Ecotoxicology of inorganic sunscreen on tropical corals in a warming ocean

Alice Tagliati

Submitted for the Degree of Doctor of Philosophy

October 2019

Heriot-Watt University
Institute of Life and Earth Sciences,
School of Energy, Geoscience, Infrastructure and Society

Research Thesis Submission

Name*:*	ALICE TAGLIATI		
School:	Energy, Geoscience, Infrastructure and Society; Institute of Life and Earth Sciences		
Version:	Final Submission	Degree Sought:	PhD

Declaration

In accordance with the appropriate regulations I hereby submit my thesis and I declare that:

1. The thesis embodies the results of my own work and has been composed by myself
2. Where appropriate, I have made acknowledgement of the work of others
3. The thesis is the correct version for submission and is the same version as any electronic versions submitted*.
4. My thesis for the award referred to, deposited in the Heriot-Watt University Library, should be made available for loan or photocopying and be available via the Institutional Repository, subject to such conditions as the Librarian may require
5. I understand that as a student of the University I am required to abide by the Regulations of the University and to conform to its discipline.
6. I confirm that the thesis has been verified against plagiarism via an approved plagiarism detection application e.g. Turnitin.

Signature of Candidate*:*		Date:	

Submission

Submitted By *(name in capitals):*	
Signature of Individual Submitting:	
Date Submitted:	

For Completion in the Student Service Centre (SSC)

Limited Access	Requested	Yes		No		Approved	Yes		No	
E-thesis Submitted (**mandatory for final theses)**										
Received in the SSC by *(name in capitals):*					Date:					

Abstract

Titanium dioxide nanoparticles ($nTiO_2$) are popular UV filter ingredients incorporated in inorganic sunscreen formulations to effectively protect human skin from the harmful effects of sun rays. Because of their extensive use, in recent years sunscreen products have emerged as potential contaminants of environmental concern, especially in coastal waters where sunscreen ingredients are washed off from the skin of bathers and discharged by sewage following showering and laundry. Various studies have documented the toxicity of organic UV filters to corals, however very little is known about the impacts of $nTiO_2$ UV filters and whole sunscreen formulations. Moreover, their potential interaction with ocean warming is unknown. The aim of this project was therefore the characterization of the photo-physiological and reproductive performances of tropical corals exposed to inorganic sunscreen ingredients and formulations, both as individual stressors and combined with elevated temperature conditions projected for the next decades. First, the potential toxicity of different $nTiO_2$ UV filters to cultured coral's endosymbiotic algae (Symbiodiniaceae) was investigated. Second, laboratory work was performed to assess the effects of a typical $nTiO_2$-based sunscreen formulation on the metabolism and photosynthetic activity of two coral species. The sea anemone *Exaiptasia pallida* was then used as a model organism to compare the toxicity of sunscreen formulations with and without UV filter. *E. pallida* experimentation allowed also the characterization of early gene expression of the stress-related heat-shock proteins (HSPs) at the onset of sunscreen-derived stress. Finally, fieldwork was conducted to evaluate the toxicity of inorganic sunscreens on corals' early life history stages, and to determine whether sunscreen toxicity change in relation to the emulsifying agents in the formulation.

Findings from this study highlight the importance of considering whole formulations, and especially the emulsifier ingredients, in evaluating sunscreen toxicity. Exposure to inorganic sunscreen's estimated environmental concentration induced significant harmful effects on reef-building corals. Symbiodiniaceae growth was reduced, coral metabolism and photosynthetic activity declined and HSPs gene expression was highly upregulated from the onset of sunscreen exposure. Inorganic sunscreen exposure also caused an increase in embryo abnormalities and a reduction of sperm motility and larvae survival. These effects were worsened under warming scenarios, suggesting that corals living in sunscreen-contaminated waters may experience a reduced resistance to thermal stress.

Acknowledgements

First I would like to thank my supervisors Prof. Teresa Fernandes and Dr Sebastian Hennige for their support, guidance and enthusiasm through my years as PhD student. I could have not asked for better supervisors.

I am also very grateful to Dr Jerome Labille, Riccardo Catalano and Danielle Slomberg that made this thesis possible by providing sunscreen formulations and ingredients, along with assistance for the many chemical analyses involved in this thesis. I thank you also for the nice time spent together during my visit to your laboratories and the SETAC conferences.
Thank you also to Dr Laetitia Hedouin and all the staff and students at CRIOBE for welcoming me in Moorea and assisting me during my field-work experiments.

A special thank you to the many great friends I shared the PhD experience with in Edinburgh: Afiq, Ana C, Ana R, Danae, Diletta, Fengjia, Francesca, Johanne, Laura, Leagh, Laurence, Margaux, Valentina. Thank you all for everything.

Laura, Paolo, grazie per essermi sempre stati vicini nonostante la lontanza, vi voglio tanto bene.

Dedico questa tesi ai miei genitori. Grazie per aver creduto in me e avermi supportato (e sopportato) sempre.

Table of Contents

List of Tables

List of Figures

List of Abbreviations and Acronyms

Al_2O_3	Aluminium oxide/Alumina
APX	Ascorbate Peroxidase
ASW	Artificial seawater
ATP	Adenosine Triphosphate
BP	Benzophenone
CASA	Computer-Aided Sperm Analysis
CAT	Enzymes catalase
cDNA	Complementary Deoxyribonucleic Acid
Chl *a*	Chlorophyll *a*
CNC	Cellulose nanocrystal
dafm	Day after the full moon
DCF	Dichlorofluorescein
DNA	Deoxyribonucleic Acid
EDX	Energy Dispersive X-ray Analysis
GLM	Generalized linear model
GLMM	Generalized linear mixed model
H_2DCFDA	2',7'-dichlorodihydrofluorescein diacetate
H_2O	Water molecule
H_2O_2	Hydrogen peroxide
HO_2	Hydroperoxyl radical
Hsp70	Heat-shock protein 70
Hsp90	Heat-shock protein 90
HSPs	Heat-shock proteins
ICP-MS	Inductively Coupled Plasma Mass Spectroscopy
ITS	Internal Transcribed Space
MHW	Marine heatwave
NP	Nanoparticle
NPS	US National Park Service
nTiO_2	Titanium dioxide nanoparticles
nZnO	Zinc oxide nanoparticles

O/W	Oil in Water emulsion
O_2	Molecular oxygen
O_2^-	Superoxide radical anion
$^{\cdot}OH$	Hydroxyl radical
OH^-	Hydroxyl group
P	Net photosynthesis
PADI	Professional Association of Diving Instructors
PAM	Pulse Amplitude Modulation
P_{gross}	Gross photosynthesis
PSI	Photosystem I
PSII	Photosystem II
qPCR	Quantitative Polymerase Chain Reaction
R	Respiration
RNA	Ribonucleic Acid
ROS	Reactive Oxygen Species
RPL11	Ribosomal protein L11
RPS7	Ribosomal protein S7
RT-PCR	Reverse transcriptase PCR
Rubisco	Enzyme ribulose-1,5-bisphate carboxylase/oxygenase
SD	Standard deviation
SEM	Standard error of the mean
SiO_2	Silicon dioxide/Silica
SML	Sea-surface microlayer
SOD	Enzyme superoxide dismutase
SPF	Sun Protection Factor
TEM	transmission electron microscopy
TiO_2	Titanium Dioxide
UV	Ultraviolet
W/O	Water in Oil emulsion
XRD	X-Ray Diffraction
ZnO	Zinc Oxide

Chapter 1

General introduction

This thesis focuses on understanding the potential impacts of inorganic sunscreen formulations and their ingredients on tropical corals, both as individual stressors and in combination with ocean warming. In this research project, each individual chapter focused on a different aspect of coral biology, life stage and model organism in order to gain a comprehensive picture of the effects of inorganic sunscreen on corals by studying cultured algal symbionts, adult corals and their early life stages, as well as the sea anemones *Exaiptasia pallida*.

Chapter 1, the general introduction, provides a general overview of the relevant literature on the research topics addressed in this thesis. Initially, the biology and characteristics of reef building corals and their algal symbionts are described, as well as an analysis of coral bleaching as coral response to stress. Coral reproduction strategies and the use of sea anemones as laboratory models for coral studies are also illustrated. Subsequently, a review of the key scientific aspects of sunscreen products composition, in particular of titanium dioxide UV filter in its nanoparticulate form, their fate in the marine environment and their potential toxicity to marine organisms, and corals principally, is presented. Finally, the objectives of the research project and the outline of the thesis are reported.

1.1 Reef-building corals

Coral reefs are among the most diverse and productive ecosystems on the planet (Connell, 1978) and offer refuge to representatives of 32 of 34 animal phyla (Spalding et al., 2001). In addition, coral reefs provide ecosystem services and support to a large number of people in the form of food, coastal protection, and tourism (Barbier et al., 2011; Moberg and Folke, 1999). Consequently, maintaining healthy reefs is of great biological and economic importance.

Hermatypic (reef-building) corals (phylum Cnidaria, order Scleractinia) are colonial animals consisting of interconnected polyps. Scleractinian corals form the basis of the reef: through the deposition of their calcium carbonate skeleton they contribute to the formation of complex three-dimensional structures that give habitat to numerous marine organisms and are spawning and nursery grounds (Hoegh-Guldberg et al., 2017; Srinivasan, 2003; Veal et al., 2010). The abundance and diversity of scleractinian corals sustain the diversity of the associated marine flora and fauna, hence any threats to reef-building corals will cause a threat to the whole ecosystem.

Scleractinian corals host in their tissues unicellular dinoflagellate symbionts of the family Symbiodiniaceae, also commonly called zooxanthellae (Schuhmacher and Zibrowius,

1985; Stambler, 2011). Zooxanthellae supply the coral with up to 95% of their energetic needs through their photosynthetic activity (Muscatine, 1990), even if coral hosts can feed heterotrophically by catching and digesting zooplankton (Houlbrèque and Ferrier-Pagès, 2009). Symbiodiniaceae produce organic matters, principally glucose and glycerol from photosynthesis, that are translocated to the coral host to supplement its metabolic processes (i.e. growth and calcification) (Burriesci et al., 2012; Wang and Douglas, 1997). The inorganic nutrients excreted by the host (CO_2, nitrogen and phosphorus) sustain Symbiodiniaceae photosynthesis and growth (Gattuso et al., 1999; Tremblay et al., 2012). The exchange of nutrients and energy between coral host and its algal symbionts allows corals, and consequently the whole coral reef communities, to survive in the low nutrients waters surrounding the reefs (Muscatine et al., 1981).

In addition to Symbiodiniaceae, corals associate also with an array of microorganisms, including bacteria, fungi, endolithic algae, archaea and viruses, to form the so-called coral holobiont (Ainsworth et al., 2010; Bourne et al., 2009; Rohwer et al., 2002). Of those microbial communities inhabiting coral tissues, the bacterial microbiome plays an essential role in coral health by supplying and/or recycling nutrients essential to coral or Symbiodiniaceae and by protecting its host against pathogens (McDevitt-Irwin et al., 2017; Rosenberg et al., 2007; van Oppen and Blackall, 2019). The survival and resilience of the coral holobiont to environmental and chemical stressors is therefore influenced not only by the responses of the coral host, but also by the characteristics of the associated Symbiodiniaceae and bacterial communities (Baker and Cunning, 2015; Glasl et al., 2017; Van Dam et al., 2011).

1.1.1 Symbiodiniaceae diversity

Coral dinoflagellate endosymbionts belong to the family Symbiodiniaceae, formerly attributed to the genus *Symbiodinium* (LaJeunesse et al., 2018). The original classification of *Symbiodinium* into nine major clades (lettered A-I) has been recently revised into seven genera (LaJeunesse et al., 2018).

Associations with Symbiodiniaceae are found in a range of marine invertebrate taxa, including Cnidaria (corals, anemones, jellyfish, zooanthidis), Mollusca (clams and nudibranchs), Porifera (sponges) and the protist Foraminifera (Stat et al., 2006). Scleractinian corals commonly associate with the genera *Symbiodinium, Breviolum, Cladocopium, Durusdinium* and occasionally with members of *Fugacium* and *Gerakladium* (formerly Clades A, B, C, D and F and G, respectively) (Baker et al., 2004;

LaJeunesse et al., 2010). Symbiodiniaceae may associate with a range of coral species ("generalist"), or associate with only one specific coral species ("specialist") (LaJeunesse et al., 2003). Furthermore, corals can host a single symbiont type or two or more simultaneously (Abrego et al., 2008; Baker and Romanski, 2007; Finney et al., 2010). In some cases within the same coral species the symbiont strain change in relation with their geographical distribution (Baker, 2003).

Coral hosts may also associate with different Symbiodiniaceae depending on the environmental conditions (Mieog et al., 2009). Indeed, different Symbiodiniaceae genera show different degrees of sensitivity and tolerance in response to environmental factors, especially temperature and light (Rowan, 2004; Tchernov et al., 2004; van Oppen and Lough, 2009). *Cladocopium* (Clade C) is the most widely distributed (LaJeunesse 2005), presumably has a wide temperature and salinity tolerance (Karako-Lampert et al. 2004; Baker 2003). *Symbiodinium* (Clade A) are considered stress-tolerant symbionts (Robison and Warner, 2006; Stat et al., 2013), and *Durusdinium* (Clade D) shows adaptation to stress tolerance (Jones et al. 2008; Van Oppen et al. 2005; Hennige et al. 2010; Abrego et al. 2008; Baker 2003), while *Breviolum* (Clade B) seems adapted to the lower light and temperature of temperate areas (Rodriguez-Lanetty et al. 2001).

Corals sensitivity to stressful conditions derive from the specific combination of symbiont and host species (Abrego et al., 2008; Fitt et al., 2009; Hoadley et al., 2015), with the Symbiodiniaceae species determining the health tolerance level of the coral hosts (Abrego et al., 2008; Berkelmans and Van Oppen, 2006; Cunning and Baker, 2013; LaJeunesse et al., 2003). For the sake of clarity and to ease comparisons with previous studies, in this thesis the Symbiodiniaceae species will be denoted with their phylotypes names (the former clade name followed by an alphanumeric identifier, e.g. A1, B1) identified with the analyses of the non-coding internal transcribed spacer (ITS) regions of rDNA (Voolstra and Berumen, 2019).

1.1.2 Coral bleaching

Coral bleaching is a stress reaction defined by the loss of some or all the algal symbionts from the host tissue or the loss of photosynthetic pigments within Symbiodiniaceae cells, resulting in the white appearance of the coral colony (Hoegh-Guldberg, 1999; Takahashi and Murata, 2008). Coral bleaching results from the exposure to various environmental stressors, such as environmental factors (e.g. high and low temperatures and light intensities, UV light, reduced pH, drastic changes in salinity) and environmental pollution

(e.g. oil, herbicides, copper, oil and sunscreens), that cause an accumulation of reactive oxygen species (ROS) and consequent oxidative stress in the algal symbionts and/or coral tissues (Baker and Cunning, 2015). As the metabolism of healthy corals depends on the photosynthetic compounds provided by the endosymbiotic algae (Muscatine, 1990), bleaching deprives corals of their major source of energy. The limited energy budget is the cause for the reduced growth, reduced reproductive outputs and the increased susceptibility to diseases observed in bleached corals (Baird and Marshall, 2002; Baker et al., 2008; Bruno et al., 2007; Hughes et al., 2019; Pratchett et al., 2015). Ultimately, If protracted in time, bleaching can lead to coral mortality (Baker et al., 2008; Brodnicke et al., 2019; Brown, 1997; Hoegh-Guldberg et al., 2017).

Heat stress from current and projected increases in sea surface temperatures, as a consequence of increased anthropogenic carbon emissions, is undeniably recognized the primary factor causing the majority of coral bleaching events worldwide (Hoegh-Guldberg et al., 2017; Hughes et al., 2017b). Scleractinian corals live close to their maximal thermal tolerance limits, hence they are vulnerable to even small changes in seawater temperature (Fitt et al., 2001; Hoegh-Guldberg, 1999). The thermally-induced breakdown of the coral-zooxanthellae symbiosis is initially linked to the ROS generated by the dysfunction of the photosynthetic processes in the symbiont. If the rate of ROS production exceed the detoxification processes of the algal symbionts, generated ROS diffuse to the host tissues leading to damage in both symbiotic partners (Downs et al., 2002; Franklin et al., 2004; Lesser, 2011; Smith et al., 2005; Weis, 2008). A schematic representation of pathways for ROS generation in *in-hospite* Symbiodiniaceae under thermal stress is presented in Figure 1.1.

The average ocean temperature has warmed by 0.2°C/decade over the past 130 years (Heron et al., 2016), and is predicted to further increase by 2-3.7°C globally by the end of the century (IPCC, 2014). In conjunction with the long-term, chronic, ocean warming, also the frequency of extreme temperature events are increasing due to anthropogenic climate change (Wernberg et al., 2013). These episodic spikes in anomalously high seawater temperatures are named “marine heatwaves” (MHW) and usually persist for a period of days to months (Hobday et al., 2016). In recent years MHW have been identified as an important environmental pressure that threaten coral reef survival (Fordyce et al., 2019; Leggat et al., 2019), being the documented cause for the severe bleaching events observed in the Great Barrier Reef, Western Australia and Japan in 2016 (Baird et al.,

2017; Hughes et al., 2017b; Le Nohaïc et al., 2017) and Hawaii in 2014 (Couch et al., 2017). The impacts of MHW and chronic thermal stress on coral holobionts are biologically and ecologically distinct (Fordyce et al., 2019; Leggat et al., 2019). Coral bleaching resulting from the prolonged exposure to warming temperatures is a gradual process causing the expulsion of algal symbionts and oxidative stress in the coral host, eventually reducing the survivorship of coral communities (Baird and Marshall, 2002; Lesser, 2011). Corals however have the capacity to recover if the warming recede (Robinson et al., 2019). Moreover, coral species differ in their susceptibility to traditional bleaching events and can be categorized as thermally-sensitive or thermally-tolerant, with the latest usually mildly- or non-affected by chronic accumulation of heat-stress (Loya et al., 2001; Van Woesik et al., 2011). Conversely, MHW cause rapid bleaching and widespread mortality even in corals normally categorized as thermally-tolerant, suggesting that the mechanisms that generally protect tolerant species from traditional bleaching are inefficient in case of acute heat-stress (Fordyce et al., 2019). The extreme warming conditions associated with MHW induce an immediate, irreversible, coral mortality, along with a catastrophic tissue loss in addition to the rapid loss of zooxanthellae (Leggat et al., 2019). Microbial bioerosion by endolithic and phototrophic microbes then degrades the exposed skeleton resulting in the decline of the structural complexity characterizing coral colonies (Leggat et al., 2019), with important ecological and socio-economic consequences (Ferrario et al., 2014; Graham and Nash, 2013).

Since MHW are directly linked to global warming (Frölicher et al., 2018) and global warming is expected to continue in the next decades even if the anthropogenic CO_2 emissions are drastically reduced (IPCC, 2014), extreme temperature anomalies are predicted to increase in frequency, magnitude and duration, particularly in tropical areas (Frölicher et al., 2018; Hobday et al., 2016; Oliver et al., 2018). Understanding how the impact of local stressors, such as sunscreens, may affect the vulnerability of corals to acute warming events is therefore essential to predict the survival of coastal and highly touristic coral reefs under the current warming scenario.

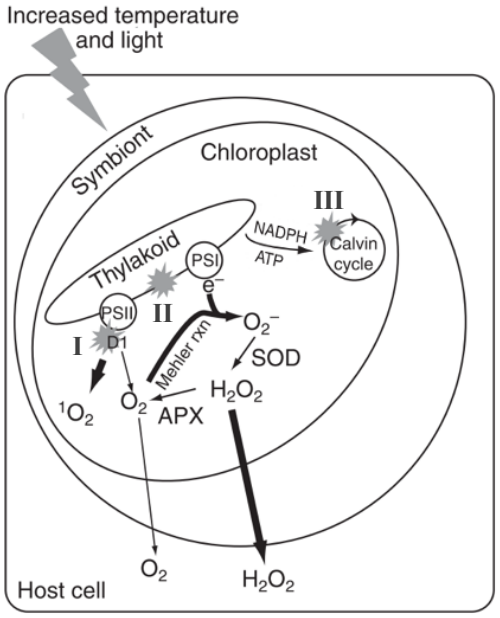

Figure 1.1 - Schematic representation of the ROS generation pathways in *in-hospite* Symbiodiniaceae under thermal stress. The proposed sites of damage are depicted as grey flashes in the figure. (**I**) Dysfunction of photosystem II (PSII) and degradation of protein D1, resulting in the triplet state of chlorophyll which reacts with O_2 to form singlet oxygen ($^1O_2$) (Takahashi et al., 2004; Warner et al., 1999). (**II**) Energetic uncoupling in the thylakoid membranes, where the proton gradient across membranes is dissipated without generating ATP (Tchernov et al., 2004). (**III**) Impairment of the Calvin cycle at the ribulose bisphospate carboxylase oxygenase (Rubisco) site, leading to reduced consumption of ATP and NADPH (Jones et al., 1998; Lesser, 1996). The build-up of electrons, resulted from the mechanisms described above, reduces O_2 in the Mehler reaction in photosystem I (PSI) to produce superoxide (O_2^-). Normally O_2 is reduced by superoxide dismutase (SOD) to hydrogen peroxide (H_2O_2), which is detoxified to water by ascorbate peroxidase (APX). When the rate of damage exceed the detoxification processes, high amount of ROS accumulate in Symbiodiniaceae cells further damaging their photosynthetic apparatus, in addition to diffusing in the host tissues where they cause oxidative damage to host cells (Smith et al., 2005; Venn et al., 2008; Weis, 2008). Figure modified from Weis (2008).

1.1.3 *Exaiptasia pallida*, a laboratory model for coral studies

The tropical sea anemone *Exaiptasia pallida* (formerly *Aiptasia pallida* (Grajales et al., 2014)) is recognized as a good laboratory model for coral studies (Lehnert et al., 2012; Sunagawa et al., 2009; Voolstra, 2013; Weis et al., 2008). Like reef-building corals, *E. pallida* is an anthozoan (a Class in the Phylum Cnidaria) and lives in symbiosis with dinoflagellate of the family Symbiodiniaceae similar to those in scleractinian corals (Thornhill et al., 2013). Although *E. pallida* anemones differs from reef-building corals in some key functional characteristics (i.e. the lack of calcareous skeleton and their indefinitely survival in an aposymbiotic state through heterotrophic feeding) (Voolstra, 2013), they offer distinct advantages that qualify them a convenient model for coral studies: they are extremely simple to maintain in aquaria, they reproduce asexually by pedal laceration, allowing the establishment of large clonal populations, and they can

survive in an aposymbiotic (symbiont-free) status (Belda-Baillie et al., 2002; Weis et al., 2008).

E. pallida anemones in the field have a wide geographical distribution, they colonize shallow waters in the tropical and subtropical regions worldwide (Grajales et al., 2014). They have been reported to associate prevalently with *Breviolum minutum* (formerly *Symbiodinium* type B1) in many locations and in aquaria, however a local population from Florida harbours the genera *Symbiodinium* and *Cladocopium* (formerly Clades A and C) (Goulet et al., 2005; Santos et al., 2003; Thornhill et al., 2013).

Whilst *E. pallida* is widely recognized as model organism for studies on coral biology, physiology, symbiosis and bleaching (Goulet et al., 2005; Lehnert et al., 2014; Núñez-Pons et al., 2017; Perez et al., 2001), it has just recently been identified as a valuable test species for laboratory ecotoxicological research (Howe et al., 2015; Patel and Bielmyer-Fraser, 2015; Siddiqui and Bielmyer-Fraser, 2015; Trenfield et al., 2017). *E. pallida* anemones provide reliable substitute of corals as animal models in toxicity studies. Their use overcomes the problem of the high number of coral colonies needed to develop statistically significant toxicity experiments with high number of replicates; coral collection is indeed a destructive practice and the required samples number might exceed the quota allowed by regulatory policies (Vijayavel and Richmond, 2012).

1.1.4 Early life-history of scleractinian corals

Gamete fertilization and larval survival are key processes to determine the persistence of coral populations (Richmond et al., 2018) but early life stages of corals are known to be more vulnerable than adults to environmental stresses (Byrne, 2011; Downs et al., 2014; Putnam et al., 2010; Reichelt-Brushett and Harrison, 1999), thus they may be particularly susceptible to sunscreen pollution.

Corals have two different types of reproduction: broadcast spawning and brooding. Most scleractinian corals are hermaphroditic broadcast spawners: they release male and female gametes simultaneously into the water column for external fertilization and pelagic larval development (Babcock et al., 1986; Carroll et al., 2006; Harrison, 2011; Hayashibara et al., 1993; Van Veghel, 1993). The released buoyant egg-sperm bundles break apart and accumulate at the sea surface (Oliver and Babcock, 1992). Coral larvae, named planulae, typically remain in the water column for 2-6 days before they become competent to settle on a substratum (Harrison and Wallace, 1990; Miller and Mundy, 2003). Brooding is the second reproduction mode and characterizes 14.3% corals worldwide (Harrison, 2011).

Brooder corals undergo within-polyps fertilization and larvae development, releasing fully developed and ready to settle larvae. Most brooded larvae contain symbiotic algae that provide energy to the planulae (Harrison and Wallace, 1990), thus they have the potential for a long-distance dispersal (Richmond, 1987).

Before settlement, gametes and planulae reside in the surface waters as planktonic stages for several days (Baird et al., 2009; Harii et al., 2007) where they are easily exposed to the anthropogenic compounds that accumulate at the air-water interface (Wurl and Obbard, 2004), including sunscreen ingredients (Gondikas et al., 2014).

1.2 Sunscreen products

Sunscreens are complex mixtures of several compounds that protect the skin from ultraviolet (UV) radiation to minimize their deleterious effects on human health. Their widespread use leads to a potential release of high quantities of sunscreen products and their ingredients in localized highly touristic areas, such as coastal coral reefs.

1.2.1 Sunscreen ingredients

Sunscreens are oil-in-water or water-in-oil emulsions of which the primary ingredients are UV filters, emulsifiers and emollients; other additives, such as perfumes, preservatives, sensory enhancers and thickeners, are added to improve the aesthetic of the cream (Figure 1.2) (Osterwalder et al., 2014).

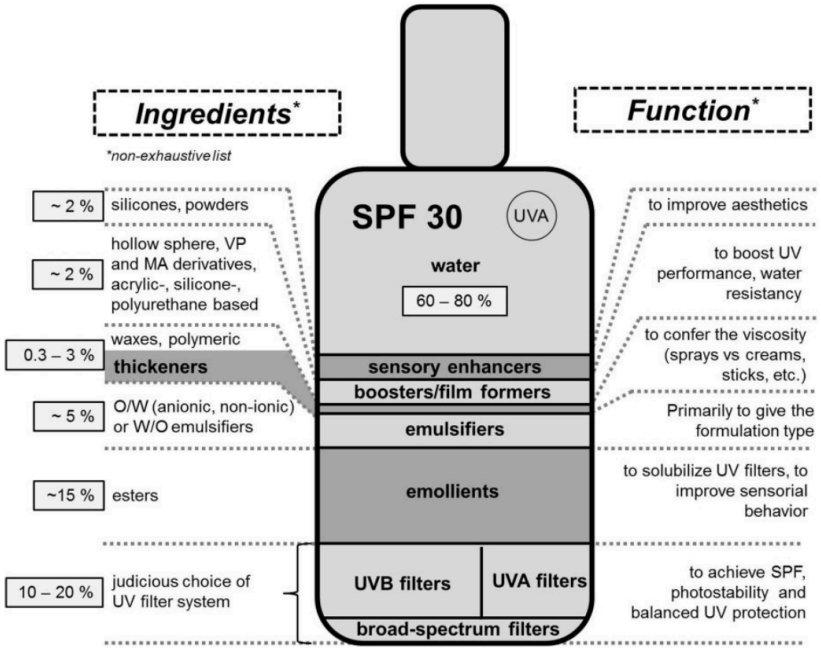

Figure 1.2 - Sunscreen ingredients and their functions (Osterwalder et al., 2014)

UV filters are the sunscreen active ingredients that protect the skin from UV radiations in the UVA (320-400 nm) and/or UVB (290-320 nm) range (Osterwalder et al., 2014). Sunscreens are conventionally divided into organic (chemical) and inorganic (physical - mineral) on the basis of the mechanism of protection. The list of UV filters, organic and inorganic, approved in Europe, United States, Australia and Japan, with their UV radiation protection range and maximum permitted concentration according to the different regulations is presented in Table 1.1. Organic sunscreens contain organic molecules that absorb UV radiations; due to their aromatic ring structures, absorbed energy is then transformed to non-radiative wavelengths and released as light or heat (Osterwalder et al., 2014). Inorganic sunscreens have metal oxides as active ingredients that prevent the UV radiations from reaching the skin due to their scattering, reflective and absorption properties (Figure 1.2). UV filters have different spectrum protection towards UV radiations (Table 1.1), thus combinations of several UV filters are used in most sunscreen formulations to maximise the total UV absorption capacity (Osterwalder et al., 2014).

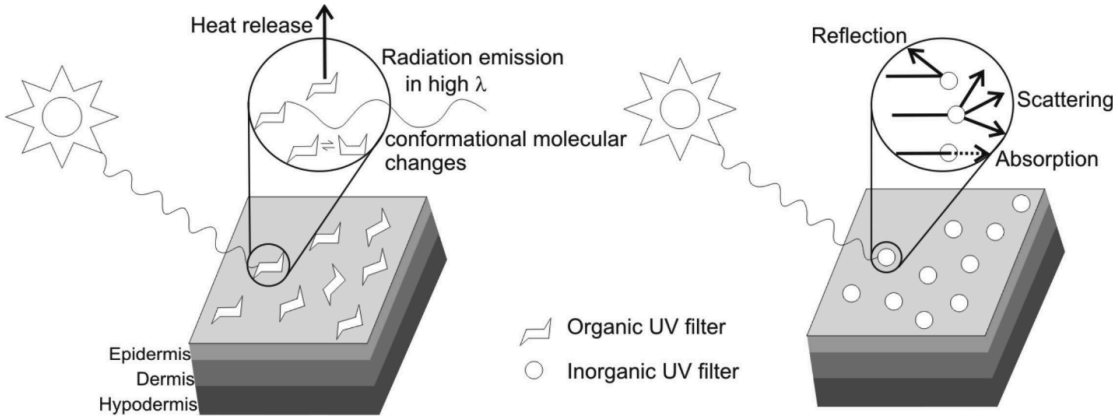

Figure 1.3 - Action mode of organic (left) and inorganic (right) UV filters (Manaia et al., 2013).

Emollients ensure the solubilization of UV filters and their homogeneous dispersion in formulation. In addition they make the sunscreen cosmetically appealing by improving its spreadability and providing a not greasy and sticky feeling on the skin (Osterwalder et al., 2014).

Emulsifiers are key compounds since they produce and stabilize the dispersion of the aqueous and oil phases creating a sunscreen emulsion. Depending on the emulsifier system, the emulsion type can either be oil-in-water (O/W) or water-in-oil (W/O)

(Osterwalder et al., 2014). Water-in-oil formulations are emulsions having an oil continuous phase and water as dispersed phase. They are a popular sunscreen system due to their high water resistance as they do not contain hydrophilic emulsifiers (Osterwalder et al., 2014) and are also the formulation type that will be tested in the experiments presented in this thesis.

Table 1.1 - List of UV filters approved in Europe, United States, Australia and Japan (Sánchez-Quiles and Tovar-Sánchez, 2015).

Active ingredients	UV action spectrum*	Concentration limits (%)			
		EU	USA	AUS	JP
Organic filters					
Oxybenzone	UVB, UVA II	10	6	10	5
Sulisobenzone	UVB, UVA II	5	10	10	10
Aminobenzophenone	UVA I	10	-	-	-
Avobenzone	UVA I	5	3	5	10
Merodimate	UVA I	-	5	5	-
Ecamsule	UVA I	10	10	10	10
Enzacamene	UVB – UVA II	4	-	4	-
Padimate-O	UVB – UVA II	8	8	8	10
Cinoxate	UVB		3		
Octinoxate	UVB – UVA II	10	7.50	10	20
Amiloxate	UVB – UVA II	10	-	10	10
Octisalate	UVB – UVA II	5	5	5	10
Homosalate	UVB – UVA II	10	15	15	10
Trolamine salicylate	UVB		12		
Octocrylene	UVB, UVA II	10	10	10	10
Ensulizole	UVB	8	4	4	3
Polysilicone-15 (BMP)	UVB, UVA II	10	-	10	10
Inorganic filters					
Titanium dioxide	UVB, UVA	25	25	25	no limit
Zinc oxide	UVB, UVA	25	25	no limit	no limit

* UVA I (340–400 nm), UVA II (320–340 nm), UVB (290–320 nm)

1.2.2 Inorganic UV filters: the case of titanium dioxide nanoparticles

Only titanium dioxide (TiO_2) and zinc oxide (ZnO) are approved as inorganic UV filters (Table 1.1). Their maximum authorized content in sunscreens in Europe, United States and Australia is 25%, whereas in Japan neither of them are considered as UV filters and their use is not restricted (Osterwalder et al., 2014). TiO_2 and ZnO are mainly used in their nanoparticle (NP) form (dimension range 1-100 nm) in order to be aesthetically pleasant (not whitening on the skin) and to ensure the optimal UV protection (Serpone et al., 2007). Inorganic UV filters are photostable and offer a broad spectrum coverage: they

effectively shield across the whole UVA and UVB spectrum due to the combination of absorption and scattering properties (Detoni et al., 2011). They are also chemically inert (do not react with other molecules) and thus are added to organic sunscreen to give additional UVA protection and increase the sunscreen sun protection factor (SPF) (Serpone et al., 2007). As a result of these characteristics, TiO_2 and ZnO have become widely popular and ubiquitous UV filters in sunscreen formulations.

Titanium dioxide has been known as UV filter since 1952, and the first sunscreen containing titanium dioxide nanoparticles ($nTiO_2$) was commercialized in 1989 (Detoni et al., 2011; Serpone et al., 2007). Titanium dioxide is available in three crystalline forms: rutile, anatase and brookite. Rutile is more stable than the other forms, thus it is generally used in cosmetic formulations (Smijs and Pavel, 2011). TiO_2 is a semi-conducting material and the nanoparticle form enhances its photocatalytic activity resulting from the absorption of UV radiation (Serpone et al., 2007).

The redox processes at the surface of radiated TiO_2 are illustrated in Figure 1.4: the absorption of UV light ($h\nu$) excites electrons from the valence band to the conduction band creating conduction band electron (e^-) and valence band holes (h^+). In aqueous solution, the electron is scavenged by molecular oxygen (O_2) to produce superoxide radical anion ($O_2^{-\cdot}$), whereas water molecules (H_2O) or hydroxyl groups (OH^-) are reactive with the valence band holes forming reactive hydroxyl radicals ($\cdot OH$) that initiate the oxidation. In acidic media, $O_2^{-\cdot}$ is protonated producing hydroperoxyl radical ($HO_2^{\cdot}$) and ultimately hydrogen peroxide (H_2O_2) (Serpone et al., 2007). The generated ROS may have harmful effects on cells and react with the organic ingredients in sunscreen contributing to their degradation (Egerton et al., 2008; Serpone et al., 2007), therefore $nTiO_2$ are modified with chemically inert substances to make them suitable for cosmetic uses (Osterwalder et al., 2014). To inactivate the photocatalytic nature of TiO_2, the $nTiO_2$ surface is coated with inorganic materials, such as silica (SiO_2) and alumina (Al_2O_3), to form a physical barrier that shields from the UV radiation leading to less UV light absorption (Detoni et al., 2011). An organic surface treatment, such as dimethicone (silicone polymer), can also be added to facilitate the dispersion of $nTiO_2$ in the oil phase and, along with the silica coating, prevent particles aggregation (Auffan et al., 2010; Choong, 2016; Labille et al., 2010).

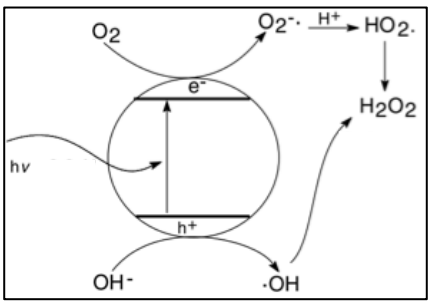

Figure 1.4 - Schematic representation of the photochemistry processes at the surface of illuminated $nTiO_2$ (modified from Serpone et al., 2007).

Studies on the composition commercial sunscreens in of United States that listed TiO_2 as an active ingredient revealed that all products contain nanoparticles (Cuddy et al., 2016; Lewicka et al., 2011). Although TiO_2 content limitation in sunscreen is 25% by weight of product, analysis of several sunscreens indicates that TiO_2 concentration range between 2-15%, equally to 14 to 90 µg TiO_2 per mg of formulation (Weir et al., 2012). Size of $nTiO_2$ in sunscreen-products range from 30 to 150 nm (Schilling et al., 2010). Lewicka et al. (2011) also established that commercially available sunscreens contain needle- or spherical-shaped $nTiO_2$ with dimensions approximately of 25 nm.

Inorganic UV filters are stated as active ingredients in 50% of suncare products sold in UK and in 23% of the products in the United States (Lewicka et al., 2011; Wahie et al., 2007), and more than 70% of the total amount of $nTiO_2$ produced worldwide is used in the cosmetic industry (Piccinno et al., 2012). Mueller and Nowack (2008) estimated that 95% of nanoparticles used in cosmetics are released during application. Moreover $nTiO_2$, are the nanoparticles type most likely to enter the environments in large quantities between all the engineered nanoparticles (Gottschalk et al., 2009).

1.2.3 Sunscreen compounds in the marine environment and their environmental toxicity

Recent studies have shown that sunscreen ingredients reach the marine environment primarily from being washed from the skin during swimming and bathing, and also indirectly via wastewater treatment plants following showering and laundry (Danovaro et al., 2008; Giokas et al., 2007; Johnson et al., 2011; Poiger et al., 2004; Tovar-Sánchez et al., 2013). Sunscreens are mixtures of hydrophobic compounds that, once released, accumulate on the water surface (Gondikas et al., 2014). The artificial aging of four commercialized sunscreen formulated with $nTiO_2$ as UV filter revealed that sunscreen in seawater forms stable colloidal suspensions characterized by submicron fractions (<1

μm) and large agglomerates (1-100 μm) consisting of the organic ingredients associated with up to 30% of the total $nTiO_2$ initially present in the formulation (Botta et al., 2011). Trapped $nTiO_2$ float on the air-water interface where they are exposed to sunlight. The intense solar radiation exposure, along with weathering by natural elements, may degrade the nanoparticle coatings (Labille et al., 2010) enhancing the titanium intrinsic photocatalytic activity, hence influencing $nTiO_2$ toxicity when they are finally dispersed in the water column.

At least 25% of the quantity of sunscreen applied on the skin is washed off when a body is immersed in water (Danovaro et al., 2008). Considering the European Union recommended quantities of sunscreen that must be applied to ensure sun protection (2 mg cm^{-2}, approximately 36 g of sunscreen), the quantity of sunscreen applied on the skin by an average size adult (60-70 kg of body weight) is estimated to be 3600 mg per application (Hansen et al., 2009). This enables us to estimate that 900 mg of sunscreen could be released from the skin during immersion, of which 90 mg are $nTiO_2$ UV filters considering a 10% $nTiO_2$ concentration in sunscreens. At present, analyses of the actual quantity of $nTiO_2$ in marine waters are limited due to the inadequacy of methods for its detection and quantification, but the predicted environmental concentrations in surface waters range from 2 to 700 ng/L (Gottschalk et al., 2009; Mueller and Nowack, 2008). Recently Gondikas et al. (2014) demonstrated that the concentration of $nTiO_2$ in a lake is steadily increasing since the late 1990s, increase that coincides with the introduction of $nTiO_2$ as sunscreen ingredients. Furthermore, $nTiO_2$ concentrations in freshwater recreational spots show seasonal and daily increases of 40-80% in conjunction with water activities, reaching values between 394 ng/L and 1.7 μg/L, with peaks of 10 and 27.1 μg/L (Gondikas et al., 2014; Reed et al., 2017; Venkatesan et al., 2017).

In recent years, environmental concerns associated with sunscreen use and release in surface waters have attracted increasing attention (Raffa et al., 2018; Richardson and Ternes, 2018; Sánchez-Quiles and Tovar-Sánchez, 2015). Sunscreen behaviours in the marine environment are summarized in Figure 1.5: because of their lipophilic characteristic and stability against biodegradation, sunscreen chemicals can accumulate in marine organisms, and from there enter food webs (Bachelot et al., 2012; Gago-Ferrero et al., 2013; Nakata et al., 2009). Under UV radiation both organic and inorganic UV filters incur degradation (Auffan et al., 2010; Labille et al., 2010; Santos et al., 2012) and can generate ROS (Allen et al., 1996; Sánchez-Quiles and Tovar-Sánchez, 2014; Serpone

et al., 2007) that may induce oxidative stress in marine organisms (Lesser, 2006). On the other hand, sunscreens may be a source of inorganic nutrients (nitrate, nitrite, phosphate, silicate and ammonium) for phytoplankton and enhance microalgal growth (Tovar-Sánchez et al., 2013).

Although sunscreens are mixtures of several ingredients, the studies investigating their environmental impacts are mainly concentrated on the individual UV filters compounds. Several studies demonstrated that the single chemical compounds can interact (Egerton et al., 2008; Sendra et al., 2017b; Seo et al., 2018), meaning it is critical the impact of whole sunscreen formulations is investigated to accurately evaluate sunscreen environmental toxicity (Fel et al., 2019).

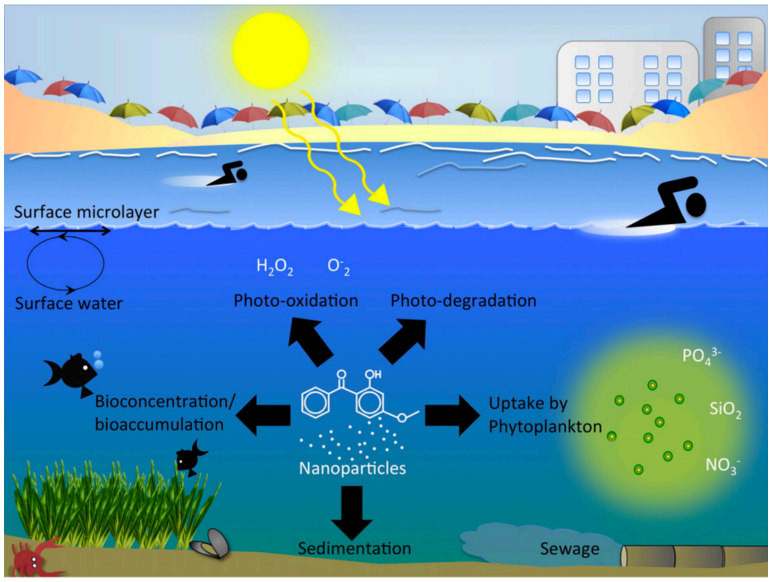

Figure 1.5 - Schematic representation of the transport and behaviour of sunscreen compounds in the marine environment (Sánchez-Quiles and Tovar-Sánchez, 2015).

Beside cosmetics, $nTIO_2$ have a wide variety of applications (e.g. cleaning agents, pigments, plastics, cements, water purification) and over 10000 tons of $nTiO_2$ are produced annually in Europe alone (Piccinno et al., 2012). Due to $nTiO_2$ broad applications, the likelihood of its uncontrolled release in the marine environment during manufacturing, transport, waste management system or by accident is high (Sun et al., 2014), hence $nTiO_2$ environmental fate and toxicity is currently under intense study. Because of its photocatalytic properties, the generation of ROS under UV radiations and the derived oxidative stress has been suggested as the main form of $nTiO_2$ toxicity in aquatic organisms (Baker et al., 2014; Barmo et al., 2013; Jovanović, 2015; Li et al., 2015; Miller et al., 2010; Zhu et al., 2011). In addition, $nTiO_2$ uptake and ingestion have

been documented in filter feeding animals (Couleau et al., 2012; Doyle et al., 2016; Marisa et al., 2018), and $nTiO_2$ internalization induce immune responses in molluscs (Ciacci et al., 2012; Grimaldi et al., 2013; Wang et al., 2014). Microalgae are more sensitive to nanoparticles compared to many other marine organisms (Aruoja et al., 2009; Zhou et al., 2014). Several studies demonstrated that $nTiO_2$ inhibit algae growth and photosynthetic activity and induce antioxidant responses (Aruoja et al., 2009; Wang et al., 2016; Xia et al., 2015). $nTiO_2$ adsorption on algal cell surface may cause physical damages to cellular membranes (Metzler et al., 2011; Wang et al., 2016; Xia et al., 2015; Zhang et al., 2016); additionally, nanoparticles agglomerations could reduce light availability for photosynthesis (shading effect) and/or uptake of nutrients (Aruoja et al., 2009; Deng et al., 2017; Li et al., 2015; Manzo et al., 2015; Sendra et al., 2017c). However, several studies showed also no evidence of growth inhibition in marine phytoplankton exposed to $nTiO_2$ up to concentrations of 20 mgL^{-1} (Griffitt et al., 2008; Hund-Rinke and Simon, 2006; Manzo et al., 2015; Miller et al., 2010; Morelli et al., 2018).

The studies described above highlight that $nTiO_2$ may alter a series of physiological properties in aquatic organisms inducing significant stress responses, while not lethal. It is also important to note that to evaluate the environmental impact of $nTiO_2$ is necessary to consider that its toxicity is dependent on nanoparticle size and coatings and environmental factors. Indeed $nTiO_2$ aggregates quickly in seawater (Keller et al., 2010) and the toxicity is enhanced when simultaneously exposed to UV radiation (Dalai et al., 2013; Miller et al., 2012; Sendra et al., 2017a).

Cosmetic (i.e. coated) $nTiO_2$ in seawater differ from the original manufactured form, as they are aged and weathered through interactions with the environment (Nowack et al., 2012). In water the external hydrophobic layer is quickly degraded and the residual is composed by the titanium core plus the inorganic coatings (Auffan et al., 2010; Labille et al., 2010; Nickel et al., 2013). This degradation promotes $nTiO_2$ dispersion in water and the formation of colloidal aggregates (Labille et al., 2010).

The impact of $nTiO_2$ derived from sunscreen has been assessed on varied organisms and the results show an overall negative impact in a concentration-dependent manner. Aged $nTiO_2$ caused growth and reproduction impairment in the crustacean *Daphnia magna* (Fouqueray et al., 2012), DNA damage in the mollusc *Mytilus galloprovincialis* (D'Agata et al., 2014), alteration of the antioxidant system and apoptosis in earthworms (Bigorgne

et al., 2011; Lapied et al., 2011), induced oxidative stress in the root system of a leguminous plant (Foltête et al., 2011) and increased genotoxicity in the bacteria *Salmonella typhimurium* (Jomini et al., 2012). Recent studies demonstrated the production of singlet oxygen ($^{\cdot}O_2$) and hydrogen peroxide (H_2O_2) in water even at low UVA intensity, suggesting that the inert coating layers of $nTiO_2$ may not be fully effective in inhibiting the formation of ROS (Sánchez-Quiles and Tovar-Sánchez, 2014; Santaella et al., 2014).

1.2.4 Sunscreen toxicity on coral reefs

In recent years the potential toxicity of sunscreen UV filters towards tropical corals has received considerable attention from scientists, media and governments, leading to the ban of selected UV-filters in popular tourist destinations, such as Hawaii, Palau, Bonaire and Mexico, with the intent to protect coral reef ecosystems (BBC News, 2018). As a consequence, many sunscreens labelled "Reef Safe" and "Reef Friendly" entered the market, claiming to not contain ingredients toxic to corals and marine life in the coral reef ecosystems. However, the sunscreen labelling depends solely on the sunscreen manufacturers, since there is no official definition for "Reef Safe/Friendly Sunscreen" as it is not regulated by any law (Wood, 2018). The US National Park Service (NPS), Professional Association of Diving Instruction (PADI) and numerous eco-tour operators recommend the use of mineral based sunscreen as safer alternative to sunscreen with oxybenzone (NPS; PADI), although studies on the effects of inorganic UV filters on coral reef ecosystems are scarce.

To date, studies on the impacts of sunscreen on tropical corals concentrated on the organic UV filters. Oxybenzone, avobenzone and octinoxate have been found to induce coral bleaching in both adult corals and their larval forms (Danovaro et al., 2008; Downs et al., 2014, 2016; He et al., 2019a), while octrocrylene accumulates in coral tissues causing mitochondrial disfunctions (He et al., 2019a; Stien et al., 2018). On the contrary, Fel et al. (2019) demonstrated that coral maximum photosynthetic efficiency was not affected by a 5-weeks exposure to a range of organic UV filters up to concentrations of 10 mgL^{-1}. Concerning inorganic UV filters, ZnO nanoparticles (nZnO) seem to be more toxic than $nTiO_2$ at the same exposure concentrations (Corinaldesi et al., 2018), causing coral bleaching (Corinaldesi et al., 2018), reduced photochemical efficiency (Fel et al., 2019) and changes in the lipid composition of the cellular membranes (Tang et al., 2017). Jovanović et al. (2014) showed that $nTiO_2$ exposure induced minor bleaching as well as

upregulation of heat shock protein 70 (Hsp70) gene expression in the coral *Montastrea faveolata*. However the nanoparticles tested in the experiment do not represent the type of $nTiO_2$ typically used as UV filter in cosmetics as the crystal structure is anatase, the more reactive form of TiO_2 (Ohno et al., 2003; Sayes et al., 2006), and without any coatings. The only study on cosmetic (coated) type $nTiO_2$ demonstrated no adverse effects on coral-algae symbiosis, even at 6.3 mgL^{-1} (Corinaldesi et al., 2018), a concentration much higher than the $nTiO_2$ predicted environmental concentrations.

Several studies have demonstrated a direct relationship between recreational activities and sunscreen compounds released inurface s water (Gondikas et al., 2014; Reed et al., 2017; Tovar-Sánchez et al., 2013, 2019; Venkatesan et al., 2017). Coral reefs annually support ~70 million trips, and tourism linked to coral reefs is constantly growing (Spalding et al., 2017). The direct release of sunscreen ingredients in coral reef areas is thus expected to be higher than in non-touristic regions. Additionally, domestic sewage also discharge sunscreen components into the environment (Giokas et al., 2007; Poiger et al., 2004) and coral reefs are mainly located in the poorest developing countries in the world (Donner and Potere, 2007) with poor or non-existent policy to address waste management (Bell, 2002). Normally the removal efficiency of $nTiO_2$ from wastewater is between 90.6 and 99.5% (Westerhoff et al., 2011), but in coral reef areas only a fraction of domestic wastewater is treated, and most of the treatment plants do not work efficiently (Bell, 2002; Musee, 2011). Indeed 80-90% of wastewaters are discharged without an adequate treatment in Southeast Asia and in the Pacific (Bryant et al., 1998; UNEP/GPA, 2006). In the Caribbean, discharges from coastal activities are the main form of pollution (Cesar et al., 2003) and although many tourists facilities have their own treatment plants, only 25% of these are in working condition (UNEP/GPA, 2006). Moreover, coral reefs are coastal marine ecosystems characterized by shallow water and long residence time (Suzuki and Kawahata, 1999). Black et al. (1990) demonstrated that sewage remains on or near a coral reef for several weeks in common weather conditions. Sunscreens may therefore pose a significant threat for coastal coral reef ecosystems subjected to intense tourism and urbanization (Baker et al., 2014).

1.2.5 Estimation of the release of sunscreen formulated with the UV filter $nTiO_2$ in a touristic beach

Although the actual environmental concentrations of sunscreen ingredients in marine waters are unknown, following data from the literature about the market of inorganic sunscreen products and their composition, the European Commission recommended a sunscreen quantity for an effective sun protection and estimated the quantity of sunscreen washed from the skin during swimming allowed to estimate the potential release of inorganic sunscreen in coastal waters by beachgoers. The assessment was based on the water volume of Palmira beach in Majorca Island, used here as a model for a typical touristic beach in tropical areas. Palmira beach was previously described in detail by Sánchez-Quiles and Tovar-Sánchez (2014): it is a cove of 300 m length with a bay of 1.5 m depth on average and 3 days of water residence time (Sánchez-Quiles and Tovar-Sánchez, 2015; Tovar-Sánchez et al., 2013).

It is thus possible to propose an estimation of the release of $nTiO_2$-based sunscreen in a touristic coastal areas using information currently in the literature:

- Inorganic sunscreen products formulated with $nTiO_2$ as UV filter were estimated to constitute one in six of the global sunscreen market in 2006, corresponding to 16.6% of the market (Botta et al., 2011);
- the recommended sunscreen application by an adult is 2 mg cm^{-2}, approximately 36g for an average-sized man (The Comission of the European Communities, 2006);
- the volume of water of the bathing zone of a touristic beach provided by Sánchez-Quiles and Tovar-Sánchez (2014) (1.2×10^7 L, for an area of 1.6×10^4 m^2 and 1.5 m depth), where the number of tourists in a typical summer day is ~ 10000 (Sánchez-Quiles and Tovar-Sánchez, 2014);
- an estimate of 25% of the sunscreen applied is considered to wash-off from the skin into the water (Danovaro et al., 2008);
- the quantity of $nTiO_2$ in a commercial inorganic sunscreen product is typically 10% (Botta et al., 2011).

Combining these points, it is possible to estimate a summer daily release of a typical $nTiO_2$-based sunscreen at approximately 1.2 mgL^{-1}, of which 0.1 mgL^{-1} is the concentration of $nTiO_2$ alone, using the following equations:

$$\text{Total sunscreen released} = \frac{\%\ sunscreen\ washed\text{-}off \times sunscreen\ applied \times \#\ tourists}{volume\ of\ water\ body}$$

$$nTiO_2\text{-sunscreen concentration} = \%\ nTiO_2\text{-}sunscreen\ in\ the\ market \times total\ sunscreen\ released$$

$$nTiO_2\ only\ concentration = \%\ nTiO_2\ in\ sunscreen \times nTiO_2\text{-}sunscreen\ concentration$$

The above estimates consider one sunscreen application from adult consumers that apply the recommended quantity of sunscreen. In real-life people typically use less sunscreen than the recommended dose, however it is applied more than one time only (De Villa et al., 2011; Reich et al., 2009). Moreover, the data from the inorganic sunscreen market are related to 12 years ago, a higher volume of sunscreen formulated with inorganic filters is likely on the market nowadays. Also, a 24h rate of water renewal is considered here, however longer residence times of several days have been recorded for several coastal coral reefs (Andréfouët et al., 2001; Choukroun et al., 2010; Suzuki and Kawahata, 2003). Therefore 1.2 mgL^{-1} is considered a safe and conservative estimate of a realistic daily release of inorganic sunscreen in coastal waters by beachgoers in a typical summer day.

1.3 Research objectives and thesis outline

Titanium dioxide is a popular cosmetic ingredient. However, ecotoxicity studies on whole sunscreen formulations with $nTiO_2$ as the active ingredient are scarce, even though significant quantities of the mineral and hydrophobic ingredients are discharged into high-touristic coral reef's waters, which interact among themselves and the environment resulting in a potential threat to tropical corals.

Additionally, the impacts of inorganic sunscreen ingredients and formulations may affect the response of corals to periods of anomalously high seawater temperature, which frequency and magnitude will increase even under the most optimistic global environmental change scenarios. The research presented here will therefore help us understand the effects of sunscreen exposure in a climate change context, a large gap in our current understanding.

Corals are complex organisms and sunscreen are complex mixtures of ingredients, the toxicity of which has rarely been studied. The objective of each chapter is thus to investigate the toxicity of different combinations of sunscreen ingredients to a different aspect of coral biology and life stage. All experiments were performed under ambient and warming conditions to question whether the effects of sunscreen exposure change in relation with projected climate change.

The specific subject and aim of each chapter are:

Chapter 2: *Subject*: Symbiodiniaceae; $nTiO_2$ UV filters and oil phase ingredients.

Aim: Evaluate $nTiO_2$ potential toxicity to coral's endosymbiotic algae. Assess whether characteristics of the nanoparticle's coatings drive the UV filter toxicity and the potential impacts of sunscreen oil phase ingredients.

Since corals are complex organisms where fitness depends on the equilibrium between animal host and algae symbionts, stress to symbionts will affect their coral host. Chapter 2 provides preliminary evidence of the possible toxicity of inorganic sunscreen to the coral-Symbiodiniaceae symbiotic association.

Chapter 3: *Subject*: Adult corals; Sunscreen formulation.

Aim: Investigate the toxicity of a typical $nTiO_2$-based sunscreen formulation on the photo-physiological responses of two coral species.

This chapter addresses the knowledge gap on understanding the effects of a whole sunscreen formulation on tropical corals. Coral metabolism and photosynthetic activity are analysed under present and predicted ocean warming scenarios to evaluate if the combination of multiple stressors reduces coral resistance to elevated seawater temperatures.

Chapter 4: *Subject*: *Exaiptasia pallida*; Sunscreen and filter-free formulations.

Aim: Compare the toxicity of a typical sunscreen formulation and a formulation with identical composition but no UV filters.

Contrary to recent studies that focused only on the toxicity of individual UV filters, results from Chapter 2 highlight the importance of taking into account sunscreen's oil phase in assessing sunscreen toxicity. In Chapter 4

the impacts of sunscreen having $nTiO_2$ as UV filter and a filter-free formulation are compared by studying the sea anemone *E. pallida*'s photosynthetic and transcriptomic responses. *E. pallida* was chosen as a model organism here due to its benefit of fast reproduction and easiness of both culturing and handling for gene expression analyses.

Chapter 5: *Subject*: Coral gametes and larvae; 3 sunscreen formulations
Aim: Assess the toxicity of inorganic sunscreens on coral early life history stages and determine whether sunscreen toxicity changes in relation to the emulsifying ingredients in the formulation.

Chapter 5 results from the fusion of findings from previous chapters on the toxicity of whole sunscreen formulation and the importance of the oil phase ingredients. In this study the effects of three sunscreen formulations, having different combinations of hydrophobic-hydrophilic $nTiO_2$ and chemical-organic oil phases, were assessed on coral fertilization success and larvae survival. The experiments presented here were conducted at the Centre for Island Research and Environmental Observatory (CRIOBE) in Moorea (French Polynesia). Results from this chapter provide not only information on the potential impacts of inorganic sunscreens on the persistence of coral communities in Moorea and their recovery after a thermal stress, but also preliminary evidence that the use of an organic emulsifier could mitigate the toxicity of sunscreen.

Finally, chapter 6 presents a summary and discussion of the work undertaken within this PhD project.

All together this thesis aims to create an integrated view of the effects of inorganic sunscreen on tropical corals in a warming ocean through a series of laboratory and field-based experiments designed to test different $nTiO_2$ types and sunscreen formulations.

Chapter 2

Effects of inorganic sunscreen ingredients on coral symbionts and their combined toxicity with global warming

2.1 Introduction

Tropical reef-building corals offer habitat and protection to numerous marine species in oligotrophic waters due to the nutritional exchanges between scleractinian corals and their photosynthetic zooxanthellae symbionts (family Symbiodiniaceae) (LaJeunesse et al., 2018; Muscatine, 1990; Spalding et al., 2001). Zooxanthellae can also live outside a host while preserving the ability to form symbiosis (Hirose et al., 2008). These free-living Symbiodiniaceae are considered important source of symbionts for corals recovering from bleaching (Pochon et al., 2010). Furthermore juveniles of the majority of coral species must acquire their symbionts from a free-living Symbiodiniaceae reservoir (Baird et al., 2009; Harrison, 2011). Rising sea surface temperatures due to climate change is recognized as the major threat to coral survival (Hoegh-Guldberg et al., 2017), nonetheless recent studies highlight sunscreen compounds as an important source of stress in coastal reef ecosystems (Tovar-Sánchez et al., 2013). With global surface temperatures and extreme temperature events forecasted to increase even under the more optimistic scenario (Frölicher et al., 2018; Hughes et al., 2018a; IPCC, 2014, 2018), it is therefore important to understand how Symbiodiniaceae respond to the multiple stressors of sunscreen and changes in water temperatures, and whether this can exacerbate a breakdown in symbiosis (bleaching) or undermine the acquisition of new symbionts.

The use of sunscreen products results in the direct release of $nTiO_2$ and other sunscreen ingredients into water bodies (Gondikas et al., 2017) where they pose a potential threat to free-living and *in-hospite* Symbiodiniaceae populations. Current knowledge on sunscreen environmental toxicity regards mainly sunscreen UV filters (Sánchez-Quiles and Tovar-Sánchez, 2015), with the potential impact of emulsifier and emollient ingredients on marine organisms still unknown. The aim of this chapter is thus to investigate the effects of both $nTiO_2$ and oil phase ingredients on cultured Symbiodiniaceae, representative of both host-algae symbioses of reef-building corals and free-living species, to understand $nTiO_2$ activity in a typical sunscreen mixture. For this purpose, three hydrophobic $nTiO_2$, commonly used in cosmetic products, but with different sizes and coatings, were dispersed in an oil phase composed by a mixture of emollients and emulsifier, to mimic the composition of commercially-available sunscreens. Additionally, a fourth $nTiO_2$ covered by a hydrophilic coating was dispersed in water and also tested on a Symbiodiniaceae species to test the direct toxicity of $nTiO_2$ nanoparticles.

$nTiO_2$ UV filters are either released into the water column or remain on the water surface where they float trapped in the hydrophobic components of the cream (Gondikas et al.,

2017). $nTiO_2$ floating on the air-water interface are exposed to direct sunlight irradiation that enhance titanium's intrinsic photocatalytic behaviour and thus its toxicity (Gondikas et al., 2017). The production of ROS following UV radiation exposure and the derived oxidative stress has been considered to be the dominant $nTiO_2$ toxicity mechanism to fish (Federici et al., 2007; Xiong et al., 2011), bivalves (Barmo et al., 2013), cyanobacteria (Cherchi et al., 2011) and freshwater (Al-Awady et al., 2015; Metzler et al., 2011) and saltwater algae (Li et al., 2015; Miller et al., 2012; Sendra et al., 2017b; Xia et al., 2015). In corals, ROS generation is acknowledged as the triggering cause of coral bleaching (Lesser, 2011; Smith et al., 2005). According to the oxidative theory of coral bleaching, elevated sea water temperatures induce the photosynthetic apparatus of Symbiodiniaceae to produce a high quantity of ROS. Those generated ROS leak into coral host tissues where they accumulate and cause cellular damage, leading the coral to expel the symbiotic algae as defence mechanism (Downs et al., 2002; Smith et al., 2005; Weis, 2008). Symbiodiniaceae species have different sensitivity to thermal stress (Rowan, 2004; Tchernov et al., 2004; van Oppen and Lough, 2009). For example, Symbiodiniaceae of the genera *Brevioulum*, particularly the ITS2 type B1, is generally recognized as a thermally sensitive type, showing a significant decline of photosynthetic activity and growth at temperatures between 31 and 33°C, coupled with the production of high amounts of ROS (Grégoire et al., 2017; Hawkins and Davy, 2012; Krueger et al., 2014; McGinty et al., 2012; Robison and Warner, 2006). Whereas Symbiodiniaceae type A1 (genera *Symbiodinium*) can maintain an elevated photosynthetic efficiency up to 32°C while its growth rate is reduced, suggesting that A1 invests energy in antioxidant protective mechanisms or to repair the photosynthetic system at the expense of algal growth (Hawkins and Davy, 2012; Karim et al., 2015; Robison and Warner, 2006). Corals' susceptibility to bleaching depends on the characteristics of their endosymbiotic algae (Abrego et al., 2008; Fitt et al., 2009; Hoadley et al., 2015) and coral hosts rely on the energy translocated from the zooxanthellae for their growth and calcification (Muscatine, 1990). Thus any change in Symbiodiniaceae growth and ROS production in relation to environmental stressors, such as sunscreen compounds, will ultimately affect corals' survival.

In order to characterize Symbiodiniaceae's response to sunscreen ingredients, two model Symbiodiniaceae species were chosen in this study: the thermo-tolerant *S. microadriaticum* (ITS2 type A1) and the thermo-sensitive *B. minutum* (ITS2 type B1). Symbiodiniaceae belonging to the genera *Symbiodinium* and *Breviolum* are also the free-

living zooxanthellae more frequently detected in the water column and sediments in Florida (Coffroth et al., 2006; Takabayashi et al., 2012), the Caribbean (Granados-Cifuentes et al., 2015; Takabayashi et al., 2012), Hawaii (Pochon et al., 2010) and Japan (Yamashita and Koike, 2013). Cultured Symbiodiniaeae do not exactly represent *in-hospite* symbionts in a natural environment. They alternate between a mastigote (motile) state in the light and a coccoid (non-motile) state in the dark (Fitt et al., 1981), while algae in symbiosis instead are coccoid cells surrounded by a series of membrane of both algal- and host-origin, all together called symbiosome (Davy et al., 2012). Also photosynthetic responses and carbon uptake mechanisms have been found to differ between cultured and *in-hospite* Symbiodiniaceae (Buxton et al., 2009). Despite these physiological and morphological differences, cultured Symbiodiniaceae are widely studied to infer stress responses and mode of actions of Symbiodiniaceae in symbiosis (Lesser, 2019; Rodríguez-Román and Iglesias-Prieto, 2005; Van Dam et al., 2015). There is wide body of research investigating the effects of thermal stress on Symbiodiniaceae and their coral hosts, however little is known about the impact of contaminants on different Symbiodiniaceae genera. Furthermore, environmental stressors such as warming, may alter organisms response to anthropogenic toxicants, ultimately lowering the threshold temperature at which the stress response is initiated (Holmstrup et al., 2010).

Here the effect of inorganic sunscreen ingredients on Symbiodiniaceae A1 and B1 under ambient (26°C) and heat-stress (32°C) conditions was investigated through a series of laboratory experiments. The specific objectives of this study were to examine the toxicity of different hydrophobic and hydrophilic TiO_2 nanoparticles commonly used in sunscreen products and the oil phase alone on cultured Symbiodiniaceae growth rate, maximum photosynthetic efficiency (Fv/Fm) and ROS production, under ambient and heat stress conditions. This work also investigated whether the different susceptibility to thermal stress of the tested Symbiodiniaceae species influenced the symbiont response, and consequently the host-coral response, to inorganic sunscreen exposure. Finally, the toxicity of the oil phase alone was determined by analysing B1 growth inhibition to increasing oil concentrations. In this chapter was investigated the hypothesis that $nTiO_2$ UV filters and oil phase ingredients lead to reduced growth and photosynthetic activity in coral symbiotic algae, likely driven by an increase of intracellular ROS. Findings from this study are the first step to evaluate both the toxicity of inorganic sunscreen products towards reef-building corals and the contribution of the oil phase into the toxicity of sunscreen products.

2.2 Material and Methods

2.2.1 $nTiO_2$ and sunscreen oil phase ingredients

$nTiO_2$ tested here are representative of sunscreen nanoparticles and were provided by the Centre Européen de Recherche et d'Enseignement des Géosciences de l'Environnement (CEREGE) in Aix-en-Provence, France (Table 2.1; nanoparticles characterization is presented in Appendix A).

Hydrophobic $nTiO_2$ (T-S, T-2000, T-Lite) were dispersed in an oil phase to mimic commercially available sunscreen formulations. The oil phase consists in a mixture of emollient ingredients, Cetiol® LC (INCI: Coco-Caprylate/Caprate. BASF, Germany) and Tegosoft® P (INCI: Isopropyl Palmitate. Evonik Goldschmidt GmbH, Germany), and an emulsifier, Easynov™ (INCI: Octyldodecanol & Octyldodecyl Xyloside & PEG-30 Dipolyhydroxystearate. SEPPIC, France). Hydrophobic $nTiO_2$-oil dispersions at 1 and 10 mgL^{-1} concentrations were made freshly before each experiment and stirred overnight to avoid nanoparticles settlement due to storage.

The hydrophilic $nTiO_2$ T-Avo was suspended in Milli-Q water at 1 mgL^{-1} concentration and then sonicated for 25 minutes twice, with ~10 seconds manual shaking in between, in a bath sonicator (35 kHz frequency, Fisherbrand FB 11010, Germany) following the protocol of D'Agata et al. (2014) and Jensen (2014).

Table 2.1 - $nTiO_2$ characteristics provided by the suppliers.

Name	ID	Crystal phase	Size	Coatings	Supplier
Eusolex® T-S	T-S	Rutile	20 nm	Alumina, Stearic acid	Merck, France
Eusolex® T-2000	T-2000	Rutile	10-15 nm	Alumina, Simethicone	Merck, France
T-Lite™ SF	T-Lite	Rutile	14-16 nm	Alumina, Dimethicone	BASF, Germany
Eusolex® T-Avo	T-Avo	Rutile	20 nm	Silica	Merck, France

2.2.2 $nTiO_2$ quantification

The actual concentrations of $nTiO_2$ in the water column was assessed by inductively coupled plasma mass spectrometry (ICP-MS) at different time points (0, 48, 96 hours) in a single experimental flask per treatment. Water samples (1 mL) were digested in a mixture of 500 µL hydrofluoric acid (HF, 40% analytical reagent grade, Fisher) and 1 mL

nitric acid (HNO_3, concentrated trace analysis grade, Fisher) in a microwave (CEM MARS, Buckingham, UK). The temperature program involved a 15 min temperature increase to 210 °C, followed by a hold time at this temperature for 45 min. After the digestion, the extracted solutions were diluted in 15 mL saturated H_3BO_3 (400 mg powder dissolved in 15 mL HNO_3 5%). The extracted, diluted and filtered sample solutions were analysed for titanium concentrations by ICP-MS.

2.2.3 Symbiodiniaceae cultures

Symbiodiniaceae used in the experiments were obtained from the National Center for Marine Algae and Microbiota (NCMA, Bigelow Laboratory for Ocean Sciences, Maine, United States). Symbiodiniaceae species belonging to *Symbiodinium microadriaticum* (CCMP 2464 formerly known as Clade A, ITS2 phylotype A1) and *Breviolum minutum* (CCMP 3450, ITS2 phylotype B1 formerly known as *Symbiodinium pseudominutum*) were grown as unialgal cultures in natural filtered seawater enriched with silica-free f/2 culture medium (salinity ~ 36, pH 8.1) (Guillard, 1975). They were maintained in a temperature-controlled incubator under a photon flux rate of ~ 90 µmol photons m^{-2} s^{-1} (LI-250A, LI-COR, USA) on a light:dark cycle of 12 h:12 h at 26°C. The stock culture medium was refreshed monthly.

2.2.4 Experimental setup

A series of consecutive experiments were conducted to assess the toxicity of $nTiO_2$-oil and -water dispersions on both Symbiodiniaceae species and the toxicity of the oil phase alone on Symbiodiniaceae B1 at both ambient (26°C) and heat stress (32°C) conditions. Fourteen days prior each experiment, Symbiodiniaceae were subcultured in 2.5 L of fresh sterile medium standardized to $1x10^6$ cells mL^{-1} to ensure log-phase growth.

Experiments were conducted in 125 mL borosilicate flasks, 3 replicates per treatment were incubated for 96 hours in a shaker incubator (Multitron-Pro, Infors HT, Switzerland) set at 130rpm to reduce the settling of algae and nanoparticles by mixing the medium, 12:12 light:dark cycle (~100 µmol photons m^{-2} s^{-1}, LI-250A light meter (LI-COR, USA)) at either 26 or 32°C. Flasks were placed randomly into the incubator to avoid any potential lighting differences. Samples were collected every 24 hours at the same time of the day to eliminate any possible variation due to the natural diurnal cell cycle. All glassware was acid washed (5% HNO_3), rinsed with MilliQ water and autoclaved before use.

Impact of $nTiO_2$-oil and -water dispersions experiments

Hydrophobic $nTiO_2$ were tested on both Symbiodiniaceae A1 and B1, the hydrophilic $nTiO_2$ was tested on Symbiodiniaceae B1 only due to the limited space capacity of the experimental incubator.

Symbiodiniaceae B1 was chosen as representative of the Symbiodiniaceae genera for the T-Avo and oil-phase alone toxicity tests among the two available Symbiodiniaceae species because it is classified as a sensitive type (McGinty et al., 2012). Additionally, it is commonly associated with the sea anemone *Exaiptasia pallida* (Thornhill et al., 2013), the model species used in the toxicity study presented in Chapter 4 of this thesis.

The selected concentrations of $nTiO_2$-oil or -water working solutions (described below) were injected in 50 mL of the exponentially growing culture medium (three replicates per treatment). In the control treatments both $nTiO_2$ and oil were absent. $nTiO_2$ and oil concentration treatments tested in the experiments are presented in Table 2.2.

Hydrophobic $nTiO_2$: For each $nTiO_2$ type, the tested concentrations were 0.1 and 1 mgL^{-1}. To distinguish between the effects due to $nTiO_2$ and the oil phase, two 1 mgL^{-1} treatments were carried out: 1 mgL^{-1} from 1 gL^{-1} $nTiO_2$-oil dispersion and 1 mgL^{-1} from a 10 gL^{-1} $nTiO_2$-oil dispersion, in order to maintain the same nanoparticle concentration but varying the oil phase quantity. Additional oil was then added to each NP-treated algae to reach a 3:1 oil:NPs ratio to mimic common commercial sunscreen formulations (Dr Jerome Labille, personal communication). Oil controls were treated with the two oil concentrations of the NP-treated algae (0.3 and 3 mgL^{-1}) without any $nTiO_2$ (No NP).

Hydrophilic $nTiO_2$: 0.1, 1 and 10 mgL^{-1} concentrations were tested.

The concentration of 0.1 mgL^{-1} simulates the estimated quantity of $nTiO_2$ released in a touristic water body (Chapter 1, Section 1.2.5), while 1 mgL^{-1} represents the quantity of $nTiO_2$ in raw sewage that could potentially be released in coral reef areas if the wastewater treatment plants do not work efficiently (Kiser et al., 2009; Westerhoff et al., 2011). The concentration of 10 mgL^{-1} is very high and presumably may never be measured in a natural environment, however it elucidates the processes of the possible $nTiO_2$ toxicity towards Symbiodiniaceae (Jovanović and Guzmán, 2014).

Table 2.2 - $nTiO_2$ and oil concentration treatments tested in Symbiodiniaceae A1 and B1 experiments.

A1 **$nTiO_2$ type**	**No NP**			**T-S**			**T-Lite**			**T-2000**		
$nTiO_2$ concentration (mgL^{-1})	0			0.1	1	1	0.1	1	1	0.1	1	1
Oil concentration (mgL^{-1})	0	0.3	3	0.3	0.3	3	0.3	0.3	3	0.3	0.3	3

B1 **$nTiO_2$ type**	**No NP**			**T-S**			**T-Lite**			**T-2000**			**T-Avo**		
$nTiO_2$ concentration (mgL^{-1})	0			0.1	1	1	0.1	1	1	0.1	1	1	0.1	1	10
Oil concentration (mgL^{-1})	0	0.3	3	0.3	0.3	3	0.3	0.3	3	0.3	0.3	3	0	0	0

Oil phase growth inhibition test

No data exist regarding the actual environmental concentration of the sunscreen oil components in coastal marine waters. Therefore 8 concentrations ranging between 0 and 25 mgL^{-1} were selected to match the concentrations tested in the previous experiments and to cover the whole spectrum from realistic environmental values (Gondikas et al., 2017) to extreme values (25 mgL^{-1}) that most likely will never be present in the marine environment but presumably induce adverse effects in the tested algae. The concentrations of oil-phase inhibiting algal growth by 10, 20, 50 and 90% (EC_{10}, EC_{20}, EC_{50} and EC_{90} respectively) were calculated.

2.2.5 Growth rate determination

Growth rates were measured by changes in chlorophyll content over time, quantified using a fluorometer (Trilogy®, Turner Design) after extraction in 4 mL of pure acetone for 48h in the dark (Patsiou et al., 2019). Cell densities were determined by converting chlorophyll values to algae numbers using a standard curve based on cell counts on the algae stock culture (calibration curves are presented in Appendix A) (Karim et al., 2015). A volume of 0.1 mL of 1.5 mg mL^{-1} locust bean gum (Sigma–Aldrich, UK) was added to the extraction protocol to promote the nanoparticles settlement in the algal samples and eliminate any interference during the readings (Kalman et al., 2015).

Daily growth rates (μ, day^{-1}) were calculated from cell densities using Eq 1.

$$\mu = \ln (N2/N1) / (t2 - t1) \qquad [Eq. 1]$$

where N_1 and N_2 are algae number at time 1 (t_1) and time 2 (t_2), respectively.

2.2.6 Maximum quantum yield of PSII fluorescence measurements

The maximum quantum yield of PSII, Fv/Fm, reveals the efficiency of the photosynthetic energy conversion in PSII and is widely used to investigate photochemical performance of photosynthetic organisms under stress (Baker, 2008; Ralph et al., 2007). At each sampling time, maximum photosynthetic yield of photosystem II (PSII), Fv/Fm = Fm – F_0/Fm, was measured in 3 mL of Symbiodiniaceae cell suspension with a Phyto-PAM chlorophyll fluorometer (Walz, Germany). Samples were quasi dark-acclimated for ~ 20 minutes before the initial fluorescence (F_0) was measured by applying a weak pulse-modulated measuring light. The maximum fluorescence (Fm) was then determined by applying a 0.8s saturation light pulse as described previously in both Symbiodiniaceae experiments and algal toxicity tests (Deng et al., 2017; Lesser, 2019; Marchello et al., 2018). Phyto-PAM instrument generates an array of LEDs covering four spectral colours: blue (470 nm), green (520 nm), light red (645 nm) and dark red (665 nm). The first wavelength (470 nm) is optimized for measuring active fluorescence in diatoms and dinoflagellates (Nicklisch and Köhler, 2001), thus only the 470 nm LED data were analysed here.

2.2.7 Quantification of *in vivo* ROS production

Measure of *in vivo* ROS production provide information for the potential levels of oxidative stress in Symbiodiniaceae cells (Lesser, 2019). *In vivo* intracellular ROS production was evaluated by 2',7'-dichlorodihydrofluorescein diacetate (H_2DCFDA) (Molecular Probes, Invitrogen), an indicator for overall ROS, (superoxide (O_2^-), singlet oxygen ($^1O_2$), hydrogen peroxide (H_2O_2), and hydroxyl radical ($OH^\bullet$). The probe is membrane permeable; it diffuses in the cell where it is hydrolysed by intracellular esterases in a polar molecule (H_2DCF) that becomes trapped and it is oxidised in the fluorescent compound dichlorofluorescein (DFC) by H_2O_2 and hydroxyl radicals (Gomes et al. 2005).

Every 24h, 1 mL of sampled algae were pelleted by centrifugation, washed twice with the culture medium and then re-suspended in the culture medium to remove nTiO_2 and oil from the samples to avoid any possible interference in the fluorescence measurements and measure just the intracellular ROS produced (Gunawan et al. 2013; Wang et al. 2016). Fluorescence intensity was measured in 96 wells black plates (to prevent autofluorescence) using a SpectraMax® M5 microplate reader with 488-525 nm

excitation-emission, after 1 hour incubation in the dark with 15 µM H_2DCFDA in each well. Because fluorescence intensity is proportional to the abundance of intracellular ROS species, thus it depends on the cell density of the measured sample, fluorescence values were corrected for the numbers of algae in each sample (derived from the chlorophyll content taken at the same time) to account for the possible differences in growth rate between treatments.

2.2.8 Statistical analyses

Each Symbiodiniaceae type was tested individually. All analyses were carried out in R (v. 3.4.1; R Core Team, 2017) with the packages 'lmerTest' (v. 3.1.0), 'car' (v. 3.0.2), 'multcomp' (v. 1.4.8), 'AICcmodavg' (v. 2.2.1) and 'drc' (v. 3.0.1).

Generalized linear model (GLM) was used to investigate 96h-growth rate whereas generalized linear mixed models (GLMM) with repeated measures over time were applied to assess the effects on Fv/Fm and ROS production. The explanatory variables tested were: nTiO_2 type (T-S, T-Lite, T-2000, T-Avo), nTiO_2 concentration (0.1, 1 and 10 mgL^{-1}), temperature (26°C and 32°C) and oil as a continuous factor, in GLMM the time of sampling is a random factor. The models (combination of factors) that best explained each endpoint were selected by backward elimination of insignificant response parameters based on the Akaike Information Criterion corrected for small sample size (AICc) (Burnham and Anderson, 2002). In the result section only the selected models are referred to.

The 'drc' package was used to model the concentration-response relationship between algal growth inhibition (in relation to the control) and oil phase concentrations and to calculate the concentrations that induced 10, 20, 50 and 90% growth inhibition (EC_{10}, EC_{20}, EC_{50} and EC_{90}, respectively) for each tested temperature.

An analysis of deviance table was then computed using the *Anova* function of the 'car' package on the selected models and on the oil phase growth inhibition test data to determine the significance of the model's factors.

Post-hoc Tukey HSD tests were then performed to assess the significant differences within the categories of the explanatory variables resulting significant from the best explanatory models (function *glht* of the 'multcomp' package (version 1.4-8) GLM and GLMM models).

2.3 Results

Experiments demonstrated that sunscreen oil phase, temperature and the simultaneous exposure of oil and temperature are the main factors ($p \leq 0.001$) that affected growth, photochemistry and ROS production in *S. microadriaticum* (ITS2 type A1) and *B. pseudominutum* (ITS2 type B1). The type of $nTiO_2$ tested (NPtype) and nanoparticle concentrations (NPconc) were often not significant factors in determining the observed toxicity.

0.1 mgL^{-1} of all hydrophobic NP types (T-S, T-Lite, T-2000) dispersed in 0.3 mgL^{-1} oil phase and the 0.3 mgL^{-1} oil control treatment are referred as the low oil (LO) treatments. Correspondingly, all the 3 mgL^{-1} oil treatments, with and without dispersed $nTiO_2$, are the high oil (HO) treatments.

2.3.1 Quantification of $nTiO_2$ in the water

Hydrophobic $nTiO_2$ tended to remain in the oil phase floating on the water surface, just small quantities of the nominal $nTiO_2$ present in the oil dispersions lose their lipophilic coating and are released into the water column in a time-dependent manner (Figure 2.2). At the end of the experiment, a small amount of nanoparticles (~17%) was dispersed into the water from the HO dispersions compared to the LO treatments. An overall larger amount of T-2000 nanoparticles were measured in the water column compared to T-S and T-Lite. At 96 hours T-2000 quantities were very close to the nominal $nTiO_2$ concentrations: 0.099 mgL^{-1} and 0.61 ± 0.03 mgL^{-1} in the 0.1 and 1 mgL^{-1} treatments, respectively. In contrast, measured $nTiO_2$ quantities in T-S and T-Lite LO treatments were 58.7% and 49.9% the nominal $nTiO_2$ concentration of the respective treatments, and 33.1% and 14.8% in the HO treatments. Quantified concentrations of $nTiO_2$ in the experimental suspensions are presented in Table 2.3 and Figure 2.1.

$nTiO_2$ shape, particle size, chemical composition characterization by scanning electron microscope coupled with EDX, thermogravimetric analysis, and XRD, performed by Vincent Bartholomei (CEA LITEN, Grenoble) and T-Lite characterization by transmission electron microscopy coupled with ICP-AES by Dr Jerome Labille (CEREGE, Aix en Provence) are presented in Appendix A.

Table 2.3 - Quantified titanium concentration (μgL^{-1}) in T-S, T-Lite and T-2000 experimental suspensions over 96 hours.

$nTiO_2$	Treatments		0h	48h	96h
T-S	0.1 mgL^{-1}	Low Oil	9.05	10.64	64.43
	1 mgL^{-1}	Low Oil	10.01	67.46	529.93
	1 mgL^{-1}	High Oil	9.27	26.52	331.18
T-Lite	0.1 mgL^{-1}	Low Oil	8.30	22.28	53.99
	1 mgL^{-1}	Low Oil	6.58	82.11	458.67
	1 mgL^{-1}	High Oil	18.59	135.29	147.77
T-2000	0.1 mgL^{-1}	Low Oil	12.69	12.15	99.88
	1 mgL^{-1}	Low Oil	35.87	18.59	613.88
	1 mgL^{-1}	High Oil	5.98	29.66	609.19

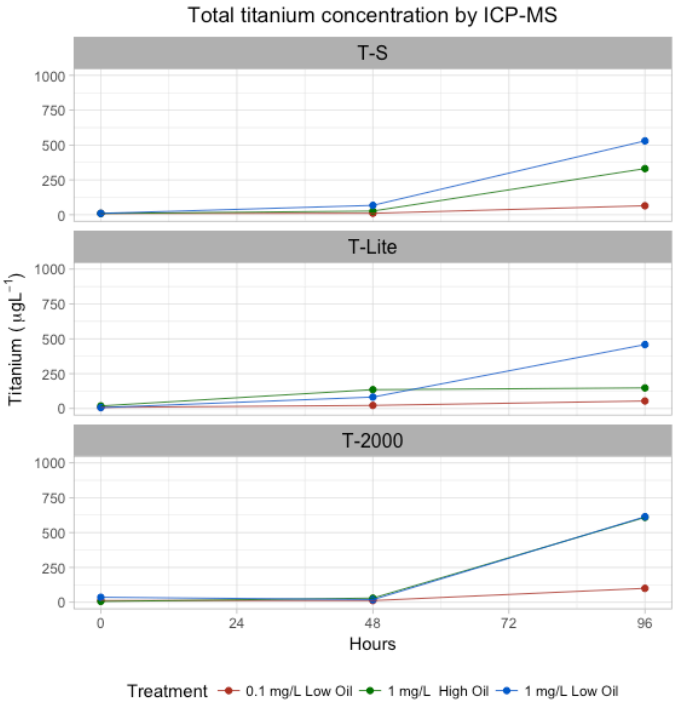

Figure 2.1 - Quantified titanium concentration (μgL^{-1}) in the different T-S, T-Lite and T-2000 experimental solutions over 96 hours.

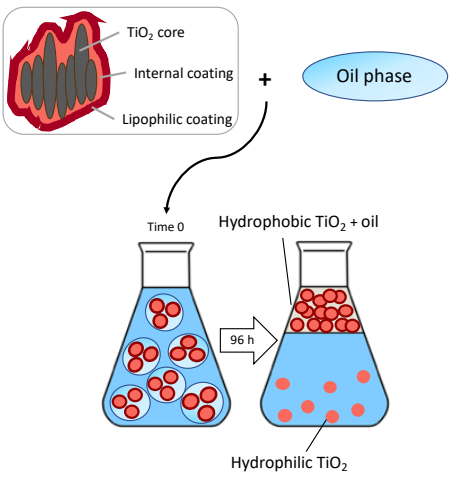

Figure 2.2 - Graphical representation of $nTiO_2$ and the oil phase behaviour in the experimental medium.

2.3.2 Symbiodiniaceae growth characterization

Symbiodiniaceae A1 and B1 exhibited the same trend in growth when exposed to the different treatments, but the specific growth rate values were different (Figure 2.3, Table 2.4). Both Symbiodiniaceae phylotypes exhibit significantly higher growth rates at 26°C compared to the correspondent growth at elevated temperature ($p_{temperature} < 0.001$; Table 2.5); increasing temperature from 26 to 32°C caused a growth decline in the control by 64% and 74% in A1 and B1 algae, respectively. Furthermore, in each Symbiodiniaceae ITS2 type, low oil treatments had comparable values regardless of the nanoparticle types and concentrations (No NP LO = NP 0.1 mg L^{-1} LO = NP 1 mg L^{-1} LO), but high oil exposure significantly decreased growth at both temperatures ($p_{oil} < 0.001$; Table 2.5). Symbiodiniaceae were highly susceptible to HO treatments as cultures exposed to both 3 mgL^{-1} oil control and 1 mgL^{-1} $nTiO_2$ dispersed in 3 mgL^{-1} of oil phase at 32°C showed negative growth indicating decline in chlorophyll content compared with the initial set-up. These trends were confirmed by GLM model selection as shown in Table 2.5: oil, temperature and their interaction were the most significant factors in both ITS2 types ($p < 0.001$).

The type of $nTiO_2$ resulted a significant factor in A1 experiment ($p_{NPtype} = 0.004$), driven by T-Lite that showed an overall higher growth than the other nanoparticles tested (results of Post-hoc Tukey HSD test are reported in Table 2.6). On the contrary, B1 T-Lite treatments at 26°C had a lower growth than the correspondent T-S and T-2000 treatments, and $nTiO_2$ type was significant in interaction with temperature ($p_{NPtype:temperature} < 0.001$; Table 2.5). Interestingly, Symbiodiniaceae B1 exposed to T-Avo 10 mgL^{-1} (the treatment with the highest NP concentration without oil) exhibited the lowest growth rate among the no-oil treatments at 32°C ($\mu = 0.008 \pm 0.05$ d^{-1}), but HO treatments maintained always a lower, negative, growth rate ($\mu = \sim -0.2 \pm 0.01$ d^{-1}).

Overall, the tolerant Symbiodiniaceae ITS2 type A1 exposed to the different $nTiO_2$-oil dispersions exhibited a smaller decrease in growth at ambient temperature compared to B1. However, when simultaneously exposed to elevated temperature, A1 had a more pronounced growth decline than B1, reaching values between -0.35 and -0.67 μ d^{-1} in the HO treatments while B1 stands at ~ -0.2 μ d^{-1}.

Table 2.4 - Growth (μ day^{-1}) for Symbiodiniaceae A1 and B1 under the different treatments (mean ± SEM, n=3).

		A1		B1	
		26°C	**32°C**	**26°C**	**32°C**
Control		0.32 ± 0.02	0.12 ± 0.03	0.38 ± 0.02	0.10 ± 0.02
Low Oil		0.38 ± 0.02	-0.03 ± 0.02	0.35 ± 0.04	0.11 ± 0.05
HighOil		0.14 ± 0.05	-0.35 ± 0.03	0.04 ± 0.02	-0.21 ± 0.03
T-S	0.1 mgL^{-1} Low Oil	0.37 ± 0.04	0.14 ± 0.08	0.38 ± 0.01	0.06 ± 0.03
	1 mgL^{-1} Low Oil	0.38 ± 0.01	0.05 ± 0.03	0.30 ± 0.01	0.09 ± 0.02
	1 mgL^{-1} High Oil	0.10 ± 0.06	-0.56 ± 0.04	0.13 ± 0.03	-0.22 ± 0.02
T-Lite	0.1 mgL^{-1} Low Oil	0.45 ± 0.09	0.08 ± 0.03	0.34 ± 0.05	0.12 ± 0.01
	1 mgL^{-1} Low Oil	0.42 ± 0.05	0.06 ± 0.01	0.26 ± 0.04	0.16 ± 0.02
	1 mgL^{-1} High Oil	0.23 ± 0.03	-0.36 ± 0.04	0.06 ± 0.01	-0.21 ± 0.02
T-2000	0.1 mgL^{-1} Low Oil	0.32 ± 0.02	0.05 ± 0.05	0.32 ± 0.01	0.11 ± 0.02
	1 mgL^{-1} Low Oil	0.35 ± 0.01	-0.03 ± 0.01	0.31 ± 0.03	0.12 ± 0.02
	1 mgL^{-1} High Oil	0.16 ± 0.06	-0.67 ± 0.15	0.15 ± 0.01	-0.18 ± 0.02
T-Avo	0.1 mgL^{-1}			0.28 ± 0.002	0.06 ± 0.06
	1 mgL^{-1}			0.34 ± 0.02	0.03 ± 0.03
	10 mgL^{-1}			0.33 ± 0.01	0.008 ± 0.005

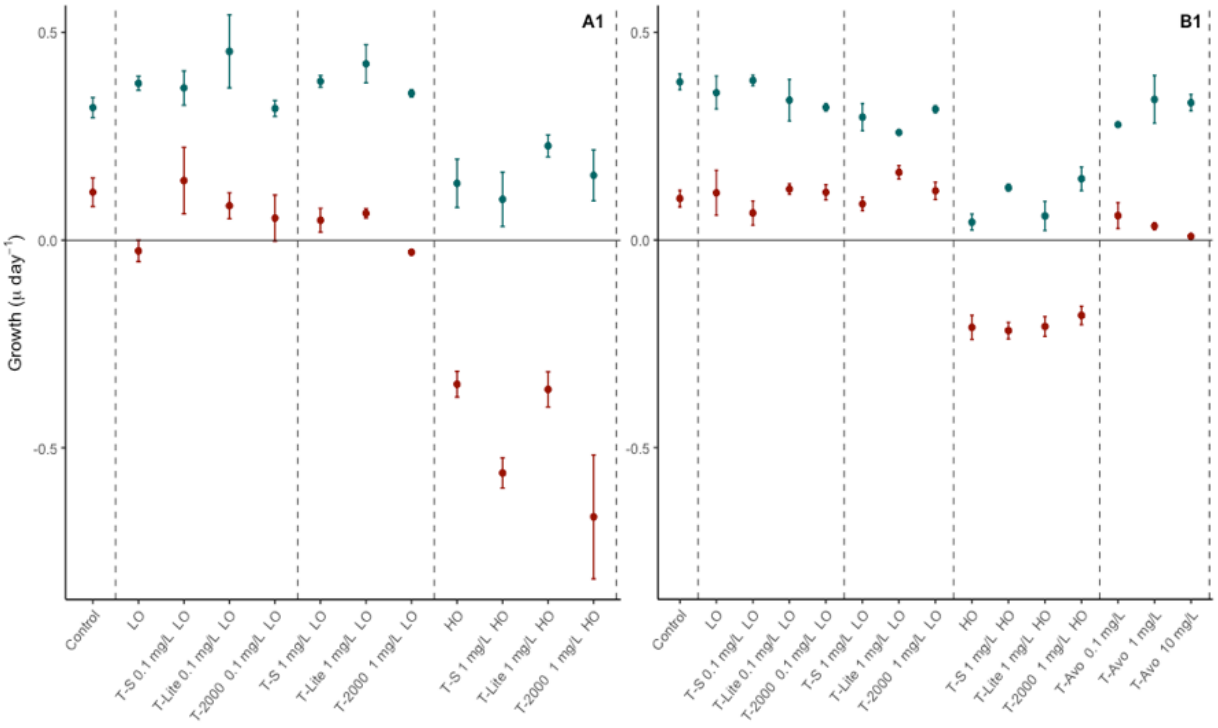

Figure 2.3 - Growth rate (μ, day^{-1}) of Symbiodiniaceae A1 (left) and B1 (right) exposed for 96h to the different $nTiO_2$ oil- and water- dispersions either under ambient (green) and heat-stress (red) conditions. Data (n=3) are expressed as mean ± standard error of the mean (SEM).

2.3.3 Maximum photochemical efficiency of PSII, Fv/Fm

Changes in maximum photochemical efficiencies of Symbiodiniaceae ITS2 types A1 and B1 in responses to $nTiO_2$ oil- and water- dispersions at ambient and elevated temperature are illustrated in Figure 2.4, and GLMM results are presented in Table 2.5. For both algal types, oil, temperature and their interactions are the main explanatory variables detected from the best-fitted models ($p < 0.001$; Table 2.5). In A1 experiment also $nTiO_2$ concentration is a significant variable ($p_{NPconc} < 0.001$; Table 2.5), with both concentrations tested resulting significantly different to control values ($p < 0.001$; Table 2.6). At 26°C, algal cells responded to the different treatments by slightly increasing their Fv/Fm over time, only B1 algae exposed to the HO treatments exhibited a 3.7% Fv/Fm decline at 96h compared to control. Elevated temperature caused a Fv/Fm increase similar to the increase observed in treated algae at ambient temperature, however a decline in Fv/Fm values was detected in the HO treatments starting from 48h. Although the modest Fv/Fm changes observed are not an evidence of impairment of photosynthetic functions, at the end of the experiment A1 algae exposed to the different treatments had an overall lower Fv/Fm compared to control algae, with the highest decline (5.6%) observed in the HO treatments. Symbiodiniaceae B1 showed a similar trend with the high oil treatments causing a 11.5% Fv/Fm decrease, while T-Avo treatments maintain Fv/Fm values comparable to control algae even at the highest $nTiO_2$ concentration of 10 mgL^{-1}.

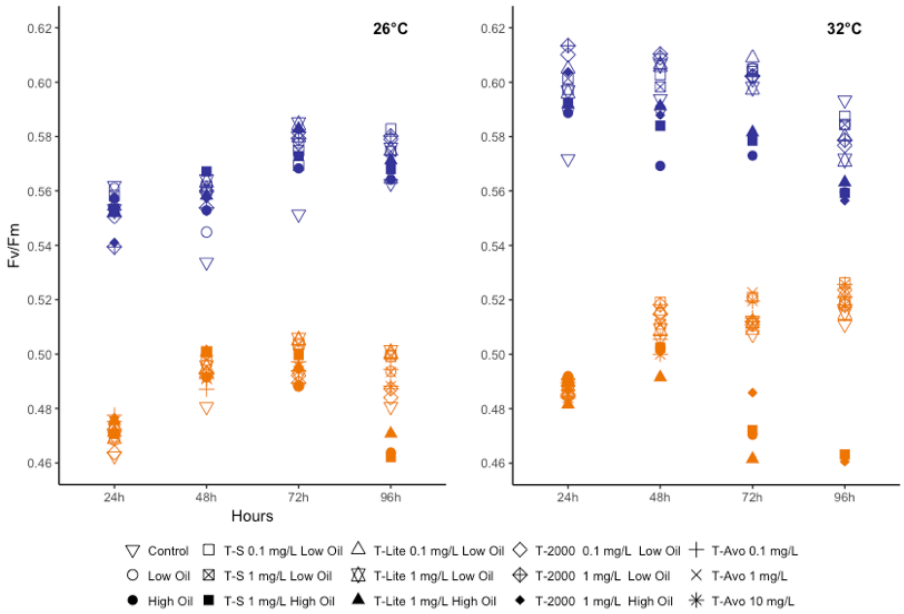

Figure 2.4 - Maximum quantum yield of PSII (Fv/Fm) of Symbiodiniaceae A1 (blue) and B1 (orange) under the different treatments at 26°C (left) and 32°C (right) (n=3, error bars not displayed to keep the graphs clearer).

2.3.4 Symbiodiniaceae *in vivo* ROS production

In-vivo ROS production in untreated algae and T-Avo treatments are presented in Figure 2.5 and 2.6. Symbiodiniaceae exposed to the different $nTiO_2$ and oil phase treatments are presented in Figure 2.7 and show an overall increase in ROS production over time and with heat stress. For both algal types, oil, temp, NPtype and their interaction had significant effects ($p < 0.001$) on ROS production (Table 2.5). At ambient temperature, Symbiodiniaceae A1 experienced the greatest ROS increase (3-6 folds) in the first 24 hours, then ROS decreased in all treatments except T-S and T-2000 HO and HO control, where a second ROS peak is observed at 96 hours. T-Lite HO at 96h exhibited ROS values lower than the LO treatments, in accordance with the higher growth rate among the HO treatments shown in Figure 2.3. At 32°C, all high oil treatments displayed significantly greater ROS values than the LO treatments, particularly the last 2 days of the experiment when ROS increased between 15 and 45 times. Overall, Symbiodiniaceae B1 generated more ROS than the corresponding A1 values, but contrary to A1, ROS produced in the first 24 hours in B1 are lower than the consecutive timepoints. At 26°C, T-Avo 10 mgL^{-1} at 24 hours caused the greatest increase in ROS (~ 7 times control values), at 48 hours showed a value comparable to the other oil treatments while in the last timepoints ROS decreased to the lowest measured values along with T-Avo 0.1 and 1 mgL^{-1}. All oil treatments were similar between each other at 26 °C, with ROS fold increase ranging from 1.4 to 8. B1 algae incubated at 32°C displayed a larger ROS increase compared to 26°C and the amount of ROS generated raise with time. At 96 hours of the elevated temperature experiment, B1 exposed to 0.3 mgL^{-1} oil phase accumulated ROS levels ~ 20 times higher than the normal metabolic production; in the HO treatments ROS levels further increase up to 50 times the control values. Interestingly, ROS generated by A1 algae exposed to the different $nTiO_2$-oil dispersions at 26°C are similar to ROS produced by control algae at warming conditions. In contrast all B1 treatments at ambient temperature, except T-Avo 0.1 and 1 mgL^{-1}, showed a larger ROS compared to ROS produced by untreated algae at 32°C.

Although for Symbiodiniaceae A1 the type of $nTiO_2$ was identified as significant variable from the model, post-hoc Tukey HSD test did not detect any significant difference among all pairwise comparisons (Table 2.6). For B1 instead the NPtype significance derives from the nanoparticle T-Avo, that resulted significantly different to all the other tested nanoparticles in the Tukey HSD test post-hoc analysis ($p < 0.001$; Table 2.6).

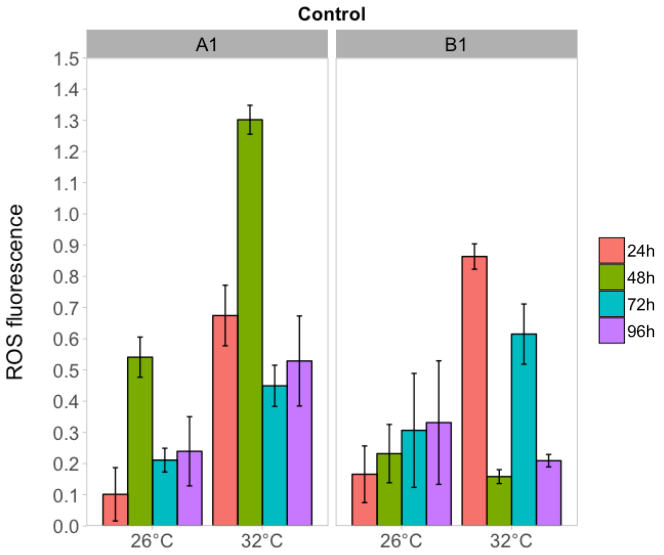

Figure 2.5 - Reactive oxygen species (ROS) production over the 96h experiment by Symbiodiniaceae A1 and B1 control algae at both ambient (26°C) and elevated (32°C) temperature. Results (mean ± SEM, n=3) are presented as fluorescence units of H_2DCFDA probe labelling ROS fold increase.

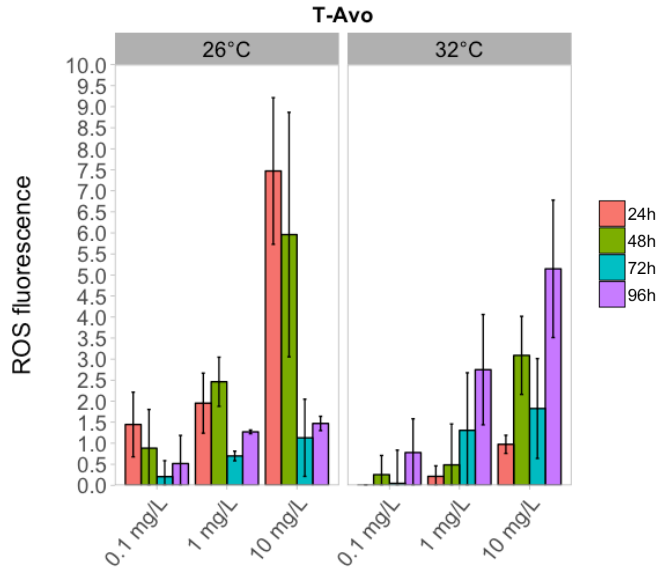

Figure 2.6 - Reactive oxygen species (ROS) production over the 96h experiment by Symbiodiniaceae B1 exposed to the T-Avo nanoparticles at both temperatures. Results (mean ± SEM, n=3) are presented as fluorescence units of H_2DCFDA probe labelling ROS fold increase respect time-matching control algae at the respective temperatures.

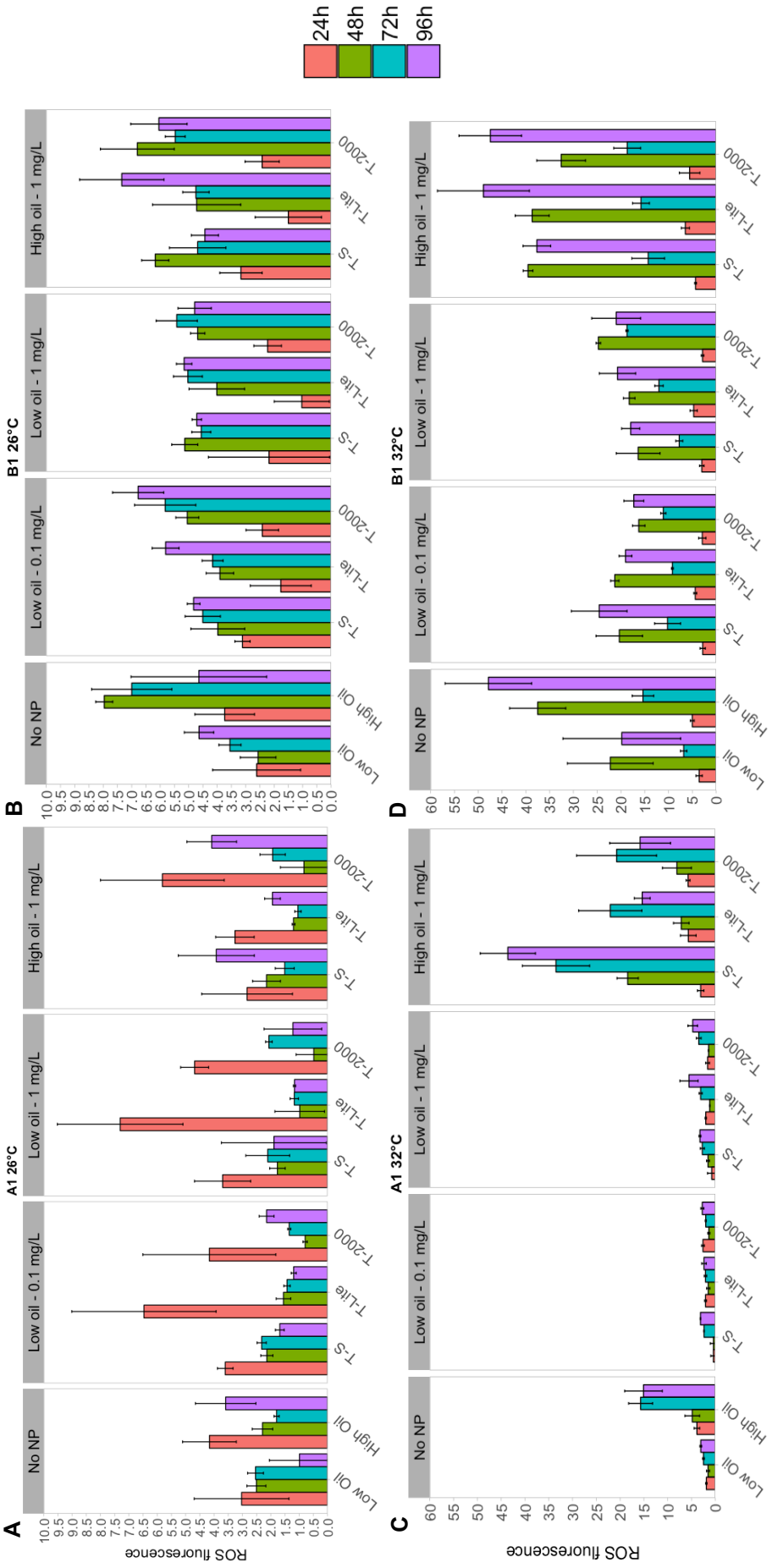

Figure 2.7 - Reactive oxygen species (ROS) production over time by Symbiodiniaceae A1 and B1 at 26°C (**A**, **B**), Symbiodiniaceae A1 and B1 at 32°C (**C**, **D**). Results are presented as fluorescence units of H_2DCFDA probe labelling ROS fold increase respect time-matching control algae at the respective temperatures (mean ± SEM, n = 3).

Table 2.5 - ANOVA test results from the selected GLM (growth rates) and GLMM (Fv/Fm, ROS) models and for the oil growth inhibition experiment.

Type	Model	Predictor	Chisq	Df	p-value
Growth rates (μ)					
A1	oil*temperature + NPtype				
		oil	237.16	1	**<0.001**
		temperature	334.53	1	**<0.001**
		oil:temperature	43.30	1	**<0.001**
		NPtype	13.15	3	**0.004**
B1	NPconc*oil*temperature + NPtype*temperature				
		oil	498.32	1	**<0.001**
		temperature	694.03	1	**<0.001**
		NPconc	0.16	2	0.9
		NPtype	6.32	3	0.09
		NPconc:oil	4.35	2	0.11
		NPconc:temperature	2.36	2	0.3
		oil:temperature	11.45	1	**<0.001**
		temperature:NPtype	22.63	3	**<0.001**
		NPconc:oil:temperature	14.05	2	**<0.001**
Maximum photochemical efficiency (Fv/Fm)					
A1	oil*temperature + NPconc				
		oil	17.46	1	**<0.001**
		temperature	264.21	1	**<0.001**
		oil:temperature	26.70	1	**<0.001**
		NPconc	19.59	2	**<0.001**
B1	oil*temperature				
		oil	67.69	1	**<0.001**
		temperature	121.91	1	**<0.001**
		oil:temperature	67.73	1	**<0.001**
ROS					
A1	oil*temperature*NPtype				
		oil	133.75	1	**<0.001**
		temperature	170.15	1	**<0.001**
		NPtype	12.29	3	**0.006**
		NPtype:oil	28.37	3	**<0.001**
		NPtype:temperature	18.41	3	**<0.001**
		oil:temperature	191.09	1	**<0.001**
		NPtype:oil:temperature	47.43	3	**<0.001**
B1	oil*temperature + NPtype				
		oil	62.22	1	**<0.001**
		temperature	384.12	1	**<0.001**
		NPtype	34.88	4	**<0.001**
		oil:temperature	151.96	1	**<0.001**
Oil induced growth inhibition					
B1	oil*temperature				
		oil	56.44	1	**<0.001**
		temperature	326.39	1	**<0.001**
		oil*temperature	2.32	1	**0.04**

NPtype = $nTiO_2$ type
NPconc = $nTiO_2$ concentrations

Table 2.6 - Tukey HSD post-hoc test results of all pairwise comparisons among $nTiO_2$ type (NPtype) and $nTiO_2$ concentrations (NPconc) that resulted significant from the best explanatory models reported in Table 2.5. Statistically significant differences are highlighted in bold.

Pairwise Comparisons			p-value			
			Growth rates	ROS		Fv/Fm
			A1	A1	B1	A1
NPtype	No NP	T-2000	0.39	1	0.07	
		T-S	0.99	0.63	0.58	
		T-Lite	0.17	0.99	0.05	
	T-2000	T-S	0.44	0.65	0.79	
		T-Lite	**0.002**	0.99	0.99	
	T-Lite	T-S	0.15	0.74	0.71	
	T-Avo	No NP			0.08	
		T-2000			**<0.001**	
		T-S			**<0.001**	
		T-Lite			**<0.001**	
NPconc	0 mgL^{-1}	0.1 mgL^{-1}				**<0.001**
		1 mgL^{-1}				**<0.001**
	0.1 mgL^{-1}	1 mgL^{-1}				0.66

2.3.5 Inhibition of growth induced by the oil phase

Sunscreen oil phase alone, without the addition of UV-filter, caused a concentration-response inhibition of *B. pseudominutum* (B1) growth. At ambient temperature, the mixture of emulsifier and emollient ingredients used as sunscreen oil phase in all the experiments caused slight growth inhibition. It was not possible to calculate the 96h-EC_{50} as the maximum tested concentration (25 mgL^{-1}) did not cause complete growth inhibition, but only a 56.8% growth reduction (Figure 2.8). In contrast, warming significantly affects algae sensitivity to oil exposure ($p < 0.001$, Table 2.5), leading to increased oil-dependent growth inhibition by about 8 fold (Figure 2.7). Indeed at 32°C just 0.1 mgL^{-1} of sunscreen oil phase induces a 10% of algal growth inhibition (96h-EC_{10}, Table 2.7) and the calculated 96h-EC_{50} is 0.46 ± 0.08 mgL^{-1}.

Table 2.7 - Sunscreen oil phase effect concentrations for inhibition of *Symbiodinium* B1 growth rates (mgL^{-1}, mean ± SE) and associated 95% confidence intervals at 32°C.

EC_{10}	0.11 ± 0.06	$[-0.005:0.23]_{95\%}$
EC_{20}	0.19 ± 0.07	$[0.04:0.34]_{95\%}$
EC_{50}	0.46 ± 0.08	$[0.28:0.64]_{95\%}$
EC_{90}	1.88 ± 0.06	$[0.61:3.15]_{95\%}$

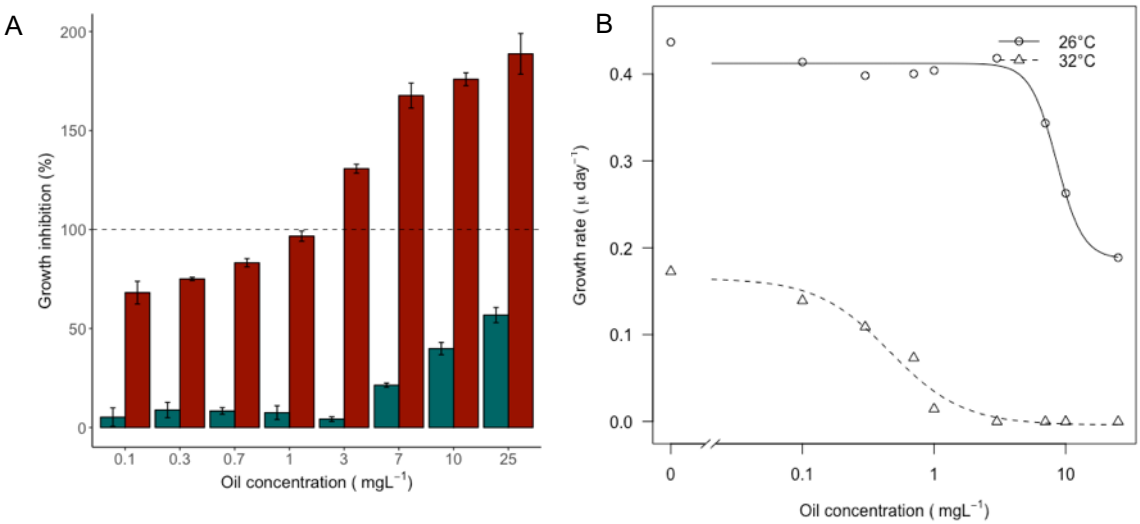

Figure 2.8 - **A**) Percentage of growth inhibition respect to control values of *B. pseudominutum* (B1) at 26°C (green) and 32°C (red) (mean ± SEM, n = 3). **B**) Growth rate concentration-response curves of *B. pseudominutum* (B1) at 26°C (circle) and 32°C (triangle).

2.4 Discussion

In recent years, the toxicity of sunscreen UV filters towards marine organisms has attracted increasing attention. Previous studies have concentrated on the assessment of individual compounds within sunscreen formulations, however, sunscreens are complex mixtures of chemicals that are released into the environment (Gondikas et al., 2017; Sánchez-Quiles and Tovar-Sánchez, 2015). Here, two species of Symbiodiniaceae, *S. microadriaticum* (A1) and *B. pseudominutum* (B1), were exposed to $nTiO_2$ UV filters and sunscreen oil phase under ambient and elevated temperature to investigate potential differences in nanoparticles toxicity, oil phase toxicity and in zooxanthellae response to inorganic sunscreen ingredients, their influence in Symbiodiniaceae thermal susceptibility and the possible toxicity interaction between sunscreen ingredients and warming.

2.4.1 Behaviour of $nTiO_2$ in culture medium

In agreement with Gondikas et al. (2017) measurements, $nTiO_2$ quantification analyses demonstrate that the effective amount of nanoparticles released into the water column from sunscreen products is lower than the quantity of UV filters in the formulation as $nTiO_2$ remain trapped into the oil phase floating on the water surface. Among the three

hydrophobic $nTiO_2$ tested, an overall higher quantity of T-2000 was measured in the water column compared to T-S and T-Lite, likely due to the amphiphilic properties (i.e. both hydrophilic and lipophilic) of T-2000 silica gel coating. Titanium core in T-S and T-Lite nanoparticles is coated with stearic acid, a natural product insoluble in water, and dimethicone respectively. Dimethicone is a silicon base polymer insoluble in both oils and water, hence the lower quantity of T-Lite measured in water at 96h.

2.4.2 Effect of sunscreen ingredients on *S. microadriaticum* (A1) and *B. pseudominutum* (B1) under ambient temperature

Growth rates integrate all the positive and negative impacts of environmental factors and is the most relevant physiological parameter to describe algal performance to stressful conditions (Gustavs et al., 2009). The calculation of algal growth rates is usually based on cell counts, however nanoparticles and oil in the experimental samples made the direct microscopical determination of algae abundance inaccurate, hence cell count was replaced by chlorophyll *a* measurement as biomass biomarker. In a natural environment intracellular chlorophyll content is influenced by abiotic parameters such as nutrient supply, light level, as well as age and size of the algal cell, hence it is not considered a reliable measurement to assess algal density (Kruskopf and Flynn, 2006). Moreover it is acknowledged that in the specific case of Symbiodiniaceae cells under thermal and/or high light stress, the reduction in chlorophyll content is often not matched by a parallel decrease in algal density (Hennige et al., 2009; Venn et al., 2006). However under laboratory conditions abiotic parameters are constant and controlled, it is also recognized that algal density based on chlorophyll extraction is commonly used in nanoparticle toxicity studies to overcome the inaccuracy issues of working with nanoparticles (Hartmann et al., 2010; Kalman et al., 2015; Li et al., 2015; Miller et al., 2012; Morelli et al., 2018; Patsiou et al., 2019; Tang et al., 2013), thus chl *a* content was valuated as a good proxy for algae number (as reported by Becker, 1994).

Symbiodiniaceae in laboratory conditions should be left undisturbed as mixing has been observed to retard algae growth (Rogers and Davis, 2006, and references therein), however growth rates in the present experiments are not affected by the gently shaking needed to reduce the settling and guarantee an even distribution of $nTiO_2$ into the experimental flasks. Growth rates measured here for untreated A1 and B1 were indeed comparable to growth rates reported previously for the same cultured Symbiodiniaceae ITS2 types. Growth values were 0.31 ± 0.02 and 0.38 ± 0.02 μ d^{-1} for Symbiodiniaceae

A1 and B1 respectively, and $\mu = 0.31$ d^{-1} and $\mu = 0.3$ d^{-1} were reported by Krämer et al. (2012) and Grégoire et al. (2017) for Symbiodiniaceae A1 and B1 grown at 25 and 27°C under 90 - 150 µmol photons m^{-2} s^{-1}.

Despite the different water behaviour of the tested $nTiO_2$ due to the nanoparticle coating type, algal response to the different $nTiO_2$ was variable but generally consistent among the treatments. In Symbiodiniaceae A1 experiments, the type of $nTiO_2$ is a significant factor in the growth rate and ROS generation models, although for ROS it was not possible to detect differences among nanoparticles with the post-hoc Tukey HSD test (Table 2.6). Differences in growth rates linked to $nTiO_2$ types likely depend on the apparent lower toxicity of T-Lite (Figure 2.3; Table 2.6). This is surprising as T-Lite dimethicone coating has been demonstrated to not efficiently prevent the generation of hydroxyl radicals by the titania core (Carlotti et al., 2009). Indeed in the first 24 hours of the A1 experiment at 26°C, T-Lite generated the highest amount of ROS among the tested $nTiO_2$ (Figure 2.5A). However ROS levels sharply declined in the following days, likely due to the activation of the algae antioxidant defences that are known to act quickly and efficiently in A1 symbionts (Krämer et al., 2012; McGinty et al., 2012); probably allowing T-Lite-exposed A1 algae to maintain an elevated growth rate.

The type of $nTiO_2$ was also a significant factor in B1 algae for ROS production and, in interaction with the oil phase and temperature, for growth rates (Table 2.5). However, in this case the differences depend on the hydrophilic nanoparticle T-Avo, which was significantly lower in toxicity than the other tested nanoparticles (Figure 2.3, Figure 2.5 and Figure 2.6; Table 2.6). T-Avo is coated with a silica layer which was demonstrated to be among the most effective agents to deactivate the titania photocatalytic behaviour (Carlotti et al., 2009). T-Avo was also the only nanoparticle treatment dispersed in water and not in the sunscreen oil phase. The lower growth of algae exposed to the combined $nTiO_2$-oil mixtures may be only partially related to the type of coating, and rather be a result of the oil exposure. Potential mode of actions are suggested below and in section 2.4.4.

At ambient temperature the HO treatments induced a decline in growth rate in both Symbiodiniaceae species (Figure 2.3). Interestingly LO treatments show a higher growth rate than HO treatments, despite both treatments induced similar ROS levels (Figure 2.7) and larger quantities of $nTiO_2$ were released into the water column in the LO treatments (Figure 2.1). Moreover, exposure to the hydrophilic $nTiO_2$ type T-Avo at concentrations up to 10 mgL^{-1}, without the addition of oil phase, did not impact algae growth. This result

is similar to that of Morelli et al. (2018), who observed no effect on the growth of the microalgae *Dunaliella tertiolecta* exposed to 0.01 – 10 mgL^{-1} $nTiO_2$. As illustrated in Table 2.8, concentrations of $nTiO_2$ (mainly having anatase or a combination of rutile and anatase as crystalline core) that induce 50% of growth inhibition in marine microalgae are heterogeneous but relatively high, ranging between 7.57 and 551.7 mgL^{-1} under visible light. Thus the observed low $nTiO_2$ toxicity in the present study is not unexpected, considering also that the crystalline structure of all four nanoparticles tested here is rutile, known to exhibit lower photocatalytic activity and toxicity than anatase (Sayes et al., 2006; Smijs and Pavel, 2011). Therefore, the oil phase is presumably a key factor responsible for the algae growth reduction observed here. Sendra et al. (2017) demonstrated that the organic sunscreen components were responsible for the majority of hydrogen peroxide (H_2O_2) generated by an inorganic sunscreen formulation under solar radiation, whilst $nTiO_2$ UV filters produced just 15% of the total measured H_2O_2. Oxidative stress induced by H_2O_2 generated by the oil phase ingredients likely caused the high levels of ROS and the severe growth reduction observed in the HO treatments here.

Table 2.8 - Toxicological characterization of $nTiO_2$ growth inhibition in marine microalgae (NOEC: No Observed Effect Concentration).

Species	Endpoint (mgL^{-1})		UVA	$nTiO_2$ crystal structure	size	Reference
Chlamydomonas reinhardtii	72h EC_{50}	2.6 551.7	✓	anatase/rutile	<100 nm	Sendra et al., 2017
Dunaliella tertiolecta	96h EC_{50}	24.10		anatase	25 nm	Manzo et al., 2015
	168h NOEC	3	✓	anatase/rutile	15–30 nm	Miller et al., 2012
Phaeodactylum tricornutum	72h EC_{50}	2 132	✓	anatase/rutile	<100 nm	Sendra et al., 2017
	96h EC_{50} 96h LOEC	203.74 20		anatase	15 nm	Wang et al., 2016
	72h EC_{50}	10.91 11.30 14.30 35.51 24.11		anatase anatase anatase anatase rutile	15 nm 25 nm 32 nm 44 μm 1 μm	Clément et al., 2013
Nitzschia closterium	96h EC_{50}	88.78 118.80 179.05		/ / /	21 nm 60 nm 400 nm	Xia et al., 2015
Karenia brevis	72h EC_{50}	10.69		anatase	5–10 nm	Li et al., 2015
Skeletonema costatum	72h EC_{50}	7.37		anatase	5–10 nm	Li et al., 2015
	168h NOEC	7		anatase/rutile	15–30 nm	Miller et al., 2012
Isochrysis galbana	168h NOEC	< 1	✓	anatase/ rutile	15–30 nm	Miller et al., 2012

2.4.3 Effects of the simultaneous exposure to sunscreen ingredients and warming

Temperatures above 32°C have been demonstrated to cause physiological stress in Symbiodiniaceae leading to negative growth and impaired photosynthetic performance (Hill and Ralph, 2006; Iglesias-Prieto et al., 1992; Jones et al., 1998; Karim et al., 2015; Lesser, 1996; Robison and Warner, 2006; Smith et al., 2005). Thermal stress disrupts the electron-transport chain in Symbiodiniaceae photosyntetic apparatus, leading to the reduction of photosynthetically derived O_2 and consequent ROS generation (Jones et al., 1998; Lesser, 2011; Smith et al., 2005; Tchernov et al., 2004). If damage is not repaired, or ROS exceed the capacity of Symbiodiniaceae antioxidant defences, ROS accumulate in the algal cell. These increases of intracellular ROS levels would cause DNA and protein damage (e.g. D1 protein in photosystem II and its repair mechanisms, thylacoid membranes and the enzyme ribulose-1,5-bisphate carboxylase/oxygenase (Rubisco), see Figure 1.1) and would ultimately undermine the algal photosynthetic functions (Lesser, 1996, 2006; Roth, 2014; Takahashi and Murata, 2008).

In this study, an apparent uncoupling of growth and photosynthetic activity was observed: exposure to sunscreen compounds and warming caused a decline in A1 and B1 growth rate that is not coupled with a reduction in Fv/Fm, which instead is maintained, in all treatments, at values not indicating a stress situation (Ragni et al., 2010; Robison and Warner, 2006; Wietheger et al., 2015). Only HO treatments caused a slight Fv/Fm decline in A1 and B1, which is however accompanied by a significant growth reduction, indicating a strong toxicity effect of the sunscreen oil phase. Fv/Fm trends observed here contrast with the reduction in photosynthetic efficiency generally observed in previous work on Symbiodiniaceae cultures under thermal stress, although Takahashi et al. (2013) measured unchanged Fv/Fm values in several types of Symbiodiniaceae with temperatures up to 33°C and Nitschke et al. (2015) observed a small but significant Fv/Fm increase in a free-living clade A at 31°C.

Regarding exposures to $nTiO_2$, published work are consistent with the Fv/Fm trends obtained here. Other microalgae, such as *Clamidomonas reinhardtii* and *Phaeodactylum tricornutum,* exhibit photosynthetic activity values similar to those presented here, or higher, under increasing $nTiO_2$ concentrations (Chen et al., 2012; Deng et al., 2017; Sendra et al., 2017a). In plants several studies have also demonstrated that moderate $nTiO_2$ concentrations enhance photosynthetic activity due to promotion of rubisco carboxilation and electron transport chain acceleration (Gao et al., 2008; Hong et al.,

2005; Hussain et al., 2019; Ze et al., 2011), sites known to be damaged in Symbiodiniaceae following heat stress. In this study, the significant increase in intracellular ROS levels in all treatments at both ambient and warming conditions following the exposure to sunscreen ingredients likely promote the algal total antioxidant capacity (Lesser, 2006). The enhanced antioxidant defences potentially protect the proteins at the site of photosynthesis from heat-induced oxidative damage. Furthermore, the relatively low quantities of $nTiO_2$ dispersed in the water column could promote rubisco and electron transport chain activity. Therefore algae are capable of maintaining functional photosyntetic activity even at 32°C, however, a severe growth decline was observed in the HO treatments.

Growth was reduced proportionally to increasing ROS levels potentially due to elevated energy requirements of the antioxidant system reducing energy available for cell proliferation. In support of this assumption, uncoupling of growth and photosynthesis was previously observed in Symbiodiniaceae, generally in thermally tolerant types (e.g. A1), under light and heat stress (Karim et al., 2015; Krämer et al., 2012; Nitschke et al., 2015; Robison and Warner, 2006). Uncoupling is suggested to be due to the relocation of metabolic energy from growth to repairing damaged PSII (D1 protein and thylakoid membranes) and antioxidant defences (Karim et al., 2015; Krämer et al., 2012). Symbiodiniaceae B1, a sensitive type, also maintained elevated photosynthetic activity when exposed to LO treatments, under both ambient and warming temperatures (Figure 2.4). McGinty et al. (2012) demonstrated that B1 was not capable of neutralising excess ROS produced at 31°C since the algae did not increase the activity of ROS scavenging enzymes catalase (CAT) and superoxide dismutase (SOD), whilst A1 activated a rapid antioxidant response to scavenge ROS and it is known to have an efficient antioxidant system (Krämer et al., 2012). Previous studies observed that $nTiO_2$ can enhance plant tolerance to temperature stresses, such as cold stress in chickpea (Mohammadi et al., 2014) and heat stress in tomato (Qi et al., 2013) by promoting antioxidant defences and photosynthesis (by stimulating rubisco and electron transport chain activity) under stress. Moderate sunscreen oil phase and moderate $nTiO_2$ concentrations may play the same role here, with the simultaneous exposure to elevated temperature and LO treatments resulting in an increase in B1 tolerance to warming by stimulating algal photosynthetic activity and antioxidant defences. However, exposure duration is a known factor in $nTiO_2$ toxicity tests (Clément et al., 2013), hence it should be noted that the phenomenon described here could be transient: a longer exposure to sunscreen ingredients alone and combined with

warming could overwhelm Symbiodiniaceae antioxidant capacity and repair systems being detrimental to algae survival. A long-term experiment should be performed to verify this assumption, along with measurements of antioxidant enzymes activity such as CAT and SOD.

2.4.4 Symbiodiniaceae A1 and B1 differential responses to inorganic sunscreen ingredients

B. pseudominutum (ITS2 type B1) was previously described as more sensitive to thermal stress than *S. microadriaticum* (ITS2 type A1) (Hawkins and Davy, 2012; Karim et al., 2015; Robison and Warner, 2006). In the experiments presented here B1 exhibits moderate differences from A1. At ambient temperature, B1 generated higher ROS quantities than A1 and showed a modest decrease in photosynthetic efficiency at HO conditions while A1 Fv/Fm remained unchanged. Also under combined thermal stress Fv/Fm reduction was higher in B1. Interestingly, the quantity of ROS produced by A1 algae not exposed to $nTiO_2$-oil mixtures at 32°C was similar to ROS produced by A1 treated algae at 26°C. B1 algae at 26°C, instead, generated higher level of ROS than untreated-control algae at 32°C. These findings support the higher sensitivity to stress of B1 described in previous studies. Nonetheless the two Symbiodiniaceae species investigated here exhibited an overall similar negative response to sunscreen ingredients toxicity, even A1 algae displayed severe effects especially under combined thermal stress. Thermally sensitive A1 is known to invest in a rapid and efficient antioxidant defence system (Krämer et al., 2012; McGinty et al., 2012), and also here it can be observed that ROS levels decrease with time at 26°C (Figure 2.7A). It is possible that the surplus of energy required to respond to the stress imposed by the HO treatments caused the severe growth decline observed under warming conditions. Whereas Symbiodiniaceae B1 antioxidant production, usually not sufficient to scavenge thermally-induced ROS (McGinty et al., 2012), may be promoted by the ROS induced by moderate sunscreen exposure, allowing B1 algae exposed to LO treatments to maintain a growth rate similar to control algae.

Symbiodiniaceae under laboratory conditions do not exactly represent *in-hospite* symbionts in a natural environment because their physiological processes are optimized to culture conditions (Van Dam et al., 2015). Nevertheless, findings from this study suggest that various Symbiodiniaceae types may experience stress from sunscreen pollution regardless of their potential tolerance to elevated temperature.

Corals have been demonstrated to associate with thermally-tolerant Symbiodiniaceae types to increase their threshold to thermal stress (Bay et al., 2016; Berkelmans and Van Oppen, 2006; Cunning et al., 2015). The benefits of associating with thermally-tolerant corals may be ineffective in areas contaminated by inorganic sunscreen ingredients. The high levels of ROS produced by the algal symbionts exposed to sunscreen ingredients at ambient as well elevated temperature likely exceed the antioxidant capacities of the coral host, potentially initiating a bleaching response in corals living in sunscreen-polluted waters even under not-stressful temperature conditions. Moreover, the high sensitivity of Symbiodiniaceae to nTiO_2-oil mixtures may reduce the availability of free-living populations for the colonization of aposymbiotic larvae and bleached corals.

2.4.5 Oil phase growth inhibition

Emulsion is the predominant formulation type for sunscreen products globally, thus the oil phase is the principal component in every sunscreen. The oil phase is the medium in which UV filters are dispersed (inorganic UV filters) or dissolved (organic UV filters), it also contains emollients and emulsifier agents that give the skin-sensory characteristics to sunscreen (Osterwalder et al., 2014). The oil phase is also the dominant sunscreen component remaining on the skin after spreading (Wang and Lim, 2016), thus it likely is the sunscreen compound most primarily released into the environment during water-recreational activities. The oily layers frequently observed floating on the water surface in tourist recreational areas are presumably the result of the oil phase discharge from sunscreen applied on bathers skin (Gondikas et al., 2017), nonetheless the environmental impacts of oil phase ingredients are a key knowledge gap to date.

Based on the results presented here, the sunscreen oil phase is likely the main driver of sunscreen toxicity towards coral algal symbionts, although UV filter type and concentration might also be key important drivers, as demonstrated by the models derived in this study (Table 2.5). With this in mind, the potential effects of the sunscreen oil phase alone, the mixture of emulsifying and emollient ingredients without the addition of UV filters, was investigated using *B. pseudominutum* (B1), as model organism. At ambient temperature the oil phase had a low impact on the growth of *B. pseudominutum*, however the synergistic effect of warming and oil phase significantly enhanced algae growth inhibition (Table 2.7). Oil phase ingredients and their potential health hazards are illustrated in Table 2.9, but lack of research on these ingredient make it difficult to determine their safety. The emulsifying agent, a lipophilic polymeric water-in-oil

emulsifier (Hassan et al., 2014), is the only ingredient reported to be a moderate hazard (Environmental Working Group, 2019), and may have an important role in driving the oil toxicity. Seo et al. (2018) demonstrated that common chemical and organic cosmetic emulsifying agents, such as cyclopentasiloxane and jojoba ester respectively, increased the toxicity of the UV filters $nTiO_2$ and nZnO towards human skin cells. In light of the results presented here and Seo et al. (2018) findings, emulsifiers are important ingredients to take into consideration when assessing sunscreen toxicity. Shading effect, algae immobilization, accumulation on membrane surfaces, hazard to membrane integrity and internalization, are possible mechanisms that, alone or in concert, can cause the observed oil toxicity. However, from the growth inhibition results, is not possible to pinpoint a single ingredient or mechanism that drives oil adverse effects on algae growth and further studies are necessary.

Table 2.9 - Information on the ingredients of the sunscreen oil phase (Environmental Working Group, 2019)

Ingredient	Function	EWG score[∂]	Toxic effect
Coco-Caprylate/Caprate	Emollient	1	/
Isopropyl Palmitate	Emollient	1	Not suspected to be an environmental toxin, persistent nor bioaccumulative[2]
Octyldodecanol	Emollient	1	Human irritant[1] Not suspected to be an environmental toxin, persistent nor bioaccumulative[2]
Octyldodecyl Xyloside	/	1	/
PEG-30 Dipolyhydroxystearate	Emulsifying Agent	3	Contamination concerns: it can contain harmful impurities (Ethylene Oxide, 1,4-dioxane)

[∂] The Environmental Working Group (EWG) score: 1–2 (low hazard), 3–6 (moderate hazard), 7–10 (high hazard).
[1] CIR (Cosmetic Ingredient Review). 2006. CIR Compendium, containing abstracts, discussions, and conclusions of CIR cosmetic ingredient safety assessments. Washington DC.
[2] EC (Environment Canada). 2008. Domestic Substances List Categorization. Canadian Environmental Protection Act (CEPA) Environmental Registry

2.5 Conclusion

This is the first study examining the ecotoxicity of sunscreen emulsifier and emollient ingredients, and $nTiO_2$ UV filters, on a marine organism. Sunscreen oil phase and $nTiO_2$ negatively affected Symbiodiniaceae growth and ROS production, yet it was not possible to determine a type of $nTiO_2$ UV filters less toxic then others. Results presented here suggest that low $nTiO_2$ concentrations could protect PSII system and promote

zooxanthellae photosynthetic activity, agreeing with Corinaldesi et al. (2018) who suggested $nTiO_2$ are likely a more eco-compatible sunscreen UV filter than nZnO.

As described in this study, the oil phase was a key component driving the observed toxicity. Oil phase ingredients accumulate at the air-water interface (Gondikas et al., 2017), in upper ocean layers known as the sea-surface microlayer (SML). SML is an important ecosystem, habitat for neuston and plankton communities, and it is a known sink of anthropogenic compounds (Wurl and Obbard, 2004). Sunscreen ingredients may thus impact a variety of aquatic organisms, including larvae and eggs of many species, as well as corals, that use SML during different life cycle stages (Zaitsev, 2005). The toxicity of oil phase ingredients could be enhanced by exposure to solar radiation, inducing photochemical reactions and formation of radicals (Zafiriou, 1986), as well as the interaction with a range of contaminants often present with the SML (Wurl and Obbard, 2004).

Impact of sunscreen ingredients is particularly important in a warming ocean scenario, with high temperature potentially enhancing any harmful effects, often leading to a significant decline in zooxanthellae growth. The findings of this study suggest that coastal sunscreen contamination may make Symbiodiniaceae more vulnerable to elevated temperatures, exacerbating bleaching responses in corals. The sensitivity of Symbiodiniaceae to sunscreen ingredients may also have important consequences in free-living Symbiodiniaceae populations, fundamental reservoirs for re-populating bleached corals and for colonization of aposymbiotic coral larvae and juveniles.

Lastly, this chapter demonstrated that ecotoxicity assessments of solely UV filters are not sufficient to evaluate the impact of sunscreen in the marine environments and highlight the importance of taking into account oil phase ingredients, particularly the emulsifying agents, in addition to UV filters when developing safer and environmentally friendly sunscreens.

Overall this chapter demonstrated that the mixture of sunscreen UV filters and oil phase ingredients induce negative effects on cultured Symbiodiniaceae, with the potential to impact both *in-hospite* and free-living Symbiodiniaceae populations. The potential toxicity of inorganic sunscreen towards corals' gametes and larvae floating in the SML will be explored in Chapter 5. In the next chapter the sunscreen ingredients tested here will be integrated in a typical sunscreen formulation in order to investigate the effects of inorganic sunscreen on adult corals.

Chapter 3

Toxicological effects of inorganic sunscreen on two coral species under ambient temperature and projected elevated temperature conditions

3.1 Introduction

In recent years the toxicity of sunscreen formulations towards coral life stages has attracted increasing attention (Corinaldesi et al., 2018; Downs et al., 2014, 2016; Fel et al., 2019; He et al., 2019b; Jovanović and Guzmán, 2014; Stien et al., 2018; Tang et al., 2017). However, very few studies have addressed the effects of whole sunscreen formulations on reef-building corals or other marine organisms despite the release of whole sunscreen product mixtures in the environment. Sunscreen products formulated with organic UV filters were found to increase viral and bacterial abundance in experimental microcosms as well as water surrounding corals, causing zooxanthellae expulsion and complete bleaching of exposed corals in 96 hours (Danovaro et al., 2008; Danovaro and Corinaldesi, 2003). Sunscreen formulated with titanium dioxide nanoparticles UV filters instead have been found to have only a moderate impact on sea urchin embryo and larval development compared to organic sunscreen (Corinaldesi et al., 2017). nTiO_2-based sunscreen formulations have also been demonstrated to reduce fish movements (Díaz-Gil et al., 2017), be toxic to marine phytoplankton (Sendra et al., 2017b; Tovar-Sánchez et al., 2013) and to induce antioxidant responses in mussels (Sureda et al., 2018). However, these studies tested commercial sunscreen products, where the exact composition, or even the exact concentration of UV filters, is unknown. It is therefore impossible to determine the ingredients exposure concentration and to compare the results across studies. Nevertheless, the evidence of toxicity of sunscreen nTiO_2-oil phase mixtures measured in the Symbiodiniaceae experiments presented previously (Chapter 2) coupled with findings from the aforementioned studies, confirm the need for further investigations looking at the impact of inorganic sunscreen on tropical corals. In this study, the effect of a laboratory-made inorganic sunscreen formulation was assessed on two common corals from the Indo-Pacific, *Porites cylindrica* and *Seriatopora hystrix*, characterized by different sensitivity to thermal stress (Loya et al., 2001). Although sunscreen toxicity studies in laboratory conditions have been recently criticized to not be representative of the natural conditions in coral reef areas (Hughes, 2019), laboratory studies allow isolation of the effects and mechanisms of sunscreen toxicity by minimizing the natural variability of a real environment in order to better assess and predict of the impact of sunscreen on reef-building corals under realistic conditions (Holmstrup et al., 2010).

Environmental conditions affected by global climate change are known to influence the toxicity of a chemical compound (Hooper et al., 2013; Kimberly and Salice, 2014;

Nikinmaa, 2013). In particular elevated temperature affects the sensitivity of marine organisms to toxicants by influencing their metabolism and membranes' properties, and thus the diffusion rates of compounds in marine organisms (Holmstrup et al., 2010; Nikinmaa, 2013). Extreme climate events are the major threat affecting coral reefs worldwide (Fordyce et al., 2019; Frölicher and Laufkötter, 2018; Hughes et al., 2018a). The frequency and intensity of those marine heatwaves is constantly increasing as a result of anthropogenic global warming (Frölicher et al., 2018; Oliver et al., 2018), with up to 90% of all coral reefs predicted to experience sever annual bleaching by 2055 (Van Hooidonk et al., 2014). The deleterious effects of severe heat stress on coral health have been extensively studied (Leggat et al., 2019; Lesser, 2011; Smith et al., 2005; Weis, 2008), as well as the combined impact of elevated seawater temperature with local stressors such as heavy metals (in particular copper (Banc-Prandi and Fine, 2019; Nyström et al., 2001), iron (Biscéré et al., 2018) and nickel (Biscéré et al., 2017)), herbicide (Van Dam et al., 2015), diesel (Kegler et al., 2015), salinity (Alutoin et al., 2001) and sedimentation (Poquita-Du et al., 2019). Generally, local stressors mentioned above have been found to enhance the negative effects of elevated seawater temperature in an additive or synergistic way, increasing coral susceptibility to bleaching and reducing coral growth and metabolic activity (references cited above). The combined impact of sunscreen and short-term acute warming events are however currently unknown.

The objective of the study described in this chapter was to assess the effects of inorganic sunscreen concentrations representing the estimated concentrations of a $nTiO_2$-based sunscreen in a touristic beach (Chapter 1, Section 1.2.5) on the photo-physiological performances of two common reef building corals described to be highly susceptible to thermal stress (Van Woesik et al., 2011). Combined sunscreen-elevated temperature experiments were also performed in order to investigate whether sunscreen toxicity change in relation to the expected projections for acute warming events over the next century (Frölicher et al., 2018). Since both thermal stress and $nTiO_2$ exposure have the potential to cause coral bleaching (Corinaldesi et al., 2018; Jovanović and Guzmán, 2014; Leggat et al., 2019; Chapter 2 of this thesis), it is hypothesized that sunscreen and warming simultaneous exposure will enhance the negative effects of both individual stressors.

3.2 Materials and Methods

3.2.1 Sunscreen formulation

Water in oil (w/o) sunscreen emulsion was custom made from cosmetic ingredients at CEREGE laboratories (Aix-en-Provence, France) under the supervision of Dr Jerome Labille. Ingredients' characteristics are presented in Table 3.1. Sunscreen was formulated with $nTiO_2$ Eusolex® T-S as UV filter at 10% concentration (Eusolex® T-S characterization is reported in Appendix A).

For a total mass of 100g of sunscreen, 40.4 g of demineralized water was mixed with 3g of glycerine using a laboratory agitator (deflocculator, Turbotest evo, VMI) at ~ 400 rpm. A quantity of 0.6 g of the gelling agent Sepiplus™ 400 was added while increasing the agitation speed around 1500-2000 rpm and stirred continuously for 10 mins until a homogeneous and well mixed gel was obtained. Separately, the oil-phase solution of 15g Easynov™, 3g Cetiol® LC and 3g of Tegosoft® P was prepared, to which were added 5g of $nTiO_2$ T-S powder. Once the $nTiO_2$ UV filter was well dispersed, the suspension was mixed for 5 mins with the deflocculator. Finally, the oil phase with dispersed $nTiO_2$ was slowly added to the gel phase under constant stirring (1800-2000 rpm) with a rotor stator mounted on the agitator to obtain a homogenous emulsion.

The final texture and the Sun Protection Factor (SPF) 20 (measured *in vitro*, Dr Jerome Labille personal communication) of the custom-made sunscreen, make it comparable to commercial sunscreen products.

3.2.2 Preparation of sunscreen test solutions

Stock suspensions of 1 gL^{-1} were prepared by dispersing the sunscreen formulation in Milli-Q water, mixing well for 48 consecutive hours. The resulting stock suspension was stored in the dark in a refrigerator throughout the experimental period.

Twenty-four hours prior to the start of each experiment and prior of each experimental sampling timepoint, sunscreen test suspensions at 0.1 and 1 mgL^{-1} nominal concentrations were prepared by adding aliquots of stock suspensions to artificial seawater (ASW, see below) and mixed overnight to allow for equilibration.

Table 3.1 - Sunscreen and filter-free formulation ingredients characteristics, as provided by the suppliers.

Commercial name	Supplier	INCI name(s)	Function
Glycerine	AmiChimie, France	Glycerine	Moisturizer
Sepiplus™ 400	Seppic, France	Polyacrylate-13 Polyisobutene Polysorbate 20	Thickening, stabilizing and texturizing polymer
Easynov™	Seppic, France	Octyldodecanol* Octyldodecyl Xyloside* PEG-30 Dipolyhydroxystearate*	W/O emulsifier
Cetiol® LC	Basf, Germany	Coco-Caprylate/Caprate*	Emollient
Tegosoft® P	Evonik, Germany	Isopropyl Palmitate*	Emollient
Eusolex® T-S	Merck, France	Rutile, Alumina, Stearic acid	UV filter

* Chemical formulas:

Octyldodecanol
(solvent)

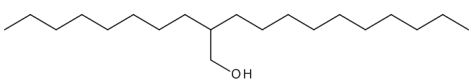

Octyldodecyl Xyloside
(tensioactive)

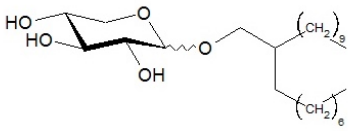

PEG-30 Dipolyhydroxystearate
(non-ionic tensioactive)

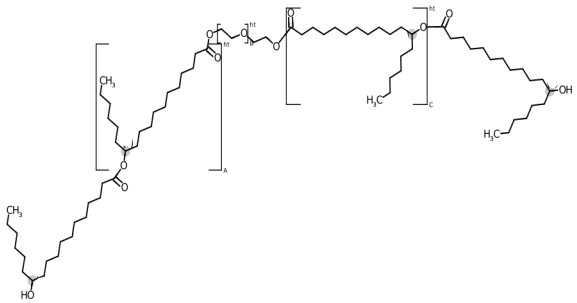

Coco-Caprylate/Caprate

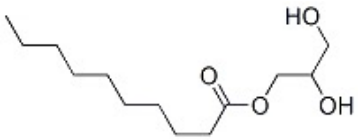

Isopropyl Palmitate

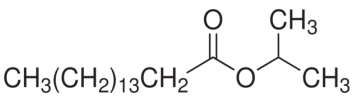

3.2.3 Coral husbandry

The branching corals *Porites cylindrica* and *Seriatopora hystrix* were purchased from Tropical Marine Centre (TMC, UK) and were maintained at the Changing Oceans laboratory at the University of Edinburgh. After one month of acclimation to aquarium conditions, coral colonies were fragmented with coral clippers or a rotary tool. Coral fragments (~ 1 - 1.5 cm long) were either hung on nylon wires and suspended into the aquaria or attached to coral plugs and placed on plastic racks, where they were allowed

to recover for at least three weeks. Aquaria were supplied with ASW prepared by mixing freshwater obtained by reverse osmosis purified and Tropic Marin® ProReef salt mixture (Tropic Marine, Germany). Temperature and salinity were kept constant using heaters connected to electronic controllers (ProfiLux, GHL, Germany) and routinely verified using an YSI Model 30 conductivity meter (Xylem Inc. USA).

3.2.4 Experimental design

A factorial experimental design was employed with two concentrations of sunscreen (0.1 and 1 mgL^{-1}) and four levels of temperature (26°C [ambient], 27.5°C, 29°C, 30.5˚C). The chosen sunscreen concentrations represent concentrations that are likely to be released in a touristic water body during a summer day based on estimations (Chapter 1, Section 1.2.5), while the temperature range includes current and future projected temperatures increase during extreme thermal events under the present-day global warming scenario (+ 1.5°C), under the current mitigation policies scenario (+3°C), and under the worst-case scenario without any mitigation policy (+4.5°C) (Frölicher et al., 2018). A schematic representation of the experimental design is depicted in Figure 3.1.

For each coral species, two consecutive experiments were performed in temperature-controlled incubators at either ambient temperature or warming conditions for 16 days (4 days of acclimation to experimental conditions followed by 12 days of experiment). LED units (Aquaray white flexi LED Twin, TMC) were added to the incubators' lights to provide an irradiance of approximately 250 μmol photons m^{-2} s^{-1} on a 12 h:12 h light:dark photoperiod (Figure 3.2A). At the start of each experiment, coral fragments were randomly distributed in 1 L glass containers (3 fragments per container, one for each sampling timepoint), fitted with an air bubbler to ensure air supply and water motion for the homogenous dispersion of the sunscreen formulation (Figure 3.1B and 3.2A). Only visually healthy fragments were used in the experiments. Containers were then placed in the temperature-controlled incubators in a completely randomised design. To prevent heat shock, temperature was gradually increased by 0.5°C per day until the target temperatures were achieved. Four fragments for each treatment were sampled for analysis from four different containers at day 4, day 8 and day 12, timepoints corresponding to 24 h of incubation at 27.5°C, 29°C and 30.5°C in the warming experiments (Table 3.2).

At the start of each experiment (time 0), four control fragments were sampled from extra containers removed thereafter. At each sampling time, 50% of the water in the containers was replaced with the appropriate sunscreen test solution or control seawater acclimatized

to the experimental temperature. The average temperature conditions at the different timepoints for each coral species is given in Table 3.2.

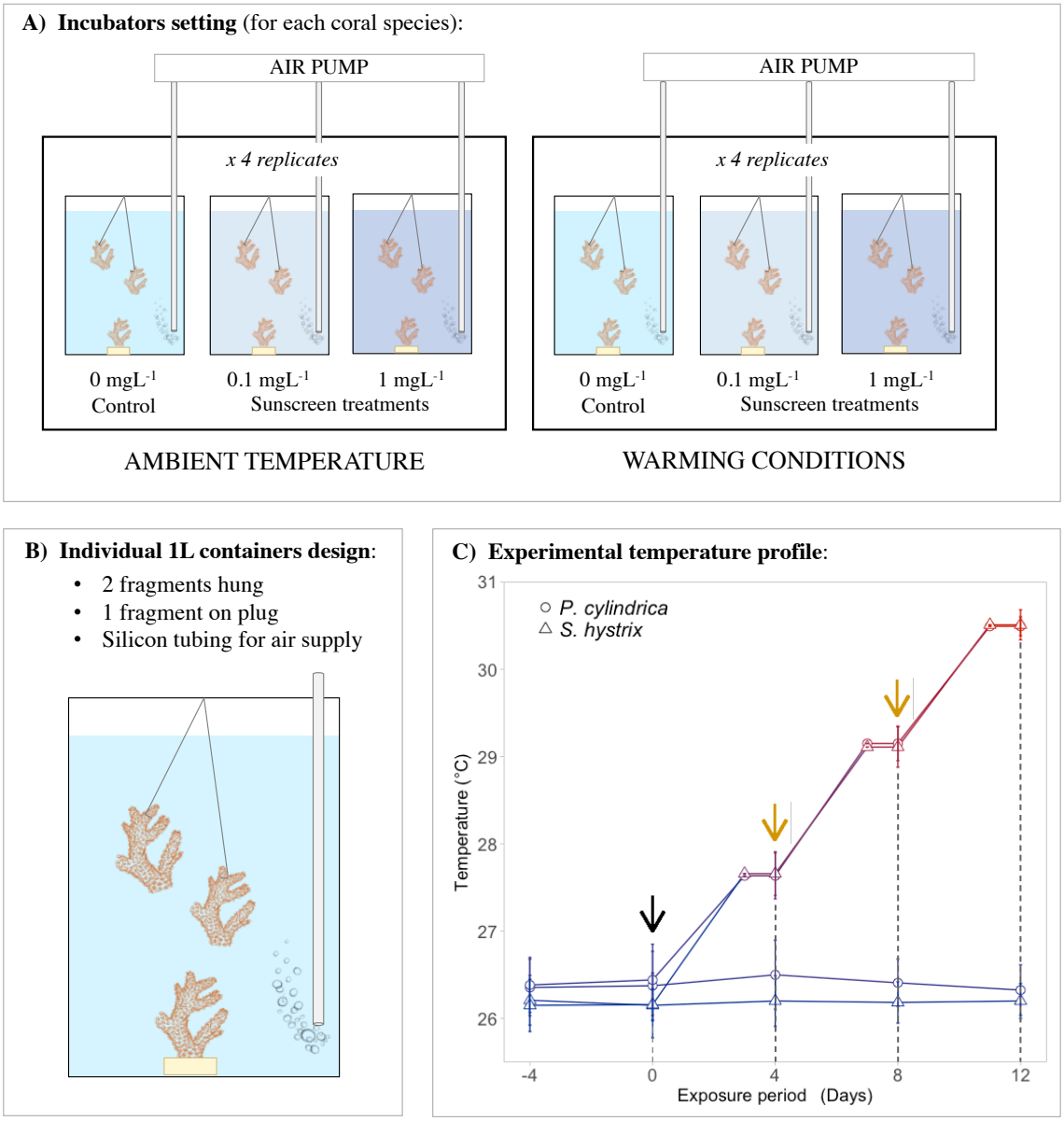

Figure 3.1 - Overview of the experimental setup. **A)** Two separate temperature-controlled incubators held at ambient or elevated temperature, for each coral species. In each incubator, 4 replicate glass containers were exposed to 0.1 mgL^{-1} sunscreen concentration, 4 containers had 1 mgL^{-1} sunscreen concentration and lastly 4 were control, seawater only, containers. **B)** Design of the individual 1L experimental containers; half of the seawater was replaced in every container after the measurements were taken. **C)** Temperature profile of the experimental treatments for *P. cylindrica* (circle) and *S. hystrix* (triangle) at 26°C (blue) and elevated temperature (gradient blue-red) during the acclimation phase (prior Day 0) and the exposure period (sampling on Days 0, 4, 8 and 12); the black arrow indicate the start of the sunscreen exposure, yellow arrows indicate each sunscreen addition and dashed segments the sampling timepoints (Error bars represent standard deviation).

Table 3.2 - Average temperature conditions at the different timepoints in the ambient temperature and warming experiments (n = 12, mean ± sd).

Timepoints (Days)	*P. cylindrica*		*S. hystrix*	
	Ambient	Warming	Ambient	Warming
- 4	26.3 ± 0.3	26.4 ± 0.3	26.2 ± 0.3	26.1 ± 0.3
0	26.4 ± 0.4	26.4 ± 0.4	26.1 ± 0.4	26.2 ± 0.2
4	26.5 ± 0.4	27.6 ± 0.3	26.2 ± 0.3	27.6 ± 0.2
8	26.4 ± 0.3	29.1 ± 0.2	26.2 ± 0.2	29.2 ± 0.2
12	26.3 ± 0.3	30.4 ± 0.1	26.2 ± 0.2	30.5 ± 0.2

3.2.5 Chlorophyll fluorescence, net photosynthesis and respiration measurements

Starting from the acclimation phase, the maximum quantum yield of photosystem II (Fv/Fm) was measured every 48 hours in 15-minutes dark-adapted coral fragments using a pulse amplitude-modulated fluorometer (Diving PAM-II, WALZ GmbH, Germany) (Hoegh-Guldberg and Jones, 1999). Coral fragments used in the Fv/Fm measurements were the same during each experiment, namely the samples for day 12 respirometry measurements.

At the experimental timepoints (day 0, day 4, day 8 and day 12), fragments were allowed to recover under the experimental light conditions for 30 minutes following Fv/Fm measurements. Coral fragments (n = 4 per treatment) were then transferred into air-tight respiration chambers (230 mL volume) filled with seawater from the respective containers and equipped with oxygen sensor spots to measure oxygen fluxes in the light (net photosynthesis, P) and in the dark (respiration, R). To maintain temperature and sunscreen concentration constant during the measurements, respiration chambers were immersed in a water-bath equipped with a temperature control system and LED units as light source (Aquaray white flexi LED Twin, TMC), and seawater in the chambers was also continuously stirred with a magnetic stir bar (the experimental apparatus for respirometry measurements is shown in Figure 3.2B). Rates of net photosynthesis and respiration were calculated as the change of oxygen concentration slopes over time. Oxygen concentrations were determined using oxygen optodes connected to an Oxy-4 Mini temperature-compensated oxygen analyser (Presens Precision Sensing GmbH, Germany). Gross photosynthetic rates (P_{gross}) were calculated as the difference between net photosynthesis and respiration, and the dimensionless ratio of gross photosynthesis to respiration (P_{gross}:R, indicating coral autotrophic capacity) were estimated, assuming a

constant respiration during light and darkness (McCloskey, 1978). Data obtained were normalized by surface area (cm^{-2}), estimated using the wax-dipping method (Stimson and Kinzie, 1991).

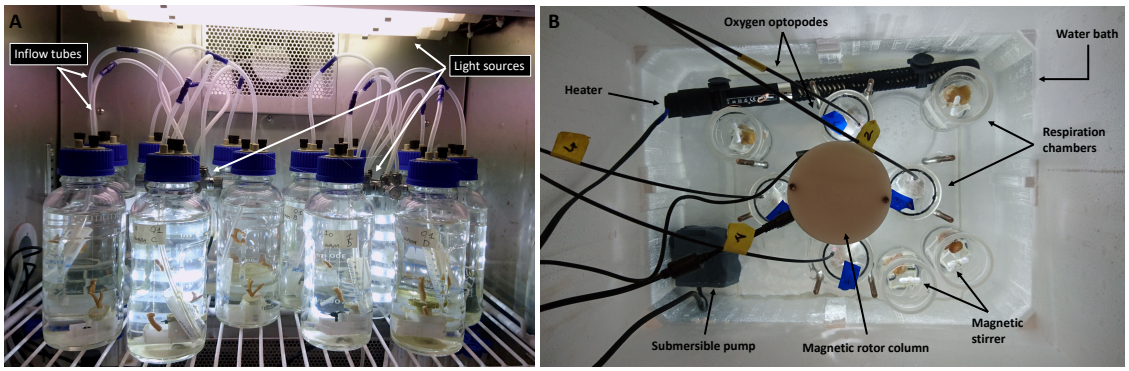

Figure 3.2 - Incubator setting and experimental apparatus for respirometry measurements. **A**) Experimental setting of the temperature-controlled incubator showing the 12 glass containers with 3 coral fragments each fitted with inflow tubes connected to an external air pump, and the three light sources: the top general light incubator and the two led stripes, each providing direct light to 6 containers. **B**) Respirometry apparatus submersed in a water bath showing the heater and submersible pump that guarantee constant temperature during the measurement; the central waterproof magnetic rotor column, fitted with two led light stripes; the respirometry chambers containing one coral fragment each, closed with a lid equipped with an oxygen spot and connected to the oxygen optode during the measurements, open to acclimatize coral fragments to the conditions during the respirometry incubation. Each respirometry chamber contain a magnetic stirrer controlled by the central rotor during the measurements.

3.2.6 Chlorophyll concentration and Symbiodiniaceae density

After the assessment of the physiological performance, coral fragments (n = 4 per treatment) were snap frozen in liquid nitrogen and stored at – 20°C. Coral tissue was removed with a Waterpik® water jet using 50 mL of ASW and homogenised with a motorized pellet pestle. The homogenate was centrifuged for 5 min at 5000 rpm, supernatant was discharged and the Symbiodiniaceae pellet was resuspended in 1 mL ASW. A 500-µL subsample was fixed in 4% formaldehyde for successive Symbiodiniaceae density counts using a haemocytometer under a light microscope (6 replicates counts per sample). For determination of chlorophyll *a*, the other subsample (500 µL) was centrifuged 5 min at 8000 rpm and resuspended in 100% methanol at 4°C. Extracts were centrifuged for 5 min secs at 5000 rpm and the absorbance of the supernatant was measured at 652, 665 and 750 nm. Chlorophyll *a* concentration was quantified according to the spectrophotometric equation of Porra (1989). Cell count and chlorophyll concentration were normalized by coral surface area.

3.2.7 Data analyses

All analyses were performed in R (version 3.4.3) and measurements from each coral were analysed separately. One-way Anova analyses with time as fixed factor (categorical variable) was used to reveal if the incubation time had an impact on all endpoints studied in coral fragments not exposed to sunscreen in the ambient temperature experiments.

Changes in chl *a*, Symbiodiniaceae density, respiration, net photosynthesis and P_{gross}:R ratio within treatments were assessed with two-way Anova analyses having sunscreen (0, 0.1 and 1 mgL^{-1}, categorical variable) and time (days of sampling, continuous variable) and their interactions as fixed factors, for both ambient and elevated temperature experiments. As Fv/Fm were measured from the same coral fragments in all sampling days, linear mixed effect models with repeated measures were applied, having sunscreen as fixed factor and sampling time as random factor (function *lme* of the package 'nlme' version 3.1-137). Post-hoc Tukey HSD test was then used when sunscreen resulted a significant factor (function *glht* of the 'multcomp' package (version 1.4-8) for Fv/Fm *lme* models).

To verify differences between treatments at ambient vs the different warming conditions, results from each temperature tested (coinciding with the sampling times, 27.5 °C day 4, 29°C day 8, 30.5°C day 12) were then analysed separately with two-way Anova analyses having sunscreen (categorical variable), temperature (continuous variable) and their interaction as fixed factors.

For each analysis, all parameters were first tested for normality and homogeneity of variances using Shapiro-Wilk and Levene's tests (package 'car', version 3.0-2), respectively, and data that did not met the assumptions were ln-, sin- or square root-transformed depending on the endpoint measured.

Graphs were created using the package 'ggplot' (version 2-2.2.1).

3.3 Results

3.3.1 Effect of inorganic sunscreen exposure at ambient temperature

Incubation conditions did not affect corals physiological performances. One-way Anova analyses of the effect of incubation time on each endpoint studied confirmed that *S. hystrix* and *P. cylindrica* control fragments maintained stable conditions through the experiment ($p > 0.05$ for all endpoints in both coral species, Table 3.3). Only *S. hystrix* experienced a slight but statistically significant decline in its net photosynthetic rates with incubation time ($p = 0.036$), in particular the production of oxygen at day 8 was significantly reduced compared to the start of the experiment (Tukey HSD Post Hoc test $p = 0.047$).

The photo-physiological responses of corals exposed to increasing sunscreen concentrations are depicted in Figure 3.3 for *P. cylindrica* and Figure 3.4 for *S. hystrix*. The two corals displayed similar trends of variation, an overall reduction of performances with increasing sunscreen concentrations was observed for all endpoints, however the effect of sunscreen was not always significant. Photosynthetic rate and symbionts density were the endpoints most affected by sunscreen in both corals (*P. cylindrica* net photosynthesis $p_{sunscreen} < 0.0001$ and Symbiodiniaceae density $p_{sunscreen} = 0.0003$, Table 3.4, *S. hystrix* net photosynthesis and Symbiodiniaceae density $p_{sunscreen} < 0.0001$, Table 3.6). Oxygen production during daylight fell below zero from the 4th day (*P. cylindrica*) and the 8th day (*S. hystrix*) of exposure to inorganic sunscreen onwards (Tukey HSD Post Hoc test $p < 0.002$ for 0.1 mgL^{-1} against control for *P. cylindrica*, $p < 0.0001$ in the other pairwise comparisons for both corals, Table 3.5 and Table 3.7), suggesting that oxygen consumption rates were greater than oxygen production through photosynthesis. While respiration rates in the dark were constant among all treatments and timepoints in *P. cylindrica*, in *S. hystrix* respiration rates were significantly affected by sunscreen exposure ($p_{sunscreen} = 0.003$), showing a significant reduction of oxygen consumption at concentrations of 0.1 mgL^{-1} (Tukey HSD post hoc test $p = 0.042$, Table 3.7) and 1 mgL^{-1} (Tukey HSD post hoc test $p < 0.0001$, Table 3.7). As consequence of sunscreen detrimental effect on corals' oxygen fluxes, the gross photosynthetic to respiration ratio was significantly affected as well ($p_{sunscreen} \leq 0.0001$), dropping below 1 in all experimental times in *P. cylindrica* and from day 8 onwards in *S. hystrix* fragments exposed to 1 mgL^{-1} concentration (Figure 3.3 and 3.4). Following the decline in

symbionts density and net photosynthesis, Fv/Fm profiles also showed a significant reduction with increasing sunscreen concentrations ($p_{sunscreen}$ = 0.03 and 0.04 for *P. cylindrica* and *S. hystrix*, respectively, Table 3.4 and 3.6). A maximum photosynthetic yield reduction was observed even after just 24 hours in sunscreen containing waters compared to control fragments (10.7 % for *P. cylindrica* and 4.4% for *S. hystrix* at the concentration of 1 mgL^{-1}). Fv/Fm declined to values of ~ 0.55 in *P. cylindrica* and ~ 0.57 in *S. hystrix* after 12 days of sunscreen exposure (Figure 3.3 F and Figure 3.4 F).

Sunscreen exposure time significantly affected corals photo-physiological performances in an additive manner, enhancing the negative impact of sunscreen. Time is a significant factor for the net photosynthetic rates of *P. cylindrica* (p_{time} = 0.002, Table 3.4) and for all *S. hystrix*'s endpoints affected by sunscreen (Table 3.6). The interaction between sunscreen and time was significant only for *S. hystrix* P_{gross}:R ratio ($p_{sunscreen:time}$ = 0.014).

Table 3.3 - One-way Anova results on the effects of incubation time on *P. cylindrica* and *S. hystrix* control fragments. Statistically significant effects are highlighted in bold. Df: degrees of freedom, SS: sum of squares.

Source of variation	*Porites cylindrica*				*Seriatopora hystrix*			
	Df	**SS**	**F-value**	**p-value**	**Df**	**SS**	**F-value**	**p-value**
Net photosynthesis								
Time	3	0.121	2.713	0.09	3	10.74	3.582	**0.0365**
Respiration								
Time	3	0.04	0.558	0.653	3	6.299	1.532	0.261
Symbionts density								
Time	3	3.797	2.104	0.153	3	11.66	3.886	0.125
Chl a concentration								
Time	3	153.9	0.254	0.857	3	2562	854	0.227
Fv/Fm								
Time	9	0.016	0.424	0.912	7	0.115	1.748	0.145

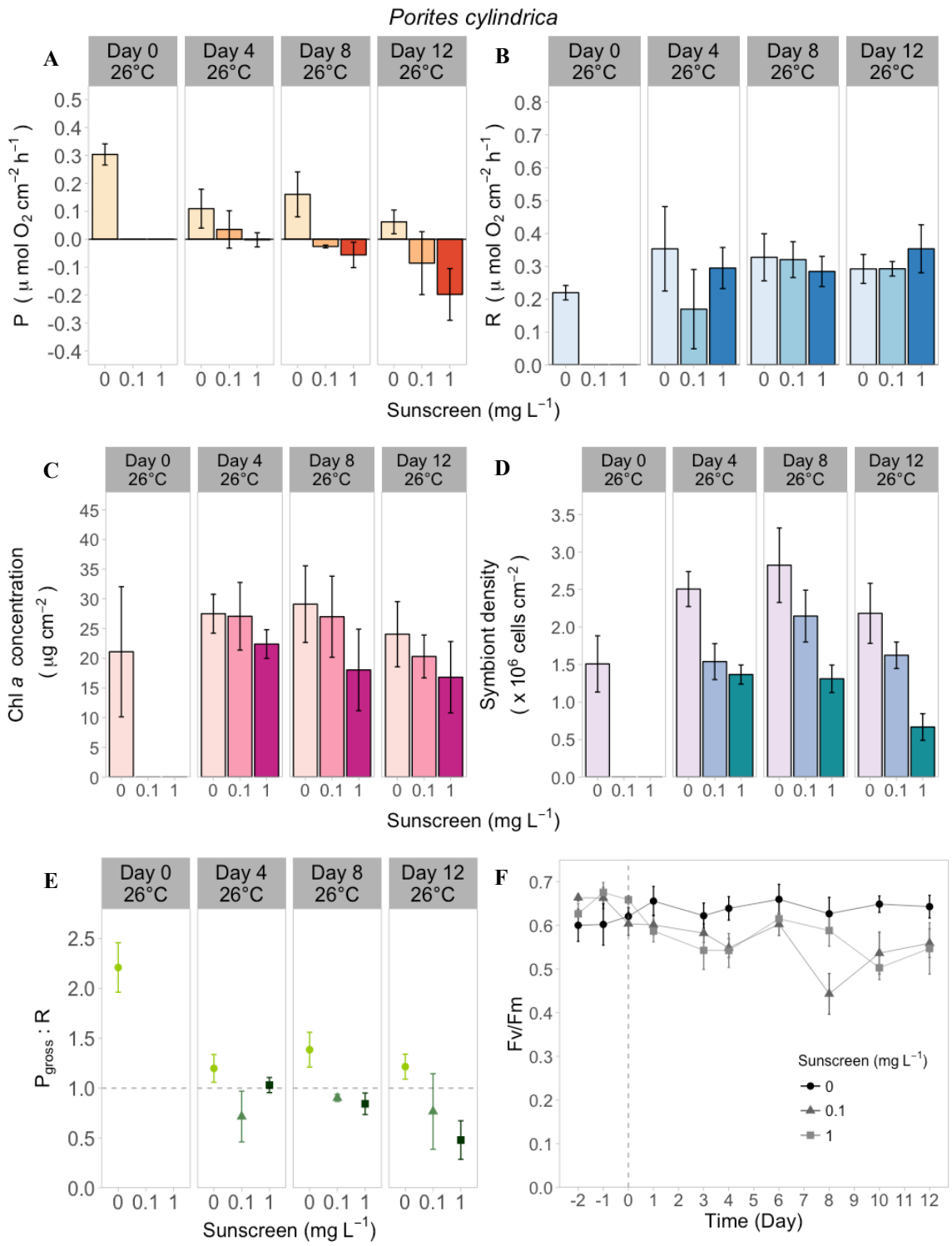

Figure 3.3 - *Porites cylindrica* physiological parameters measured at ambient temperature (mean ± SEM, n=4). **A**) net photosynthesis, **B**) respiration, **C**) chlorophyll *a* concentration, **D**) Symbiodiniaceae density, **E**) gross photosynthesis to respiration ratio and **F**) Fv/Fm. Darker colours in the graphs A-E indicate increasing sunscreen concentration as stated in the *x*-axis.

Table 3.4 - Two-way Anova results on *Porites cylindrica* measurements from the ambient temperature experiment. Data were ln-transformed (‘‘*’’) when appropriate and statistically significant effects are highlighted in bold. Df: degrees of freedom, SS: sum of squares.

Source of variation	Df	SS	F-value	p-value
Net photosynthesis				
Sunscreen	12	0.4718	14.12	**<0.0001**
Day	1	0.1796	10.75	**0.002**
Sunscreen:Day	12	0.0067	0.2	0.82
Respiration			*	
Sunscreen	12	0.012	0.49	0.62
Day	1	0.0252	2.057	0.16
Sunscreen:Day	12	0.0102	0.415	0.66
P_{GROSS} *: R*				
Sunscreen	12	4.016	12.445	**0.0001**
Day	1	1.258	7.797	**0.009**
Sunscreen:Day	12	0.435	1.348	0.27
Symbionts density				
Sunscreen	12	8.914	10.477	**0.0003**
Day	1	0.137	0.322	0.57
Sunscreen:Day	12	1.95	2.292	0.12
Chl a concentration			*	
Sunscreen	12	0.617	1.283	0.291
Day	1	0.005	0.022	0.882
Sunscreen:Day	12	0.727	1.512	0.236
Fv/Fm				
Sunscreen	2		5.2333	**0.03**
Error	9			

Table 3.5 - Tukey Post-hoc test results of all pairwise comparisons among sunscreen treatments for *P. cylindrica* measurements in the ambient temperature experiment. Statistically significant differences are highlighted in bold.

Pairwise comparisons		p-value
Net photosynthesis		
0 mgL^{-1}	0.1 mgL^{-1}	**0.002**
0 mgL^{-1}	1 mgL^{-1}	**<0.0001**
1 mgL^{-1}	0.1 mgL^{-1}	0.501
P_{GROSS} *: R*		
0 mgL^{-1}	0.1 mgL^{-1}	**0.001**
0 mgL^{-1}	1 mgL^{-1}	**<0.0001**
1 mgL^{-1}	0.1 mgL^{-1}	0.994
Symbionts density		
0 mgL^{-1}	0.1 mgL^{-1}	0.141
0 mgL^{-1}	1 mgL^{-1}	**<0.0001**
1 mgL^{-1}	0.1 mgL^{-1}	**0.049**
Fv/Fm		
0 mgL^{-1}	0.1 mgL^{-1}	**0.007**
0 mgL^{-1}	1 mgL^{-1}	**0.032**
1 mgL^{-1}	0.1 mgL^{-1}	0.867

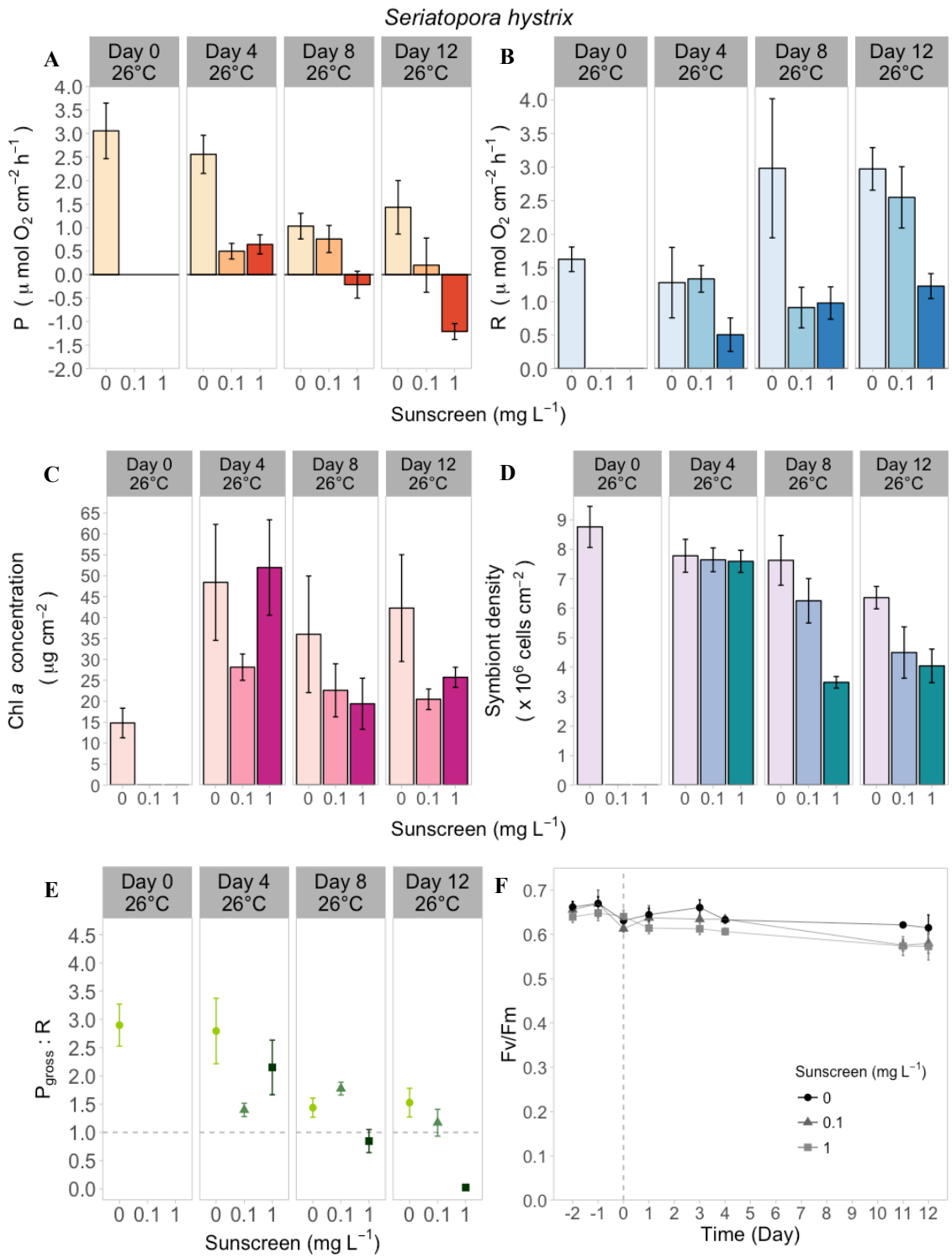

Figure 3.4 - *Seriatopora hystrix* physiological parameters measured at ambient temperature (mean ± SEM, n=4). **A**) net photosynthesis, **B**) respiration, **C**) chlorophyll *a* concentration, **D**) Symbiodiniaceae density, **E**) gross photosynthesis to respiration ratio and **F**) Fv/Fm. Darker colours in the graphs A-E indicate increasing sunscreen concentration as stated in the *x*-axis.

Table 3.6 - Two-way Anova results on *Seriatopora hystrix* measurements from the ambient temperature experiment. Data were either ln- (‘‘*’’) or square root- (‘‘$’’) transformed, and statistically significant effects are highlighted in bold. Df: degrees of freedom, SS: sum of squares.

Source of variation	Df	SS	F-value	p-value
Net photosynthesis				
Sunscreen	12	38.24	30.811	**<0.0001**
Day	1	12.71	20.489	**<0.0001**
Sunscreen:Day	12	2.51	2.026	0.15
Respiration			*	
Sunscreen	12	1.536	10.236	**0.0004**
Day	1	0.8434	11.24	**0.002**
Sunscreen:Day	12	0.0269	0.179	0.84
P_{GROSS} *: R*				
Sunscreen	12	8.097	12.734	**<0.0001**
Day	1	9.5	29.88	**<0.0001**
Sunscreen:Day	12	3.099	4.874	**0.014**
Symbionts density				
Sunscreen	12	47.31	13.578	**<0.0001**
Day	1	47.83	27.453	**<0.0001**
Sunscreen:Day	12	7.98	2.291	0.12
Chl a concentration			$	
Sunscreen	12	5.49	1.159	0.33
Day	1	0.05	0.02	0.89
Sunscreen:Day	12	16.99	3.59	0.04
Fv/Fm				
Sunscreen	2		4.458	**0.04**
Error	9			

Table 3.7 - Tukey Post-hoc test results of all pairwise comparisons among sunscreen treatments for *S. hystrix* measurements in the ambient temperature experiment. Statistically significant differences are highlighted in bold.

Pairwise comparisons		p-value
Net photosynthesis		
0 mgL^{-1}	0.1 mgL^{-1}	**<0.0001**
0 mgL^{-1}	1 mgL^{-1}	**<0.0001**
1 mgL^{-1}	0.1 mgL^{-1}	0.067
Respiration		
0 mgL^{-1}	0.1 mgL^{-1}	**0.042**
0 mgL^{-1}	1 mgL^{-1}	**<0.0001**
1 mgL^{-1}	0.1 mgL^{-1}	0.153
P_{GROSS} *: R*		
0 mgL^{-1}	0.1 mgL^{-1}	**0.011**
0 mgL^{-1}	1 mgL^{-1}	**<0.0001**
1 mgL^{-1}	0.1 mgL^{-1}	0.157
Symbionts density		
0 mgL^{-1}	0.1 mgL^{-1}	**0.014**
0 mgL^{-1}	1 mgL^{-1}	**<0.0001**
1 mgL^{-1}	0.1 mgL^{-1}	0.122

Table 3.7 - Continue

Pairwise comparisons		p-value
Fv/Fm		
0 mgL^{-1}	0.1 mgL^{-1}	0.097
0 mgL^{-1}	1 mgL^{-1}	**0.011**
1 mgL^{-1}	0.1 mgL^{-1}	0.681

3.3.2 Effect of sunscreen and combined temperature increase

Two-way Anova analysis on the measurements taken during *S. hystrix* and *P. cylindrica* warming experiments was employed to reveal significant effects of simultaneous elevated temperature and inorganic sunscreen exposure as well as elevated temperature alone.

Under warming conditions, *P. cylindrica* respiration rates, chlorophyll *a* concentration, symbionts density and Fv/Fm were not affected either by sunscreen exposure or temperature increase. Conversely net photosynthesis was significantly affected by sunscreen ($p_{sunscreen}$ = 0.014, Table 3.8), with both concentration treatments significantly reducing oxygen fluxes under light conditions (Tukey post hoc test $p_{0.1\ mgL\text{-}1}$ = 0.003 and $p_{1\ mgL\text{-}1}$ = 0.004, Table 3.9). As a consequence, sunscreen also significantly reduced the ratio of photosynthesis to respiration ($p_{sunscreen}$ = 0.0001, Table 3.8), that fell below 1 in both sunscreen treatments at day 4 and day 8 (Figure 3.5). In contrast, *S. hystrix* was acutely affected by sunscreen, which exposure significantly reduced chlorophyll a concentration ($p_{sunscreen}$ = 0.008), Symbiodiniaceae density ($p_{sunscreen}$ = 0.0009), Fv/Fm (p = 0.02) and net photosynthesis ($p_{sunscreen}$ = 0.003) (Table 3.10), with sunscreen treatments significantly reduced compared to control (Table 3.11). The photosynthesis/respiration ratio also declined under sunscreen exposure ($p_{sunscreen}$ = 0.003), although its values remained above 1 in all timepoints (Figure 3.6, Table 3.10).

Overall, inorganic sunscreen was the main factor driving the variations of the studied endpoints in the warming experiments. Temperature is significant, along with sunscreen, only in two-way Anova analyses of *P. cylindrica* P_{gross}:R ratio ($p_{temperature}$ = 0.0007, Table 3.8) and *S. hystrix* symbionts density ($p_{temperature}$ = 0.0006) and P_{gross}:R ratio ($p_{temperature}$ = 0.03). Only in *S. hystrix* net photosynthetic rate a significant interaction of sunscreen and temperature was revealed ($p_{sunscreen}$:time = 0.04, Table 3.10).

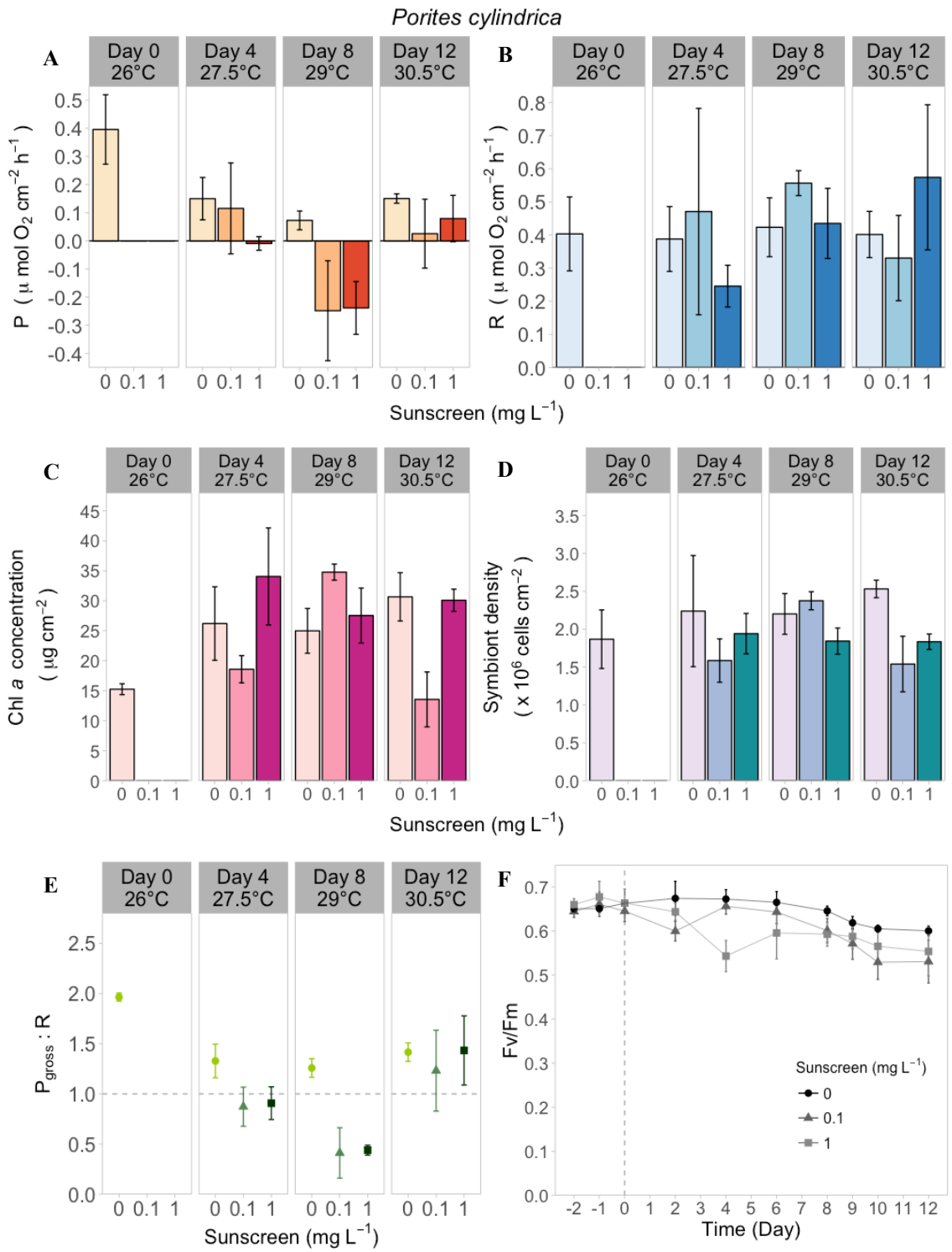

Figure 3.5 - *Porites cylindrica* endpoint measures of sunscreen exposure under thermal stress on physiological parameters (mean ± SEM, n=4): **A**) net photosynthesis, **B**) respiration, **C**) chlorophyll *a* concentration, **D**) Symbiodiniaceae density, **E**) gross photosynthesis to respiration ratio and **F**) Fv/Fm. Darker colours in the graphs A-E indicate increasing sunscreen concentration as stated in the *x*-axis.

Table 3.8 - Two-way Anova results on *Porites cylindrica* measurements from the elevated temperature experiment. Data were ln-transformed (''*'') when appropriate and statistically significant effects are highlighted in bold. Df: degrees of freedom, SS: sum of squares.

Source of variation	Df	SS	F-value	p-value
Net photosynthesis				
Sunscreen	12	0.5613	4.892	**0.014**
Day	1	0.0688	1.199	0.28
Sunscreen:Day	12	0.0867	0.756	0.48
Respiration			*	
Sunscreen	12	0.0004	0.006	0.99
Day	1	0.0133	0.414	0.52
Sunscreen:Day	12	0.0824	1.281	0.29
P_{GROSS} *: R*			*	
Sunscreen	12	0.8605	12.145	**0.0001**
Day	1	0.8034	7.559	**0.0007**
Sunscreen:Day	12	0.2237	1.579	0.21
Symbionts density			*	
Sunscreen	12	0.1053	1.002	0.38
Day	1	0.0458	0.872	0.37
Sunscreen:Day	12	0.0713	0.678	0.51
Chl a concentration				
Sunscreen	12	453	2.318	0.11
Day	1	81	0.828	0.37
Sunscreen:Day	12	406	2.076	0.14
Fv/Fm				
Sunscreen	2		3.779	0.06
Error	9			

Table 3.9 - Tukey Post-hoc test results of all pairwise comparisons among sunscreen treatments for *P. cylindrica* measurements in the elevated temperature experiment. Statistically significant differences are highlighted in bold.

Pairwise comparisons		p-value
Net photosynthesis		
0 mgL^{-1}	0.1 mgL^{-1}	**0.041**
0 mgL^{-1}	1 mgL^{-1}	**0.025**
1 mgL^{-1}	0.1 mgL^{-1}	0.976
P_{GROSS} *: R*		
0 mgL^{-1}	0.1 mgL^{-1}	**<0.0001**
0 mgL^{-1}	1 mgL^{-1}	**0.001**
1 mgL^{-1}	0.1 mgL^{-1}	0.900

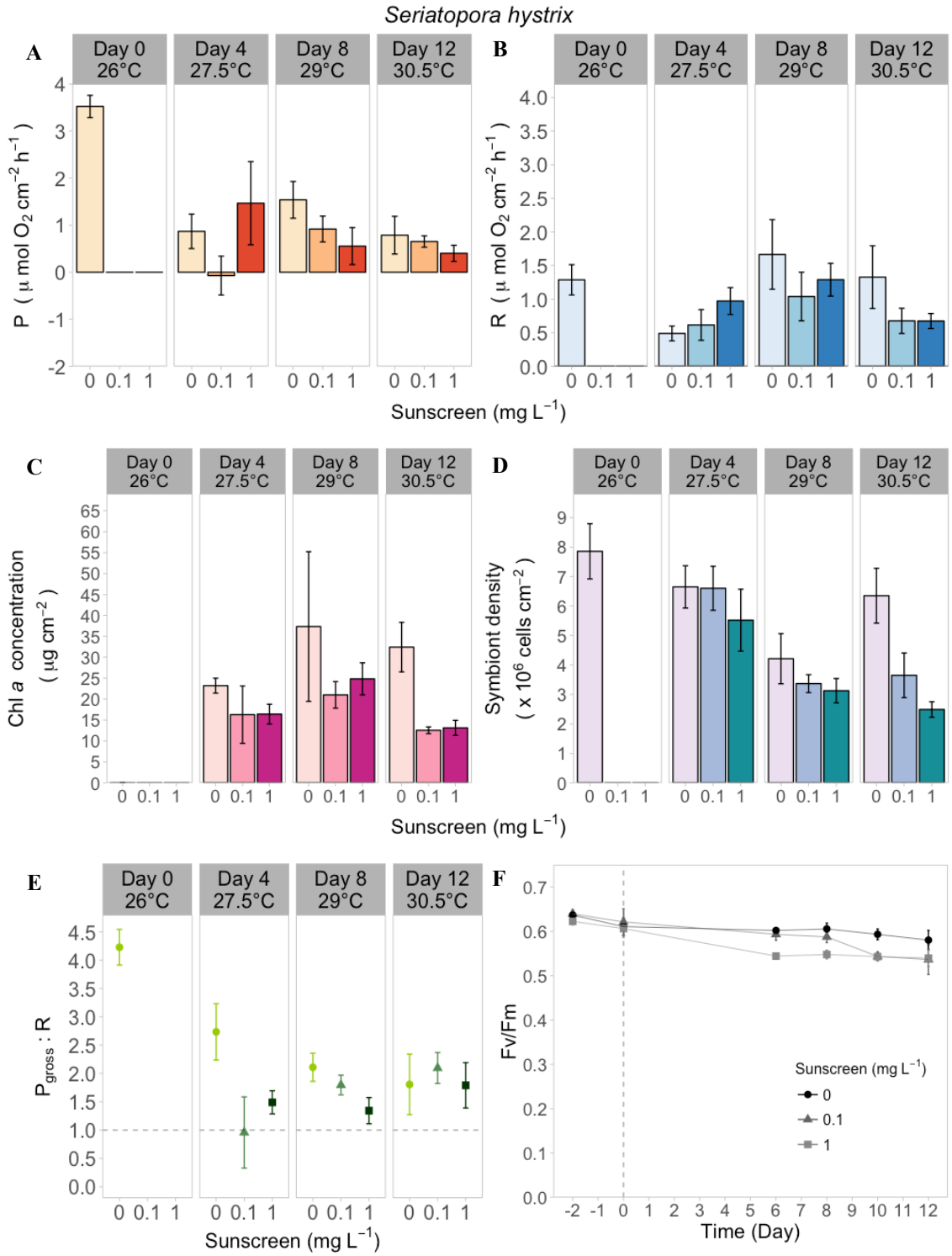

Figure 3.6 - *Seriatopora hystrix* endpoint measures of sunscreen exposure under thermal stress on physiological parameters (mean ± SEM, n=4): **A**) net photosynthesis, **B**) respiration, **C**) chlorophyll *a* concentration, **D**) Symbiodiniaceae density, **E**) gross photosynthesis to respiration ratio and **F**) Fv/Fm. Darker colours in the graphs A-E indicate increasing sunscreen concentration as stated in the *x*-axis.

Table 3.10 - Two-way Anova results on *Seriatopora hystrix* measurements from the elevated temperature experiment. Data were either ln- (''*'') or square root- (''$'') transformed, and statistically significant effects are highlighted in bold. Df: degrees of freedom, SS: sum of squares.

Source of variation	Df	SS	F-value	p-value
Net photosynthesis			*	
Sunscreen	12	2.67	6.836	**0.003**
Day	1	0.026	0.135	0.72
Sunscreen:Day	12	2.222	5.689	**0.008**
Respiration			*	
Sunscreen	12	0.0497	0.318	0.73
Day	1	0	0	0.99
Sunscreen:Day	12	0.137	0.877	0.43
P_{GROSS} *: R*			$	
Sunscreen	12	1.1925	7.417	**0.003**
Day	1	0.8672	3.596	**0.03**
Sunscreen:Day	12	0.8422	2.619	0.059
Symbionts density				
Sunscreen	12	48.09	8.624	**0.0009**
Day	1	39.77	14.264	**0.0006**
Sunscreen:Day	12	5.7	1.022	0.37
Chl a concentration			*	
Sunscreen	12	2.051	5.852	**0.008**
Day	1	0.008	0.044	0.83
Sunscreen:Day	12	0.263	0.751	0.48
Fv/Fm				
Sunscreen	2		5.657	**0.02**
Error	9			

Table 3.11 - Tukey Post-hoc test results of all pairwise comparisons among sunscreen treatments for *S. hystrix* measurements in the elevated temperature experiment. Statistically significant differences are highlighted in bold.

Pairwise comparisons		p-value
Net photosynthesis		
0 mgL^{-1}	0.1 mgL^{-1}	**0.003**
0 mgL^{-1}	1 mgL^{-1}	**0.004**
1 mgL^{-1}	0.1 mgL^{-1}	0.999
P_{GROSS} *: R*		
0 mgL^{-1}	0.1 mgL^{-1}	**0.010**
0 mgL^{-1}	1 mgL^{-1}	**0.008**
1 mgL^{-1}	0.1 mgL^{-1}	1.000
Symbionts density		
0 mgL^{-1}	0.1 mgL^{-1}	**0.028**
0 mgL^{-1}	1 mgL^{-1}	**0.001**
1 mgL^{-1}	0.1 mgL^{-1}	0.454
Chl a concentration		
0 mgL^{-1}	0.1 mgL^{-1}	**0.009**
0 mgL^{-1}	1 mgL^{-1}	**0.039**
1 mgL^{-1}	0.1 mgL^{-1}	0.762
Fv/Fm		
0 mgL^{-1}	0.1 mgL^{-1}	0.186
0 mgL^{-1}	1 mgL^{-1}	**0.002**
1 mgL^{-1}	0.1 mgL^{-1}	0.242

3.3.3 Effect of sunscreen and combined temperature at each timepoint

Measurements taken at each sampling timepoint (coinciding with the different temperatures tested) were analysed with two-way Anova to compare the effects of sunscreen at ambient temperature versus simultaneous elevated temperature conditions. Results from the two-way Anova analyses for *P. cylindrica* measurements are presented in Table 3.12 and for *S. hystrix* in Table 3.13. *S. hystrix* Fv/Fm values between 29th June and 3rd July 2018, corresponding to days 7-10 of the ambient temperature experiment and days 2-5 of the elevated temperature experiment, are missing due to a malfunction of the Diving-PAM storage capacity. Thus the comparison of Fv/Fm values between control and heated experiment was possible only for day 12.

Temperature alone did not have a marked negative effect on coral physiological performances and the two coral species exhibited different responses. Nevertheless, chlorophyll and symbionts contents, Fv/Fm and oxygen production and consumption were significantly influenced by both sunscreen and elevated temperature in the majority of treatments.

The increase of 1.5°C above ambient temperature (27.5°C, day 4) did not have an effect on *P. cylindrica*, which exhibited unchanged physiological performances compared to ambient temperature, only Fv/Fm was significantly reduced by the effect of sunscreen. *S. hystrix* instead was significantly affected by temperature, that reduced chl *a* concentration (~ 54%), Symbiodiniaceae density (~ 18%), and respiratory and net photosynthetic rates (~ 74% altogether for control and 0.1 mgL^{-1} fragments). The metabolic performances were also significantly reduced by sunscreen exposure, but only dark respiration showed an interactive effect of sunscreen and temperature (Table 3.13).

At + 3°C above ambient (day 8), the two coral species displayed divergent responses towards elevated temperature. Warming induced a general decrease in all endpoints studied for *S. hystrix*, although it was only significant for Symbiodiniaceae density ($p_{temperature}$ = 0.0003) and P_{gross}:R ratio ($p_{temperature}$ = 0.02). Contrarily, *P. cylindrica* exhibited a significant increase in dark respiration ($p_{temperature}$ = 0.02) along with a slight, not significant, increase of chl *a* and symbionts in fragments simultaneously exposed to sunscreen. Contrary to elevated temperature, sunscreen alone had a definite negative effect in both corals, significantly reducing P_{gross}:R ratio ($p_{sunscreen}$ = 0.003 in *S. hystrix* and <0.0001 in *P. cylindrica*) and Symbiodiniaceae density ($p_{sunscreen}$ = 0.002 in *S. hystrix*

and 0.01 in *P. cylindrica*), in addition to net photosynthesis and respiration of *S. hystrix* ($p_{sunscreen}$ = 0.009 and 0.04, respectively) and Fv/Fm of *P. cylindrica* ($p_{sunscreen}$ = 0.009). Finally, at 30.5°C (4.5°C above ambient, day 12) coral responses were similar to those at 29°C. *S. hystrix* fragments simultaneously exposed to elevated temperature and sunscreen exhibited the lowest amount of chl *a* and symbiont densities (approximately 50% less than untreated fragments, which showed values similar to the time-matching control at 26°C). Similarly, temperature and sunscreen exposure significantly decreased *S. hystrix* dark respiration and net photosynthesis ($p_{sunscreen}$ = 0.003 and 0.005 for net photosynthesis and respiration, respectively; $p_{temperature}$ respiration < 0.0001 and $p_{temperature:sunscreen}$ net photosynthesis = 0.03). In contrast, fragments of *P. cylindrica* under warming conditions maintained the increase of chl *a* and Symbiodiniaceae contents and dark respiration compared to time-matching values at 26°C observed at day 8, in addition to an increase in the net photosynthetic rates too, despite this temperature effect not being significant for respiration but significant for Symbiodiniaceae density ($p_{temperature}$ = 0.03), net photosynthesis ($p_{temperature}$ = 0.04) and P_{gross}:R ratio ($p_{temperature}$ = 0.03). The negative impact of sunscreen exposure was also mitigated in *P. cylindrica* when combined with elevated temperatures, nevertheless its effect remained significant for Symbiodiniaceae density ($p_{sunscreen}$ = 0.001).

Tables summarizing the responses of each endpoint are presented in Table 3.14 and Table 3.15 for P. cylindrica and S. hystrix, respectively.

Table 3.12 - Two-way Anova results on *Porites cylindrica* measurements from each temperature tested. Data were either ln- (‘‘*’’) or sin- (‘‘†’’) transformed, and statistically significant effects are highlighted in bold. Df: degrees of freedom.

	Day 4: 26 vs 27.5 °C			**Day 8: 26 vs 29 °C**			**Day 12: 26 vs 30.5 °C**		
	Df	**F-value**	**p-value**	**Df**	**F-value**	**p-value**	**Df**	**F-value**	**p-value**
Net photosynthesis		†							
Sunscreen	2	2.049	0.16	*Friedman rank sum test*			2	1.979	0.17
Temperature	1	0.074	0.79	*Df*	*χ2*	*p-value*	1	4.818	**0.04**
Sunscreen:Temp	2	0.056	0.95	2	3	0.2	2	0.654	0.15
Respiration									
Sunscreen	*Friedman rank sum test*			2	0.359	0.7	*Friedman rank sum test*		
Temperature	*Df*	*χ2*	*p-value*	1	6.67	**0.02**	*Df*	*χ2*	*p-value*
Sunscreen:Temp	2	1	0.6	2	0.432	0.65	2	3	0.22
P_{GROSS} : *R*									
Sunscreen	2	4.042	**0.04**	2	18.636	**<0.0001**	12	0.908	0.42
Temperature	1	0.037	0.85	1	10.429	**0.005**	1	5.245	**0.03**
Sunscreen:Temp	2	0.762	0.48	2	1.128	0.35	12	0.813	0.46
Symbionts density									
Sunscreen	2	2.883	0.08	2	5.463	**0.014**	2	10.144	**0.001**
Temperature	1	0.153	0.7	1	0.038	0.85	1	5.385	**0.03**
Sunscreen:Temp	2	0.663	0.53	2	2.087	0.15	2	3.18	0.06
Chl a concentration								*	
Sunscreen	2	0.6	0.56	2	0.984	0.39	2	2.773	0.09
Temperature	1	0.022	0.88	1	0.929	0.35	1	1.227	0.28
Sunscreen:Temp	2	1.992	0.16	2	1.012	0.38	2	3.518	0.052
Fv/Fm									
Sunscreen	2	8.108	**0.003**	2	6.107	**0.009**	2	2.044	0.16
Temperature	1	4.274	0.053	1	5.08	**0.03**	1	0.387	0.54
Sunscreen:Temp	2	1.916	0.17	2	3.305	0.059	2	0.178	0.84

Table 3.13 - Two-way Anova results on *Seriatopora hystrix* measurements from each tested timepoint. Data were either ln- (‘‘*’’) or square root- (‘‘$’’) transformed, and statistically significant effects are highlighted in bold. Df: degrees of freedom.

	Day 4: 26 vs 27.5 °C			**Day 8: 26 vs 29 °C**			**Day 12: 26 vs 30.5 °C**		
	Df	**F-value**	**p-value**	**Df**	**F-value**	**p-value**	**Df**	**F-value**	**p-value**
Net photosynthesis									
Sunscreen	2	11.528	**0.0007**	2	6.063	**0.009**	2	7.999	**0.003**
Temperature	1	8.831	**0.008**	1	3.31	0.08	1	2.793	0.11
Sunscreen:Temp	2	3.26	0.06	2	0.448	0.64	2	4.134	**0.03**
Respiration					*				
Sunscreen	2	1.849	0.19	2	3.302	0.06	2	7.124	**0.05**
Temperature	1	5.131	**0.04**	1	0.001	0.98	1	27.352	**<0.0001**
Sunscreen:Temp	2	8.693	**0.003**	2	1.991	0.17	2	2.455	0.11
P_{GROSS} : *R*									
Sunscreen	2	6.518	**0.01**	2	8.101	**0.003**	12	2.345	0.13
Temperature	1	1.06	0.32	1	6.514	**0.02**	1	14.116	**0.002**
Sunscreen:Temp	2	0.229	0.79	2	1.364	0.28	12	2.548	0.1
Symbionts density					*				
Sunscreen	2	0.546	0.59	2	8.627	**0.002**	2	11.254	**0.0007**
Temperature	1	6.451	**0.02**	1	19.497	**0.0003**	1	2.126	0.16
Sunscreen:Temp	2	0.35	0.7	2	2.727	0.09	2	0.656	0.53
Chl a concentration		*						$	
Sunscreen	2	2.251	0.14	2	1.529	0.25	2	1.655	0.22
Temperature	1	16.807	**0.001**	1	0.051	0.82	1	0.002	0.97
Sunscreen:Temp	2	0.607	0.56	2	0.074	0.93	2	1.254	0.31
Fv/Fm									
Sunscreen							2	1.548	0.24
Temperature							1	2.904	0.11
Sunscreen:Temp							2	0.021	0.98

Table 3.14 - Summary table with the main responses of all physiological variables for *P. cylindrica* at each sampling day relative to the time-matching control treatment (26°C). Trends are indicated as decrease (↓), increase (↑), or no change (↔).

P. cylindrica	**Day 4 27.5 °C**	**Day 8 29 °C**	**Day 12 30.5 °C**
Net photosynthesis	↔	↔	↓
Respiration	↔	↑	↔
P_{GROSS} : R	↓	↓	↓
Symbionts density	↔	↓	↓
Chl *a* concentration	↔	↔	↔
Fv/Fm	↓	↓	↔

Table 3.15 - Summary table with the main responses of all physiological variables for *S. hystrix* at each sampling day relative to the time-matching control treatment (26°C). Trends are indicated as decrease (↓), increase (↑), or no change (↔).

S. hystrix	**Day 4 27.5 °C**	**Day 8 29 °C**	**Day 12 30.5 °C**
Net photosynthesis	↓	↓	↓
Respiration	↓	↔	↓
P_{GROSS} : R	↓	↓	↓
Symbionts density	↓	↓	↓
Chl *a* concentration	↓	↔	↔
Fv/Fm	/	/	↔

3.4 Discussion

In this study, the effects of isolated and combined inorganic sunscreen and elevated temperatures projected for the end of the century (IPCC, 2014, 2018) were examined on two common reef-building coral species. Sunscreen exposure caused an overall decline of *S. hystrix* and *P. cylindrica* photo-physiological performances, both alone and with simultaneous temperature increase. Results suggest that inorganic sunscreen formulations have a greater detrimental impact on corals photo-physiological performances than short term thermal stress resulting from a gradual temperature increase, and no interacting effect with high temperature was detected.

3.4.1 Effect of inorganic sunscreen formulation on coral physiology

At ambient temperature, exposure to increasing sunscreen concentrations had a significant negative impact on coral physiological performances. Consistently between the two species studied, net respiration, Fv/Fm, symbionts density and chl *a* concentration significantly decreased under sunscreen exposure and the effect was intensified with the exposure time.

Respiration and net photosynthesis values measured in control fragments were comparable to those measured in previous studies for the same coral species. For example, *P. cylindrica* respiration rates measured by Nyström et al. (2001) ranged between approximately 8 and 18 µg O_2 cm^{-2} h^{-1} in control conditions, equivalent to 0.25 – 0.56 µmol O_2 cm^{-2} h^{-1}, while Noonan and Fabricius (2016) and Strahl et al. (2015) measured *S. hystrix* net photosynthetic rate in ~ 40 µg O_2 cm^{-2} h^{-1}, equivalent to 1.25 µmol O_2 cm^{-2} h^{-1}. Net oxygen production was the parameter most significantly affected by sunscreen exposure, which induced a shift from production to consumption under illumination (Figure 3.4A and Figure 3.5A). Similar negative net photosynthetic rates were measured by Lürig and Kunzmann (2015) and Middlebrook et al. (2012) in corals exposed to elevated temperature (3 and 7°C, respectively, above ambient) for 24-48 hours. Moreover, declined coral net photosynthesis was measured as a response to copper (Alutoin et al., 2001; Banc-Prandi and Fine, 2019; Nyström et al., 2001) and the herbicide diuron (Råberg et al., 2003). In all the aforementioned studies, it was suggested that heat-stress, copper and diuron directly damaged the photosynthetic apparatus of the algal symbionts by inhibiting the electron transport rate of PSII. Similarly, photoinhibition of Symbiodiniaceae photosynthetic activity, leading to symbionts expulsion from coral host,

was detected in the corals *Montastreaea faveolata* and *Acropora* spp. exposed to both uncoated (10 mgL^{-1}) (Jovanović and Guzmán, 2014) and dimethicone and manganese coated (6.3 mgL^{-1}) (Corinaldesi et al., 2018) $nTiO_2$, as a result of $nTiO_2$-induced oxidative stress. In this study, the decline in photosynthetic rate occurred along with an important decrease in the number of symbionts inhabiting corals tissue. Indeed, Symbiodiniaceae experienced a decline of 33% and 45% in the 0.1 mgL^{-1} treatment group and 25% and 61% under 1 mgL^{-1} concentration, for *S. hystrix* and *P. cylindrica* respectively, values indicating partial bleaching of the coral fragments (Desalvo et al., 2008). Here sunscreen exposure had a greater impact on coral photosynthetic rates and zooxanthellae density than the effects observed for copper, diuron and $nTiO_2$ individual exposure (Alutoin et al., 2001; Banc-Prandi and Fine, 2019; Corinaldesi et al., 2018; Jovanović and Guzmán, 2014; Nyström et al., 2001; Råberg et al., 2003), likely because corals are exposed to the whole mixture of sunscreen ingredients, and not the single UV filter (results similar to the ones presented in Chapter 2). $nTiO_2$ contained in sunscreen and released in surface water through bathing activities produce high quantities of hydrogen peroxide in seawater (Sánchez-Quiles and Tovar-Sánchez, 2014), more than $nTiO_2$ alone due to interaction with organic compounds in the formulation (Sendra et al., 2017b). The production of hydrogen peroxide in *in-hospite* Symbiodiniaceae following heat-stress is suggested to be the triggering signal that lead to symbionts expulsion from coral host during a bleaching event (Smith et al., 2005). Thus sunscreen is likely to impact both algal symbionts and coral host simultaneously, resulting in a detrimental impact on coral health. The mechanism proposed here for inorganic sunscreen toxicity comprises two modes of action acting simultaneously. $nTiO_2$ UV filters, alone or together with the other sunscreen ingredients, induce oxidative stress in *in-hospite* Symbiodiniaceae causing the production of ROS, the decline of their photosynthetic activity and, lastly, the symbionts expulsion from the host. At the same time, hydrogen peroxide produced by sunscreen ingredients in the water surrounding coral colonies acts directly on the coral host leading to symbiont expulsion. As a result, coral net oxygen production and zooxanthellae density are highly affected by sunscreen exposure while Fv/Fm values undergo a moderate but significant decline, as observed in the present study and in the Symbiodiniaceae experiments (Chapter 2).

S. hystrix and *P. cylindrica* respiration rates maintained constant values among treatments, consequently the gross photosynthetic production to respiration ratio fell below 1. P_{gross}:R ratio reveals the autotrophic capacity of corals, with P_{gross}:R > 1

indicating that *in-hospite* Symbiodiniaceae are able to support the coral host through their photosynthetic activity while P_{gross}:R < 1 indicates the necessity of heterotrophic carbon uptake (Muscatine et al., 1981). Here the observed *P. cylindrica* and *S. hystrix* P_{gross}:R < 1 with increasing sunscreen concentration and exposure time suggests that the energetic costs associated with sunscreen exposure elicit the consumption of the energy reserves of the coral host. The reduction of energy reserves prior to a bleaching event has been linked to higher mortality after the bleaching event (Anthony et al., 2009), hence sunscreen may increase the vulnerability of corals to bleaching and following mortality. Calcification and respiration in symbiotic corals are coupled processes (Allemand et al., 2004; Gattuso et al., 1999) and calcification requires a considerable amount of energy (Allemand et al., 2011). The increased metabolic demand due to sunscreen exposure may therefore reduce the capacity of corals to maintain their calcification rates. Measurement of coral calcification was not part of this study, however as support of this suggestion Al-Horani et al. (2005) measured a decrease of *Galaxea fascicularis* calcification at elevated temperature rate that was directly linked to the coral's negative net photosynthetic rate. Coral calcification is thus suggested to be an important endpoint to be evaluated in future sunscreen toxicity experiments.

3.4.2 Combined effect of sunscreen and temperature increase

Contrary to the original hypothesis, combined temperature and sunscreen exposure had a significant effect on coral physiological performances but to a lesser extent than sunscreen alone. It was originally hypothesized that the oxidative stress induced by elevated temperature would have been enhanced by the simultaneous exposure to increasing sunscreen concentrations, as observed in corals simultaneously exposed to heat-stress and metals such as copper (Banc-Prandi and Fine, 2019) and iron (Biscéré et al., 2018). However, sunscreen is the main factor driving the negative effects observed here under elevated temperature, and elevated temperature seems to mitigate the impact of sunscreen in the combined treatments.

Coral species tested here are common branching corals in the Indo-Pacific known to have different sensitivity to thermal stress: while *P. cylindrica* is a tolerant species (Fitt et al., 2009; Loya et al., 2001; Palmer, 2018; Veron, 2000), *S. hystrix* is highly susceptible to environmental perturbations (Baird and Marshall, 2002; Hughes et al., 2018b; Loya et al., 2001; Noonan and Fabricius, 2016; Van Woesik et al., 2011). Findings here are in agreement with the known susceptibility of the tested coral species, with *P. cylindrica*

appearing more tolerant than *S. hystrix* towards temperature stress conditions studied here. While warming induced a general reduction of *S. hystrix* tested parameters, *P. cylindrica* showed an increase of respiration, net photosynthesis and Symbiodiniaceae density at 29°C and 30.5°C (Figure 3.5 and 3.6). The differences in thermal tolerance between *P. cylindrica* and *S. hystrix* observed in this study may be influenced by their symbiont population as well the characteristics of the coral host (Baker, 2003). It is not possible here to attribute the observed different sensitivities to corals *in-hospite* Symbiodiniaceae types, as Symbiodiniaceae assessment was not performed. Different symbionts types have different temperature tolerance (Berkelmans and Van Oppen, 2006), so coral fragments here belonging to different parental colonies were divided evenly among treatments to reduce biasing caused by different symbiont identities or coral genotypes. Nevertheless, the relative tolerance of *P. cylindrica* to thermal stress is not surprising, as previous studies demonstrated that *P. cylindrica* was able to tolerate up to 5 days exposure to a 2°C and 4°C temperature increase without reducing symbionts density or Fv/Fm (Fitt et al., 2009; Nordemar et al., 2003), similar to results reported here. Although temperature is widely recognized as the main stressor affecting coral health (Fitt et al., 2001; Lesser, 2011; Weis, 2008; Wild et al., 2011), a positive effect of temperature in corals simultaneously exposed to multiple stressors has been observed in previous studies. For example, Krueger et al. (2017) measured a significant increase in *P. cylindrica* P_{gross}:R ratio under combined warming and low pH. Also, *Mussismilia harttii* was more tolerant to the negative effects of copper exposure when pre-exposed to elevated temperature (Fonseca et al., 2017). Moreover, the simultaneous exposure to elevated salinity and warming mitigated the negative effect of each stressor alone on *Montastrea annularis* respiration rates (Porter et al., 1999). It is possible that the induction of heat shock proteins by elevated temperatures increases coral tolerance towards sunscreen exposure, as suggested for the improved tolerance of *P. cylindrica* to copper toxicity under combined thermal stress (Nyström et al., 2001). High temperatures may also induce changes in the lipid composition and properties of cellular membranes that alter their diffusion rates and thus the toxicity of a chemical substance (Van Dam et al., 2011). As a result, only minor effects of elevated temperatures on coral physiological performances, symbiont density and chlorophyll *a* concentration were measured in this study, and no interacting effect with sunscreen was detected. Contrary to the ambient temperature experiment where the ratio of gross photosynthesis to respiration was <1, the P:R of ~ 1.2-2 measured in *P. cylindrica* at 30.5°C and *S. hystrix* under all temperatures

suggests that algal symbionts are able to support completely their coral host through the translocation of photosynthates (Muscatine et al., 1981).

In natural environments, coral bleaching is induced when corals experience 1-2°C above average seawater temperature for several weeks or by an acute exposure of 3-4°C above ambient temperatures over few days (Fitt et al., 2001; Fordyce et al., 2019; Jokiel and Coles, 1990; Leggat et al., 2019). In a controlled experimental environment, corals have been demonstrated to vary their responses towards thermal stress according to the heating method used in the experimental design and the coral thermal history. Different cellular pathways are indeed induced in corals slowly taken to warming conditions compared to rapid heating (Krueger et al., 2015). Here corals were subjected to short term, not acute thermal stress, following a gradual temperature increase over several days. The heating rate of 0.5°C day^{-1} used in this experiment is representative of a realistic temperature profile occurring during a natural bleaching event (Krueger et al., 2015), but it significantly delayed *Acropora formosa* physiological responses compared to a rapid heating of 1°C day^{-1} (Middlebrook et al., 2010). Likewise, coral acclimated to elevated, sub-lethal temperatures significantly increased Fv/Fm, photosynthetic rate and chlorophyll content during heat stress (Barott et al., 2018; Middlebrook et al., 2008; Nyström et al., 2001). This may explain the lack of significant detrimental effects here during the thermal stress experiment, while the increase in physiological performances observed at 30.5°C may indicate compensation mechanisms in order to repair the metabolic processes previously altered during the gradual temperature increase (Gates and Edmunds, 1999). The absence of interacting effects between sunscreen exposure and elevated temperature on corals photo-physiological performances within the experimental thermal range may be due to the increased rates of protein repair in the coral host as well as in the symbionts' PSII under thermal stress (Jones, 2004). Indeed Fitt et al. (2009) measured high expression of both heat shock proteins and PSII protein D1 in *P. cylindrica* at 32°C with just a slight change in its Fv/Fm values. A similar effect was proposed in Chapter 2 to explain the positive impact of combined $nTiO_2$ and temperature stress on Symbiodiniaceae photosynthetic activity.

It is unknown whether a longer period of exposure to sunscreen and elevated temperature would have resulted in a significant negative effect of temperature, but the positive effects of temperature observed here when combined with sunscreen treatments are likely temporary. As support of this, previous studies described the detrimental effects of

temperature in long term experiments (Courtial et al., 2017; Silverstein et al., 2015). Moreover, the mitigating effect of combined temperature and salinity exposure on *Montastrea annularis* P:R ratios observed by Porter et al. (1999) disappeared in the longer exposure time and corals died. Also, Banc-Prandi and Fine (2019) observed that Fv/Fm and net photosynthesis of corals at 4°C above ambient temperature significantly changed from 72h to two-weeks exposure time, suggesting that longer exposures are better to explain coral responses under stressful conditions. Further studies should thus evaluate corals response under a chronic exposure to sunscreen and elevated temperature, both alone and combined, to verify the hypothesis of the detrimental impact of both stressors in the long term and the recovery capacity of corals once the stressors are over.

3.5 Conclusion

Results here show for the first time, the effects of a common sunscreen product formulated with $nTiO_2$ on two common coral species. Levels of sunscreen actually released into coastal surface waters are currently unknown, however the nominal highest sunscreen concentration tested in this study represents the concentration of inorganic $nTiO_2$-sunscreen expected to be released in a touristic beach during a summer day (Chapter 1, section 1.2.5). Despite the different sensitivity of *P. cylindrica* and *S. hystrix* observed under thermal stress, twelve days exposure to sunscreen expected environmental concentrations induced significant detrimental effects on the photo-physiological performances of both corals. These effects were intensified with time. Inorganic sunscreen formulations may exert a double pressure on reef-building corals, with sunscreen ingredients directly impacting *in-hospite* Symbiodiniaceae populations inducing oxidative stress, and hydrogen peroxide produced in the surrounding waters through photocatalytic reactions acting on the coral host to promote zooxanthellae expulsion. As a consequence, sunscreen exposure here led to partial bleaching in the exposed coral fragments, in addition to a reduction of metabolic performances, instigating a shift from oxygen production to net oxygen consumption, and Fv/Fm decline even at the lowest tested concentration.

The effects of heat stress on corals have been widely studied, however the combined impacts of elevated temperature with local stressors are poorly understood, and results vary depending on stressor, coral species and the nature of heat stress experimental design (Baker et al., 2008; Krueger et al., 2015; Middlebrook et al., 2008). In this study temperature was slowly increased by 0.5°C day^{-1}, and coral physiological performances

were measured after a short-term exposure (24h) at the target thermal conditions. While the heating rate applied here is more representative of a natural bleaching event than rapid heating conditions (Krueger et al., 2015), it likely caused a delay in coral responses due to acclimation to sub-lethal temperatures (Barott et al., 2018; Middlebrook et al., 2008, 2010). Overall, elevated temperatures induced less detrimental effects on corals' oxygen fluxes, Symbiodiniaceae density and chlorophyll *a* concentration than inorganic sunscreen exposure, and the combination of stressors mitigated the negative effects of sunscreen alone.

Although results from the combined stressors experiments indicate that short-term heat stress conditions following a gradual temperature increase are unlikely to acutely affect coral metabolic activities, chronic elevated temperature experiments mimicking a real prolonged exposure to bleaching heat stress (as described by Eakin et al., 2016) would be necessary to accurately evaluate the consequences of inorganic sunscreen exposure during a natural bleaching event. Long-term experiments would also characterize coral response under environmentally relevant sunscreen conditions, since sunscreen compounds are likely quickly diluted soon after being released into the water column, and sunscreen products are also continuously released in highly populated coral reef areas due to constant touristic load.

In conclusion, this study provides insight into the photo-physiological responses of reef-building corals living in near-shore waters contaminated with $nTiO_2$-based sunscreen products. The inability of corals to cope with sunscreen exposure of 0.1 mgL^{-1} could compromise coral growth and calcification processes, eventually influencing reef functionality and stability in highly touristic coastal areas. To elucidate the mechanisms underlying potential stress, the next chapter explores the molecular impact of short-term sunscreen exposure.

Chapter 4

Photosynthetic and transcriptomic responses to short-term inorganic sunscreen and filter-free formulations exposure, alone and in combination with acute heat stress, in the coral model *Exaiptasia pallida*

4.1 Introduction

The aim of this chapter is to examine the findings of Chapter 2 that indicated the oil phase ingredients as the key drivers of sunscreen toxicity on Symbiodiniaceae, highlighting the importance of taking into account sunscreen's oil phase ingredients when assessing sunscreen toxicity. Therefore in this chapter the effects of a custom-made inorganic sunscreen formulation, resembling a commercially available sunscreen having $nTiO_2$ as active ingredient, were compared with the effects of its counterpart lacking UV filters but maintaining an identical composition formulation. The tropical sea anemone *Exaiptasia pallida* was chosen as model organism for this study because of its easiness of both handling and culturing in laboratory in large numbers. *E. pallida* has a wide geographic distribution and is commonly found in tropical and subtropical near-shore coastal environments (Shick, 2012), areas predicted to have the highest discharge of sunscreen products (Gondikas et al., 2014; Mitchelmore et al., 2019; Tovar-Sánchez et al., 2013). This species reproduces both asexually by pedal laceration and sexually by spawning (Trenfield et al., 2017), and lives in symbiotic relationship with dinoflagellate of the family Symbiodiniaceae. In the Indo-Pacific this anemone associate only with *Breviolum minutum* (ITS2 type B1), while local populations in the Atlantic can also harbour *Symbiodinium linucheae* (A4) and rarely the genus *Cladocopium* (Thornhill et al., 2013) Despite *E. pallida* anemones lack the calcareous skeleton characterizing reef-building corals and, contrarily to corals, are able survival indefinitely in an aposymbiotic state through heterotrophic feeding (Voolstra, 2013), they provide a reliable substitute of corals as model organism in toxicity studies (Howe et al., 2012, 2015; Lehnert et al., 2012; Rädecker et al., 2018; Trenfield et al., 2017; Voolstra, 2013). Exactly as in corals, environmental stressors such as global warming and contaminants may disrupt the symbiotic relationship between host anemones and their photosynthetic symbionts (Perez et al., 2001; Weis et al., 2008), inducing transcriptional responses that lead to the activation of stress-inducible genes (Black et al., 1995; Ellison et al., 2017; Rosic et al., 2011; Sunagawa et al., 2009) and causing a decline of *E. pallida in-hospite* Symbiodiniaceae photosynthetic efficiency (Howe et al., 2017; Patel and Bielmyer-Fraser, 2015).

Although the experiments presented in Chapter 2 showed that the effects of $nTiO_2$ sunscreen UV filters (i.e. having rutile core and hydrophobic or hydrophilic external protective coatings) on cultured Symbiodiniaceae were negligible, recent studies described the loss of symbionts from corals exposed to elevated concentrations of $nTiO_2$.

Acropora spp. showed reduction in Symbiodiniaceae abundance, but not visible bleaching, when exposed to 6.3 mgL^{-1} of sunscreen-type $nTiO_2$ (Corinaldesi et al., 2018) and *Montastraea faveolata* exhibited slight bleaching after exposure to 0.1 and 10 mgL^{-1} of anatase-$nTiO_2$ (i.e. not cosmetic type) (Jovanović and Guzmán, 2014). $nTiO_2$ photoactivation and consequent oxidative stress is considered the main form of $nTiO_2$ toxicity (von Moos et al., 2014) and it was hypothesized to be the cause of zooxanthellae expulsion in the aforementioned studies. As support of this theory, Jovanović and Guzmán (2014) measured upregulation of the gene for heat-shock protein 70 (Hsp70) in *Montastraea faveolata* samples showing reduction in symbiont abundance. Induction of Hsp70 gene expression has indeed been demonstrated to protect coral metabolic pathways from oxidative damage and restore cellular homeostasis during oxidative stress (Downs et al., 2002; Kalmar and Greensmith, 2009; Lesser, 2006; Seveso et al., 2016).

Heat-shock proteins (HSPs) are molecular chaperones well known for their defence role under environmental stress (Sørensen et al., 2003) thanks to their activity in repairing stress-damaged proteins thus helping them to recover their biological activity (Richter et al., 2010). Hsp70 and heat-shock protein 90 (Hsp90) are the two major HSPs families and their upregulation has been widely documented in corals and anemones under thermal stress (see review by Louis et al., 2017, and Kitchen and Weis, 2017). Alterations in Hsp70 and Hsp90 gene expression have also been reported for corals and *E. pallida* exposed to various anthropogenic contaminants, such as sedimentation (Poquita-Du et al., 2019), copper (Schwarz et al., 2013; Venn et al., 2009), oil dispersant (Venn et al., 2009), anthracene (Overmans et al., 2018), herbicide (Ishibashi et al., 2018), bacterial infections (Brown et al., 2013) and salinity stress (Ellison et al., 2017). Characterization of Hsp70 and Hsp90 expression profiles can therefore reveal the impacts of chemical contaminants as well as acute heat stress in symbiotic cnidarian. Upregulation of HSPs in corals during warming is detected at the initial stages of the stress response, prior to any photo-physiological dysfunction that ultimately leads to bleaching. Induction of HSPs at the onset of stress is indeed suggested to be a protective mechanism to prevent the onset of adverse physiological conditions as well as to postpone bleaching (Maor-Landaw et al., 2014; Rosic et al., 2014). Early changes in corals' transcriptomic profiles are thus important to determine corals' capacity to both react to warming and to return to normal cellular functions post stress conditions (Ainsworth et al., 2008; Seneca and Palumbi, 2015; Traylor-Knowles et al., 2017).

The experiments reported in Chapter 3 of this thesis showed that the simultaneous exposure to the sunscreen, having the same formulation that will be tested here, with short term thermal stress conditions, following a gradual temperature increase, did not significantly affect corals metabolic activities and photosynthetic efficiency. However, the molecular mechanisms of sunscreen effects on symbiotic cnidarians, alone and combined with acute thermal stress, remain unknown.

To test the hypothesis that sunscreen ingredients induce a rapid stress response in exposed anemones regardless the presence of UV filters in the formulation and that negative effects are intensified under simultaneous heat stress, in the study presented here Hsp70 and Hsp90 early gene expression responses were characterized in the sea anemone *E. pallida*, along with its maximum photosynthetic activity, following exposure to sunscreen and filter-free formulations under ambient (26°C) and elevated temperature (32°C) conditions. Specifically, the objectives of this study were: to i) measure the toxicity of an inorganic sunscreen on the tropical anemone *E. pallida*, ii) determine whether cosmetic formulations induce toxicity even lacking UV filters, iii) assess the combined effects of the tested formulations with elevated temperature known to induce bleaching in symbiotic cnidarians, iv) characterize the temporal expression of Hsp70 and Hsp90 at the onset of stress, precisely at 0h, the start of the experiment, and 3, 6, 24 hours post exposure to the two formulations and increased temperature, alone and combined.

Using *E. pallida* as model organism, findings from this study provide insight into the potential expression of stress-related genes in reef-building corals exposed to inorganic sunscreen, as well their transcriptomic responses in a bleaching scenario.

4.2 Materials and Methods

4.2.1 *Exaiptasia pallida* maintenance

Exaiptasia pallida (formerly *Aiptasia pallida*) sea anemones of the clonal strain CC7 (Sunagawa et al., 2009) were reared in static small tanks (1 or 1.5 L) with Instant Ocean® artificial seawater (35 ppt, pH = 8.2) (Figure 4.1).

Stock anemones were maintained in an incubator at 26°C under 40 µmol photons m^{-2} s^{-1} light intensity on a 12h light:12h dark cycle. Animals were fed with freshly hatched *Artemia salina* (brine shrimp larvae) three times per week and water was exchanged after ~ 5h from feeding, to allow time for the food to be consumed.

Figure 4.1 - *Exaiptasia pallida* anemones reared at Heriot-Watt university laboratories.

4.2.2 Sunscreen and filter-free formulation

Water in oil (w/o) sunscreen emulsion and filter-free formulation were custom made from cosmetic ingredients at CEREGE laboratories (Aix-en-Provence, France) under the supervision of Dr Jerome Labille as described in Chapter 3, section 3.2.1. Ingredients' characteristics are presented in Table 3.1.

Sunscreen was formulated with nTiO_2 Eusolex® T-S as UV filter at 10% concentration (the same formulation tested in the previous chapter); the filter-free formulation has the

same composition of the sunscreen but lacks UV filter (which is replaced by demineralized water).

4.2.3 Preparation of test solutions

Stock suspensions of 1 gL^{-1} were prepared by dispersing sunscreen and filter-free formulation in Milli-Q water and mixed well for 48 consecutive hours. Stock suspension bottles were stored in the dark in a refrigerator throughout the experimental period.

Twenty-four hours prior to test initiation, sunscreen and filter-free formulation test suspensions were prepared (nominal concentration: 50, 100, 500, 1000 μgL^{-1}) by adding aliquots of stock suspensions to filtered seawater and mixed overnight to allow for equilibration.

4.2.4 Experimental design

All animals used in the experiments were clones of the same parental anemones reproduced by pedal laceration. Forty-eight hours prior the start of the experiment, adult anemones with similar size (6.5 ± 1.5 cm) were removed from the culture tanks by gently scraping them from the tank surface. Anemone size was estimated using oral disc diameter, the widest distance between opposite tentacle (Perez et al., 2001), measured with a digital calliper placed above the oral disk without touching the animal (Figure 4.2 A). Oral disc diameter has been demonstrated to be correlated with wet weight of the anemone (Clayton and Lasker, 1985). Animals were then randomly placed into 6 well plates (1 anemone per well) and allowed to acclimate for 48 hours (Figure 4.2 B). Anemones that did not attach to the side of the well and/or did not expand fully were excluded from the experiment. Two simultaneous experiments were carried in two different temperature-controlled incubators set at 26°C for the ambient-temperature experiment and 32°C for the heat-stress experiment (Figure 4.3). In the heat-stress experiment, during the acclimation stage, temperature was raised from 26°C 1 degree per hour to reach 32°C at the start of the experiment (6°C above ambient temperature). On the day of the experiment, seawater into each well was replaced with sunscreen or filter-free formulation test solutions heated at the appropriate experimental temperature. For the qPCR assay, anemones were sampled at the start (0h) then after 3h, 6h and at the end (24h) (n=3 per timepoint per treatment). At the designated timepoints, anemones were flash-frozen in liquid nitrogen and stored at -80°C. Timepoints for gene expression

analysis were selected from a preliminary experiment designed to investigate the early expression of candidate genes in *Exaiptasia pallida* anemones under heat-stress at the same condition of the main experiment (Appendix B).

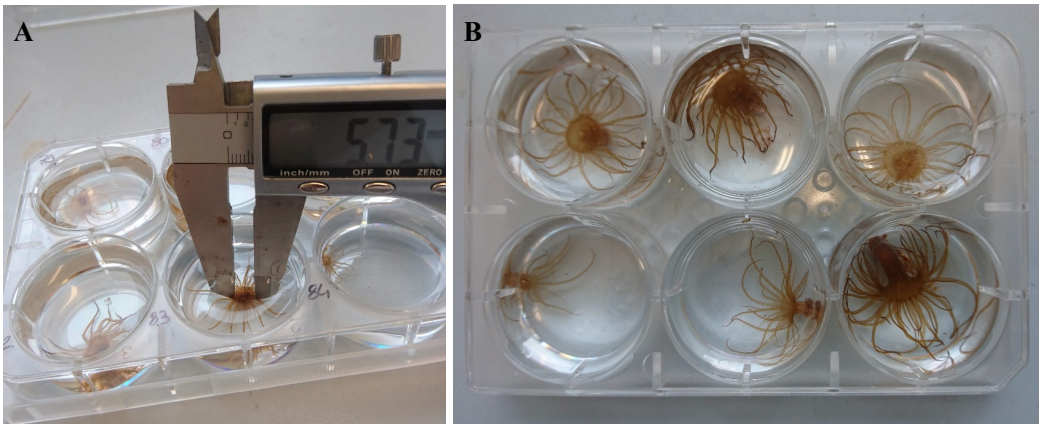

Figure 4.2 - **A**) Example of *E. pallida* anemones in the experimental 6-well plates, **B**) Calliper measurement of the anemone's oral disk diameter.

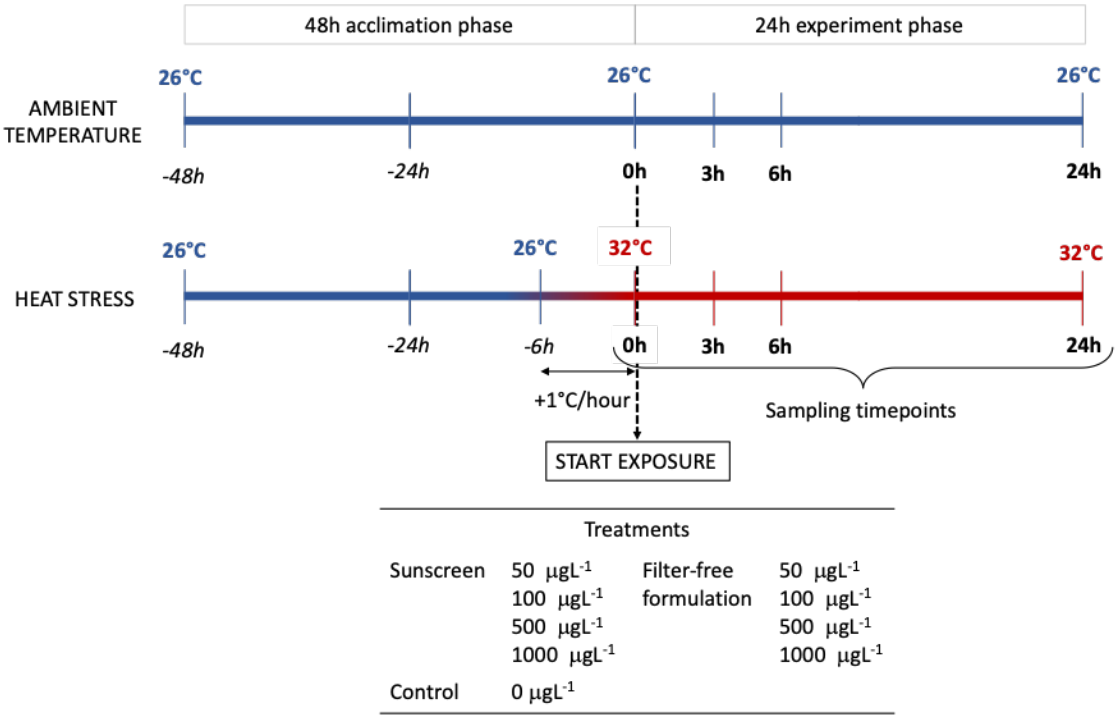

Figure 4.3 - Experimental design of *Exaiptasia pallida* exposure to the different treatments under ambient and heat stress conditions.

4.2.5 Photosynthetic measurements

Pulse amplitude modulated (PAM) fluorometry is a non-invasive technique widely used to measure changes in PSII photochemical efficiency of corals symbionts under heat and contaminant stress (Fitt et al., 2001; Fonseca et al., 2017; Jones et al., 1999; Jones and Kerswell, 2003; Warner et al., 1999). Recently it has also been recognized as a valuable tool for toxicological studies to measure pollutant effects on *Exaiptasia pallida* symbionts (Howe et al., 2017; Patel and Bielmyer-Fraser, 2015).

To determine the effects of sunscreen, filter-free formulation and heat exposure on anemones' photosynthetic efficiency, maximum quantum yield (Fv/Fm) of *E. pallida* anemones was measured using a Diving PAM chlorophyll fluorometer (Walz, Germany) at the start (0h) and at the end of the experiment (24h). Measurements were taken in randomly selected anemones from each treatment and temperature tested (n = 3 per treatment), after 20 minutes of dark-adaptation (lights off in the incubator), by placing the fibre optic of the Diving PAM 1–2 cm above the apical part of the anemone following the protocol by Howe et al. (2017). Twenty-four hours before the start of the experiment, during the acclimation stage, Fv/Fm was measured in random anemones (n = 10) from both incubators to confirm the animals were not stressed by the experimental incubation.

4.2.6 RNA extraction and cDNA synthesis

Total RNA was extracted from each anemone using the TRI Reagent® (Sigma-Aldrich) method following the manufacturer's protocol. To prevent sample contamination from DNA, traces of genomic DNA were removed with DNase treatment following the instruction provided by the DNase kit used (Primerdesign Ltd). RNA quality and quantity were then assessed by NanoDrop™ spectrophotometer (NanoDrop™ 2000, ThermoFisher Scientific (UK)). Only RNA samples that met the quality criteria (260/230 and 260/280 ratio of 1.8-2.2) were used for further analyses. RNA samples were stored at -80°C until required.

To obtain cDNA, reverse transcriptase PCR (RT-PCR) was performed on RNA samples diluted to a concentration of 100 ng/µL, using nanoScript™ 2 Reverse Transcription kits (PrimerDesign Ltd) following manufacturer's instructions. The annealing step of the RT-PCR was conducted at 65°C for 5min. After that, the extension step was carried out in 30 cycles of 42°C for 20min followed by the heat-inactivating transcriptase step at 75°C for 10min. cDNA samples were stored at -20°C until qPCR was performed. Both RT-PCR

steps were conducted on an Applied Biosystems Veriti™ 96-Well Thermal Cycler (ThermoFisher Scientific, UK). cDNA was stored at -20°C until the gene expression analyses were performed.

4.2.7 Quantitative Polymerase Chain Reaction (qPCR)

Hsp70 and Hsp90 were chosen as target genes based on their known role in oxidative stress response (Downs et al., 2002; Lesser, 2006) and being the most studied genes in corals transcriptomic responses to heat stress (Louis et al., 2017). The reference genes ribosomal protein L11 (RPL11) and ribosomal protein S7 (RPS7) were identified as the most stably expressed genes in *E. pallida* under a range of stress conditions (Lehnert et al., 2014). Primer sets characteristics and sequence references are presented in Table 4.1. Amplicon size was verified by 2% agarose gel electrophoresis, stained in GelRed™ (VWR, UK) after PCR amplification.

For each primer pair, qPCR reaction efficiency was optimised prior to running the experimental samples by comparing the change in Ct value for the gene transcript relative to the concentration of the standard, based on a 4-point standard curve. The efficiency of the PCR reaction was computed from the equation described by Radonić et al. (2004):

$$\text{Efficiency} = (10^{(-1/\text{slope})}-1) \times 100$$

Only efficiencies between 95% and 102% were used for further analysis (Pfaffl, 2001).

qPCR was performed on the sample cDNA using Precision PLUS Mastermix with SYBRGreen (PrimerDesign Ltd). Fluorescence was detected in a StepOne Real-Time PCR System, Applied Biosystems (ThermoFisher Scientific, UK) with thermal profile set as follows: initial denaturation of 10 min at 95°C, followed by 40 two-step cycles of 95°C for 15 s and 60°C for 1 min. At the end, a dissociation step was included: 95°C for 15 s, 60°C for 1 min and 95°C for 15 s. A standard curve of cDNA template (from a known sample) was run on each plate for each gene to allow for within experiment plate normalization. Relative fold change in expression of each target gene in exposed samples relative to control (n = 3) was then determined for each timepoint using the ΔΔCt method (Henry et al., 2009). Relative quantities are presented in the $\log_2$ scale ($\log_2$FC).

Table 4.1 - Primer sets characteristics. Primer name, sequence, annealing temperature (Tm) and amplicon size (bp) is given for target genes heat shock protein 70 (Hsp70), heat shock protein 90 (Hsp90), and reference genes 60S ribosomal protein L11 (RPL11), 40S ribosomal protein S7 (RPS7).

Gene		Primer Sequence (5'-3')	Tm (°C)	Product size (bp)	Reference
Hsp70	F	TCCTCCAGCACAGAAGCAAG	57.1	118	Ellison et al., 2017
	R	GACACGAGCGGAACAGATCA	57.3		
Hsp90	F	TCACGCATGAAGGATAACCA	56.9	150	Kitchen and Weis, 2017
	R	CTGGACGGCATACTCATCAA	57.4		
RPL11	F	AGCCAAGGTCTTGGAGCAGCTTA	60.6	125	Lehnert et al., 2014
	R	TTGGGCCTCTGACAGTACAGTGAACA	61.5		
RPS7	F	ACTGCAGTCCACGATGCTATCCTT	60.2	125	Lehnert et al., 2014
	R	GTCTGTTGTGCTTTGTCGAGATGC	58.6		

4.2.8 Statistical analyses

All statistical analyses were performed in R (v. 3.4.1; R Core Team, 2017). Anemones oral disk size and results from Fv/Fm and gene expression were tested for normal distribution and homoscedasticity with Shapiro and Levene's tests, data were transformed where appropriate. To confirm that anemones used in the experiment were all of similar size, differences in oral disk measurements of anemones from each experimental condition were tested with One-way Anova.

One-way Anova was applied to identify any significant differences on Fv/Fm between treatments at each timepoint (0h, 24h) and temperature (26°C, 32°C). Two-way Anova was used to verify that incubation had no effect on anemones health by testing Fv/Fm of untreated anemones against time (24h before the start of the experiment and time 0h) and incubators (A-26°C and B-32°C).

To test for statistical differences in log_2FC of each target gene, two-way Anova was conducted for each timepoint considering treatments, temperature and their interaction as main factors.

Whenever a factor resulted significant from the Anova test, post-hoc tests were conducted using the Tukey pairwise multi-comparison test.

4.3 Results

4.3.1 Chlorophyll fluorescence (Fv/Fm)

Exaiptasia pallida anemones throughout the experiments appeared healthy (maintained a normal colour and tentacle length). Two-way Anova of Fv/Fm data confirmed that anemones in both incubators were unstressed at the start of the experiment (Incubator and Incubator x Time $p > 0.8$, Time $p = 0.075$; Figure 4.4, Table 4.2.)

Control anemones exhibit Fv/Fm values between 0.84 to 0.94 at both ambient and warming temperatures, while Fv/Fm values of anemones exposed to sunscreen and filter-free formulation treatments show an overall similar trend in the different experimental conditions (Figure 4.5). At time zero no significant differences in Fv/Fm were observed among sunscreen and filter-free formulation treatments in both temperature experiments (One-way Anova $p = 0.7$ at 26°C, $p = 0.6$ at 32°C). However, anemones exposure to the different treatments reduced photosynthetic efficiency over time, leading to marginally significant differences at 26°C (One-way Anova $p = 0.054$; Figure 4.4, Table 4.2) and statistically significant differences at 32°C (One-way Anova $p = 0.001$; Figure 4.4, Table 4.2) at 24 hours of exposure. At the end of the experiment, at ambient temperature sunscreen treatments display a decrease in Fv/Fm values dependent on the sunscreen concentration, with 50 μgL^{-1} treatment (0.95 ± 0.01) identical to the time-matching control (0.94 ± 0.01) (Tukey HSD $p = 1$) but significantly different to 1000 μgL^{-1} treatment (0.79 ± 0.05) (Tukey HSD $p = 0.04$; Figure 4.5 A, Table 4.3). Exposure to the filter-free formulation caused a slight decrease in Fv/Fm (Figure 4.5 B). In the heat-stress experiment, the simultaneous exposure to warming enhanced the concentration-dependent reduction in the maximum photosynthetic yield at 24h exposure, with the lowest Fv/Fm in anemones exposed to 1000 μgL^{-1} concentration of both sunscreen (0.6 ± 0.02) and filter-free formulation (0.65 ± 0.02). Sunscreen treatments induced a more marked Fv/Fm decrease (Tukey HSD 100 μgL^{-1} $p = 0.003$, 500 μgL^{-1} $p = 0.01$, 1000 μgL^{-1} $p = 0.0002$; Figure 4.5 C) than filter-free formulation treatments (Tukey HSD 100 μgL^{-1} $p = 0.04$, 500 μgL^{-1} $p = 0.02$, 1000 μgL^{-1} $p = 0.005$; Figure 4.5 D) compared to control Fv/Fm at the same time and temperature condition (0.84 ± 0.02) (Table 4.3).

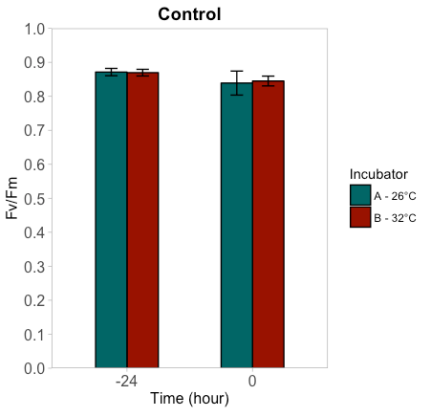

Figure 4.4 - Maximum photosynthetic yield (Fv/Fm) of control (untreated) anemones in the experimental incubators (A-26°C and B-32°C) 24 hour prior the starting of the experiment (-24h) and at the start of the experiment (0h), Data are expressed as mean ± SEM.

Table 4.2 - Two-way Anova results on Fv/Fm data in the different experimental conditions. Data were either arcsin (‘‘*’’) or ln (‘‘†’’) transformed, and statistically significant differences are highlighted in bold.

		Factor	Df	F-value	Sig.
Acclimation phase		Incubator	1	0.061	0.8
		Time	1	3.521	0.075
		Incubator:Time	1	0.066	0.8
0h	**26°C**	Treatment	8	0.653	0.7
	32°C *	Treatment	8	0.808	0.6
24h	**26°C ***	Treatment	8	2.139	0.054
	32°C †	Treatment	8	4.321	**0.001**

Table 4.3 - Tukey post-hoc test comparisons. Only significant pairwise comparisons are presented (p-value < 0.05).

Temperature	**Treatments Comparisons**					**Sig**
26°C	Sunscreen	50 μgL^{-1}	*vs*	Sunscreen	1000 μgL^{-1}	0.04
32°C	Control	0 μgL^{-1}	*vs*	Sunscreen	100 μgL^{-1}	0.003
					500 μgL^{-1}	0.01
					1000 μgL^{-1}	0.0002
				Filter-free formulation	100 μgL^{-1}	0.04
					500 μgL^{-1}	0.02
					1000 μgL^{-1}	0.005

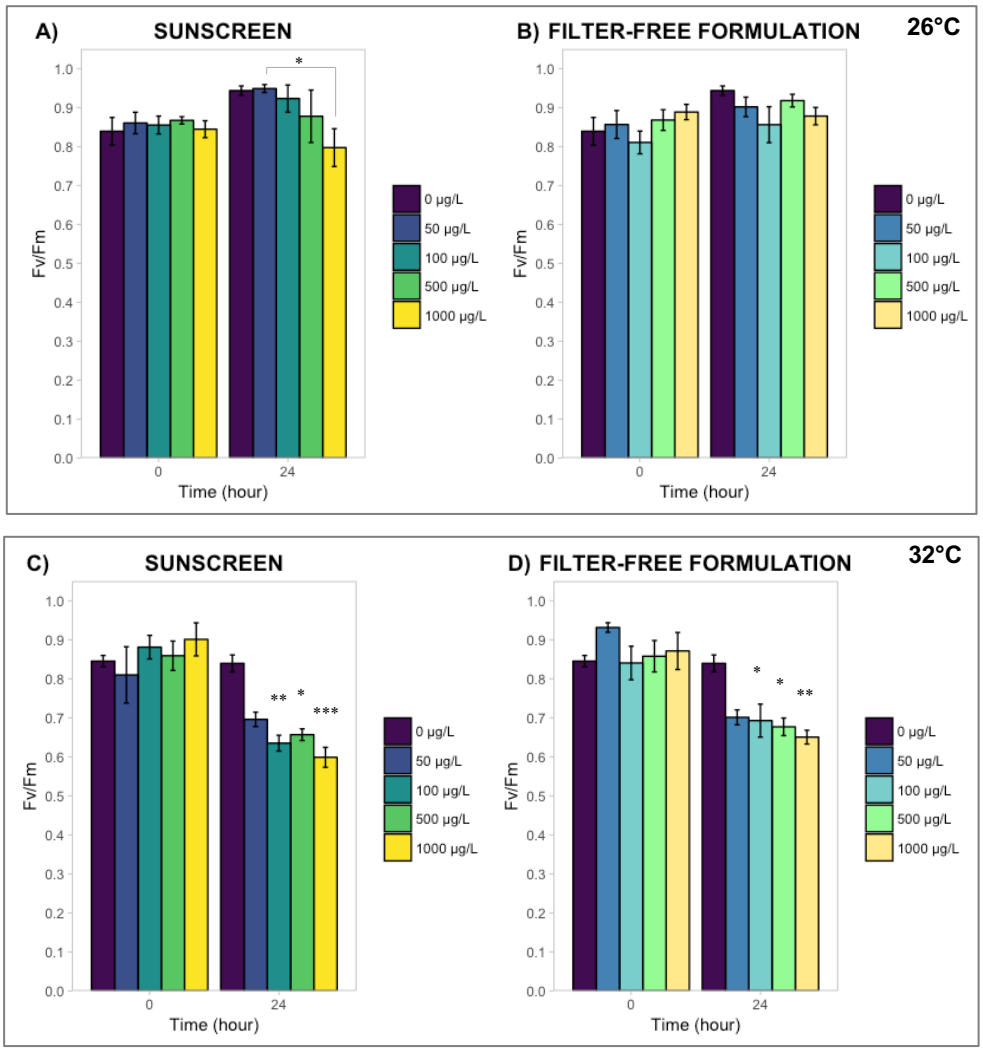

Figure 4.5 - Maximum photosynthetic yield (Fv/Fm) of anemones exposed to different concentrations of sunscreen and filter-free formulation at ambient temperature (A and B) and under heat-stress (C and D). Data are expressed as mean ± SEM. Asterisks indicate significant difference from the time-matching control (* = $p < 0.05$, ** = $p < 0.01$, *** =$P<0.001$).

4.3.2 Changes in Hsp70 and Hsp90 gene expression

Hsp70 and Hsp90 genes expression was measured in *Exaiptasia pallida* anemones exposed to increasing concentrations of sunscreen and filter-free formulation, incubated in ambient (26°C) and warming (32°C) temperatures, at several time points. Log_2FC of candidates genes expression was assessed relative to the untreated counterparts at the corresponding timepoint using quantitative real-time qPCR and the relative ΔΔCt method (Henry et al., 2009), with ribosomal protein L11 and ribosomal protein S7 as reference genes for symbiotic *E. pallida* (Lehnert et al., 2014). All anemones investigated were of similar size, as confirmed by One-way Anova test ($p = 0.15$; Table 4.4), thus they were of the same weight and, presumably, age (Clayton and Lasker, 1985).

In untreated anemones, heat-stress initiated an over-expression of Hsp70 and Hsp90 starting from time 0, with the greatest expression observed after 6 hours (log_2FC 3.9 ± 0.9) followed by a decrease towards log_2FC value similar to the one at the beginning of the experiment (log_2FC 1.3 ± 2; Figure 4.6).

Sunscreen and filter-free formulation exposure stimulated the expression of *E. pallida* Hsp70 and Hsp90 genes compared to control, even at 26°C and under the lowest tested concentration (log_2FC range: 0.5 – 6.26), except at 6h exposure when HSPs expression was mainly down-regulated (Figure 4.7). Treatment was a significant factor, alone and under the simultaneous temperature exposure, in all timepoints for Hsp90 and at 3h and 24h for Hsp70 (Table 4.5). The presence of the UV filter $nTiO_2$ in the formulation did not influence HSPs' induction patterns: filter-free formulation induced a HSPs transcript abundance similar to the correspondent sunscreen concentration.

At 32°C (6°C above mean ambient temperature) Hsp70 transcript levels were overall similar to the correspondent treatments at ambient temperature, whilst the expression of Hsp90 at 32°C was higher than its expression at 26°C for all timepoints except at 24h. For the majority of treatments, the pattern of HSPs gene induction at both experimental temperatures displayed a double peak of expression: the first peak was observed at 3h (prior to the HSPs expression peak of untreated anemones under heat-stress which occurred at 6h) and a second one at the end of the experiment. At 24 hours the transcript levels remained significantly higher compared to controls at 26°C (Tukey HSD $p \leq 0.03$ for Hsp70 and Hsp90; Table 4.6). A different pattern of Hsp70 and Hsp90 genes expression was observed for the highest concentration tested, 1000 μgL^{-1}, of both sunscreen and filter-free formulation. At ambient temperature, 1000 μgL^{-1} exhibited the greatest HSPs expression at time 0 (Hsp70 ~ 3.8, Hsp90 ~ 2.9 fold increase respect control

values), the transcript abundance then decreased at 3h and 6h while at the end of the final timepoint the expression was high again. In contrast, under warming conditions HSPs transcript abundance was lower than heat-stressed controls at time 0, the expression then increased with time. At 24h, 1000 μgL^{-1} sunscreen and filter-free formulation displayed the highest transcript increment at both ambient and warming temperatures (Hsp70 26°C filter-free formulation: 4.1 ± 1, Hsp90 26°C: 5.5 ± 0.8, Hsp70 32°C: 2.6 ± 0.8, Hsp90 32°C: 3.4 ± 0.1 fold increase respect control values), except for Hsp70 expression in sunscreen treatment concentration 1000 μgL^{-1} at 26°C (1.6 ± 2 fold) (Figure 4.7).

Table 4.4 - *Exaiptasia pallida* oral-disc size in mm (mean ± SD) for each experimental timepoint and temperature.

	26°C	**32°C**
0h	6.9 ± 0.5	7 ± 0.7
3h	6.1 ± 1.5	6.5 ± 1.7
6h	6.4 ± 1.9	5.8 ± 1.5
24h	6.2 ± 2.4	6.6 ± 0.8

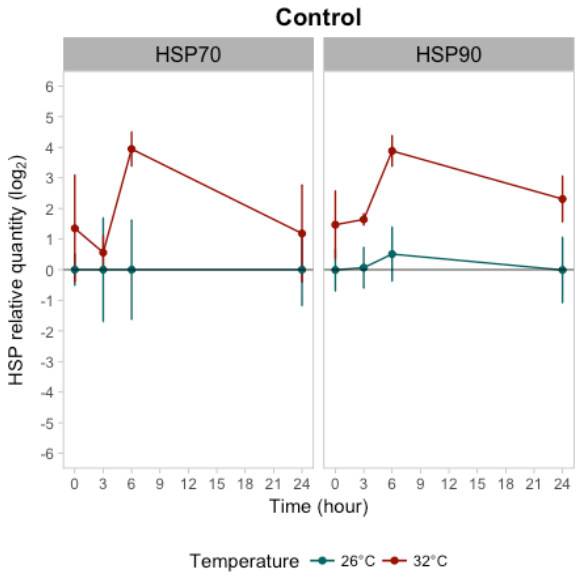

Figure 4.6 - Log_2 relative expression values (± SEM) of candidate genes in control (untreated) anemones shown with respect to temperature treatment.

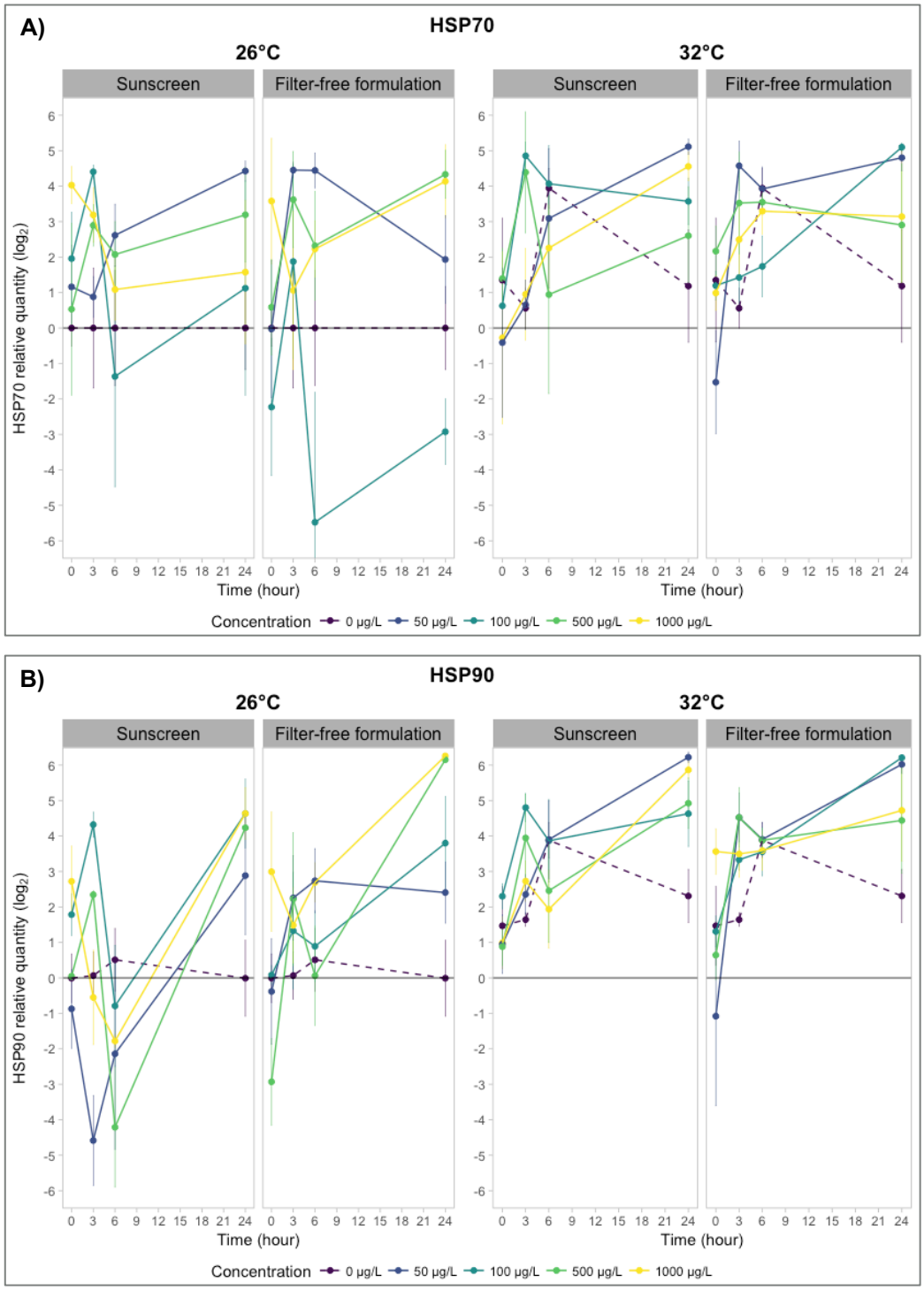

Figure 4.7 - Log_2 relative expression values (± SEM) of Hsp70 (**A**) and Hsp90 (**B**) in treated anemones shown with respect to temperature treatment. Expression levels of genes are plotted as ratio of relative expression of treated versus control anemones at each time point. The relative expression for these selected genes was normalized to RPL11 and RPS7.

Table 4.5 - Two-way Anova results on log_2FC of candidate genes at each timepoints. Statistically significant differences are highlighted in bold.

Timepoint	Factor	Df	Hsp70		Hsp90	
			F-value	Sig.	F-value	Sig.
0h	Treatment	8	0.779	0.624	3.423	**0.005**
	Temperature	1	0.079	0.781	3.244	0.08
	Treatment:Temperature	8	1.207	0.324	0.948	0.49
3h	Treatment	8	2.897	**0.014**	4.678	**< 0.0001**
	Temperature	1	0.035	0.85	27.731	**< 0.0001**
	Treatment:Temperature	8	0.37	0.93	1.481	0.2
6h	Treatment	8	2.082	**0.06**	2.521	**0.03**
	Temperature	1	7.699	**0.009**	49.613	**< 0.0001**
	Treatment:Temperature	8	1.386	0.24	1.586	0.17
24h	Treatment	8	1.419	0.23	1.431	0.2
	Temperature	1	10.69	**0.003**	10.767	**0.0025**
	Treatment:Temperature	8	2.548	**0.03**	2.566	**0.03**

Table 4.6 - Tukey post-hoc test comparisons for treatments interaction at the different timepoints. Only significant pairwise comparisons are presented (pvalue < 0.05).

Timepoint	Treatments Interaction						Sig.	
							Hsp70	Hsp90
0 h	Filter-free formulation	1000 µgL^{-1}	*vs*	Filter-free formulation		50 µgL^{-1}	/	0.014
						500 µgL^{-1}	/	0.005
3 h	Control	0 µgL^{-1}	*vs*	Sunscreen		100 µgL^{-1}	0.059	0.018
	Sunscreen	50 µgL^{-1}	*vs*	Sunscreen		100 µgL^{-1}	/	0.001
						500 µgL^{-1}	/	0.028
				Filter-free formulation		50 µgL^{-1}	/	0.015
						500 µgL^{-1}	/	0.016
		100 µgL^{-1}	*vs*	Sunscreen		1000 µgL^{-1}	/	0.032
24h	Control	0 µgL^{-1} 26°C	*vs*	26°C	Filter-free formulation	500 µgL^{-1}	0.037	0.036
						1000 µgL^{-1}	0.031	0.03
				32°C	Sunscreen	500 µgL^{-1}	0.013	0.012
						1000 µgL^{-1}	0.024	0.023
					Filter-free formulation	500 µgL^{-1}	0.019	0.018
						1000 µgL^{-1}	0.013	0.013

4.4 Discussion

This experiment was designed to improve the understanding whether sunscreens' emulsifying and emollient ingredients, besides UV filters, are involved in sunscreen toxicity by testing how *Exaiptasia pallida* anemones respond to increasing concentrations of two custom-made sunscreen formulations having the same oil phase ingredients but differing in the presence-absence of $nTiO_2$ as UV filter. Results demonstrated that the filter-free formulation induced the same changes in anemones photochemical efficiency and HSPs early gene expression of sunscreen exposure. Additionally, when both formulations were combined with an acute short-term heat stress treatment (32°C, + 6°C above ambient, for 24h), enhanced negative responses were observed.

4.4.1 *Exaiptasia pallida* responses under ambient temperature

E. pallida photochemical efficiency has been demonstrated to be a direct indicator of its *in-hospite* Symbiodiniaceae responses to stress (Howe et al., 2017). In this experiment, *E. pallida* exposed to sunscreen at ambient temperature exhibited a reduction of photosynthetic efficiency in a concentration-response manner, whilst formulation lacking UV filters did not affect Fv/Fm (Figure 4.5). On the contrary, qPCR analyses did not show differences in Hsp70 and Hsp90 expression under sunscreen and filter-free formulation exposure. HSPs were overall significantly up-regulated by exposure to both formulations and at 24 hours exposure reached even higher values than control anemones under heat stress (Figure 4.7). Heat shock proteins are well-known protective mechanisms for thermal stress and consequent oxidative damage (Louis et al., 2017). High HSPs levels unmatched by changes in Fv/Fm under filter-free formulation exposure may indicate that at ambient temperature the formulation lacking UV filters induce stress directly on *E. pallida* animal cells, while the algal symbionts are not affected. The observed Fv/Fm reduction in anemones exposed to sunscreen may be therefore mediated by the UV filter $nTiO_2$, which photocatalytic activity induce the production of ROS in the algal chloroplast (Li et al., 2015), with consequent photosystem damage and oxidative stress in algae and animal cells derived by ROS accumulation. This finding is consistent with the double mechanism of toxicity proposed for inorganic sunscreen in Chapter 3 and is supported by Jovanović and Guzmán (2014) who measured simultaneous Hsp70 upregulation and Symbiodiniaceae expulsion in the coral *Montastraea faveolata* after 48 hours exposure to 0.1 and 10 mgL^{-1} $nTiO_2$. Previous studies showed that exposure to

$nTiO_2$ did not affect the photosynthetic efficiency of freshwater and marine microalgae (Chen et al., 2012; Deng et al., 2017; Marchello et al., 2018). However, anemones responses cannot be directly compared to algae's, furthermore, in this experiment, organisms were not exposed to $nTiO_2$ alone, and the interaction with other sunscreen ingredients could have enhanced $nTiO_2$ intrinsic photocatalytic behaviour, as observed by Sendra et al. (2017) who measured a higher H_2O_2 production after exposure to sunscreen compared to $nTiO_2$ alone. These results agree with findings in Chapter 2 where a reduction of Fv/Fm was observed in stress-sensitive Symbiodiniaceae exposed to hydrophobic $nTiO_2$ dispersed in the sunscreen oil phase but not to hydrophilic $nTiO_2$ dispersed in water.

4.4.2 Combined effects of sunscreen/filter-free formulation and temperature increase

Measurement of Fv/Fm is also a standard method to determine the effect of warming on the cnidarian-Symbiodiniaceae relationship, being an indicator of heat-induced damage to PSII (Fitt et al., 2001; Roth, 2014; Warner et al., 1999). Here the photosynthetic activity of control anemones was not altered by heat stress alone. This result is consistent with Hawkins and Warner (2017) who showed that Fv/Fm of *E. pallida* at 32°C was stable for 7 days before showing a decline, and it was also observed in Symbiodiniaceae and corals previously in this thesis (Chapter 2 and 3). Notably, the combination of both formulations with elevated temperature aggravated the negative effect of sunscreen ingredients and temperature as individual stressors on the maximum photosynthetic capacity of *E. pallida* (Figure 4.5). At 32°C both sunscreen and filter-free formulation caused a significant Fv/Fm reduction, although under sunscreen exposure the decline was more marked (Tukey HSD $p_{sunscreen} \leq 0.01$, $p_{filter\text{-}free\ formulation} \leq 0.04$; Table 4.3).

Heat shock proteins are common biomarkers for thermal stress response in symbiotic cnidarians (see review by Louis et al., 2017) and their expression levels vary depending on type, intensity and duration of the stress applied and the sampling time (Kvitt et al., 2016; Leggat et al., 2011; Levy et al., 2011; Rodriguez-Lanetty et al., 2009; Rosic et al., 2011; Venn et al., 2009). Here HSPs upregulation in anemones at 32°C is accompanied by a drop in photosynthetic efficiency under both sunscreen and filter-free formulation, suggesting that the combined warming-formulations stress impact both *E. pallida* and its endosymbionts. Interestingly, the response of HSPs genes was significantly stimulated by the different sunscreen and filter-free formulation treatments already at 3 hours of

exposure under both ambient and elevated temperature (Two-way Anova $p \leq 0.01$), prior to the peak of HSPs transcript levels in anemones exposed solely to thermal stress observed at 6 h. Concentrations of 1000 μgL^{-1} highly upregulated Hsp70 and Hsp90 expression even at time 0 at 26°C. This suggests that the mechanism of early response to both formulations might be similar to the one for heat stress alone, but it is activated more rapidly. HSPs expression in symbiotic cnidarians under thermal stress is regulated in two phases (Kitchen and Weis, 2017; Kvitt et al., 2016; Rosic et al., 2011, 2014; Seneca and Palumbi, 2015). An initial acute response during the first 24 hours, in which HSPs are upregulated in order to counteract heat stress and regulate stress-induced apoptosis, followed by a HSPs decline to basal levels from 18-24 h onwards. For example Kvitt et al. (2016) noticed that the coral *Stylophora pistillata* at 34°C showed the maximum Hsp70 gene expression after 6 hours of heat stress and Rodriguez-Lanetty et al. (2009) observed a higher expression of Hsp70 and Hsp90 in coral larvae after 3 h at 31°C than 10 h. Kitchen and Weis (2017) also measured Hsp90 gene expression in *E. pallida* anemones exposed at 33°C for 7 days and the transcript quantities in the first 24 hours were upregulated to approximately the same extent presented here: between 3 and 6 hours the expression was at the maximum level ($\log_2 FC \sim 4$) then decreased, but still remaining upregulated, at 24h ($\log_2 FC \sim 1.9$). The stimulated HSPs expression at the onset of stress is suggested to be an acclimatization mechanism to elevated temperatures (Barshis et al., 2013; Kitchen and Weis, 2017; Kvitt et al., 2016; Rosic et al., 2014). The rapid high levels of HSPs expression at the start of the experiment and at 3 hours of exposure observed here may indicate that exposure to cosmetic formulations, with and without UV filters, cause a stronger stress to *E. pallida* compared to elevated temperatures alone, inducing an almost instant stress response. A similar effect was observed in Chapter 3, where sunscreen was demonstrated to be the main driver of toxicity in corals simultaneously exposed to sunscreen and gradual temperature increase.

Furthermore, high levels of HSPs transcripts measured at the end of the experiment, contrary to heat stress alone, may suggest that animals have difficulty in resisting the stress induced by both sunscreen and filter-free formulation, and as a consequence the heat shock proteins' defensive mechanism is upregulated for a longer period. However, the capacity of return to normal cellular functions after a stress is essential for the survival of the organism (De Nadal et al., 2011). The continuous expression of HSPs is detrimental as the organism redirects all its energy to heat shock protein synthesis, and the synthesis of non-essential proteins is stopped (Morimoto, 1993). Moreover Seneca and Palumbi

(2015) hypothesized that the return to control levels in genes up- or down- regulated during heat stress is directly connected to the bleaching performance of corals. They observed that corals totally bleached were the ones that at 20 hours of warming exposure continued to upregulate their gene expression; in contrast, those corals that at 20h returned gene expression to control levels showed just slight or no bleached tissues. Here the unusually high HSPs levels lingering at 24 hours exposure to both formulations, at 26°C as well as 32°C, may have instigated bleaching in *E. pallida* anemones and be a symptom of physiological stress. Apoptosis, the programmed cell death, is one of the mechanism involved during bleaching and it has been described in corals (Kvitt et al., 2011, 2016; Pernice et al., 2011) and anemones (Richier et al., 2006) under thermal stress. Further investigations of the expression of genes involved in *Exaiptasia pallida* apoptotic system, such as the anti-apoptotic and pro-apoptotic mediators Bcl-2 and Bax (whose activities inhibit and promote apoptosis, respectively) and Caspase (directly involved in cell death), may help gaining insight into the similarities between bleaching and sunscreen responses in symbiotic cnidarian. The possibility of an acclimation stage after the 24 hours HSPs expression peak as observed in corals exposed to $nTiO_2$ (Jovanović and Guzmán, 2014) cannot be excluded. Further studies are also necessary to determine if HSPs induction by sunscreen and filter-free formulation exposure is transient or sustained over time, finally leading to bleaching and probably death of the organism.

Although *E. pallida* anemones are accepted as cnidarian representative in ecotoxicity tests (Duckworth et al., 2017; Howe et al., 2017; Trenfield et al., 2017), at present it is not clear whether results presented here can be valid for corals. The lack of calcium carbonate skeleton and the consequent inability to withdraw the tissue exposed to the surrounding contaminated water into the skeletal cavity (a common stress response in adult corals (Brown et al., 1994; Van Dam et al., 2011)), may make *E. pallida* anemones more sensitive to chemical contamination at the onset of stress. Moreover, anemones used here were clonal animals, thus results do not account for the genetic variability of coral hosts in a natural environment. Corals also may show higher tolerance to warming under simultaneous sunscreen exposure, as observed in Chapter 3 of this thesis and for corals at high salinity conditions (Gegner et al., 2017).

Nonetheless *E. pallida* is widely recognized as a valuable model system for studies on coral biology, physiology, symbiosis and bleaching (Goulet et al., 2005; Lehnert et al., 2014; Núñez-Pons et al., 2017; Perez et al., 2001), and new discoveries on cnidarian

bleaching and innate immune system first described in *E. pallida* have already been validated in corals (Weis, 2019). Therefore, findings from this study allow for a certain degree of extrapolation to HSPs dynamics in the coral holobiont under sunscreen stress. However, additional long-term experiments with *E. pallida* anemones from natural populations are suggested (as proposed by Gegner et al., 2017), they will allow to acknowledge and investigate the potential role of host genetic variability into sunscreen toxicity, facilitating the direct comparison with corals.

4.5 Conclusion

This study expands the current state of knowledge on the toxicity of sunscreen products by considering them as chemical mixtures and assessing the toxicity of formulations in presence and absence of the UV filter active ingredients. Results presented here show that cosmetic formulations induce toxicity effects similar to sunscreen even when lacking UV filters. Moreover, the important photochemical and HSPs expression effects observed in the sea anemone *Exaiptasia pallida* suggest that sunscreen exposure is detrimental to symbiotic cnidarians, in particular under short-term acute warming conditions.
HSPs expression profiles measured here are from the whole anemones; it was not possible to determine HSPs levels in the algal symbiont cells. Further investigation into the Symbiodiniaceae-specific differential effects of formulations, with and without $nTiO_2$ UV filter, will help to verify $nTiO_2$ direct involvement in sunscreen toxicity as hypothesized. Nevertheless, a better understanding of HSPs gene expression at the onset of stress is crucial to detect those cellular responses that occur before any physiological effect is measured (Ainsworth et al., 2008), and HSPs transcriptomic profiles observed in this study indicate that sunscreen exposure cause considerable stress in *E. pallida*. Although additional studies to measure the actual protein turnover stimulated by sunscreen exposure will help to reveal also the direct physiological impacts, the significant and prolonged high levels of HSPs detected here under combined sunscreen and elevated temperature suggest that the elevated energetic cost required to cope with sunscreen exposure may limit the energy still available for recovery after bleaching.

In summary, the study presented in this chapter follow findings from Chapter 2 that highlight the importance of taking into account sunscreen's oil phase in assessing sunscreen toxicity. By using *E. pallida* as a model organism, photosynthetic and HSPs gene expression responses observed here represent the potential early reactions of

symbiotic cnidarians in general, and reef-building corals in particular, to inorganic sunscreen exposure and simultaneous acute heat stress. It was confirmed that sunscreen induce important detrimental effects in coral, as also observed in Chapter 3. Furthermore, results corroborate findings from Chapter 2 regarding the importance of considering the whole formulation ingredients in assessing sunscreen toxicity. In the next chapter the contribution of the oil phase into sunscreen toxicity will be further explored by investigating the differential impacts of sunscreens formulated with diverse $nTiO_2$ and emulsifying agents on coral fertilization, sperm motility and larvae survival.

Chapter 5

The individual and combined effects of different inorganic sunscreen formulations and thermal stress on early life history stages of tropical corals

5.1 Introduction

In the previous chapters it was demonstrated that an inorganic sunscreen formulation negatively affected adult corals and the sea anemone *Exaiptasia pallida*, however its effects on coral early life history stages are unknown.

Early life history stages of corals are more sensitive to changes in environmental conditions than adults (Byrne, 2011; Putnam et al., 2010; Reichelt-Brushett and Harrison, 1999; Richmond et al., 2018), and since fertilization and early development occur in surface waters, gametes and larvae are particularly vulnerable to waterborne contaminants such as sunscreen products (Jones et al., 2015; Reichelt-Brushett and Hudspith, 2016). The purpose of this study was to evaluate the effects of exposure to environmentally relevant concentrations of inorganic sunscreen formulations on fertilization, sperm motility and larval survival of the reef-building corals *Acropora hyacinthus*, *Acropora globiceps* and *Pocillopora damicornis* from the island of Moorea in French Polynesia (Figure 5.1). Moorea is a remote location with modest tourist pressure (Gössling et al., 2018). The likely low background level of sunscreen contamination in its waters designates Moorea an ideal control site for sunscreen toxicity testing. Impacts of sunscreen exposure were tested on coral early life history stages since they are critical stages for coral recovery after disturbance events (Knowlton, 2001; van Oppen et al., 2008). This will provide better insight into the persistence of coral communities exposed to sunscreen-polluted waters.

The tested species are common corals in the Indo-Pacific, and in particular *Acropora* and *Pocillopora* spp. support the successful recovery of the reefs in Moorea after severe disturbances (Adjeroud et al., 2018; Bramanti and Edmunds, 2016; Edmunds, 2018). The studied corals are characterized by different life strategies. *A. hyacinthus* and *A. globiceps* are spawning corals, and they release buoyant egg-sperm bundles into the water columns where fertilization occurs. Larvae remain in the planktonic stage for a minimum of 2-6 days before they are ready to settle, metamorphose and acquire symbiotic zooxanthellae from the environment (Harrison and Wallace, 1990) (Figure 5.2). *P. damicornis* instead is a brooding coral which release symbiotic free-swimming larvae monthly according to the lunar cycle (Fan et al., 2002; Richmond and Hunter, 1990), and larvae are ready to settle soon after their release (Rivest and Hofmann, 2015) (Figure 5.3). Although both broadcast and brooded larvae usually reside just few days in the water column before settlement, they have the capacity for long-distance dispersal (Graham et al., 2008; Nozawa and Harrison, 2002; Richmond, 1987).

Fertilization and larval dispersal are fundamental processes for reproductive success and recovery of coral reef ecosystems after stressful conditions (Knowlton, 2001; van Oppen et al., 2008), and warming is known to have a detrimental impact on early life history stages of corals (Bassim et al., 2002; Chui and Ang, 2015; Edmunds et al., 2001; Hédouin et al., 2015; Hughes et al., 2019; Keshavmurthy et al., 2014). Fertilization rates decline at 34°C (Negri et al., 2007; Puisay et al., 2018), while temperatures from 1°C above ambient increase the amount of abnormalities in embryo development (Bassim et al., 2002; Keshavmurthy et al., 2014; Negri et al., 2007; Puisay et al., 2018; Randall and Szmant, 2009). Elevated temperature also negatively impact the survival of larvae (Bassim and Sammarco, 2003; Puisay et al., 2018; Randall and Szmant, 2009; Yakovleva et al., 2009) and shorten their pelagic stage (Edmunds et al., 2001; Nozawa and Harrison, 2007), resulting in increased local larval retention and decrease connectivity among distant reefs (Figueiredo et al., 2014). Since seawater temperatures are expected to increase 2-4°C in the coming decades (IPCC, 2014), a better understanding of the effects of inorganic sunscreens alone and combined with thermal stress is critical to predict the survival of reef-building corals in coastal areas. Fertilization success and larval survivorship are ecologically important endpoints for toxicological studies. The use of coral early life stages also avoid the destructive fragmentation of adult corals needed for the necessary amount of replicates required in ecotoxicity experiments (Gissi et al., 2017; Negri and Heyward, 2000; Reichelt-Brushett and Harrison, 2000). Organic sunscreen UV filters belonging to the benzophenone (BP) family, BP-1, BP-2, BP-4 and BP-8, have been reported to negatively affect survival and settlement of larvae of the corals *Stylophora pistillata* and *Seriatopora caliendrum*, in addition to inducing bleaching and DNA damage (Downs et al., 2014, 2016; He et al., 2019b). In contrast, larvae of *P. damicornis* were not affected up to 1 mgL^{-1} of BP-1 and BP-8 (He et al., 2019b). The aforementioned studies demonstrated that coral larvae are potentially sensitive to sunscreen exposure and responses are not homogeneous among coral species, yet the effects of whole sunscreen formulations on gametes and larvae behaviour are still unknown. This study therefore aimed to reveal the effects of inorganic sunscreen, elevated temperature and their combinations on the various early life history stages of two of the most abundant reef-building corals in Moorea and representative of the different reproductive modes, *Acropora* and *Pocillopora* spp. Since the effects of filter-free formulation on the sea anemone *E. pallida* were similar to the effects of a common inorganic sunscreen (Chapter 4), it is here hypothesized that sunscreen toxicity varies

depending on the ingredients incorporated in the oil phase. In particular it is tested whether a sunscreen formulated with an organic, plant-derived, emulsifier is less toxic than a common chemical emulsifying agent. The study consisted of three parts: first, the fertilization success and the ratio of abnormally developed embryos under different sunscreen formulations was assessed on gametes of the coral *A. hyacinthus* at ambient and elevated temperature. Then a second experiment was designed to investigate sperm motility of *A. globiceps* exposed to the different sunscreen formulations at ambient temperature only. Lastly, survivorship of *A. globiceps* and *P. damicornis* larvae exposed to increasing sunscreens concentrations was examined.

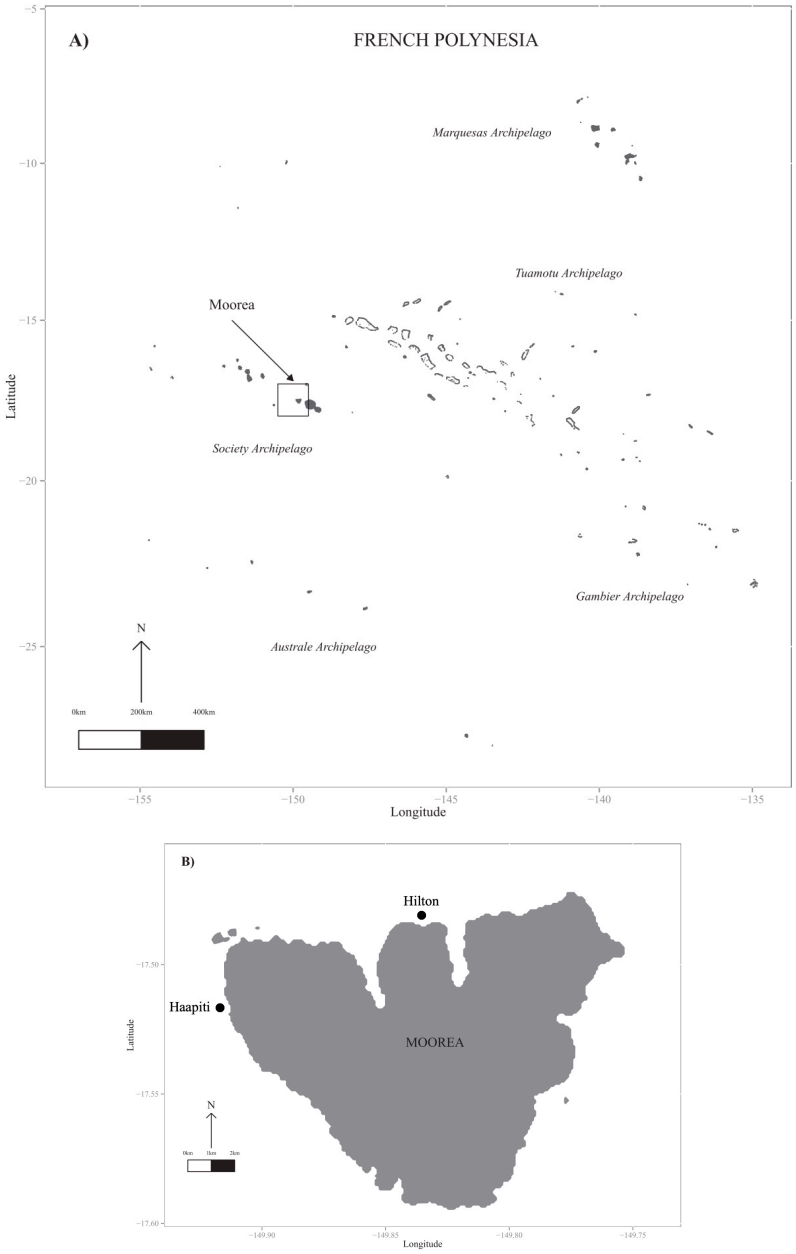

Figure 5.1 – Location of the study. **A**) Map of French Polynesia. **B**) Coral sampling sites in Moorea (modified from Hédouin et al.(2015)).

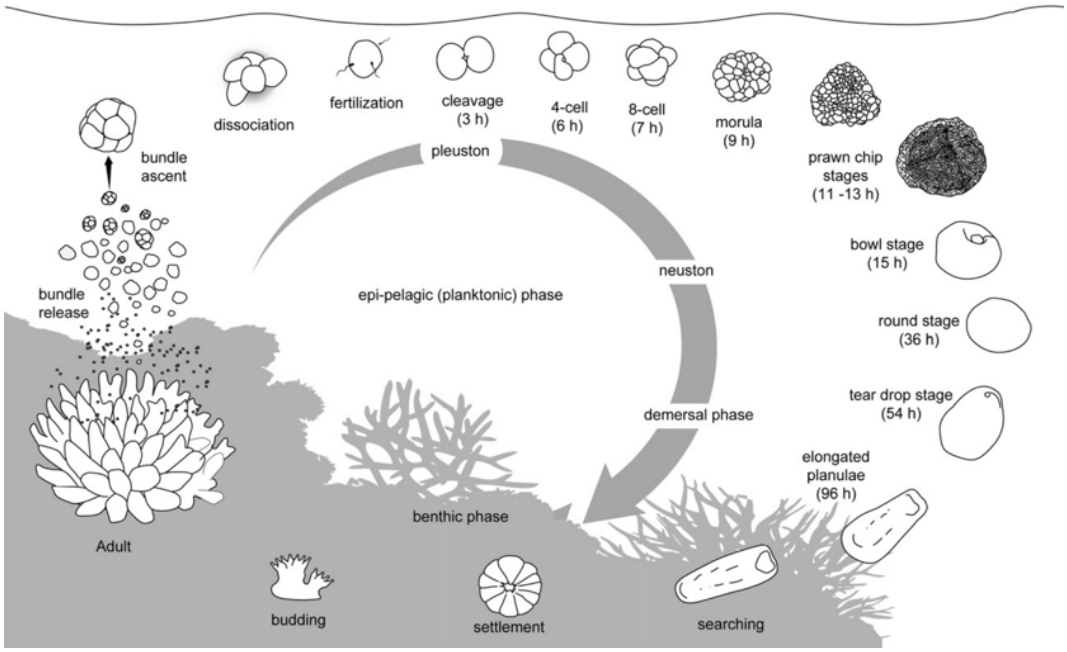

Figure 5.2 - Reproductive cycle of *Acropora* spp. corals, from Jones et al., 2015.

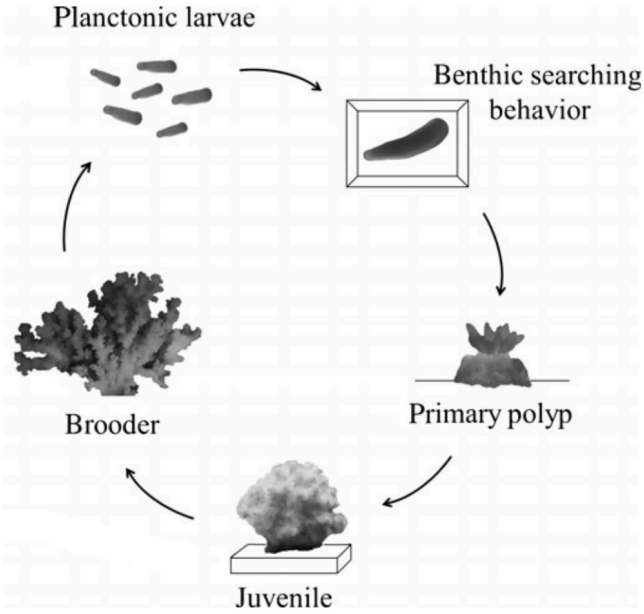

Figure 5.3 - Reproductive cycle of *Pocillopora* spp. corals, from Leal et al. (2016).

5.2 Materials and Methods

5.2.1 Coral collection and husbandry

Experiments were conducted at the Centre for Island Research and Environmental Observatory (CRIOBE) in Moorea (French Polynesia) during the spawning events in October and November 2018.

Experiments (summarised in Table 5.1) were designed to assess the effects of different sunscreen formulations on:

- *Acropora hyacinthus* fertilization and embryos development at 27 and 31°C,
- *Acropora globiceps* sperm motility at 27°C,
- *Acropora globiceps* larvae survival at 27 and 31°C,
- *Pocillopora damicornis* larvae survival at 27°C.

Experiments were conducted in two water baths equipped with a Hobby® Biotherm Pro to maintain a stable temperature throughout the experiments. One bath was at 27°C, the annual average temperature on the outer reef of Moorea (Leichter, 2015), while the second one represented the thermal stress scenario (31 °C, i.e. ambient + 4°C) projected in the coming decades (IPCC, 2014; Wang et al., 2018b).

Because of the short time between spawning events, experiments were often executed simultaneously. Consequently, a diverse number of replicates and temperatures were tested for each coral species (see Table 5.1), as a result of the balance between the number of gametes and larvae produced by parental colonies and the space available in the experimental water baths.

Acropora hyacinthus and *Acropora globiceps* (Figure 5.4 A, B) in Moorea spawn between 8 and 13 nights after the full moon from September to November (Carroll et al., 2006), hence mature colonies (showing pink oocytes, Figure 5.5 A and B) were collected around the full moon of October 2018 from the lagoons of Moorea. Larvae of the coral *Pocillopora damicornis* (Figure 5.4 C) in Moorea are released every month around 6-9 days after the new moon (Fan et al., 2006; Rivest and Hofmann, 2014), thus colonies were collected on November 09 2018 (two days after the new moon). Corals sampling sites are depicted in Figure 4.1. Corals were kept in outdoor flow-through aquaria under indirect sunlight (Figure 5.5 C). Temperatures in the tanks were consistent with reef temperatures (Leichter, 2015), varying between 26 and 28°C during daytime (Salinity: 36 ppt, pH = 8.03).

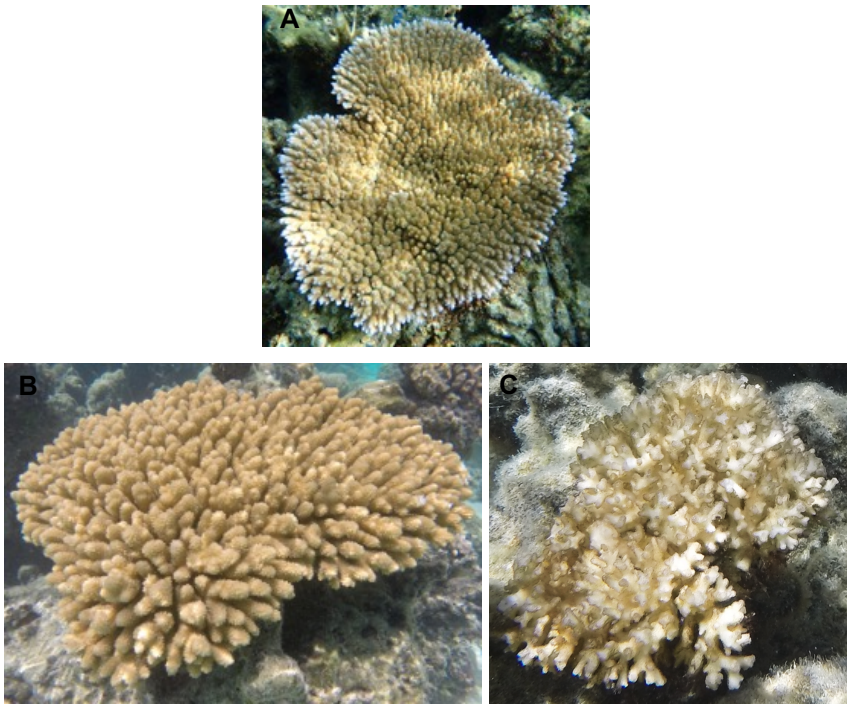

Figure 5.4 - Representative pictures of *Acropora hyacinthus* (**A**), *Acropora globiceps* (**B**), *Pocillopora damicornis* (**C**).

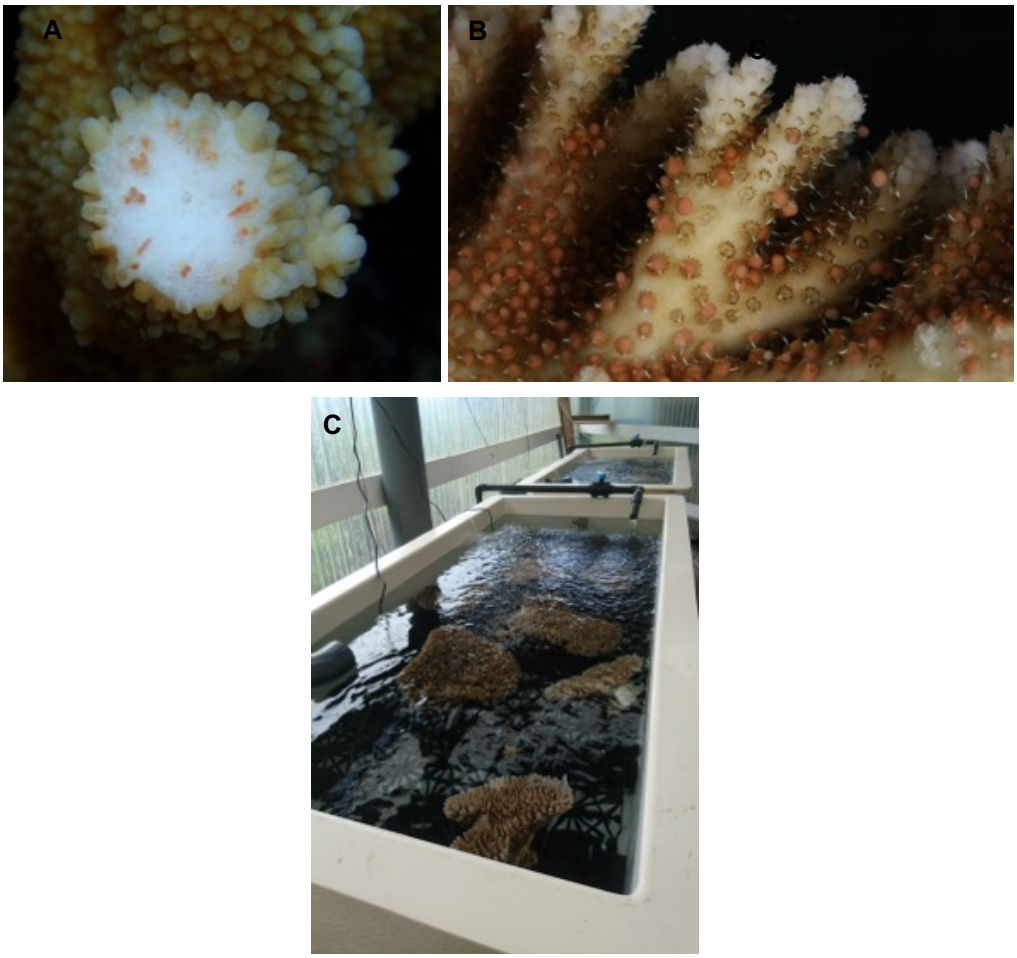

Figure 5.5 - Mature colony with pink oocytes (**A**), setting colony (**B**), outdoor aquaria (**C**)

Table 5.1 - Outline of each experiment, performed at different temperature and sunscreen concentrations.

Stage	Coral species	Nature of exposure	Exposure duration	Response variable	Methods section
Gametes	*Acropora hyacinthus*	Sperm and eggs (from 2 consecutive spawning nights: 01-02 Nov 2018) exposed to sunscreen formulations at 27 and 31°C (6 and 10 replicates, respectively).	5h	Fertilisation success Embryo development	Section 5.2.3
Gametes	*Acropora hyacinthus*	Sperm and eggs (from the third spawning night: 04 Nov 2018) exposed to sunscreen formulations at 27°C only (10 replicates).	5 h	Fertilisation success Embryo development	Section 5.2.3
Sperm	*Acropora. globiceps*	Sperm exposed to 1 mgL^{-1} of sunscreen formulations at 27°C (3 replicates).	15 min	Sperm motility	Section 5.2.4
Larvae	*Acropora globiceps*	Competent (4 days old) larvae exposed to sunscreen formulations at 27°C (6 replicates).	12 days	Larval survival	Section 5.2.5
	Acropora globiceps	Competent (4 days old) larvae exposed to sunscreen formulations at 31°C (6 replicates).	7 days	Larval survival	Section 5.2.5
	Pocillopora damicornis	Freshly released larvae exposed to sunscreen formulations at 27°C (6 replicates).	12 days	Larval survival	Section 5.2.5

5.2.2 Preparation of sunscreen test solutions

Three different sunscreen formulations were custom made from ingredients commonly used in the cosmetic industry by Riccardo Catalano and Dr Jerome Labille at CEREGE (Aix-en-Provence, France). The composition of the three tested sunscreens is outlined in Table 5.2. Sunscreens formulation was: $nTiO_2$ as UV filter, hydrophobic (Eusolex® T-S) or hydrophilic (Eusolex® T-Avo), and 15% of oil phase. The oil phase was composed of 80% plant derived emollients (40% Cetiol®LC - Coco-Caprylate/Caprate and 40% TEGOSOFT® P - Isopropyl Palmitate) and 20% by an emulsifier. Two different emulsifiers were tested: the chemical EasyNov™ (Octyldodecanol, Octyldodecyl Xyloside, PEG-30 Dipolyhydroxystearate) and the organic Cellulose NanoCrystals (CNC). T-S formulation was the same formulation tested in the previous chapters.

A 10 gL^{-1} stock solution for each sunscreen type was prepared at Heriot-Watt University by dispersing the sunscreen in milli-Q water as described in Chapter 3. Approximately four hours prior the start of each experiment, a series of test solutions were freshly prepared by dispersing the appropriate amount of stock solution in 0.7 µm freshly filtered seawater and mixing with a magnetic stirrer. For each sunscreen formulation, the concentrations tested were: 0.05, 0.1, 0.5 and 1 mgL^{-1}, to represent a range of environmentally relevant concentrations (the daily release of inorganic sunscreen in a touristic beach in a summer day is estimated at 1.2 mgL^{-1}, Chapter 1, Section 1.2.5), and to allow for comparisons with previous experiments in this thesis.

All working test solutions were kept in the experimental water baths a few hours prior the start of each experiment to acclimate them to the experimental temperatures.

Table 5.2 - Composition characterization of the tested sunscreens

Sunscreen ID	**T-S**	**T-Avo**	**CNC**
UV filter	Eusolex® T-S 10%	Eusolex® T-Avo 5%	Eusolex® T-S 10%
Emulsifying agent	EasyNov™ * 3%	EasyNov™ * 3%	Cellulose NanoCrystal 3%
Water	70%	75%	70%
Other ingredients	Emollient oils: Isopropyl Palmitate 6.5% Coco-Caprilate 6.5 % Moisturizer: Glycerol 2% Gelly agents: Polycrilate-13, polyisobutene, polysorbate, sorbitane, isooctadecanoate 2%		

* EasyNov™ ingredients: Octyldodecanol, Octyldodecyl Xyloside 1.5
PEG-30 Dipolyhydroxystearate 1.5%

5.2.3 Experiment 1: Effects of sunscreen and elevated temperature on fertilization and embryo development

Coral colonies were monitored every day from 7 pm to midnight to check for the release of egg-sperm bundles. Spawning of *A. hyacinthus* occurred on November 01 (8 days after the full moon (8 dafm)), November 02 (9 dafm) and 04 (11 dafm). Colonies showing sign of setting behaviour (bundles visible through the mouth of the polyps ready to be released into the water, Figure 5.5 B) were individually isolated in plastic buckets to allow the collection of bundles from each colony while avoiding mixing. Once collected, egg-sperm bundles were gently mixed to break the bundles, passed through 50 µm size mesh to separate eggs from sperm and eggs on the mesh were rinsed several times with 0.7 µm sperm-free seawater (following the protocol of Hédouin et al. (2015) and Puisay et al. (2015)) (Figure 5.6 A). Fertilization experiments were conducted in 50 mL polystyrene flat-base tubes, with each treatment having six (8 dafm experiment) or 10 (9 and 11 dafm experiments) replicate tubes. A total of 26 treatments were established, with 3 sunscreen formulations (T-S, T-Avo and CNC) x 4 concentrations (0.05, 0.1, 0.5, 1 mgL^{-1}) and 2 levels of temperature (27 and 31°C), a control-untreated treatment was also added to each temperature experiment. In the 11 dafm experiment, fertilization was assessed at ambient temperature only due to the reduced number of spawning colonies and consequent gametes available. At the beginning of each experiment, sperm-free eggs collected from four or five colonies were mixed together and placed in 50 mL plastic vials containing 20 mL of sunscreen working solutions or filtered seawater (approximately 150 eggs x vial) and immersed in water baths at either 27 or 31°C to maintain stable temperature throughout the experiment (Figure 5.7 A). Sperm were mixed together, sperm concentration was assessed spectrophotometrically and a quantity of sperm was added in each vial to reach a final concentration of 10^6 sperm mL^{-1} (optimal sperm concentration to maximize fertilization according to Oliver and Babcock (1992) and Willis et al. (1997)). Vials were left undisturbed and after 6 h embryos were fixed with a 90% EtOh solution. Samples were observed under a M80® Leica binocular microscope. The proportion of normal (2 cells, 4 cells, >4 cells) and abnormally developed embryos, as well as unfertilized eggs, were determined using the ImageJ software (https://imagej.nih.gov/ij/). Fertilization rate was calculated as the quantity of fertilized eggs divided by the total amount of eggs. Abnormal development rate was determined as the proportion of deformed embryos to the total number of fertilized eggs. Coral embryos were considered normal when they showed normal cleavage shapes (Figure 5.2), whilst

abnormal ones showed irregular, deformed and asymmetrical cell divisions and/or fragmentation (Hédouin et al., 2015; Keshavmurthy et al., 2014). Results from different spawning nights were analysed separately to account for the possible variations in the quality of gametes released from the same coral colony over several spawning nights, that could lead to biologically different fertilization rates (Chui and Ang, 2015; Hédouin and Gates, 2013; Padilla-Gamiño et al., 2013).

Figure 5.6 - *A. hyacinthus* eggs and sperms (**A**) and *A. globiceps* larvae (**B**).

5.2.4 Experiment 2: Sperm motility under sunscreen exposure

Sperm motility test was conducted on the night of November 03 2018 with pooled sperm from three *A. globiceps* spawning colonies. Approximately two hours after spawning (time allowed to setup the fertilization batch to rear larvae for the following experiment), pooled sperm were diluted in the 1 mgL^{-1} test solution of each sunscreen formulation to reach 10^7 sperm concentration and were incubated for 15 mins at room temperature (~ 26°C) in 1.5 mL microcentrifuge tubes (Fisherbrand™) (n=3). Sperm motility was analysed with the Computer-Aided Sperm Analysis (CASA) tracking software (Kime et al., 2001) in collaboration with Michael Henley and Claire Lager from the Smithsonian Conservation Biology Institute (USA). Sperm-sunscreen solution was loaded into special microscope slides and the motility was recorded after ~ 30 seconds (time requested for the sperm to recover and resume movement) with at least 5 videos per sample. CASA software then automatically assessed the average the total motility percentage in each sample, as well as the progressive and slow motility proportion (Figure 5.7 A). The replicates number in this experiment is just three per treatment (4 treatments x 3 replicates = 12 total), due to the short time available for both analysing sperm motility and starting the fertilization process to rear larvae for the subsequent experiment in the about 2 hours

sperm viability and successful fertilization time span (Oliver and Babcock, 1992; Ricardo et al., 2015).

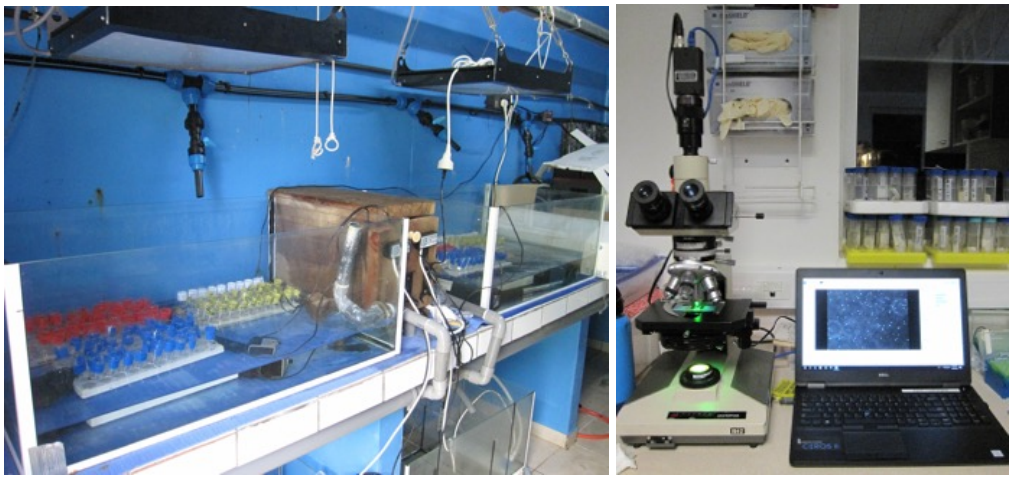

Figure 5.7 - Sperm motility assay (A) and experimental set-up (B).

5.2.5 Experiment 3: Effects of sunscreen and elevated temperature on larval survivorship and settlement

Larval survival was assessed on larvae that were not previously exposed to sunscreen nor elevated temperature (i.e. raised in control conditions). Two separate and consecutive larvae experiments were performed: 3a) survival rates of *A. globiceps* larvae in response to four sunscreens concentrations (0.05, 0.1, 0.5 and 1 mgL^{-1}) for each sunscreen formulation and two temperatures (27 and 31°C); 3b) survival of *P. damicornis* larvae exposed to four sunscreens concentrations (0.05, 0.1, 0.5 and 1 mgL^{-1}) for each sunscreen formulation at ambient temperature only (27°C). The survival experiment with *P. damicornis* larvae was carried out at ambient temperature only as the experiment timeframe conflicted with *A. globiceps* larvae survival test, constraining available water bath space. Gametes from the same *A. globiceps* colonies tested in the sperm motility assay were mixed together and after 12h the fertilized eggs were transferred to a 20L flow-through conical container with gentle bubbling. Larvae were tested 5 days post-fertilization (i.e. 08 November 2018) when they displayed active swimming behaviour (Figure 5.6 B). Six *P. damicornis* colonies were isolated in individual buckets every night and checked in the morning for larvae release. The morning of 14 November 2018, 7 days after the new moon, swimming larvae were collected and pooled together for the experiment. Larval experiments were conducted in six-wells microplate (Thermo Scientific™), each treatment having 6 replicates (10 larvae each replicate). At the

beginning of each experiment, 10 larvae were placed in each well of a 6 well plate filled with 10 mL of sunscreen working solution or filtered seawater (control treatment) and the plates were kept in water baths either at 27 or 31°C under natural dark:light regime (PAR average value: 140 µmol photons m^{-2} s^{-1} measured using a LI- 190SA quantum sensor, Licor, USA). During the 12- and 7-days experiments (ambient and elevated temperature, respectively) half of the seawater in each well was replaced every 48h, at the same time larvae mortality was recorded. Larvae were defined as alive when their movement and/or integrity was observed (Puisay et al., 2018).

5.2.6 Data analyses

All statistical analyses were performed using R version 3.4.3 (R Core Team, 2017). Generalized Linear Models (GLM) were used to analyse fertilization success and abnormal development rate as a function of treatment (11 dafm experiment data) and both treatment, temperature and their interaction (8 and 9 dafm experiment data). GLM were fitted with a quasi-binomial error distribution and logit link function when models showed overdispersion. Because no interaction between treatment and temperature was observed, significant differences among treatments were assessed for each temperature experiment separately with the post-hoc Tukey's HSD test from GLM models having just treatment as explanatory variable (function *ghlt* of the 'multcomp' package (v 1.4-8)).
Survivorship curves of coral larvae were estimated using the Kaplan- Meier method (Kaplan and Meier, 1958), a non-parametric statistic that estimates the probability of the event of interest occurring at each time point. Kaplan-Meier curves were compared with the logrank test and multiple pairwise comparisons test with the functions *survdiff* and *pairwise_survdiff* of the package 'survival' (v 2.41-3). The package 'survminer' (v 0.4.3) was then used to draw the survival curves plots.

5.3 Results

5.3.1 Effects of sunscreen and temperature stress on coral fertilization (Experiment 1)

A. hyacinthus fertilization rates (the proportion of eggs developed into embryos) were high across all treatments up to 1 mgL^{-1} in all spawning nights: range 89 ± 4.8 % - 97 ± 1.7 % (mean ± sd) at ambient temperature (Figure 5.8 A-C) and 85 ± 6.6 - 97 ± 4.1% under thermal stress (Figure 5.8 D-E), with the majority of normally developed embryos between the 8- and 32- cells stage (Figure 5.8, cell stages illustrated in Figure 5.2). Results from different spawning nights were similar, a slight decrease in fertilization 9 dafm (~ 5% at 27°C, 10% at 31°C) and an overall lower rate of aberrations in embryo development during 11 dafm was observed.

GLM analyses did not detect any significant effect of sunscreen nor temperature exposure during the 8 and 11 dafm spawning nights, while a significant effect of elevated temperature was revealed in the 9 dafm spawning event ($p_{temperature} < 0.0001$, Table 5.3). Interestingly, although total fertilization rates are high in all conditions, an elevated amount of abnormal embryos were observed as a result of sunscreen and warming exposure (Figure 5.8). Increasing temperature halved the proportion of normally developed embryos, representing the rate of successfully fertilized eggs, in all treatments compared to corresponding values at 27°C, even in control samples (Table 5.4). The observed reductions in the rate of embryos that developed normally for high sunscreen concentrations and temperature independently ranged from ~ 80% (T-Avo 0.5-1 mgL^{-1} and T-S 1 mgL^{-1}) to ~ 47% (control at 32°C), indicating that elevated temperature had a greater impact than sunscreen (Table 5.3 and Figure C.1). GLM analyses revealed that both sunscreen and temperature had significant effect on the proportion of successfully fertilized eggs ($p_{treatment}$ = 0.03 and < 0.0001, 8 dafm and 9-11 dafm respectively; $p_{temperature} < 0.0001$, 8-9 dafm, Table 5.3), however the interaction between sunscreen and temperature was not significant, indicating an additivity of effects ($p_{treatment:temp}$ = 0.87 and 0.123, 8 and 9 dafm respectively, Table 5.3).

Although at 27°C sunscreens exposures caused just a modest reduction in successful fertilized eggs compared to control (the maximum difference is ~ 8%), post hoc Tukey HSD test showed that the declines caused by some T-Avo and T-S concentrations on the 9 and 11 dafm were significant (Table C.1). At 32°C the lowest successful fertilization rates were reached in the 1 mgL^{-1} T-S and T-Avo treatments, which triggered a 39.6%

and 30.3% successful fertilization rate drop respectively, compared to control values at elevated temperature (Figure C.1), and a difference of 64% and 58% from unexposed samples at ambient temperature (Table 5.4).

5.3.2 Effects of sunscreen and temperature stress on coral embryonic development (Experiment 1)

An elevated number of aberrations in embryo development were observed in all the experiments, and the proportion of abnormal embryos compared with the total amount of fertilized embryos counted is reported in Figure 5.9. At ambient temperature, the abnormal development rate was relatively low across all treatments: 7 ± 1.7% - 8 dafm, 8 ± 2 - 9 dafm and 2 ± 2.3 - 11 dafm, although there was still a significant impact of sunscreen exposure ($p_{treatment} < 0.005$ – 8 dafm and $p_{treatment} < 0.0001$, 9-11 dafm, Table 5.3). Warming significantly increased the number of abnormalities ($p_{temperature} < 0.0001$, 8-9 dafm, Table 5.3). Control samples showed ~ 45% of aberrant embryos at 32°C, whilst they constitute more than 50% of the total number of fertilized embryos under sunscreen exposure. The highest abnormal development rate, ~ 67%, was reached under 1 mgL^{-1} T-S and T-Avo treatments, which displayed a 27% increase of abnormalities from control values compared to CNC 1 mgL^{-1} (Figure 5.9.). As for the fertilization rate, the effect of simultaneous temperature and sunscreen exposure was not significant ($p_{treatment:temp} = 0.99$ and 0.85, 8 and 9 dafm respectively, Table 5.3), thus the stressors did not induce a synergistic impact on the abnormal development rate. The results from Tukey HSD pairwise comparisons for abnormal developmental data are reported in Table C.2.

Table 5.3 - Effects of sunscreen treatments (Treatm) and temperature (Temp) on total fertilization rate, successfully fertilized eggs rate and embryo abnormal development rate of *Acropora hyacinthus* at the different spawning events (dafm). Significance at $p < 0.05$ is shown in bold. Df: degrees of freedom.

Experiment		Factor	Df	Deviance	F-value	p-value
Total fertilization	8 dafm	Treatm	12	0.25	0.7186	0.7312
		Temp	1	0.007	0.2376	0.6268
		Treatm:Temp	12	0.476	1.3687	0.1889
	9 dafm	Treatm	12	0.374	1.4172	0.1588
		Temp	1	0.747	33.948	**<0.0001**
		Treatm:Temp	12	0.167	0.6325	0.8135
	11 dafm	Treatm	12	0.0729	0.4471	0.9405
Successfully fertilized eggs	8 dafm	Treatm	12	0.742	2.0116	**0.03**
		Temp	1	36.713	1195.1	**<0.0001**
		Treatm:Temp	12	0.210	0.5708	0.87
	9 dafm	Treatm	12	1.703	6.7271	**<0.0001**
		Temp	1	61.667	2923.3	**<0.0001**
		Treatm:Temp	12	0.381	1.5037	0.123
	11 dafm	Treatm	12	1.158	6.3826	**<0.0001**
Abnormal development	8 dafm	Treatm	12	0.870	2.5250	**<0.005**
		Temp	1	45.085	1570.9	**<0.0001**
		Treatm:Temp	12	0.093	0.2689	0.993
	9 dafm	Treatm	12	2.324	7.9753	**<0.0001**
		Temp	1	78.024	3212.8	**<0.0001**
		Treatm:Temp	12	0.134	0.4590	0.936
	11 dafm	Treatm	12	2.779	20.137	**<0.0001**

Table 5.4 - Percentage of reduction in the rate of successfully fertilized eggs of *A. hyacinthus* for each treatment exposed to elevated temperature (average 8-9 dafm values ± sd).

Treatment		27 - 31°C reduction (%)
Control	0 mgL^{-1}	44.9 ± 1.7
CNC	0.05 mgL^{-1}	47.2 ± 0.1
	0.1 mgL^{-1}	50.4 ± 3.4
	0.5 mgL^{-1}	52.3 ± 1.1
	1 mgL^{-1}	50.2 ± 0.5
T-Avo	0.05 mgL^{-1}	53.1 ± 0.2
	0.1 mgL^{-1}	53.4 ± 10.4
	0.5 mgL^{-1}	56.2 ± 4.2
	1 mgL^{-1}	58.5 ± 10.8
T-S	0.05 mgL^{-1}	50.3 ± 4.1
	0.1 mgL^{-1}	52.0 ± 3.0
	0.5 mgL^{-1}	57.4 ± 1.1
	1 mgL^{-1}	64.8 ± 2.1

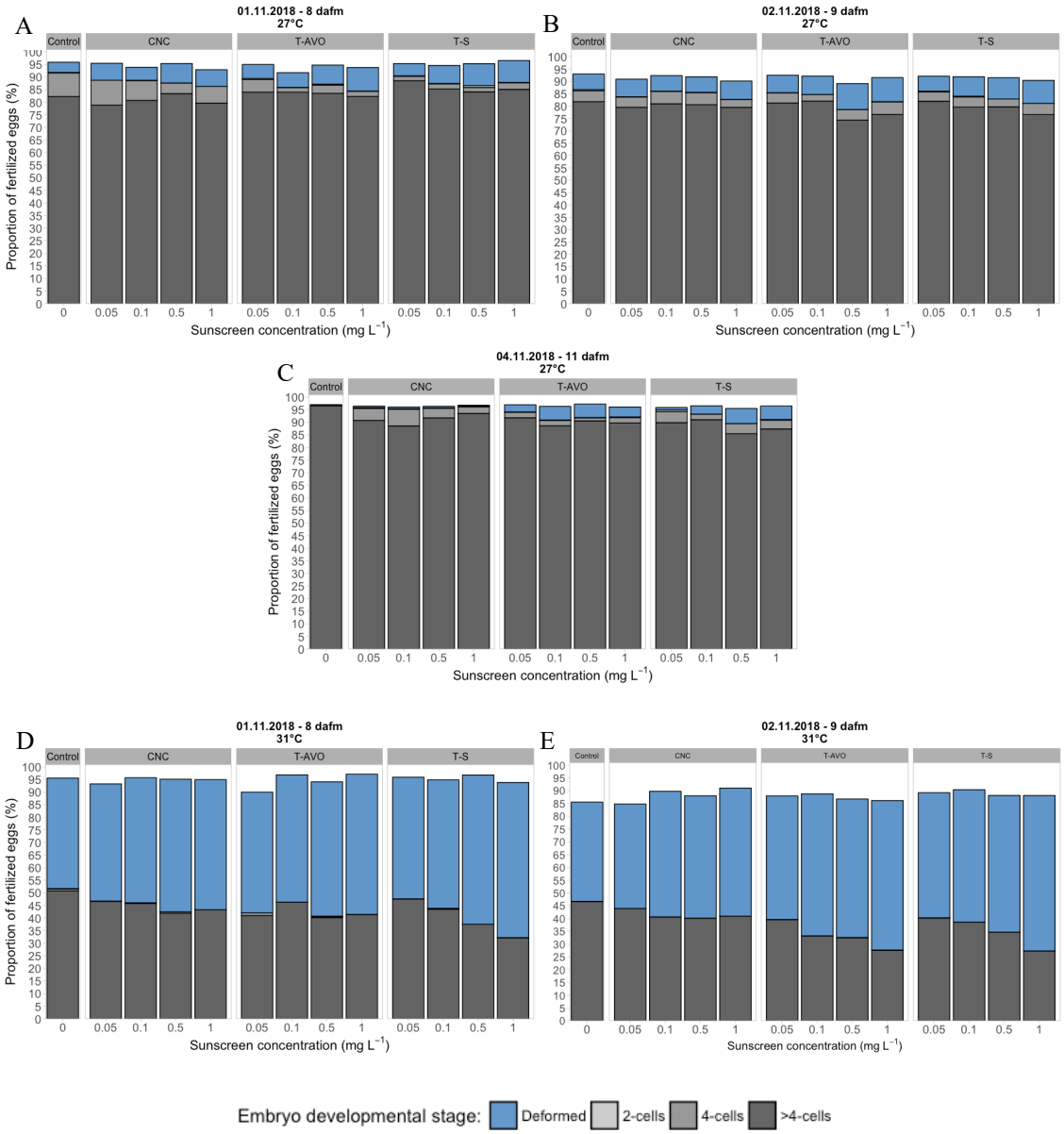

Figure 5.8 - Proportion of the different embryonic developmental stages on the total amount of fertilized eggs of *A. hyacinthus* under increasing sunscreen concentrations at either ambient (27°C) (**A-C**) or elevated (31°C) (**D-E**) temperature during the different night of spawning.

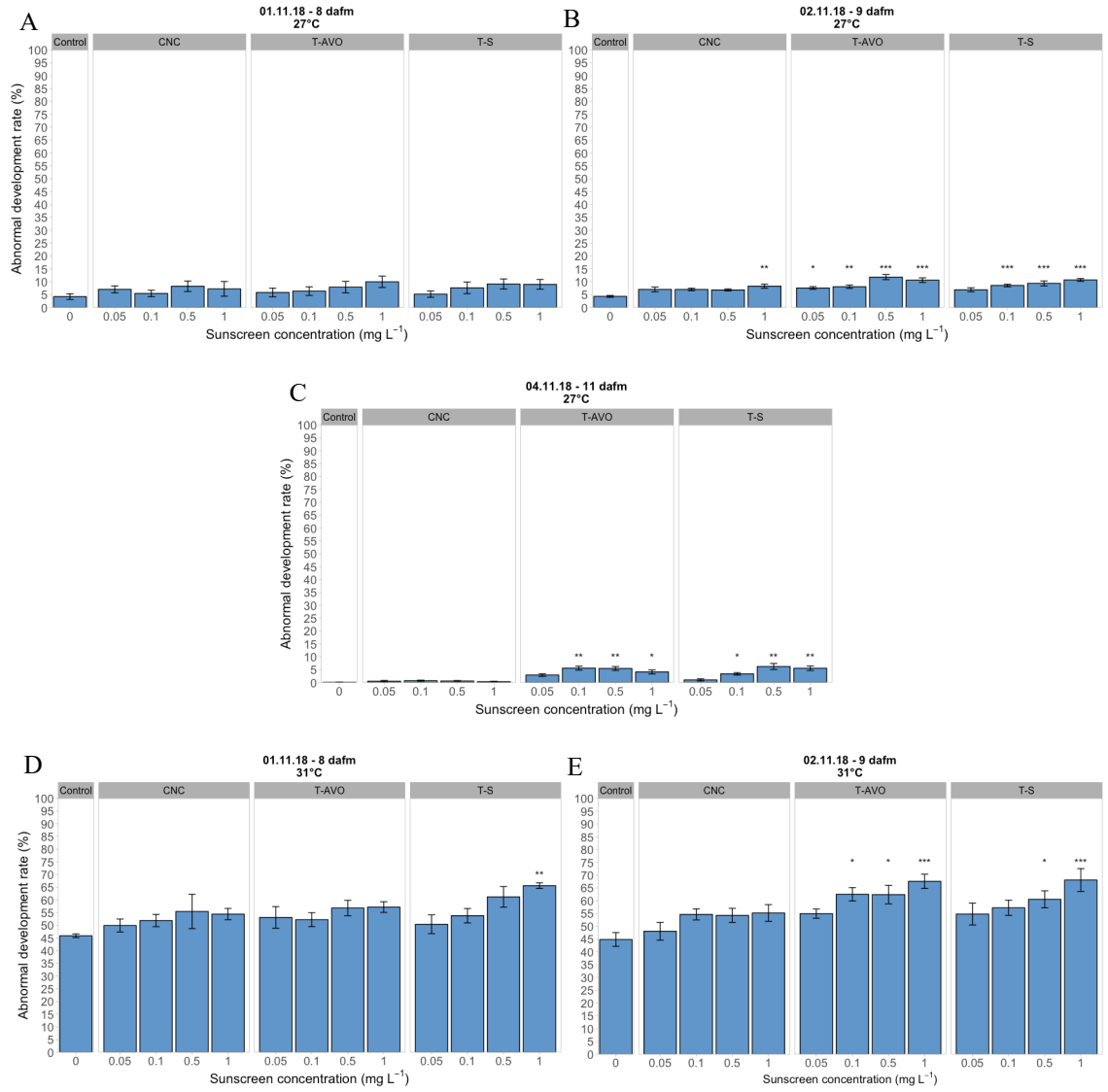

Figure 5.9 - Abnormal developmental rate of *A. hyacinthus* under increasing sunscreen concentrations at either ambient (27°C) (**A-C**) or elevated (31°C) (**D-E**) temperature during the different night of spawning. Error bars represent the standard error of mean. "*", "**" and "****" indicated significant difference between control and the other sunscreen treatments with $p < 0.05$, 0.01 and 0.001, respectively.

5.3.3 Sperm motility test (Experiment 2)

Here CASA is used to analyse the motility of *A. globiceps* sperms exposed for 15 minutes to 1 mgL^{-1} of the different sunscreen formulations and the percentage of total, progressive and slow motility is presented in Figure 5.10. In the unexposed samples, 78.7 ± 5.1% of the sperm were in movement and 45.6 ± 9% of them showed progressive motility, while just 9.1 ± 1.6% are slow. GLM analyses revealed that exposure to sunscreen impacted significantly total and slow motility (p_{total} = 0.05 and p_{slow} = 0.005, Table 5.5 A). T-S caused the highest reduction in total motility, ~ 17% than control ($p_{T\text{-}S}$ = 0.048 according to Tukey HSD post hoc test, Table 5.5 B, Figure 5.10 A), in addition to significantly increase the proportion of slow motility along with T-Avo ($p_{T\text{-}S}$ = 0.01 and $p_{T\text{-}AVO}$ = 0.004 according to Tukey HSD post hoc test, Table 5.5 B, Figure 5.10 C).

Table 5.5 - **A**) GLM analyses on the effects of 1 mgL^{-1} of sunscreen formulations on the total, progressive and slow motility of *A. globiceps* sperm. **B**) Tukey post-hoc test comparisons on total and slow sperm motility. Significance at $p < 0.05$ is shown in bold. Df: degrees of freedom

A)

Motility type	Df	F-value	p-value
Total	3	3.7501	**0.05**
Progressive	3	0.0617	0.97
Slow	3	9.5457	**0.005**

B)

Motility type	Comparisons		p-value
Total	Control	CNC	0.25
		T-Avo	0.15
		T-S	**0.048**
	CNC	T-Avo	0.97
		T-S	0.65
	T-Avo	T-S	0.85
Slow	Control	CNC	0.1
		T-Avo	**0.004**
		T-S	**0.01**
	CNC	T-Avo	0.15
		T-S	0.62
	T-Avo	T-S	0.66

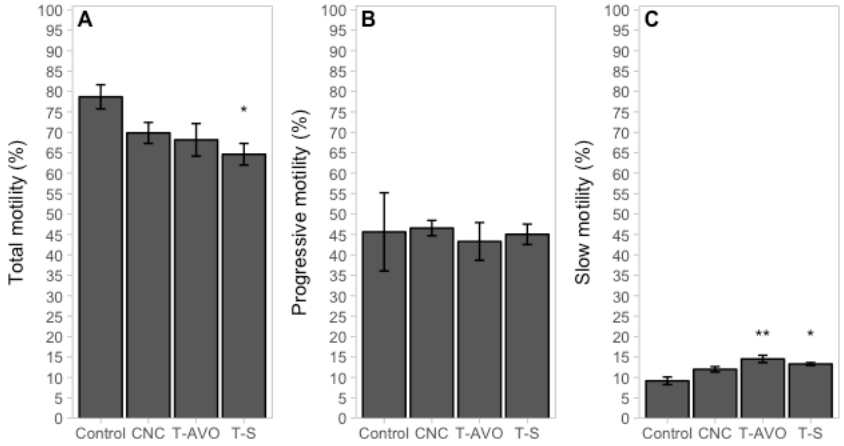

Figure 5.10 - **A**) Total, **B**) Progressive, **C**) Slow motility of *A. globiceps* sperm exposed to 1 mgL^{-1} of each inorganic sunscreen formulation. Error bars represent standard error of means. "*" and "**"indicated significant difference between the control treatment and the other sunscreen treatments with $p < 0.05$ and 0.01, respectively.

5.3.4 Effects of sunscreen and temperature stress on larval survivorship (Experiment 3)

Survival of *A. globiceps* larvae (Experiments 3a) in the control treatment at ambient temperature was high for the entire duration of the experiment (83% after 12 days, the last day of experiment, Figure 5.11). Thermal stress halved the survival of control larvae after 7 days; when a survival of 45% was observed (Figure 5.12), the experiment was terminated. Significant differences in larval survivorship between treatments were observed both under ambient and warming conditions (Log-rank test at 27°C: $\chi^2 = 21.3$, df = 12, p = 0.047; log-rank test at 31°C: $\chi^2 = 35.3$, df = 12, p = 0.0001, Table C.3). At ambient temperature, larvae exposed to T-Avo showed an overall lower survival rate among all sunscreen formulations, with the curves of all concentrations constantly between 13 and 25% lower than control curve from day 4 and reaching an average survival of 62 ± 0.03% for 0.1, 0.5 and 1 mgL^{-1} at the 12th day of experiment (value however similar to CNC 1 mgL^{-1} survival rate, 65 ± 0.06%, Figure 5.11). The lowest survival rate at the end of the experiment was observed for T-S 1 mgL^{-1} (53 ± 0.06%), the only curve to be significantly different from the control (Log-rank test pairwise comparisons p = 0.03, Table C.3). Survivorship curves of *A. globiceps* larvae under warming conditions are presented in Figure 5.12. The fitted Kaplan-Meier function estimated that 50% of the larvae population in control conditions at 32°C would die after 5 days, with a 95% confidence interval between 4 to 7 days (Table C.4). Under sunscreen

exposure instead 50% of mortality is reached already at day 2 for all concentrations and formulations tested (except for T-Avo 0.1 mgL^{-1} and CNC 0.05 mgL^{-1} when it is reached at day 3, Table C.4).

Survivorship curves of *P. damicornis* larvae (Experiment 3b) exposed to sunscreen treatments are depicted in Figure 5.13. The survival of *P. damicornis* larvae was significantly affected by sunscreen (Log-rank test survivorship: $\chi^2 = 64.8$, df = 12, p <0.0001, Table C.5). Larvae showed the lowest survival rate exposed to T-S and T-Avo 1 mgL^{-1} (58 ± 0.06% and 60 ± 0.06%, respectively), while the lower survival rate exhibited by CNC formulation was 73 ± 0.06% for 1 mgL^{-1} concentration. Log-rank test pairwise comparisons are reported in Table C.5 and the larvae survival probability in Table C.6.

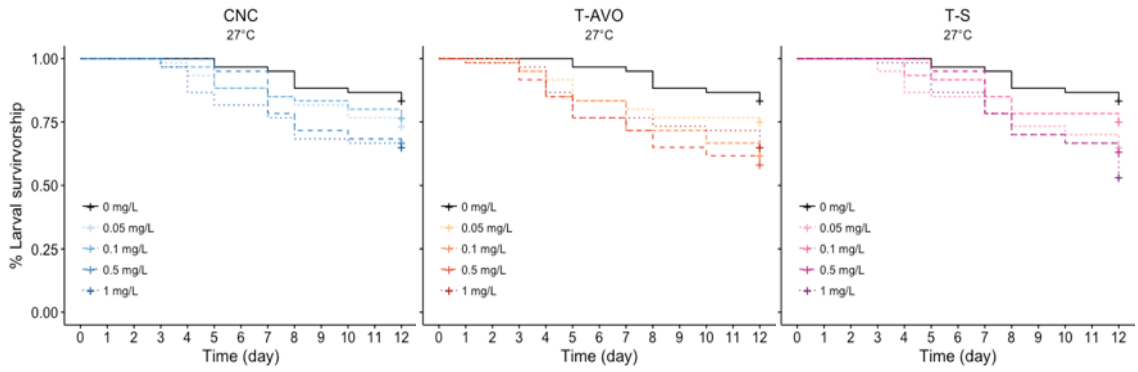

Figure 5.11 - Kaplan-Meyer survivorship curves of 5 days old larvae of *A. globiceps* exposed to different concentrations of CNC, T-Avo and T-S sunscreens at ambient temperature (27°C).

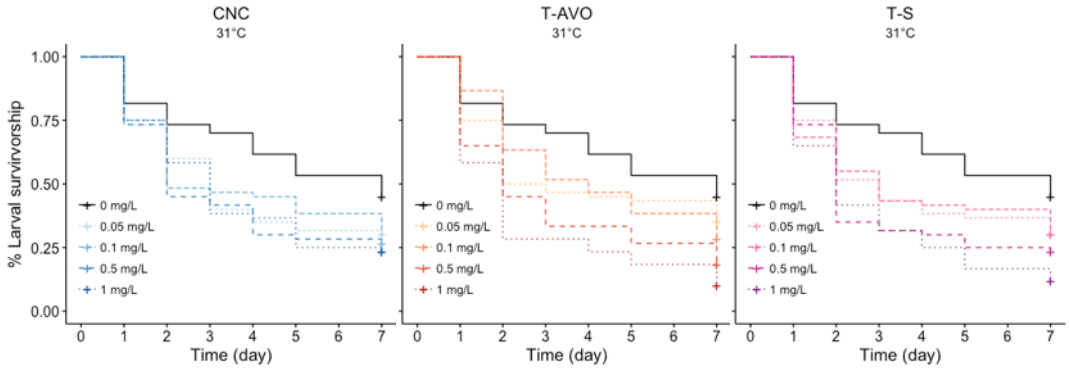

Figure 5.12 - Kaplan-Meyer survivorship curves of 5 days old larvae of *A. globiceps* simultaneously exposed to different concentrations of CNC, T-Avo and T-S sunscreens and warming conditions (31°C).

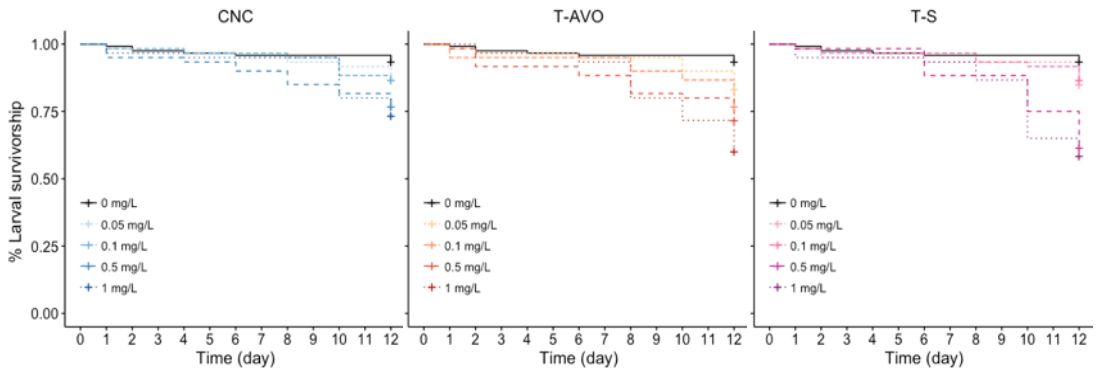

Figure 5.13 - Kaplan-Meyer survivorship curves of *P. damicornis* larvae exposed to different concentrations of CNC, T-Avo and T-S sunscreen formulations at ambient temperature.

5.4 Discussion

This is the first study to test the effects of inorganic sunscreen on corals early life history stages, and also to compare the toxicity of different sunscreen formulations in order to investigate their differential toxicity in relation with the type of emulsifying agent and $nTiO_2$ UV filter used as sunscreen ingredients. Results demonstrated that the final outcome of the exposure of coral early life history stages to environmentally realistic concentrations of inorganic sunscreen formulations was an increase of aberrations in embryo development, a reduction of sperm motility and a decline of larval survivorship. Although temperature increase is the main driver of the detrimental impacts on fertilization and larval survivorship in a warming ocean, sunscreen enhanced those effects in a combined exposure, demonstrating that it is an important factor in coral population dynamics and for corals' resilience to ocean warming.

5.4.1 Fertilization and embryo development under sunscreen and heat stress

Results from this study suggests a high tolerance of fertilization against sunscreen exposure since *Acropora hyacinthus* fertilization rates were high across all sunscreen formulations up to the estimated inorganic sunscreen concentration in a touristic beach (1 mgL^{-1}), even when simultaneously exposed to temperature of 4°C above ambient. This is not surprising as relatively high levels of fertilization have been reported for gametes of various coral species exposed to a variety of stressors, such as 1-4°C seawater temperature increase (Bassim et al., 2002; Negri et al., 2007; Puisay et al., 2018), up to 100 μgL^{-1} of

copper (Kwok et al., 2016), 25 mgL^{-1} of iron (Leigh-Smith et al., 2018), 500 μgL^{-1} of zinc as well as a range of salinities (Chui and Ang, 2015; Hédouin et al., 2015), sediments (Humphrey et al., 2008) and nutrients levels (Humanes et al., 2016; Humphrey et al., 2008). *A. hyacinthus* from subtropical environment, in particular, showed an almost 100% fertilization rate at temperatures between 25°C and 33°C (Keshavmurthy et al., 2014). High fertilization rates in the study presented here as well many of the studies reported above, were accompanied by an increase of aberrations in embryo development proportional to the stress applied to the gametes. Here temperature had a greater impact on fertilization success and abnormal development ratio than sunscreen. The quantity of abnormally developed embryos under inorganic sunscreens at 27°C was significant, although low, whilst embryos under control conditions at 31°C exhibited an abnormal development rate of ~ 45%, consistent with previous studies on *Acropora* spp. (Negri et al., 2007; Puisay et al., 2018). While with the experimental design applied here it is impossible to pinpoint the mechanisms inducing the observed aberrations following sunscreen exposure, possible explanations can be originated from the literature. Thermal stress has been widely demonstrated to increase the proportion of abnormally developed embryos (Keshavmurthy et al., 2014; Randall and Szmant, 2009; Voolstra et al., 2009), and ROS produced during heat stress and consequent oxidative damage has been suggested to cause impairments in functional enzymes and structural proteins (Negri et al., 2007), downregulation of metabolic processes (Voolstra et al., 2009) and a breakdown of gene expression (Portune et al., 2010) during embryo development. Results from Chapter 4 of this thesis indicate that in *E. pallida* anemones the sunscreen oil phase is responsible for a quick heat-shock protein gene induction similar to high temperature stress response. Moreover, oxidative stress is an important component of the stress induced by hydrophobic and hydrophilic $nTiO_2$ UV filter agents towards $nTiO_2$-oil phase mixtures on Symbiodiniaceae (Chapter 2) , as well as zebrafish embryos (Faria et al., 2014). Hence this study suggests that the exposure to inorganic sunscreen induces stress mechanisms similar to warming in coral embryos, but in lower doses.

The future of abnormal embryos is uncertain due to the lack of continued observation from fertilization to the larval development and juvenile recruitment under stressful conditions, however it will most likely lead to consequences at population-level (Berry et al., 2017; Humanes et al., 2016; Puisay et al., 2015). Keshavmurthy et al. (2014) observed degradation of *A. hyachintus* abnormal embryos 9 hours post fertilization, and studies on other marine invertebrates suggested that aberrations lead to higher mortality rates in

subsequent larval stages (Caldwell, 2009). The high levels of abnormalities described here may indicate that the quantity of viable larvae might be diminished under inorganic sunscreen exposure, possibly reducing coral recruitment. Chui and Ang (2015) observed that elevated temperature could alleviate the negative effects of low salinity on coral fertilization. On the contrary, in this study the combination of inorganic sunscreen formulations and elevated temperature affected *A. hyacinthus* fertilization and the amount of embryo abnormalities in an additive manner, suggesting that sunscreen exposure likely exacerbates the impacts of warming on fertilization in places where high temperatures and high touristic load coincide with natural spawning events.

5.4.2 Inorganic sunscreen exposure affects sperm motility of corals

The quality of gametes, in particular sperm, strongly influence fertilization success rate in aquatic invertebrates, and sperm motility is considered a proxy for sperm quality (Lewis and Ford, 2012). Computer-Aided Sperm Analysis (CASA) automatically measure sperm curvilinear velocity (μm s^{-1}) , straight line velocity (μm s^{-1}) and the straightness (%) of the distance covered by single sperm, to assess the percentage of motile sperm in a sample (Amann and Waberski, 2014). Moreover, CASA analyses each sperm track in a sample to classify them in progressive or slow, weakly motile. Motility is classified as progressive when spermatozoa show vigorous motion on a straight path, while slow sperms cover a shorter distance than progressive ones (Goodson et al., 2011). CASA has been a valuable tool for toxicological studies on the effects of toxicant on both human and animal sperm, and is commonly used to assess spermatozoa quality for cryopreservation and their fertilizing ability in aquaculture and breeding to preserve and transport sperm as well as in human medicine (see reviews by Kathiravan et al., 2011; Kime et al., 2001; van der Horst et al., 2018).

Reduction in the motility of sperm has been suggested as a possible reason for the reduced fertilization rates observed in corals exposed to nickel, copper, nutrient, acidified water and elevated temperature (Albright and Mason, 2013; Gissi et al., 2017; Humanes et al., 2016; Iguchi et al., 2015; Puisay et al., 2015). Although the study of sperm flagellar motility of marine organisms is commonly used in ecotoxicity assessment of contaminants (Catarino et al., 2008; Dietrich et al., 2010; Fitzpatrick et al., 2008; Özgür et al., 2018, in particular see the reviews of Gallo and Tosti, 2019, and Lewis and Ford, 2012), only three studies looked at the flagellar sperm motility of corals. Morita et al. (2010) and Nakamura et al. (2012) documented a reduction in motility of *Acropora*

digitifera spermatozoa under projected CO_2 conditions, while Omori et al. (2001) observed a reduction in motility of sperm from corals recovering from a mass bleaching event. Here exposure for just 15 minutes to 1 mgL^{-1} of all three inorganic sunscreen formulations tested reduced the motility of *A. globiceps* sperms while increasing the proportion of spermatozoa moving in slow motion (Figure 5.10).

The exposure time of 15 minutes was chosen in order to have three replicates measurements for each treatment while setting-up the fertilization process for the subsequent larvae experiment in the restricted time of sperm viability post-spawning. Although it is about half the time used in a previous experiment with coral gametes (Ricardo et al., 2015), the exposure time used here is within the limits of the 15-30 mins time occurring to an egg to become mature and for gametes to interact in the field (Heyward and Babcock, 1986; Oliver and Babcock, 1992).

ROS induction by sunscreen exposure could be the possible mechanism of action also in the case of sperm motility. Sperm are particularly vulnerable to ROS as they attack mitochondria, the organelles that provide energy to swim, through lipid peroxidation and protein denaturation (Wang et al., 2003) and $nTiO_2$ is a known ROS-inducer (von Moos et al., 2014). Experiments on Symbiodiniaceae presented in Chapter 2 support this hypothesis, demonstrating an increase of ROS in algal cells under sunscreen $nTiO_2$ and oil phase mixtures. Rainbow trout sperm cells exposed to increasing $nTiO_2$ concentrations showed a significant increase in superoxide dismutase, an important antioxidant defence system, starting from 0.1 mgL^{-1} $nTiO_2$, although normal flagellar motility was observed up to a concentration of 10 mgL^{-1} (Özgür et al., 2018). Sunscreen could also interfere with sperm movements by attaching to the spermatozoa surface and causing them to sink, as proposed for sediments in contact with coral gametes (Jones et al., 2015). The negative effect of sunscreen towards coral sperm cells observed here is likely caused by a combination of physical constraints, due to the hydrophobic properties of the sunscreen ingredients that may stick on the cells surface and impede movements, and biochemical impact from the exposure to $nTiO_2$ and other ingredients in the formulation, further studies are necessary to verify these hypothesis.

The quantity of sperm having quick, progressive movements reflects the amount of sperm available for coral fertilization (Nakamura and Morita, 2012). Omori et al. (2001) and Albright and Mason (2013) suggested that the elevated, optimal, sperm concentration used in laboratory experiments could mitigate the negative effects of decreased sperm motility and reduction of egg-sperm interactions on fertilization, and this could explain

why in this study no reduction of fertilization was observed up to 1 mgL^{-1} of sunscreen exposure. However in real spawning conditions gametes are released in surface waters where they are rapidly diluted and sink into the water column, hence the potential of fertilization of coral eggs is naturally limited (Nakamura and Morita, 2012; Oliver and Babcock, 1992). During natural spawning events, even the slight decrease of sperm flagellar motility induced by sunscreen could therefore seriously reduce coral fertilization success. To better predict the impact of sunscreen exposure on fertilization, further studies should test a range of sperm concentrations, as suggested for ecotoxicological research on coral fertilization, in order to avoid this mitigation effect of laboratory fertilization studies (Gissi et al., 2017; Jones et al., 2015; Marshall, 2006).

5.4.3 Larval survivorship under sunscreen and heat stress

Contrary to coral fertilization, the effect of sunscreen UV filters on coral larvae has been described in previous studies. Larvae of *S. pistillata* were highly susceptible to BP-2 and BP-3 and showed 50% of mortality after 24 hours at concentration of 0.2 mgL^{-1} (Downs et al., 2014, 2016). Conversely, He et al. (2019) reported that larvae of *S. caliendrum* showed low mortality (range 2.5 - 30%) when exposed to BP-1 and BP-8 up to concentration of 1 mgL^{-1}, and none of the tested compound affected *P. damicornis*. Those studies suggest that coral larvae might be affected by sunscreen compounds, but the effects are species-specific and they have been tested on individual UV filters of organic nature, the effects of whole sunscreen products remain unknown.

In the present study, exposure to inorganic sunscreen formulations at ambient temperature significantly reduced the survival of *A. globiceps* and *P. damicornis* larvae with increasing concentrations. Although *A. globiceps* exhibited in overall lower survival rates than *P. damicornis*, reaching a ~ 15% higher mortality at the end of the experiment in all treatments included control, the differences in survival rates with each time-matching control were similar for both species. Interestingly, *P. damicornis* larvae started to show reduced survival only after 8-10 days of exposure, while *A. globiceps* exhibits the same values earlier, from day 4 (Figure 5.11 and Figure 5.13). *P. damicornis* and *A. globiceps* have different reproductive strategies and those corals were chosen in the present study to expressly investigate the effects of sunscreen exposure on brooder versus spawned larvae. *P. damicornis* release free-swimming larvae which receive endosymbiotic Symbiodiniaceae from the parental colony (Harrison and Wallace, 1990). *A. globiceps* larvae instead develop in the water column following external fertilization and are

aposymbiotic (Oliver and Babcock, 1992). Larvae are coral dispersing stages with elevated energy requirements and their different susceptibilities to anthropogenic stressors are thought to be related to the amount of endogenous energy reserves (Graham et al., 2008; Kwok et al., 2016). While Symbiodiniaceae provides *P. damicornis* larvae with photosynthetically fixed carbon (Richmond, 1987), *A. globiceps* aposymbiotic larvae relies solely on stored lipids as energy reserve (Graham et al., 2008). Sunscreen compounds might induce the activation of energetic costly stress-response mechanisms in coral larvae, as observed for copper, nutrients and elevated temperature (Kwok and Ang, 2013; Lam et al., 2015; Puisay et al., 2015). The earlier mortality exhibited by *A. globiceps* larvae compared to *P. damicornis* could therefore be the consequence of the metabolism depletion induced by sunscreen exposure, while *P. damicornis* larvae use energy translocated by zooxanthellae to maintain their metabolism and swimming activity. Nevertheless algal symbiont in coral larvae makes them highly susceptible to oxidative stress, resulting in increasing mortality under stressful conditions (Yakovleva et al., 2009). Thus the high but delayed response of *P. damicornis* under 0.5 and 1 mgL^{-1} sunscreen exposure could possibly be the result of the accumulation of oxidative damage in Symbiodiniaceae and, therefore, inside larval cells. The negative effects of sunscreen exposure to adult corals and their *in-hospite* Symbiodiniaceae was presented in Chapter 3, suggesting that sunscreen directly affects both algal symbionts and coral hosts. However to verify the hypothesis presented here, future study should investigate larval metabolism and oxidative stress under sunscreen exposure through respirometry analyses and measurements of the levels of oxidative damage indicators, such as superoxide dismutase enzyme activity and malondialdehyde, a product of lipid peroxidation (Yakovleva et al., 2009).

The time-dependent increase in mortality observed in the present study agree with previous larvae toxicological studies (Bassim and Sammarco, 2003; Hédouin et al., 2015; Kwok and Ang, 2013) and has the potential to affect larvae dispersal range in the natural environment. Larvae of both *P. damicornis* and *Acropora* spp. are able to remain competent in the plankton for more than 100 days (Graham et al., 2008; Richmond, 1987), which suggests they could experience a variety of anthropogenic stressors during their long-range dispersal, including sunscreen and elevated seawater temperature. Warming is well-known to significantly affects larvae survival (Heyward and Negri, 2010; Olsen et al., 2013; Puisay et al., 2018; Woolsey et al., 2015) and previous studies demonstrated that nutrients and copper interact with elevated temperature enhancing the negative

effects warming on larvae survival (Bassim and Sammarco, 2003; Kwok and Ang, 2013; Negri and Hoogenboom, 2011). Here the simultaneous exposure to sunscreen levels expected in a touristic beach (Chapter 1, Section 1.2.5) and warming conditions projected in the coming decades (IPCC, 2014) halved the survival of *A. globiceps* after just 2 days of exposure, whereas under thermal stress alone the exposure time needs to be increased to 5 days to reach the same effect. This result indicates that exposure to inorganic sunscreen formulations is of particular concern in the view of coral reefs under pressure from climate change.

5.4.4 Comparative toxicity between sunscreens

One of the aims of the present study was to investigate if sunscreen toxicity depends on the characteristics of its ingredients, since different UV filter coatings and their dispersant medium are not usually taken into account in sunscreen toxicity studies. In particular, here it was examined if the toxicity of an inorganic sunscreen formulation varied according to the type of emulsifying agent in the oil phase or to the coating of the $nTiO_2$ UV filter. To do so, a sunscreen formulated with 10% Eusolex® T-S $nTiO_2$ and 3% of the chemical emulsifier EasyNov™ (the same sunscreen formulation tested in the experiments presented in previous chapters) was tested against a formulation having the same UV filter type and concentration but 3% of an organic emulsifier (Cellulose NanoCrystal) and a third formulation having the same chemical emulsifier but different $nTiO_2$ UV filter (specifically with Eusolex® T-Avo at 5%) (Table 5.2).

Eusolex® T-S and Eusolex® T-Avo are hydrophobic and hydrophilic $nTiO_2$, respectively, and their characterization is presented in Appendix A. EasyNov™ is an emulsifier commonly used in cosmetic industry while CNC is a nanomaterial used as surface-stabilizing agent in emulsions which use and characteristic in a sunscreen product having $nTiO_2$ as UV filter has been recently described by Shandilya and Capron (2017). CNC derives from cellulose, it is thus considered a biodegradable and environmentally friendly nanomaterial (George and Sabapathi, 2015), with no significant cytotoxicity on human cell lines (Roman, 2015). Because of those characteristics, it was originally hypothesized that sunscreen formulated with CNC as the emulsifier could have been a less toxic solution than the chemical emulsifier Easinov™ (which toxicity on Symbiodiniaceae, *E. pallida* and adult corals was presented in the previous chapters of this thesis). Although coral larvae under CNC treatments did not present striking differences compared to the

other tested formulations, a decrease of toxicity was still observed in all endpoint studied especially when gametes are exposed. The ratio of abnormal embryo development is the endpoint showing the greatest differences among sunscreen formulations, and results from Tukey HSD post hoc test indicating the treatment comparisons having significant differences are presented in Table C.2. *A. hyacinthus* gametes exposed to CNC formulation exhibited in overall the lower amount of aberrant embryos among sunscreen treatments, being significantly higher than control only during the 9 dafm at 27°C experiment at the 1 mgL^{-1} concentration. Also, the abnormal development rates of gametes exposed to CNC up to the concentration of 0.5 mgL^{-1} are significantly different to various T-S and T-Avo concentrations, particularly the 9 and 11 dafm at ambient temperature. Similarly, *A. globiceps* sperm exposed to 1 mgL^{-1} CNC showed a slight and not significant reduction of motility compared to untreated sperm (Table 5.5). Conversely, all of the sunscreen formulations were observed to affect larvae in a similar way. Larvae of *P. damicornis* only showed slight differences in their survival curves, although under CNC exposure exhibit always the lower mortality among treatments (Figure 5.13). All together these results indicate that CNC show overall less toxicity than T-Avo and T-S towards coral gametes. Because CNC and T-S formulations share the same type of $nTiO_2$ at equal dose, the organic emulsifying agent cellulose nanocrystal is likely a safer emulsifier than the chemical one. The comparable toxicity levels in larvae survival between CNC treatments and the other treatments could be the consequence of an increasing dispersion of $nTiO_2$ from the oil carrier into the water media due to the longer experimental time, as observed in the ICMPS analyses presented in Chapter 2.

Differences between the type of $nTiO_2$ UV filter in the sunscreen formulation were not as marked as for CNC. T-S and T-Avo treatments showed an overall a similar toxicity both in the gametes and larvae experiments, despite the concentration of $nTiO_2$ differs in the two chemical emulsifier formulations. Eusolex® T-Avo is characterized by a silica hydrophilic coating while Eusolex® T-S has an alumina plus stearic acid hydrophobic coating (Appendix A). The hydrophilicity of Eusolex® T-Avo makes it well dispersed in the water phase of the sunscreen emulsion and is consequently more easily dispersed in seawater than Eusolex® T-S that, because of its hydrophobicity, remains trapped in the sunscreen oil droplets and less available to interact with the environment (Dr Labille, personal communication, and results from ICPMS analyses in Chapter 2). However, Eusolex® T-Avo demonstrated low toxicity towards Symbiodiniaceae in the experiment presented in Chapter 2, hence the toxicity observed here is probably mainly due by the

sunscreen oil phase with organic emulsifier in both T-S and T-Avo sunscreen treatments. Future studies should develop chemical analyses of the sunscreen formulations dispersions in seawater in order to verify these assumptions and describe sunscreen behaviour in the water column.

5.4.5 Consequences of sunscreen pollution on corals' reproductive success

The persistence and recovery of coral populations depend on the performance of every step of their reproductive cycle, from fertilization success to post-settlement survival and growth (Ritson-Williams et al., 2009). Perturbations in one or more phase of their life cycle have the potential to affect species distribution leading to important ecological consequences (Woods et al., 2016). Spawning corals are particularly endangered by the detrimental impacts of sunscreen formulations because both fertilization and larvae development occur in surface waters where sunscreen ingredients are released and concentrated (Gondikas et al., 2017). Fertilization success is the first key step in the reproductive cycle of spawning corals. In this study fertilization success was not directly impacted by sunscreen exposure, yet sunscreen reduced sperm motility. Lower than normal sperm concentration has been linked to reduced fertilization success in field studies (Oliver and Babcock, 1992; Omori et al., 2001; Willis et al., 1997), hence sunscreen contamination has the potential to indirectly impair coral fertilization. Notably, sunscreen formulations affected embryo development by causing an increased amount of abnormalities in spite of the fertility of their gametes. This could induce important consequences in the number of larvae that will be available for settlement, since abnormally developed embryos incur degradation or can lead to higher larvae mortality (Caldwell, 2009; Keshavmurthy et al., 2014).

The next critical phase in life cycle of corals is the survival of developed and brooded larvae, fundamental process for coral recruitment (Ritson-Williams et al., 2009). Here it was proved that sunscreen exposure causes elevated larvae mortality in a dose-dependent manner. This results in limited dispersal capacity, particularly for broadcast spawners that have a longer planktonic period (Harrison and Wallace, 1990; Nozawa and Harrison, 2007). Laboratory experiments demonstrated that larvae can survive up to 244 days in the water column in absence of settlement substrate (Graham et al., 2008). Swimming larvae have thus the capacity to survive in the plankton for a long time until they found a

suitable site to settle (Graham et al., 2008; Richmond, 1987), multiplying the chances to experience sunscreen pollution and consequently further decreasing their survival rate.

All together, results from the study presented here indicate that in sunscreen polluted waters fewer larvae reach the final phase of the reproductive cycle, the processes of settlement and metamorphos into coral recruits. Settlement behaviour under sunscreen exposure was not addressed in the present study, however settlement is known to be influenced by water quality and substrate conditions (Ritson-Williams et al., 2010). Larvae must have an appropriate substrate for settlement, and respond to chemical cues likely induced by microbial/algal biofilm on the substratum (Harrington et al., 2004; Ritson-Williams et al., 2010; Webster et al., 2004). Negri and Heyward (2000) demonstrated that oil and dispersal surfactant affect larvae metamorphosis and settlement. Similarly, sunscreen could alter the physical and chemical characteristics of the substratum by creating an oily slick on its surface and/or affect the associated microbial and algal communities, likely impeding larval settlement and negatively influencing coral recruitment success.

Once settled, larvae undergo metamorphosis into a sessile primary polyp, the coral recruit. At this point the 80% of broadcast spawning species with aposymbiotic larvae must acquire their symbiont from the surrounding waters (Baird et al., 2009). Findings from Chapter 2 demonstrated that free-living Symbiodiniaceae have a higher mortality in sunscreen-polluted waters, consequently symbionts acquisition by coral recruits is likely more arduous. Moreover, the limited energy resources in coral recruits, due to their small size and small symbionts population (Negri et al., 2005), suggests they may be susceptible to sunscreen contamination. As support of this theory, settled larvae have been demonstrated to be more sensitive than swimming larvae to the UV filter benzophenone and the herbicide diuron (He et al., 2019b; Negri et al., 2005). Hence sunscreen exposure may induce negative impacts in coral recruits, similar to the metabolic and photosynthetic effects observed in Chapter 3 for adult corals.

Overall, this study show that sunscreen use in coastal and highly touristic areas and the consequent discharge of sunscreen ingredients in coral reef waters has the potential to affect coral recruitment by impairing key processes in the reproductive cycles of corals. Furthermore, sunscreen contamination increases the detrimental impacts of elevated seawater temperature on coral embryo development and larvae survival. Thereby sunscreen pollution may have important implications for the resilience and recovery of coral reefs in a global warming scenario.

5.5 Conclusion

The study presented here demonstrated that inorganic sunscreens enhanced the negative impacts of warming on the viability coral gametes and larvae. Moreover, even without thermal stress the exposure to sunscreen have small but significant impact on sperm motility, embryo development and larvae survival that could compromise larval dispersal and the replenishment success of coral communities.

Specifically, in Moorea coral populations have suffered several large-scale disturbances in the past years that caused elevated mortality (e.g. cyclones, outbreaks of crown-of-thorns starfish *Acanthaster* spp. and coral bleaching events), but surprisingly they demonstrated high recovery capacity (Edmunds, 2018; Holbrook et al., 2018). This recovery was mainly driven by the recruitment of *Pocillopora* and *Acropora* spp. and the supply of larvae from nearby islands (Adjeroud et al., 2018; Bramanti and Edmunds, 2016). Findings from this study demonstrated that larval survival of *A. globiceps* and *P. damicornis* decrease with time under sunscreen exposure, hence larvae may need to settle closer to their parental reef. Consequently, the combination of the increase in abnormally developed embryos with the reduction of the distance of larval dispersal caused by sunscreen exposure could ultimately affect coral communities in Moorea. Moreover those effects could be enhanced when anomalously elevated temperature coincide with spawning events, such as October and November 2002 when temperatures reached 32.4°C (Puisay et al., 2018).

Further studies should investigate the possible mechanisms by which inorganic sunscreen affects gametes and larvae development, as suggested in the discussion paragraphs above, in addition to larval settlement in a sunscreen polluted water. Finally, dose-response relationships on successful fertilization and larvae survival should be evaluated to quantitatively assess the effects of sunscreen exposure in order to provide information useful for management

There is limited information on the concentration of sunscreen in tropical water bodies, however in this study toxic effects on coral gametes and larvae occurred at concentrations estimated to occur on a touristic beach (Chapter 1, Section 1.2.5). Although the concentration of sunscreen could decrease with time due to dilution and currents, fertilization and larval development take place in the upper seawater layers where sunscreen compounds are likely to form films and accumulate (Gondikas et al., 2014; Mitchelmore et al., 2019; Padilla-Gamiño et al., 2013) and anomalously high seawater surface temperature can occur (Bassim et al., 2002). Therefore the impacts of inorganic

sunscreen are particularly important in coastal reefs in highly urbanized and touristic areas, where the elevated and continuous input of sunscreen in the water bodies (Gondikas et al., 2014; Mitchelmore et al., 2019) could result in a carryover bottleneck effect for the success of corals in the future. Finally, results from this study highlight how the use of cellulose nanocrystals as emulsifying agent could mitigate sunscreen detrimental effects on coral fertilization and embryo development. Findings of the differential impacts of diverse sunscreen formulations on coral gametes and larvae provide preliminary evidence that not only is crucial to assess the toxicity of whole sunscreen product mixtures, but that the selection of less toxic cosmetic ingredients could reduce the stress of sunscreen pollution on coral early life history stages.

Chapter 6

General discussion and Conclusions

6.1 Overview of findings

Sunscreens are cosmetic products that protect the skin from the deleterious effects of solar rays. UV filters, the active compounds that directly protect the skin due to their absorption and/or reflective properties, are the ingredients that characterize sunscreen products. Emollient and emulsifying agents are the other core components of sunscreen formulations having aesthetic and stabilizing purposes and ensuring homogeneous dispersion of the UV filters (Osterwalder et al., 2014). Sunscreen products are conventionally divided into organic and inorganic on the base of the type of UV filters ingredients in their composition. This thesis focused on the second type: inorganic sunscreen formulated with metal oxides as active ingredients. Specifically, the type of UV filter studied here was titanium dioxide in its nanoparticulate form.

Inorganic sunscreens formulated with $nTiO_2$ as UV filter once released in seawater form stable colloidal suspensions of aggregates containing up to 30% of the nanoparticles initially present in the formulation embedded in the organic ingredients of the cream (Botta et al., 2011). Those aggregates accumulate in the upper surface layers of the oceans (Gondikas et al., 2014), where trapped $nTiO_2$ are exposed to sunlight radiations that may degrade the nanoparticles coatings (Labille et al., 2010) enhancing the titanium intrinsic photocatalytic activity. The remaining 70% of nanoparticles settle out of the water column and accumulate in the sediments with part of the organic components of the cream escaping the agglomerates (Botta et al., 2011). Sunscreen use lead also to the release of metals and inorganic nutrients in coastal waters (Rodríguez-Romero et al., 2019; Tovar-Sánchez et al., 2013), which ecological consequences have been scarcely studied.

The scarcity of information regarding the toxicity of inorganic sunscreen on reef-building corals is currently a crucial knowledge gap, particularly for tropical coastal areas where sunscreen pollution is of growing concern as result of the high amounts of sunscreen discharged due to elevated tourism and lack of efficient wastewater treatment plants (Baker et al., 2014; Bell, 2002; Reed et al., 2017; Tovar-Sánchez et al., 2019; Venkatesan et al., 2017). Despite sunscreen ingredients are all together released into surface water, most sunscreen toxicity studies are based on the evaluation of individual UV filters, from which it is difficult to extrapolate information about the whole formulation toxicity. With regard to the UV filters type examined in this thesis, another challenge is the diversity of $nTiO_2$ that can potentially be used as active ingredients in suncare products, since $nTiO_2$ often have different sizes, morphologies and coatings (Botta et al., 2011). In recent years an increasing number of publications have assessed the toxicity of whole sunscreen

products, organic as well inorganic, to different marine organisms (Corinaldesi et al., 2017; Danovaro et al., 2008; Danovaro and Corinaldesi, 2003; Díaz-Gil et al., 2017; Sendra et al., 2017b; Sureda et al., 2018; Tovar-Sánchez et al., 2013). However, the exact composition of the tested sunscreen formulations, or even the exact concentration of UV filters, is unknown. This makes it impossible to determine ingredient exposure concentrations and to compare the results between studies. Additionally, organic sunscreen formulations have been found to induce bleaching in tropical corals (Danovaro et al., 2008), but the effects of inorganic sunscreen on corals are currently unknown.
This research project aimed to address these knowledge gaps by assessing the toxicity of sunscreen $nTiO_2$ UV filters and oil phase ingredients, as well as whole inorganic sunscreen formulations of known compositions, on various stages of coral life cycle and on the coral model organism *Exaiptasia pallida*. Every experiment presented in this thesis have been performed under ambient and heat stress conditions typical of marine heatwaves in order to assess sunscreen toxicity in a global warming scenario, the primary factor causing the majority of recent coral bleaching events worldwide (Fordyce et al., 2019; Leggat et al., 2019). A summary of the main findings of this thesis will be presented in the following sections.

6.1.1 Comprehensive picture of the toxicity of inorganic sunscreen to tropical corals

The first step in assessing sunscreen toxicity towards tropical corals has been to determine the impact of different $nTiO_2$ types that are commonly used in sunscreen products as UV filters, on cultured Symbiodiniaceae (Chapter 2). Only slight differences in algae growth and ROS production were observed and depended on the $nTiO_2$ coatings and concentrations, while they were particularly affected by the sunscreen oil phase, highlighting the importance of considering emulsifying agents when assessing the toxicity of sunscreen products. Hence following the findings of this first study, two main line of investigations were originated: to assess the toxicity of inorganic sunscreen and to explore the influence of the oil-phase ingredients on the overall sunscreen toxicity. Summaries of the two arguments will be illustrated in this and the following section.

Inorganic sunscreens, formulated with common cosmetic ingredients, induced significant harmful effects in adult and early life stages of corals as well as sea anemones. Sunscreen concentrations up to 1 mgL^{-1} caused a similar reduction of Fv/Fm in both corals and

anemones (Chapter 3 and 4), while Fv/Fm of cultured Symbiodiniaceae was not affected by $nTiO_2$-oil phase mixtures (Chapter 2). Corals' net photosynthetic rates decreased drastically under sunscreen exposure, indicating that coral respiration during daylight was greater than oxygen production through zooxanthellae photosynthetic activity and inducing a reduction of the photosynthesis to respiration ratio below the autotrophic threshold. The density of Symbiodiniaceae in coral fragments was also significantly reduced, denoting partial bleaching (Chapter 3). Similarly, cultured Symbiodiniaceae experienced an important growth reduction under $nTiO_2$-oil phase mixtures, as well as an increase of ROS inside their cells (Chapter 2). Elevated ROS levels are likely the reason for the significant upregulation of Hsp70 and Hsp90 genes expression measured in sea anemones during a short-term exposure to inorganic sunscreen (Chapter 4).

All the effects observed in the experiments presented here could indeed be related to oxidative stress induced by $nTiO_2$ and oil phase ingredients. It is therefore proposed that the toxicity of inorganic sunscreen towards symbiotic cnidarians depends on two mechanisms acting simultaneously: $nTiO_2$ and oil phase ingredients directly impact *in-hospite* Symbiodiniaceae population inducing oxidative stress; furthermore sunscreen ingredients also indirectly affect cnidarian host by promoting zooxanthellae expulsion due to the high quantities of hydrogen peroxide generated in the waters surrounding coral. Oxidative stress following the exposure to inorganic sunscreen, coupled presumably with the physical constrain due to the hydrophobic properties of the sunscreen ingredients that may stick on cells surface, significantly impaired also coral early life stages development by reducing sperm motility as well as increasing the rate of embryo abnormalities and larvae mortality (Chapter 5).

6.1.2 Summary of the differential impacts of different $nTiO_2$ and emulsifying agents composing sunscreen formulation

The production of ROS by $nTiO_2$ photoactivation under UV light is the principal cause of $nTiO_2$ toxicity towards aquatic organisms (Haynes et al., 2017; Hou et al., 2019; Minetto et al., 2014). Here $nTiO_2$ UV filters with different coatings did not induce differential toxicity in Symbiodiniaceae nor coral gametes and larvae (Chapter 2 and 5), indicating that the different types of coatings protected the titanium core from photoactivation in a similar way. Conversely, one of the main findings of this thesis is that cosmetic formulations induce toxicity effects similar to sunscreen even when lacking UV filters. Hsp70 and Hsp90 expressions were indeed comparable in *E. pallida* anemones

exposed to sunscreen and filter-free formulations (Chapter 3). Thus in the early-life stages study presented in Chapter 5, the toxicity of different sunscreen formulations were compared to evaluate whether sunscreen toxicity towards coral gametes and larvae change in relation to the emulsifying ingredients in the formulation. Results show that sunscreen formulated with the emulsifier cellulose nanocrystal, derived from natural ingredients, reduced sunscreen toxicity, in particular towards sperm and embryos, resulting a possible eco-friendly solution for the formulation of sunscreen products.

6.1.3 Summary of the combined sunscreen and elevated temperature effects

Corals are particularly sensitive to thermal stress, the detrimental effects of which have been widely studied (Hoegh-Guldberg, 1999; Lesser, 2011; Smith et al., 2005; Weis, 2008). These effects can also be exacerbated by local stressors such as heavy metals and chemical pollutants (Banc-Prandi and Fine, 2019; Biscéré et al., 2017; Kegler et al., 2015; Nyström et al., 2001; Van Dam et al., 2015). Localized events of severe and rapid heating are growing in frequency and intensity under the current global warming scenario (Frölicher et al., 2018), driving mass bleaching events worldwide (Eakin et al., 2019; Hughes et al., 2017b, 2018a; McClanahan et al., 2019). The scale of heat stress used in the study presented here replicates the rapid onset of warming of short duration typical of marine heatwaves (Hobday et al., 2016), like the extreme heating measured in the Dongsha Atoll in 2015 and in the Great Barrier Reef in 2016 with 6°C above the climatological mean (Bainbridge, 2017; DeCarlo et al., 2017). Findings from this thesis indicate that the combined exposure to sunscreen and extreme events of anomalously high temperature enhances the negative impacts of heat stress on cnidarian and algal symbionts stress responses, and the viability of coral gametes and larvae.

A short-term acute exposure to 6°C above ambient temperature significantly interacted with the sunscreen oil phase in inducing ROS production and consequent mortality in cultured Symbiodiniaceae (Chapter 2). Under similar thermal stress, the expression of heat-shock proteins was also increased in *E. pallida* simultaneously exposed to sunscreen or filter free formulations, along with a significant Fv/Fm reduction (Chapter 4). Combined exposure (+ 4°C above ambient temperature) significantly affected coral fertilization and embryo development in an additive way, along with halving the time occurred to reach 50% of larvae mortality (Chapter 5).

While temperature had a greater impact on coral gametes than sunscreen, sunscreen was the main driver of the negative effects observed in adult corals under the combined exposure (Chapter 3). Elevated temperature indeed seemed to mitigate the harmful impact of inorganic sunscreen individual exposure, presumably because corals were subjected to a gradual temperature increase instead to acute heat-stress as in the other studies presented here, causing thus acclimation of corals to thermal stress conditions.

6.2 Ecological implications of sunscreen pollution for coral reefs

The experimental work performed in this thesis aimed to assess the direct impacts of inorganic sunscreen on corals photo-physiological and reproductive performances, as well the effects on coral algal symbionts growth in culture conditions and the expression of stress-related genes in symbiotic cnidarians. However, sunscreen can also influence other aspects of coral reef ecosystems causing a cascade of effects that indirectly affect coral health. The suggested impacts of sunscreen exposure on coral reefs food web, the availability of inorganic nutrients and coral microbiome are here presented.

Corals can acquire nutrients via the translocation of photosynthates produced by their symbiotic dinoflagellate and via zooplankton predation and uptake of particulate matter by the animal (Goldberg, 2018). Heterotrophy in particular is an important component of coral nutrition under stress conditions, as in the case of bleaching, when zooplankton feeding is fundamental for the survival and recovery of stressed corals (Grottoli et al., 2006; Levy et al., 2016; Rodrigues and Grottoli, 2007). Ergo any factor causing a reduction of zooplankton abundance in coral reef waters, that in turn affects corals heterotrophic capacity, likely induces negative consequence on the coral holobiont. The direct impacts of inorganic sunscreen on zooplankton species are currently unknown, however sunscreens formulated with $nTiO_2$ as UV filters have been found to reduce the growth of different marine microalgae and cause a drift in the species composition of phytoplankton communities (da Silva Abe et al., 2017; Schiavo et al., 2018; Sendra et al., 2017b; Tovar-Sánchez et al., 2013). Phytoplankton is the food source of numerous species of zooplankton (Enochs and Glynn, 2017), thus sunscreen may indirectly influence the distribution of zooplankton and affect coral's feeding capacity. Oxidative stress through ROS generation is the principal mode of action proposed to explain the negative impacts of $nTiO_2$-sunscreen on phytoplankton (Schiavo et al., 2018; Sendra et al., 2017b), cultured Symbiodiniaceae (Chapter 2 of this thesis) and the mussel *Mytilus*

galloprovincialis (Sureda et al., 2018). It is thus pertinent to expect also a direct effect of sunscreen on those zooplankton species prey of corals.

Recently Rodríguez-Romero et al. (2019) measured the release and behaviour of inorganic components from commercialized inorganic sunscreen in seawater. They demonstrated that metals not associated with the nanoparticle UV filters (i.e. aluminium, cadmium, copper, manganese, nickel and lead), either incorporated in sunscreen formulations to fulfil a precise function or resulting from the breakdown or the inadequate purification of other ingredients, after an initial release in the water column remain associated to the stable colloidal suspension formed upon sunscreen discharge in seawater. Elements associated with nanoparticles (i.e. titanium and silicon), instead, are adsorbed to the organic ingredients in the cream and are released in seawater with increasing concentration with time (a similar behaviour of titanium was measured in Chapter 2 of this thesis). Rodríguez-Romero et al. (2019) also observed that the concentrations of metals released in coastal waters from the use of sunscreen could induce toxic effects on phytoplankton growth. At the same time, sunscreen products are also a source of inorganic nutrients (i.e. nitrate, nitrite, phosphate, silicate and ammonium) in marine waters (Rodríguez-Romero et al., 2019; Tovar-Sánchez et al., 2013). Those authors suggested that the input of inorganic nutrients in oligotrophic waters from sunscreen use facilitates the growth of phytoplankton. A modest increase in nutrient levels has been found to enhance also coral growth (Bongiorni et al., 2003; Dunn et al., 2011; Koop et al., 2001), however higher than normal nutrients load is usually considered a threat to coral reefs (D'Angelo and Wiedenmann, 2014; Koop et al., 2001), especially when associated with elevated seawater temperature (Ban et al., 2014; Fabricius et al., 2013; Humanes et al., 2016). An exhaustive description of the direct and indirect adverse effects of nutrient enrichment to corals is presented by D'Angelo and Wiedenmann (2014). Briefly, elevated nutrients have been suggested to favour diseases due to alterations of the microbial communities in the coral holobiont (Bruno et al., 2003; Harvell et al., 2007; Voss and Richardson, 2006; Wang et al., 2018a), to cause the uncontrolled proliferation of the *in-hospite* algal populations compromising coral's energy budget (Shantz and Burkepile, 2014; Wooldridge, 2012), to reduce corals reproductive success and skeletal density (Dunn et al., 2011; Humphrey et al., 2008; Lam et al., 2015; Loya et al., 2004), to enhance the susceptibility to bleaching, ocean acidification and diseases (DeCarlo et al., 2015; Vega Thurber et al., 2014; Wiedenmann et al., 2013; Zaneveld et al., 2016) and, indirectly, to prevent coral recruitment due to the

enhanced macroalgal growth that reduces suitable settlement substrate (Lapointe, 1997; McCook et al., 2001; Schaffelke and Klumpp, 1998).

Corals can thus potentially suffer from indirect effects of sunscreen release in coral reef waters due to the alteration of their natural food web dynamics and nutrient environment. Another aspect of sunscreen toxicity towards corals, that however was not part of this study, is its impact on coral microbiome. Coral-associated bacteria are an important component of the coral holobiont and environmental stress and anthropogenic pollution, such as nickel, copper and oil, are known to destabilize the functioning and composition of the coral microbiome and facilitate the invasion of pathogens and opportunistic bacteria (Fragoso Ados Santos et al., 2015; Gissi et al., 2019; McDevitt-Irwin et al., 2017). The higher frequency of coral diseases in near-shore shallow reefs also suggests that coastal pollution exerts adverse effects on coral microbiome (Klaus et al., 2007). Moreover, titanium dioxide nanoparticles have been shown to induce changes in the bacterial communities composing the gut microbiome of zebrafish (Chen et al., 2018). Similarly, sunscreen could disrupt the bacterial communities associated with the benthic substratum essential for larval settlement, ergo affecting coral recruitment (Harrington et al., 2004; Negri and Heyward, 2000; Webster et al., 2004). Therefore, the exposure to $nTiO_2$-based sunscreen has the potential to impact the coral microbiome with unknown adverse physiological and reproductive consequences.

The presented summary of the proposed direct and indirect impacts of inorganic sunscreen in coral reef areas suggests that the effects of sunscreen pollution are negative for both the physiological performances of the coral individual and for ecosystem functioning, particularly under the projected changes in seawater temperature.

6.3 Implication for reef management

Sunscreen formulations and their ingredients are subjected to rigorous human safety and efficacy evaluation before commercialization (Nohynek et al., 2010). However, limited studies exist to determine the risks induced by sunscreen, inorganic or organic, to marine organisms following their release in the environment. Sunscreen enters coastal waters by two primary pathways: the direct release during swimming and bathing activities and through the indirect wastewater route following showering and laundry of consumers goods (Danovaro et al., 2008; Poiger et al., 2004; Tovar-Sánchez et al., 2013). The growth of tourism linked to coral reef areas and the increasing awareness on the harmful effects of UV rays exposure led to a widespread use and consequently release of sunscreen

products in waters surrounding coral reefs (Sánchez-Quiles and Tovar-Sánchez, 2015; Tsui et al., 2014). Current estimates indicate that between 8000 and 16000 tons of sunscreen are released into coral reef waters (DiNardo and Downs, 2018). The actual levels of inorganic sunscreen have not been quantified yet, however it has been demonstrated that $nTiO_2$ concentrations in rivers and lakes increase up to 80% due to recreational activities (Gondikas et al., 2014; Venkatesan et al., 2017), therefore it is pertinent to expect high quantities of inorganic sunscreen to be released in highly urbanized and highly touristic coastal areas.

Findings from this research project are the first step for a realistic evaluation of the potential impacts of inorganic sunscreen formulations on tropical corals and to support the development of water quality guidelines. The maximum sunscreen concentration tested in the experiments presented here (1 mgL^{-1}) correspond to the estimated quantity of inorganic sunscreen, formulated with $nTiO_2$ UV filter, released in a typical touristic beach (Chapter 1). Moreover, the negative effects on corals photo-physiological performances as well as embryo development and larvae survival appear to be consistent among the different species studied, suggesting that the results measured here could be applied for other coral species.

Global warming is undoubtedly the most important stressor currently affecting coral reef ecosystems (Bellwood et al., 2019; Hughes et al., 2017a) and it is expected to continue in the next decades even with active mitigation strategies to reduce the emissions of greenhouse gases (IPCC, 2018). Nonetheless local actions are important to aid in the management of climate change threats, and the resistance of coral communities to bleaching events have been demonstrated to increase with the implementation of local management strategies (Shaver et al., 2018). The studies presented here show how the exposure to inorganic sunscreen formulations and ingredients can potentially magnify the impacts of thermal stress on tropical corals. Local strategies therefore aimed at reducing or removing the harmful inputs of sunscreen in reef waters could support the resilience to climate change of corals living in highly urbanized and touristic coastal areas.

The reduction of coastal pollution in coral reefs expected to survive to global warming is crucial to facilitate the restoration of coral populations and thus guarantee their persistence in the future (Hoegh-Guldberg et al., 2018). Those reefs are mainly located in the Coral Triangle, SE Asia, Indian Ocean and Caribbean (Beyer et al., 2018), highly populated and highly touristic regions characterized by poor or non-working sewage

treatments (Bell, 2002; Bryant et al., 1998; Cesar et al., 2003; Musee, 2011; UNEP/GPA, 2006), areas where the management of sunscreen pollution is particularly important.

6.4 Implication for the cosmetic industry

The global suncare products market is constantly increasing along with a raising awareness for environmentally friendly sunscreens (Raffa et al., 2018; Sánchez-Quiles and Tovar-Sánchez, 2015). In recent years, a growing number of sunscreens entered the marked claiming to be safe and non-toxic for corals, although the definition of "Reef Safe/Friendly Sunscreen" placed in the label of many commercialized sunscreen products is currently not regulated by any law (Wood, 2018). Sunscreen manufacturers declares their products are reef friendly when the formulations lack the UV filters found to be toxic towards marine life by scientific studies, as illustrated in Figure 6.1, however no concerns are raised towards the emulsifier ingredients in the formulation.

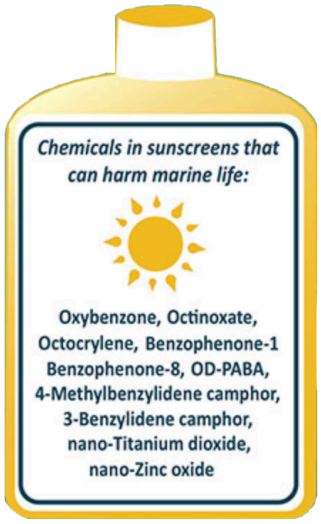

Figure 6.1 - Infographic on sunscreen chemicals that can harm marine life (modified from NOAA, 2019)

Based on the toxicity data collected within this research, it is likely that $nTiO_2$ are safer active ingredients than the organic UV filters previously demonstrated to be toxic to adult corals and their larval stages (Danovaro et al., 2008; Downs et al., 2014, 2016; He et al., 2019b, 2019a; Tsui et al., 2014). However it was also demonstrated the importance of considering the whole formulation in assessing sunscreen toxicity since a formulation lacking UV filters was as toxic as a common sunscreen having $nTiO_2$ as active ingredient (Chapter 4), and sunscreens formulated with different emulsifiers induced a different degree of toxicity towards the early life stages of corals (Chapter 5). A sunscreen product

labelled “Reef Friendly”, because formulated without toxic UV filters, can thus still exerts adverse effects on coral reefs because of its oil phase ingredients.

The reduction of sunscreen toxicity towards coral embryo development and sperm motility with the use of the emulsifying agent cellulose nanocrystal, as revealed in Chapter 5 of this thesis, is a starting point in the identification of less-toxic ingredients to support the manufacture of reef-friendly sunscreen. Findings from this research will thus aid cosmetic industries and policy makers in charge of regulations in the optimization of the eco-design of a sunscreen product from the earliest stages of the production, that is the choice of UV filter and emulsifying agents and their integration in a cosmetic formulation.

6.5 Recommendations for future research

This research project represents the first study to assess the effects of inorganic sunscreen formulations to reef-building corals, alone and in combination with climate change-induced thermal stress. While results presented here provide valuable information in regard to the toxicity of inorganic sunscreens to coral reefs, the research on sunscreen toxicity is still in its infancy and a number of unanswered questions remain.

Regarding this specific work, results of toxicity tests using sunscreen formulations are based on nominal sunscreen concentrations. Along with the detailed composition of sunscreen used in toxicity tests, further studies should measure the actual concentration of each sunscreen compound dispersed in the experimental seawater. The detection of all sunscreen oil phase compounds with liquid chromatography-mass spectrometry is costly and time consuming. The measure of solely $nTiO_2$ UV filters is more accessible, although it is not a precise proxy for the actual sunscreen concentration because they remain trapped in the organic compounds of the oil phase, as observed here in Chapter 2 and by Gondikas et al. (2014).

$nTiO_2$ and the organic component of sunscreen formulations can act as a carrier of other chemical compounds, where interactions can potentially alter toxicant bioavailability and consequent impacts to marine organisms (Hartmann et al., 2012; Qiang et al., 2015). Multiple stressor experiments are therefore recommended to provide a more realistic picture of the risks of chemical mixtures that can be found in a natural environment (Mitchelmore et al., 2019).

Furthermore, coral reefs experience and are threatened by the decrease in pH, along with ocean warming, as consequence of global climate change (Hoegh-Guldberg et al., 2017; Pandolfi et al., 2011). Ocean acidification not only affects the metabolism, calcification and photosynthetic activity of reef-building corals (Comeau et al., 2015; Kaniewska et al., 2012; Nakamura et al., 2017), but also induces changes in the water chemistry that could affect the toxicity of anthropogenic pollutants (Carere et al., 2011; Nikinmaa, 2013; Schiedek et al., 2007). Further studies testing the simultaneous impact of acidification and warming on sunscreen toxicity are thus needed to provide a better understanding of the impact of sunscreen contamination in a changing ocean.

Chemical and environmental stressors may also not appear simultaneously but at different times, thus sequential exposure studies of sunscreen and projected climate change conditions will complement the work presented in this thesis.

More data are also required to provide realistic environmental concentrations of sunscreen ingredients along with models for sunscreen dispersal in different water bodies (e.g. close bay, atoll, fringing reef) to identify those areas more vulnerable to sunscreen pollutions, and ultimately where to implement conservation and management policies.

Further studies investigating the direct and indirect effects of inorganic sunscreen to coral reef food webs, the availability of inorganic nutrients and coral microbiome are needed to verify the effects of sunscreen toxicity suggested above, in section 6.2.

Corals are key species that provide habitat and refuge to a variety of reef organisms (Spalding et al., 2001), thus evaluating the toxicity of sunscreen and other pollutants that could compromise coral health is of primary importance. Nevertheless the lack of toxicity data for tropical corals is a major limitation for the management of local pollution in coral reef areas (Van Dam et al., 2011). The primary constraint for toxicity tests with corals is the destructive fragmentation of coral colonies to provide the adequate number of replicates. Experiments presented in Chapter 4 support the use of sea anemones as good proxy for corals in toxicity tests, as suggested by Howe et al. (2015) and Trenfield et al. (2017).

6.6 Conclusions

This thesis aimed to develop a comprehensive evaluation of the effects of inorganic sunscreen formulations and ingredients on reef-building corals, providing information on both ecological effects (quantification of bleaching, fertilization success and larval survival) as well as the related physiological mechanisms (Fv/Fm reduction, impairment of the oxygen fluxes, HSPs gene expression and embryo abnormal development rate). The following main conclusions were derived:

1. Mixtures of $nTiO_2$ UV filters and oil phase ingredients reduced the growth of cultured Symbiodiniaceae while increasing intracellular ROS production. Sunscreen contamination may thus affect coral communities by impacting their algal symbionts and also have detrimental effects on free-living Symbiodiniaceae populations, crucial reservoirs of endosymbionts for bleached adults and their aposymbiotic larval and juvenile stages.

2. The large use of sunscreen products in highly urbanized and touristic areas have the potential to impact coral communities. Sunscreen concentrations simulating those encountered in a touristic beach exerted negative effects on corals metabolic and photosynthetic performances and induced partial bleaching in exposed fragments.

3. *E. pallida* HSPs expression was highly sensitive to sunscreen exposure, its effects were evident soon after exposure. Hsp70 and Hsp90, genes which expression is normally associated with warming conditions, were upregulated in sea anemones during a 24h period. This result indicates that the molecular responses of symbiotic cnidarians to sunscreen exposure may be similar to the responses identified for thermal stress. The shared molecular pathway may overwhelm the antioxidant defensive mechanisms inducing detrimental consequences under simultaneous sunscreen and elevated temperature stress.

4. Exposure to inorganic sunscreen increased abnormal embryonic development, it also reduced sperm motility and larvae survival. These harmful effect on the early developmental processes of reef-building corals have the potential to influence coral reproductive capacity and population maintenance in near-shore, touristic, reefs.

5. The combined inorganic sunscreen and elevated temperature stress enhanced the negative effects of warming on adult corals and their early life stages, as well on cultured Symbiodiniaceae and the sea anemone *E. pallida*. In the majority of experiments performed here an additivity of effects, rather than interaction between sunscreen and thermal stress, was observed. In the view of global warming, reducing sunscreen load could facilitate the survival of symbiotic cnidarian under elevated seawater temperature projected for the near future.

6. Different $nTiO_2$ types induced similar impacts in cultured Symbiodiniaceae and corals' early history stages despite having diverse external coatings. However, because $nTiO_2$ are usually applied in cosmetic products, it is important to understand the effects of sunscreen mixtures as a whole.

7. Experiments presented in this thesis highlight the importance of taking into consideration the oil phase ingredients, especially the emulsifying agents, in evaluating the potential hazards and risks of inorganic sunscreen to marine organisms.

8. Sunscreen formulated with cellulose nanocrystal as emulsifying agent resulted less toxic to coral gametes and larvae than sunscreen formulated with the chemical emulsifier EasyNov™, hence CNC represents a potential reef-friendly solution for sunscreen products.

This thesis revealed the potentially detrimental impacts of sunscreen formulations to improvements of different coral life stages and holobiont constituents, both in present day and projected future ocean conditions. While the results of this thesis highlight several areas of concern with regard to coral in areas with high potential of sunscreen contamination, it also presents the gaps in our current understanding and areas for future research and mitigation of detrimental impacts (e.g. new emulsifying agents).
Altogether, findings from this thesis are directly relevant to improvements of environmental regulations and the management of tropical coastal regions in order to promote the survival of corals now and in the future.

Appendix A

Supplementary information on Chapter 2

A1. Physical-chemical characterization of $nTiO_2$

$nTiO_2$ characterization was performed at CEREGE (Aix-en-Provence, France) under the supervision of Dr Jerome Labille.

The shape and primary size of T-S, T-2000 and T-Avo were assessed by scanning electron microscopy (SEM) and T-Lite by transmission electron microscopy (TEM). The mineralogical composition was analysed by X-Ray Diffraction (XRD), also the chemical composition of nTiO2 were determined by Energy Dispersive X-ray Analysis (EDX).

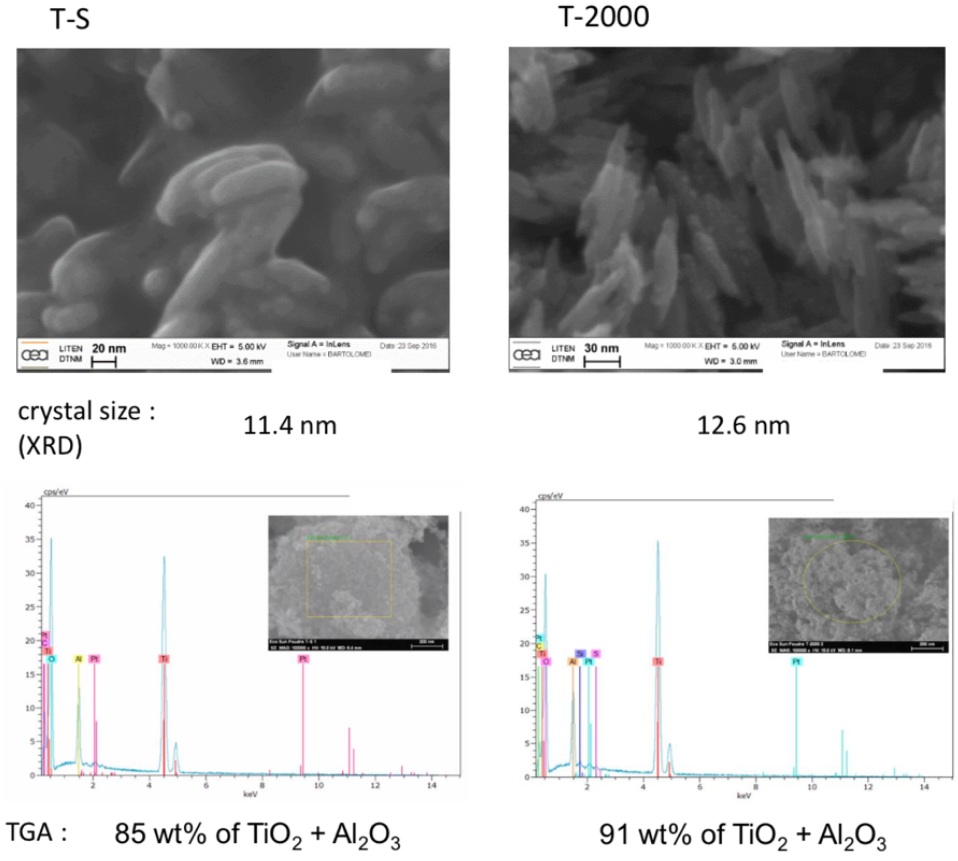

T-AVO

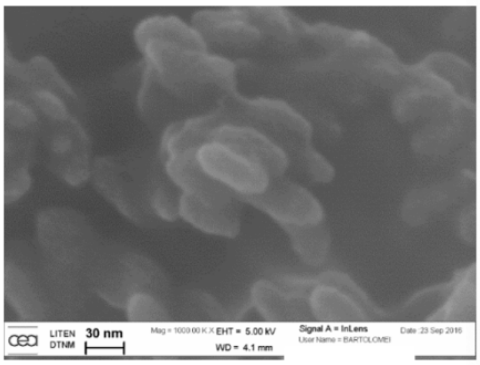

19.2 nm

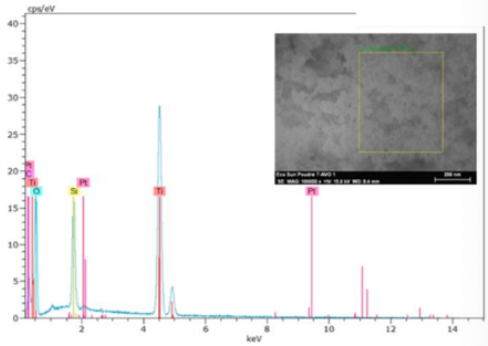

96.5 wt% of TiO_2 + SiO_2

T-Lite SF

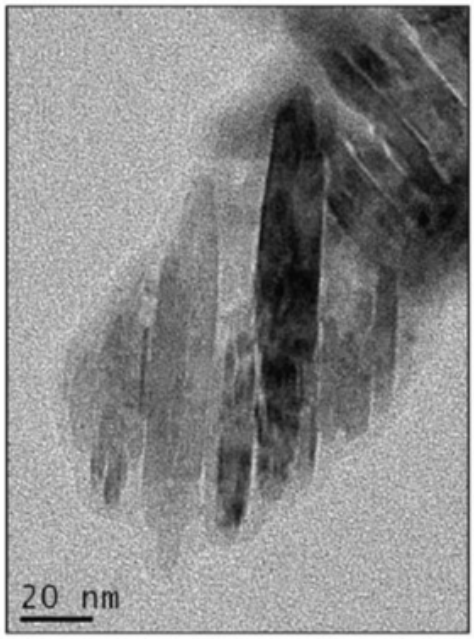

79-89 wt% TiO_2 + $Al(OH)_3$ + $Si\text{-}O(CH_3)_2$ (Labille et al., 2010)

A2. Calibration curves for Symbiodiniaceae A1 and B1 cell densities

Calibration curves for both Symbiodiniaceae A1 and B1 correlating chlorophyll *a* concentrations (µg/mL) measured with a fluorometer (Trilogy®, Turner Design) (3 replicates reading per sample) and cell density (cells/mL) calculated using a haemocytometer under a light microscope (6 replicates counts per sample).

In the experimental samples, algal densities could be estimated from chlorophyll measurements using the equations describing the relationship between chl *a* values and cell numbers.

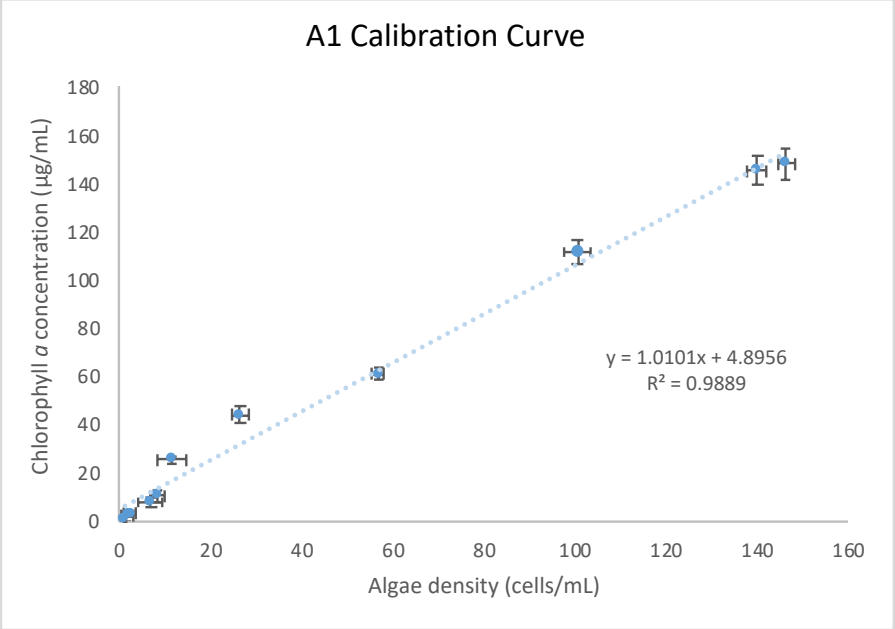

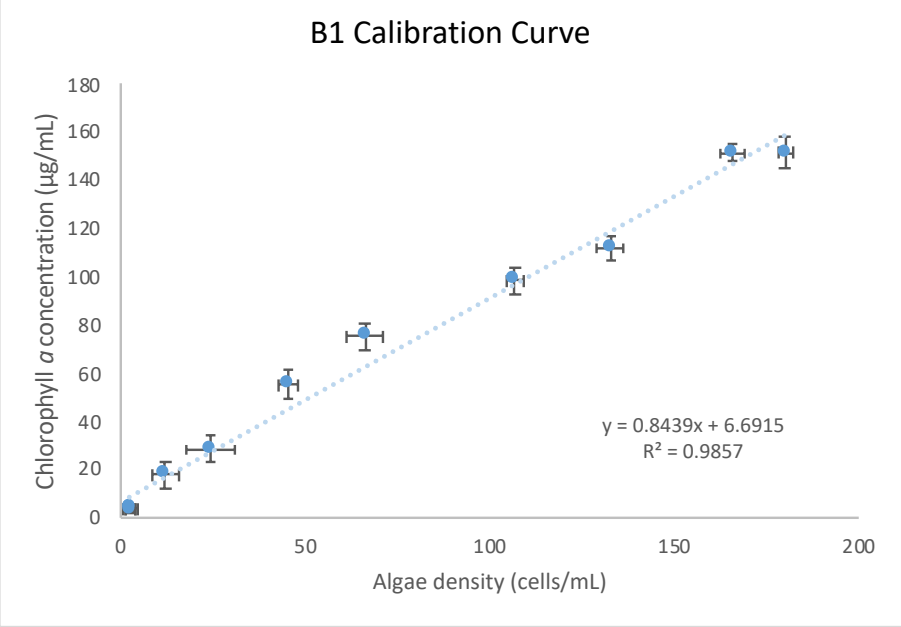

Appendix B

Supplementary information on Chapter 4

B 1. Overview

This appendix describes the results from the preliminary experiment conducted on *Exaiptasia pallida* exposed to warming to determine the sampling timepoints in the main experiment presented in Chapter 4.

Gene expression in response to stress in cnidarians is known to be transient, with changes in the transcript levels fluctuating with time very quickly (Császár et al., 2009). The expression of Hsp70 and Hsp90 gene transcripts at the onset of stress have been investigated in various species of symbiotic cnidarians but as the duration and amplitude of transcript levels vary with the magnitude of the stress (Moya et al., 2012), it was necessary to investigate the transcript profiles directly at the exact experimental conditions.

Hsp70 and Hsp90 gene expression profiles of *Exaiptasia pallida* were studied after exposure to high temperature to pinpoint the times at which HSPs are induced in order to not miss, any important changes in gene expression.

B 2. Material and methods

The experimental methodology followed was similar to the one presented in Chapter 3: 48 hours prior to the star of the preliminary experiment, cultured anemones of similar size were randomly placed into 6-well plates and allowed to acclimate prior to the start of the experiment. During the acclimation stage the temperature was raised from 26°C 1 degree per hour to reach 32°C (6°C above ambient temperature) at the start of the experiment. On the day of the experiment, seawater in each well was replaced with freshly made Instant Ocean® artificial seawater heated at 32°C. Anemones were flash-frozen in liquid nitrogen and stored at -80°C at time 0, 30 min, 1, 2, 3 ,4 5, 6 hours (3 anemones per timepoint). RNA extraction, cDNA synthesis and qPCR analyses were then carried out for each frozen anemone, as explained in chapter 3. Relative fold change in expression of each target gene to time 0 ($\log_2$ FC) was then determined for all timepoints using the ΔΔCt method (Henry et al., 2009)

B 3. Results

Hsp70 and Hsp90 transcript levels of *Exaiptasia pallida* through 6 hours of heat stress are presented in Figure B1. Both genes steadily increased their expression in the first

hours to reach the maximum expression at 2h for Hsp70 and 3h for Hsp90. Then the expression decreased and it was back at high levels at 5h for Hsp70 and 6h for Hsp90.

The selected timepoints for the main experiment were 3 and 6 hours because they represent the times when a clear peak of Hsp90 expression is observed and they is close to the times of Hsp70 maximum expression too. Moreover, high HSPs expression has been observed at 3 and 6 hours of thermal stress also in previous studies on both corals (Kvitt et al., 2016; Rodriguez-Lanetty et al., 2009) and *Exaiptasia pallida* (Kitchen and Weis, 2017).

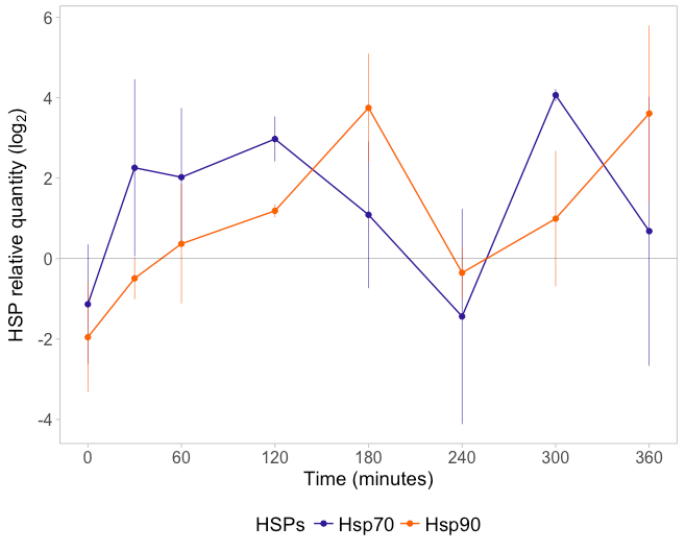

Figure B.1 - Hsp70 (violet) and Hsp90 (orange) transcript levels of *Exaiptasia pallida* under heat stress. Error bars represent standard error of the mean.

Appendix C

Supplementary information on Chapter 5

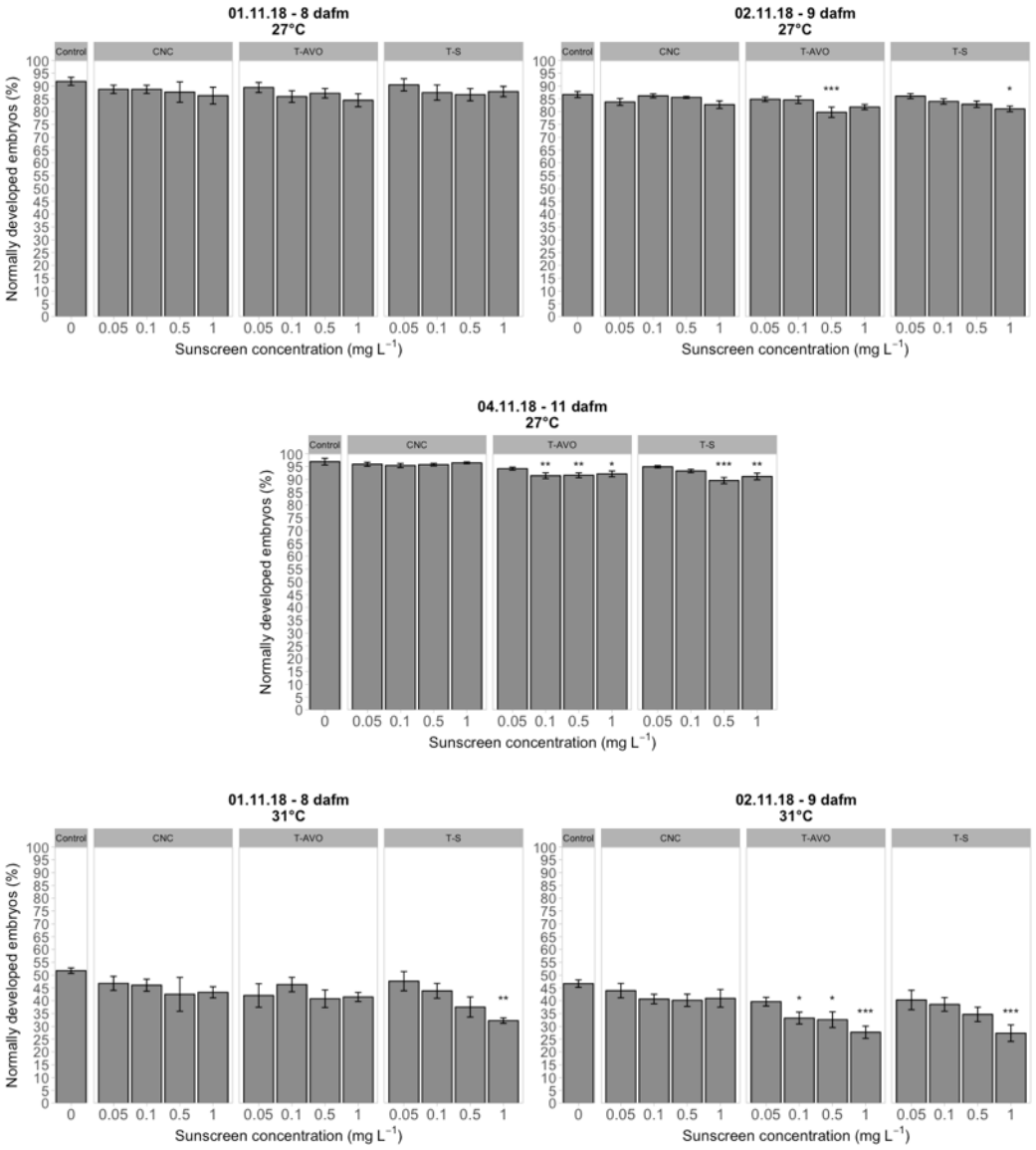

Figure C.1 - Proportion of normally developed embryos/successfully fertilized eggs of *A. hyacinthus* under increasing sunscreen concentration under either ambient (27°C) or elevated (31°C) temperature during the different night of spawning. Error bars represent the standard error of mean. "*", "**" and "****" indicated significant difference between the control treatment and the other sunscreen treatments with $p < 0.05$, 0.01 and 0.001, respectively.

Table C.1 - Tukey post-hoc test comparisons on successfully developed eggs ratio of *A. hyacinthus* during the different spawning nights. Only significant pairwise comparisons are presented (p-value < 0.05).

Treatments comparisons				p-value			
				8 dafm	9 dafm		11 dafm
				31°C	27°C	31°C	27°C
Control	0 mgL^{-1}	T-Avo	0.1 mgL^{-1}			0.045	<0.01
			0.5 mgL^{-1}		<0.001	0.028	<0.01
			1 mgL^{-1}			<0.001	0.013
		T-S	0.5 mgL^{-1}				<0.001
			1 mgL^{-1}	<0.01	0.046	<0.001	<0.01
CNC	0.05 mgL^{-1}	T-Avo	1 mgL^{-1}			<0.01	
		T-S	0.5 mgL^{-1}				<0.01
			1 mgL^{-1}			<0.01	0.032
	0.1 mgL^{-1}	T-Avo	0.5 mgL^{-1}		<0.01		
			1 mgL^{-1}			0.038	
		T-S	0.5 mgL^{-1}				<0.01
			1 mgL^{-1}			0.027	
	0.5 mgL^{-1}	T-Avo	0.5 mgL^{-1}		<0.01		
		T-S	0.5 mgL^{-1}				<0.01
			1 mgL^{-1}			0.04	0.046
	1 mgL^{-1}	T-Avo	0.1 mgL^{-1}				0.012
			0.5 mgL^{-1}				0.019
			1 mgL^{-1}			0.03	
		T-S	0.5 mgL^{-1}				<0.001
			1 mgL^{-1}			0.022	<0.01
T-AVO	0.5 mgL^{-1}	T-Avo	0.05 mgL^{-1}		<0.01		
T-S	0.05 mgL^{-1}	T-Avo	0.5 mgL^{-1}		<0.01		
		T-S	0.5 mgL^{-1}				0.02
			1 mgL^{-1}			0.036	

Table C.2 - Tukey post-hoc test comparisons on abnormal development rate of *A. hyacinthus* during the different spawning nights. Only significant pairwise comparisons are presented (p-value < 0.05).

Treatments comparisons				p-value			
				8 dafm	9 dafm		11 dafm
				31°C	27°C	31°C	27°C
Control	0 mgL^{-1}	CNC	1 mgL^{-1}		<0.01		
		T-Avo	0.05 mgL^{-1}		<0.01		
			0.1 mgL^{-1}		<0.01	0.012	<0.01
			0.5 mgL^{-1}		<0.001	0.012	<0.01
			1 mgL^{-1}		<0.001	<0.001	0.023
		T-S	0.1 mgL^{-1}		<0.001		0.046
			0.5 mgL^{-1}		<0.001	0.05	<0.01
			1 mgL^{-1}	<0.01	<0.001	<0.001	<0.01
CNC	0.05 mgL^{-1}	T-Avo	0.05 mgL^{-1}				0.034
			0.1 mgL^{-1}				<0.001
			0.5 mgL^{-1}		<0.001		<0.001
			1 mgL^{-1}		0.03	<0.01	<0.01
		T-S	0.1 mgL^{-1}				0.01
			0.5 mgL^{-1}				<0.001
			1 mgL^{-1}	0.049	0.02	<0.001	<0.001
	0.1 mgL^{-1}	T-Avo	0.1 mgL^{-1}				<0.001
			0.5 mgL^{-1}		<0.001		<0.001
			1 mgL^{-1}		0.012		<0.01
		T-S	0.1 mgL^{-1}				0.02
			0.5 mgL^{-1}				<0.001
			1 mgL^{-1}		0.02		<0.001
	0.5 mgL^{-1}	T-Avo	0.05 mgL^{-1}				0.046
			0.1 mgL^{-1}				<0.001
			0.5 mgL^{-1}		<0.001		<0.001
			1 mgL^{-1}		0.015		<0.01
		T-S	0.1 mgL^{-1}				0.012
			0.5 mgL^{-1}				<0.001
			1 mgL^{-1}		<0.01		<0.001
	1 mgL^{-1}	T-Avo	0.05 mgL^{-1}				0.02
			0.1 mgL^{-1}				<0.001
			0.5 mgL^{-1}				<0.001
			1 mgL^{-1}				<0.01
		T-S	0.1 mgL^{-1}				<0.01
			0.5 mgL^{-1}				<0.001
			1 mgL^{-1}				<0.001
T-AVO	0.5 mgL^{-1}	T-Avo	0.05 mgL^{-1}		<0.01		
			0.1 mgL^{-1}		0.041		
T-S	0.05 mgL^{-1}	T-Avo	0.1 mgL^{-1}				<0.001
			0.5 mgL^{-1}		<0.001		<0.001
			1 mgL^{-1}		0.017		<0.01
		T-S	0.5 mgL^{-1}				<0.001
			1 mgL^{-1}		0.013		<0.001

Table C.3 - Log-rank test results evaluating if the survival of *A. globiceps* larvae differed between treatments at ambient (**A**) and elevated (**B**) temperature. A) 26°C: N = 780, $\chi 2 = 21.3$, df = 12, p = 0.047; B) 31°C: N = 780, $\chi 2 = 35.3$, df = 12, p = 0.0001

A) 27°C		N	Observed survival	Expected survival	(O-E)^2/E	(O-E)^2/V
Control	0 mgL^{-1}	60	10	21.6	6.267	7.275
T-S	0.05 mgL^{-1}	60	21	18.9	0.236	0.271
	0.1 mgL^{-1}	60	15	20.3	1.367	1.577
	0.5 mgL^{-1}	60	22	19.8	0.235	0.271
	1 mgL^{-1}	60	28	19.3	3.887	4.466
T-Avo	0.05 mgL^{-1}	60	16	20.1	0.826	0.951
	0.1 mgL^{-1}	60	23	18.3	1.199	1.371
	0.5 mgL^{-1}	60	25	19.6	1.517	1.746
	1 mgL^{-1}	60	21	18.8	0.27	0.309
CNC	0.05 mgL^{-1}	60	15	19.4	0.988	1.135
	0.1 mgL^{-1}	60	14	20.3	1.959	2.259
	0.5 mgL^{-1}	60	20	18	0.225	0.257
	1 mgL^{-1}	60	22	17.7	1.06	1.209

B) 31°C		N	Observed survival	Expected survival	(O-E)^2/E	(O-E)^2/V
Control	0 mgL^{-1}	60	33	54.8	8.6528	12.5289
T-S	0.05 mgL^{-1}	60	42	45.7	0.3048	0.4376
	0.1 mgL^{-1}	60	42	45.5	0.2741	0.392
	0.5 mgL^{-1}	60	46	40.9	0.6312	0.9089
	1 mgL^{-1}	60	53	38.6	5.3807	7.7104
T-Avo	0.05 mgL^{-1}	60	39	47.2	1.4122	2.029
	0.1 mgL^{-1}	60	43	50.5	1.1029	1.5944
	0.5 mgL^{-1}	60	49	41	1.5753	2.2507
	1 mgL^{-1}	60	54	35.9	9.1237	13.0613
CNC	0.05 mgL^{-1}	60	46	45.2	0.2199	0.3155
	0.1 mgL^{-1}	60	46	46.4	0.122	0.1752
	0.5 mgL^{-1}	60	42	42.9	0.2203	0.3162
	1 mgL^{-1}	60	44	44.5	0.0497	0.0714

Table C.4 - Estimated values of *A. globiceps* larvae survival probability and their 95% confidence interval (CI) under sunscreen exposure at either 27 or 31°C at the different timepoints. Values calculated using Kaplan-Meier survival estimator.

Day	27°C				31°C			
	Survival %	std.err	lower 95% CI	upper 95% CI	Survival %	std.err	lower 95% CI	upper 95% CI
	Control							
1					81.7	0.05	0.724	0.921
2					73.3	0.0571	0.63	0.854
3					70	0.0592	0.593	0.826
4					61.7	0.0628	0.505	0.753
5	96.7	0.0232	0.922	1.000	53.3	0.0644	0.421	0.676
7	95	0.0281	0.896	1.000	45	0.0642	0.34	0.595
8	88.3	0.0414	0.806	0.968				
10	86.7	0.0439	0.785	0.957				
12	83.3	0.0481	0.744	0.933				
	T-S 0.05 mgL^{-1}							
1					73.3	0.0571	0.63	0.854
2					35	0.0616	0.248	0.494
3	95	0.0281	0.896	1.000	31.7	0.0601	0.218	0.459
4	86.7	0.0439	0.785	0.957	30	0.0592	0.204	0.442
5	85	0.0461	0.764	0.945	25	0.0559	0.161	0.388
7	78.3	0.0532	0.686	0.895	23.3	0.0546	0.147	0.369
8	73.3	0.0571	0.63	0.854				
10	70	0.0592	0.593	0.826				
12	65	0.0616	0.54	0.783				
	T-S 0.1 mgL^{-1}							
1					68.3	0.0601	0.575	0.812
2					55	0.0642	0.437	0.691
3					43.3	0.064	0.324	0.579
4	93.3	0.0322	0.872	0.999	41.7	0.0636	0.309	0.562
5	91.7	0.0357	0.849	0.989	40	0.0632	0.293	0.545
7	85	0.0461	0.764	0.945	30	0.0592	0.204	0.442
8	78.3	0.0532	0.686	0.895				
12	75	0.0559	0.648	0.868				
	T-S 0. 5 mgL^{-1}							
1					75	0.0559	0.648	0.868
2					51.7	0.0645	0.405	0.66
3					43.3	0.064	0.324	0.579
4					38.3	0.0628	0.278	0.528
5	95	0.0281	0.896	1.000	36.7	0.0622	0.263	0.511
7	78.3	0.0532	0.686	0.895	30	0.0592	0.204	0.442
8	70	0.0592	0.593	0.826				
10	66.7	0.0609	0.557	0.797				
12	63.3	0.0622	0.522	0.768				
	T-S 1 mgL^{-1}							
1					65	0.0616	0.5399	0.783
2					41.7	0.0636	0.3089	0.562
3	98.3	0.0165	0.951	1.000	31.7	0.0601	0.2184	0.459
5	86.7	0.0439	0.785	0.957	25	0.0559	0.1613	0.388
7	78.3	0.0532	0.686	0.895	16.7	0.0481	0.0947	0.293
8	70	0.0592	0.593	0.826	11.7	0.0414	0.0582	0.234
10	66.7	0.0609	0.557	0.797				
12	53.3	0.0644	0.421	0.676				

Table C.4 - Continue

Day	27°C				31°C			
	Survival %	std.err	lower 95% CI	upper 95% CI	Survival %	std.err	lower 95% CI	upper 95% CI
	T-Avo 0.05 mgL^{-1}							
1					75	0.0559	0.648	0.868
2					50	0.0645	0.388	0.644
3	95	0.0281	0.896	1	46.7	0.0644	0.356	0.612
4	91.7	0.0357	0.849	0.989	45	0.0642	0.34	0.595
5	83.3	0.0481	0.744	0.933	43.3	0.064	0.324	0.579
7	80	0.0516	0.705	0.908	35	0.0616	0.248	0.494
8	76.7	0.0546	0.667	0.882				
10								
12	73.3	0.0571	0.63	0.854				
	T-Avo 0.1 mgL^{-1}							
1	98.3	0.0165	0.951	1.000	86.7	0.0439	0.785	0.957
2					63.3	0.0622	0.522	0.768
3	95	0.0281	0.896	1.000	51.7	0.0645	0.405	0.66
4	85	0.0461	0.764	0.945	46.7	0.0644	0.356	0.612
5	83.3	0.0481	0.744	0.933	38.3	0.0628	0.278	0.528
7	71.7	0.0582	0.611	0.840	28.3	0.0582	0.189	0.424
10	66.7	0.0609	0.557	0.797				
12	61.7	0.0628	0.505	0.753				
	T-Avo 0. 5 mgL^{-1}							
1		0.0357	0.849	0.989	65	0.0616	0.54	0.783
2		0.0461	0.764	0.945	45	0.0642	0.34	0.595
3	91.7	0.0546	0.667	0.882	33.3	0.0609	0.233	0.477
4	85	0.0582	0.611	0.84				
5	76.7	0.0616	0.54	0.783	26.7	0.0571	0.175	0.406
7	71.7	0.0628	0.505	0.753	18.3	0.05	0.107	0.313
8	65	0.0636	0.471	0.722				
10	61.7	0.0357	0.849	0.989				
12	58.3	0.0461	0.764	0.945				
	T-Avo 1 mgL^{-1}							
1	98.3	0.0165	0.951	1.000	58.3	0.0636	0.471	0.722
2					28.3	0.0582	0.1895	0.424
3	96.7	0.0232	0.922	1.000				
4	86.7	0.0439	0.785	0.957	23.3	0.0546	0.1475	0.369
5	76.7	0.0546	0.667	0.882	18.3	0.05	0.1075	0.313
7					10	0.0387	0.0468	0.214
8	73.3	0.0571	0.63	0.854				
10	71.7	0.0582	0.611	0.840				
12	65	0.0616	0.54	0.783				

Table C.4 - Continue

Day	27°C				31°C			
	Survival %	std.err	lower 95% CI	upper 95% CI	Survival %	std.err	lower 95% CI	upper 95% CI
	CNC 0.05 mgL^{-1}							
1					73.3	0.0571	0.63	0.854
2					60	0.0632	0.488	0.738
3	98.3	0.0165	0.951	1	40	0.0632	0.293	0.545
4	93.3	0.0322	0.872	0.999	35	0.0616	0.248	0.494
5	88.3	0.0414	0.806	0.968	31.7	0.0601	0.218	0.459
7	85	0.0461	0.764	0.945	30	0.0592	0.204	0.442
8	81.7	0.05	0.724	0.921				
12	76.7	0.0546	0.667	0.882				
	CNC 0.1 mgL^{-1}							
1					75	0.0559	0.648	0.868
2					48.3	0.0645	0.372	0.628
3	96.7	0.0232	0.922	1.000	46.7	0.0644	0.356	0.612
5	88.3	0.0414	0.806	0.968	45	0.0642	0.34	0.595
7	85	0.0461	0.764	0.945	38.3	0.0628	0.278	0.528
8	83.3	0.0481	0.744	0.933	26.7	0.0571	0.175	0.406
10	80	0.0516	0.705	0.908				
12	76.7	0.0546	0.667	0.882				
	CNC 0.5 mgL^{-1}							
1					73.3	0.0571	0.63	0.854
2					45	0.0642	0.34	0.595
3					41.7	0.0636	0.309	0.562
4					30	0.0592	0.204	0.442
5	95	0.0281	0.896	1	28.3	0.0582	0.189	0.424
7	78.3	0.0532	0.686	0.895	23.3	0.0546	0.147	0.369
8	71.7	0.0582	0.611	0.84				
10	68.3	0.0601	0.575	0.812				
12	66.7	0.0609	0.557	0.797				
	CNC 1 mgL^{-1}							
1					75	0.0559	0.648	0.868
2					58.3	0.0636	0.471	0.722
3	96.7	0.0232	0.922	1	38.3	0.0628	0.278	0.528
4	86.7	0.0439	0.785	0.957	36.7	0.0622	0.263	0.511
5	81.7	0.05	0.724	0.921	25	0.0559	0.161	0.388
7	76.7	0.0546	0.667	0.882	23.3	0.0546	0.147	0.369
8	68.3	0.0601	0.575	0.812				
10	66.7	0.0609	0.557	0.797				
12	65	0.0616	0.54	0.783				

Table C.5 - Log-rank test results evaluating if the survival of *P. damicornis* larvae differed between treatments. N = 840, $\chi 2 = 63.8$, df = 12, $p < 0.0001$.

		N	Observed survival	Expected survival	(O-E)^2/E	(O-E)^2/V
Control	0 mgL^{-1}	120	8	27.9	14.175	17.6097
T-S	0.05 mgL^{-1}	60	9	13.6	1.5779	1.7959
	0.1 mgL^{-1}	60	8	13.7	2.3404	2.6629
	0.5 mgL^{-1}	60	23	12.5	8.7395	9.8641
	1 mgL^{-1}	60	25	12	14.0406	15.7916
T-Avo	0.05 mgL^{-1}	60	10	13.6	0.9554	1.0867
	0.1 mgL^{-1}	60	14	13.2	0.0488	0.0554
	0.5 mgL^{-1}	60	17	12.4	1.6995	1.9176
	1 mgL^{-1}	60	24	12.1	11.5764	13.0282
CNC	0.05 mgL^{-1}	60	8	13.6	2.3187	2.6378
	0.1 mgL^{-1}	60	8	13.6	2.2828	2.5952
	0.5 mgL^{-1}	60	14	12.6	0.1446	0.1634
	1 mgL^{-1}	60	16	13.1	0.6437	0.7294

Table C.6 - Estimated values of *P. damicornis* larvae survival probability and their 95% confidence interval (CI) at the different timepoints. Values calculated using Kaplan-Meier survival estimator.

Day	Survival %	std.err	lower 95% CI	upper 95% CI	Survival %	std.err	lower 95% CI	upper 95% CI
	Control							
1	99.2	0.0083	0.976	1				
2	97.5	0.0143	0.947	1				
4	96.7	0.0164	0.935	0.999				
6	95.8	0.0182	0.923	0.995				
12	93.3	0.0228	0.89	0.979				
	T-S 0.05 mgL^{-1}				**T-S 0.1 mgL^{-1}**			
1	98.3	0.0165	0.951	1	98.3	0.0165	0.951	1
2	95	0.0281	0.896	1	96.7	0.0232	0.922	1
6	93.3	0.0322	0.872	0.999				
8					93.3	0.0322	0.872	0.999
10					91.7	0.0357	0.849	0.989
12	85	0.0461	0.764	0.945	86.7	0.0439	0.785	0.957
	T-S 0.5mgL^{-1}				**T-S 1 mgL^{-1}**			
1	98.3	0.0165	0.951	1	95	0.0281	0.896	1
6	88.3	0.0414	0.806	0.968	93.3	0.0322	0.872	0.999
8	75	0.0559	0.648	0.868	86.7	0.0439	0.785	0.957
10	61.7	0.0628	0.505	0.753	65	0.0616	0.54	0.783
12	98.3	0.0165	0.951	1	58.3	0.0636	0.471	0.722
	T-Avo 0.05 mgL^{-1}				**T-Avo 0.1 mgL^{-1}**			
1	98.3	0.0165	0.951	1	95	0.0281	0.896	1
2	96.7	0.0232	0.922	1				
6	95	0.0281	0.896	1				
8					90	0.0387	0.827	0.979
10	90	0.0387	0.827	0.979	86.7	0.0439	0.785	0.957
12	83.3	0.0481	0.744	0.933	76.7	0.0546	0.667	0.882
	T-Avo 0.5 mgL^{-1}				**T-Avo 1 mgL^{-1}**			
1	98.3	0.0165	0.951	1				
2	91.7	0.0357	0.849	0.989	96.7	0.0232	0.922	1
6	88.3	0.0414	0.806	0.968	93.3	0.0322	0.872	0.999
8	81.7	0.05	0.724	0.921	80	0.0516	0.705	0.908
10	80	0.0516	0.705	0.908	71.7	0.0582	0.611	0.84
12	71.7	0.0582	0.611	0.84	60	0.0632	0.488	0.738
	CNC 0.05 mgL^{-1}				**CNC 0.1 mgL^{-1}**			
1	98.3	0.0165	0.951	1	98.3	0.0165	0.951	1
2	96.7	0.0232	0.922	1				
4					96.7	0.0232	0.922	1
6	95	0.0281	0.896	1				
8	93.3	0.0322	0.872	0.999	95	0.0281	0.896	1
10	91.7	0.0357	0.849	0.989	88.3	0.0414	0.806	0.968
12	86.7	0.0439	0.785	0.957	86.7	0.0439	0.785	0.957
	CNC 0.5 mgL^{-1}				**CNC 1 mgL^{-1}**			
1	95	0.0281	0.896	1	96.7	0.0232	0.922	1
4	93.3	0.0322	0.872	0.999	95	0.0281	0.896	1
6	90	0.0387	0.827	0.979				
8	85	0.0461	0.764	0.945				
10	81.7	0.05	0.724	0.921	80	0.0516	0.705	0.908
12	76.7	0.0546	0.667	0.882	73.3	0.0571	0.63	0.854

References

Abrego, D., Ulstrup, K. E., Willis, B. L., and van Oppen, M. J. H. (2008). Species-specific interactions between algal endosymbionts and coral hosts define their bleaching response to heat and light stress. *Proc. Biol. Sci.* 275, 2273–82.

Adjeroud, M., Kayal, M., Iborra-Cantonnet, C., Vercelloni, J., Bosserelle, P., Liao, V., et al. (2018). Recovery of coral assemblages despite acute and recurrent disturbances on a South Central Pacific reef. *Sci. Rep.* 8, 9680.

Ainsworth, T. D., Hoegh-Guldberg, O., Heron, S. F., Skirving, W. J., and Leggat, W. (2008). Early cellular changes are indicators of pre-bleaching thermal stress in the coral host. *J. Exp. Mar. Bio. Ecol.* 364, 63–71.

Ainsworth, T. D., Thurber, R. V., and Gates, R. D. (2010). The future of coral reefs: a microbial perspective. *Trends Ecol. Evol.* 25, 233–240.

Al-Awady, M. J., Greenway, G. M., and Paunov, V. N. (2015). Nanotoxicity of polyelectrolyte-functionalized titania nanoparticles towards microalgae and yeast: role of the particle concentration, size and surface charge. *RSC Adv.* 5, 37044–37059.

Al-Horani, F. A. (2005). Effects of changing seawater temperature on photosynthesis and calcification in the scleractinian coral *Galaxea fascicularis*, measured with O_2, Ca^{2+} and pH microsensors. *Sci. Mar.* 69, 347–354.

Al-Horani, F. A., Ferdelman, T., Al-Moghrabi, S. M., and De Beer, D. (2005). Spatial distribution of calcification and photosynthesis in the scleractinian coral *Galaxea fascicularis*. *Coral Reefs* 24, 173–180.

Albright, R., and Mason, B. (2013). Projected Near-Future Levels of Temperature and pCO2 Reduce Coral Fertilization Success. *PLoS One* 8, 56468.

Allemand, D., Ferrier-Pagès, C., Furla, P., Houlbrèque, F., Puverel, S., Reynaud, S., et al. (2004). Biomineralisation in reef-building corals: From molecular mechanisms to environmental control. *Comptes Rendus - Palevol* 3, 453–467.

Allemand, D., Tambutté, É., Zoccola, D., and Tambutté, S. (2011). *Coral Calcification, Cells to Reefs*.

Allen, J. M., Gossett, C. J., and Allen, S. K. (1996). Photochemical formation of singlet molecular oxygen ($^1O_2$) in illuminated aqueous solutions of p-aminobenzoic acid (PABA). *J. Photochem. Photobiol. B Biol.* 32, 33–37.

Alutoin, S., Boberg, J., Nyström, M., and Tedengren, M. (2001). Effects of the multiple stressors copper and reduced salinity on the metabolism of the hermatypic coral *Porites lutea*. *Mar. Environ. Res.* 52, 289–299.

Amann, R. P., and Waberski, D. (2014). Computer-assisted sperm analysis (CASA): capabilities and potential developments. *Theriogenology* 81, 5-17.e1–3.

Andréfouët, S., Pagès, J., and Tartinville, B. (2001). Water renewal time for classification of atoll lagoons in the Tuamotu Archipelago (French Polynesia). *Coral Reefs* 20, 399–408.

Anthony, K. R. N., Hoogenboom, M. O., Maynard, J. A., Grottoli, A. G., and Middlebrook, R. (2009). Energetics approach to predicting mortality risk from environmental stress: A case study of coral bleaching. *Funct. Ecol.* 23, 539–550.

Aruoja, V., Dubourguier, H. C., Kasemets, K., and Kahru, A. (2009). Toxicity of nanoparticles of CuO, ZnO and TiO_2 to microalgae *Pseudokirchneriella subcapitata*. *Sci. Total Environ.* 407, 1461–1468.

Auffan, M., Pedeutour, M., Rose, J., Masion, A., Ziarelli, F., Borschneck, D., et al. (2010). Structural degradation at the surface of a TiO_2-based nanomaterial used in cosmetics. *Environ. Sci. Technol.* 44, 2689–2694.

Babcock, R. C., Bull, G. D., Harrison, P. L., Heyward, A. J., Oliver, J. K., Wallace, C. C., et al. (1986). Synchronous spawnings of 105 scleractinian coral species on the Great Barrier Reef. *Mar. Biol.* 90, 379–394.

Bachelot, M., Li, Z., Munaron, D., Le Gall, P., Casellas, C., Fenet, H., et al. (2012). Organic UV filter concentrations in marine mussels from French coastal regions.

Bainbridge, S. J. (2017). Temperature and light patterns at four reefs along the Great Barrier Reef during the 2015–2016 austral summer: understanding patterns of observed coral bleaching. *J. Oper. Oceanogr.* 10, 16–29.

Baird, A. H., Guest, J. R., and Willis, B. L. (2009). Systematic and Biogeographical Patterns in the Reproductive Biology of Scleractinian Corals. *Annu. Rev. Ecol. Evol. Syst.* 40, 551–571.

Baird, A. H., Keith, S. A., Woolsey, E., Yoshida, R., and Naruse, T. (2017). Rapid coral mortality following doldrums-like conditions on Iriomote, Japan. *F1000Research* 6, 1728.

Baird, A. H., and Marshall, P. A. (2002). Mortality, growth and reproduction in scleractinian corals following bleaching on the Great Barrier Reef. *Mar. Ecol. Prog. Ser.* 237, 133–141.

Baker, A. C. (2003). Flexibility and Specificity in Coral-Algal Symbiosis: Diversity, Ecology, and Biogeography of *Symbiodinium*. *Annu. Rev. Ecol. Evol. Syst.* 34, 661–689.

Baker, A. C., and Cunning, R. (2015). Coral "Bleaching" as a Generalized Stress Response to Environmental Disturbance. *Dis. Coral*, 396–409.

Baker, A. C., Glynn, P. W., and Riegl, B. (2008). Climate change and coral reef bleaching: An ecological assessment of long-term impacts, recovery trends and future outlook. *Estuar. Coast. Shelf Sci.* 80, 435–471.

Baker, A. C., and Romanski, A. M. (2007). Multiple symbiotic partnerships are common in scleractinian corals, but not in octocorals: Comment on Goulet (2006). *Mar. Ecol. Prog. Ser.* 335, 237–242.

Baker, A. C., Rosenberg, E., and Loya, Y. (2004). Diversity, distribution and ecology of Symbiodinium on coral reefs and its relationship to bleaching resistance and resilience. 177–194.

Baker, N. R. (2008). Chlorophyll Fluorescence: A Probe of Photosynthesis In Vivo. *Annu. Rev. Plant Biol.* 59, 89–113.

Baker, T. J., Tyler, C. R., and Galloway, T. S. (2014). Impacts of metal and metal oxide nanoparticles on marine organisms. *Environ. Pollut.* 186, 257–271.

Ban, S. S., Graham, N. A. J., and Connolly, S. R. (2014). Evidence for multiple stressor interactions and effects on coral reefs. *Glob. Chang. Biol.* 20, 681–697.

Banc-Prandi, G., and Fine, M. (2019). Copper enrichment reduces thermal tolerance of the highly resistant Red Sea coral *Stylophora pistillata*. *Coral Reefs* 38, 285–296.

Barbier, E. B., Hacker, S. D., Kennedy, C., Koch, E. W., Stier, A. C., and Silliman, B. R. (2011). The value of estuarine and coastal ecosystem services. *Ecol. Monogr.* 81, 169–193.

Barmo, C., Ciacci, C., Canonico, B., Fabbri, R., Cortese, K., Balbi, T., et al. (2013). In vivo effects of n-TiO_2 on digestive gland and immune function of the marine bivalve *Mytilus galloprovincialis*. *Aquat. Toxicol.* 132–133, 9–18.

Barott, K. L., Gibbin, E. M., Krueger, T., Putnam, H. M., Bodin, J., Gates, R. D., et al. (2018). Short-Term Thermal Acclimation Modifies the Metabolic Condition of the Coral Holobiont. *Front. Mar. Sci.* 5, 1–11.

Barshis, D. J., Ladner, J. T., Oliver, T. A., Seneca, F. O., Traylor-Knowles, N., and Palumbi, S. R. (2013). Genomic basis for coral resilience to climate change. *Proc. Natl. Acad. Sci.* 110, 1387–1392.

Bassim, K. M., and Sammarco, P. W. (2003). Effects of temperature and ammonium on larval development and survivorship in a scleractinian coral (*Diploria strigosa*). *Mar. Biol.* 142, 241–252.

Bassim, K. M., Sammarco, P. W., and Snell, T. L. (2002). Effects of temperature on success of (self and non-self) fertilization and embryogenesis in *Diploria strigosa* (Cnidaria, Scleractinia). *Mar. Biol.* 140, 479–488.

Bay, L. K., Doyle, J., Logan, M., and Berkelmans, R. (2016). Recovery from bleaching is mediated by threshold densities of background thermo-tolerant symbiont types in a reef-building coral. *R. Soc. open Sci.* 3, 160322.

BBCNews (2018). Coral: Palau to ban sunscreen products to protect reefs. https://www.bbc.com/news/science-environment-46046.

Becker, E. W. (1994). *Microalgae: biotechnology and microbiology*. Cambridge University Press.

Belda-Baillie, C. A., Baillie, B. K., and Maruyama, T. (2002). Specificity of a model cnidarian-dinoflagellate symbiosis. *Biol. Bull.* 202, 74–85.

Bell, R. G. (2002). Environmental policy for developing countries. *Issues Sci. Technol.* 18, 63–70.

Bellwood, D. R., Pratchett, M. S., Morrison, T. H., Gurney, G. G., Hughes, T. P., Álvarez-Romero, J. G., et al. (2019). Coral reef conservation in the Anthropocene: Confronting spatial mismatches and prioritizing functions. *Biol. Conserv.*

Berkelmans, R., and Van Oppen, M. J. H. (2006). The role of zooxanthellae in the thermal tolerance of corals: A “nugget of hope” for coral reefs in an era of climate change. *Proc. R. Soc. B Biol. Sci.* 273, 2305–2312.

Berry, K. L. E., Hoogenboom, M. O., Brinkman, D. L., Burns, K. A., and Negri, A. P. (2017). Effects of coal contamination on early life history processes of a reef-building coral, *Acropora tenuis*. *Mar. Pollut. Bull.* 114, 505–514.

Beyer, H. L., Kennedy, E. V., Beger, M., Chen, C. A., Cinner, J. E., Darling, E. S., et al. (2018). Risk-sensitive planning for conserving coral reefs under rapid climate change. *Conserv. Lett.* 11, 1–10.

Bigorgne, E., Foucaud, L., Lapied, E., Labille, J., Botta, C., Sirguey, C., et al. (2011). Ecotoxicological assessment of TiO_2 byproducts on the earthworm Eisenia fetida. *Environ. Pollut.* 159, 2698–2705.

Biscéré, T., Ferrier-Pagès, C., Gilbert, A., Pichler, T., and Houlbrèque, F. (2018). Evidence for mitigation of coral bleaching by manganese. *Sci. Rep.* 8, 16789.

Biscéré, T., Lorrain, A., Rodolfo-Metalpa, R., Gilbert, A., Wright, A., Devissi, C., et al. (2017). Nickel and ocean warming affect scleractinian coral growth. *Mar. Pollut. Bull.* 120, 250–258.

Black, K. P., Gay, S. L., and Andrews, J. C. (1990). Residence times of neutrally-buoyant matter such as larvae, sewage or nutrients on coral reefs. *Coral Reefs* 9, 105–114.

Black, N. A., Voellmy, R., Szmant, A. M., Black, N. A., Voellmy, R., and Szmant, A. M. (1995). Elevated Temperatures Heat Shock Protein Induction in Montastraea faveolata and *Aiptasia pallida* Exposed to Elevated Temperatures. *Biol. Bull.* 188, 234–240.

Bongiorni, L., Shafir, S., Angel, D., and Rinkevich, B. (2003). Survival, growth and gonad development of two hermatypic corals subjected to in situ fish-farm nutrient enrichment. *Mar. Ecol. Prog. Ser.* 253, 137–144.

Botta, C., Labille, J., Auffan, M., Borschneck, D., Miche, H., Cabié, M., et al. (2011). TiO_2-based nanoparticles released in water from commercialized sunscreens in a life-cycle perspective: Structures and quantities. *Environ. Pollut.* 159, 1543–1550.

Bourne, D. G., Garren, M., Work, T. M., Rosenberg, E., Smith, G. W., and Harvell, C. D. (2009). Microbial disease and the coral holobiont. *Trends Microbiol.* 17, 554–562.

Bramanti, L., and Edmunds, P. J. (2016). Density-associated recruitment mediates coral population dynamics on a coral reef. *Coral Reefs* 35, 543–553.

Brodnicke, O. B., Bourne, D. G., Heron, S. F., Pears, R. J., Stella, J. S., Smith, H. A., et al. (2019). Unravelling the links between heat stress, bleaching and disease: fate of tabular corals following a combined disease and bleaching event. *Coral Reefs* 38, 591–603.

Brown, B. E. (1997). Coral bleaching causes and consequences. *Coral Reefs* 16, 129–138.

Brown, B. E., A Le Tissier, M. D., and Dunne, R. P. (1994). Tissue retraction in the scleractinian coral Coeloseris mayeri, its effect upon coral pigmentation, and preliminary implications for heat balance.

Brown, T., Bourne, D., and Rodriguez-Lanetty, M. (2013). Transcriptional Activation of c3 and hsp70 as Part of the Immune Response of *Acropora millepora* to Bacterial Challenges. *PLoS One* 8.

Bruno, J. F., Petes, L. E., Harvell, C. D., and Hettinger, A. (2003). Nutrient enrichment can increase the severity of coral diseases. *Ecol. Lett.* 6, 1056–1061.

Bruno, J. F., Selig, E. R., Casey, K. S., Page, C. A., Willis, B. L., Harvell, C. D., et al. (2007). Thermal stress and coral cover as drivers of coral disease outbreaks. *PLoS Biol.* 5, 1220–1227.

Bryant, D., Burke, L., McManus, J., and Spalding, M. D. (1998). *Reefs at risk*.

Burnham, K. P., and Anderson, D. R. (2002). *Model Selection and Multimodel Inference: A Practical Information-Theoretic Approach (2nd ed)*.

Burriesci, M. S., Raab, T. K., and Pringle, J. R. (2012). Evidence that glucose is the major transferred metabolite in dinoflagellate-cnidarian symbiosis. *J. Exp. Biol.* 215, 3467–3477.

Buxton, L., Badger, M., and Ralph, P. (2009). Effects of moderate heat stress and dissolved inorganic carbon concentration on photosynthesis and respiration of *Symbiodinium* sp. (*Dinophyceae*) in culture and in symbiosis. *J. Phycol.* 45, 357–365.

Byrne, M. (2011). Impact of ocean warming and ocean acidification on marine invertebrate life history stages: vulnerabilities and potential for persistence in a changing ocean. *Oceanogr. Mar. Biol. An Annu. Rev.* 49, 1–42.

Caldwell, G. S. (2009). The influence of bioactive oxylipins from marine diatoms on invertebrate reproduction and development. *Mar. Drugs* 7, 367–400.

Carere, M., Miniero, R., and Cicero, M. R. (2011). Potential effects of climate change on the chemical quality of aquatic biota. *TrAC - Trends Anal. Chem.* 30, 1214–1221.

Carlotti, M. E., Ugazio, E., Fubini, B., Sapino, S., Greco, G., and Fenoglio, I. (2009). Role of particle coating in controlling skin damage photoinduced by titania nanoparticles. *Free Radic. Res.* 43, 312–322.

Carroll, A., Harrison, P., and Adjeroud, M. (2006). Sexual reproduction of *Acropora* reef corals at Moorea, French Polynesia. *Coral Reefs* 25, 93–97.

Catarino, A. I., Cabral, H. N., Peeters, K., Pernet, P., Punjabi, U., and Dubois, P. (2008). Metal concentrations, sperm motility, and RNA/DNA ratio in two echinoderm species from a highly contaminated fjord (the Sørfjord, Norway). *Environ. Toxicol. Chem.* 27, 1553–1560.

Cesar, H., Burke, L., and Pet-soede, L. (2003). The The Economics Economics of of Worldwide Worldwide Coral Coral Reef Reef Degradation Degradation. *Atlantic* 14, 24.

Chen, L., Guo, Y., Hu, C., Lam, P. K. S., Lam, J. C. W., and Zhou, B. (2018). Dysbiosis of gut microbiota by chronic coexposure to titanium dioxide nanoparticles and bisphenol A: Implications for host health in zebrafish. *Environ. Pollut.* 234, 307–317.

Chen, L., Zhou, L., Liu, Y., Deng, S., Wu, H., and Wang, G. (2012). Toxicological effects of nanometer titanium dioxide (nano-TiO_2) on *Chlamydomonas reinhardtii*. *Ecotoxicol. Environ. Saf.* 84, 155–162.

Cherchi, C., Chernenko, T., Diem, M., and Gu, A. Z. (2011). Impact of nano titanium dioxide exposure on cellular structure of *Anabaena variabilis* and evidence of internalization. *Environ. Toxicol. Chem.* 30, 861–869.

Choong, K. (2016). Titanium Dioxide in Sunscreen.

Choukroun, S., Ridd, P. V., Brinkman, R., and McKinna, L. I. W. (2010). On the surface circulation in the western Coral Sea and residence times in the Great Barrier Reef. *J. Geophys. Res. Ocean.* 115, 1–13.

Chui, A. P. Y., and Ang, P. (2015). Elevated temperature enhances normal early embryonic development in the coral *Platygyra acuta* under low salinity conditions. *Coral Reefs* 34, 461–469.

Ciacci, C., Canonico, B., Bilaniĉovă, D., Fabbri, R., Cortese, K., Gallo, G., et al. (2012). Immunomodulation by Different Types of N-Oxides in the Hemocytes of the Marine Bivalve *Mytilus galloprovincialis*. *PLoS One* 7, e36937.

Clayton, W. S., and Lasker, H. R. (1985). Individual and population growth in the asexually reproducing anemone *Aiptasia pallida* Verrill. *J. Exp. Mar. Bio. Ecol.* 90, 249–258.

Clément, L., Hurel, C., and Marmier, N. (2013). Toxicity of TiO_2 nanoparticles to cladocerans, algae, rotifers and plants - Effects of size and crystalline structure. *Chemosphere* 90, 1083–1090.

Coffroth, M. A., Lewis, C. F., Santos, S. R., and Weaver, J. L. (2006). Environmental populations of symbiotic dinoflagellates in the genus *Symbiodinium* can initiate symbioses with reef cnidarians. *Curr. Biol.* 16, R985–R987.

Comeau, S., Carpenter, R. C., and Edmunds, P. J. (2015). Effects of pCO_2 on photosynthesis and respiration of tropical scleractinian corals and calcified algae.

Connell, J. H. (1978). Diversity in Tropical Rain Forests.pdf. *Science (80-.).* 199, 1302–1310.

Corinaldesi, C., Damiani, E., Marcellini, F., Falugi, C., Tiano, L., Brugè, F., et al. (2017). Sunscreen products impair the early developmental stages of the sea urchin *Paracentrotus lividus*. *Sci. Rep.* 7, 7815.

Corinaldesi, C., Marcellini, F., Nepote, E., Damiani, E., and Danovaro, R. (2018). Impact of inorganic UV filters contained in sunscreen products on tropical stony corals (*Acropora* spp.). *Sci. Total Environ.* 637–638, 1279–1285.

Couch, C. S., Burns, J. H. R., Liu, G., Steward, K., Gutlay, T. N., Kenyon, J., et al. (2017). Mass coral bleaching due to unprecedented marine heatwave in Papahānaumokuākea Marine National Monument (Northwestern Hawaiian Islands). *PLoS One* 12.

Couleau, N., Techer, D., Pagnout, C., Jomini, S., Foucaud, L., Laval-Gilly, P., et al. (2012). Hemocyte responses of *Dreissena polymorpha* following a short-term in vivo exposure to titanium dioxide nanoparticles: Preliminary investigations. *Sci. Total Environ.* 438, 490–497.

Courtial, L., Roberty, S., Shick, J. M., Houlbrèque, F., and Ferrier-Pagès, C. (2017). Interactive effects of ultraviolet radiation and thermal stress on two reef-building corals. *Limnol. Oceanogr.* 62, 1000–1013.

Császár, N. B. M., Seneca, F. O., and Van Oppen, M. J. H. (2009). Variation in antioxidant gene expression in the scleractinian coral *Acropora millepora* under laboratory thermal stress. *Mar. Ecol. Prog. Ser.* 392, 93–102.

Cuddy, M. F., Poda, A. R., Moser, R. D., Weiss, C. A., Cairns, C., and Steevens, J. A. (2016). A weight-of-evidence approach to identify nanomaterials in consumer products: a case study of nanoparticles in commercial sunscreens. *J. Expo. Sci. Environ. Epidemiol.* 26, 26–34.

Cunning, R., and Baker, A. C. (2013). Excess algal symbionts increase the susceptibility of reef corals to bleaching. *Nat. Clim. Chang.* 3, 259–262.

Cunning, R., Gillette, P., Capo, T., Galvez, K., and Baker, A. C. (2015). Growth tradeoffs associated with thermotolerant symbionts in the coral *Pocillopora damicornis* are lost in warmer oceans. *Coral Reefs* 34, 155–160.

D'Agata, A., Fasulo, S., Dallas, L. J., Fisher, A. S., Maisano, M., Readman, J. W., et al. (2014). Enhanced toxicity of "bulk" titanium dioxide compared to "fresh" and "aged" nano-TiO_2 in marine mussels (*Mytilus galloprovincialis*). *Nanotoxicology* 8, 549–58.

D'Angelo, C., and Wiedenmann, J. (2014). Impacts of nutrient enrichment on coral reefs: New perspectives and implications for coastal management and reef survival. *Curr. Opin. Environ. Sustain.* 7, 82–93.

da Silva Abe, A. S. F., Dias da Cunha, R. L., Salomon, P. S., Ricci Júnior, E., Santos Valença, S. dos, and Brito Gitirana, L. de (2017). Nanoecotoxicological Effects of a Sunscreen Formulation based on TiO_2 Nanoparticles on Microalgae from Guanabara Bay (Rio de Janeiro, Brazil). *MOJ Polym. Sci.* 1, 99–107.

Dalai, S., Pakrashi, S., Joyce Nirmala, M., Chaudhri, A., Chandrasekaran, N., Mandal, A. B., et al. (2013). Cytotoxicity of TiO_2 nanoparticles and their detoxification in a freshwater system. *Aquat. Toxicol.* 138–139, 1–11.

Danovaro, R., Bongiorni, L., Corinaldesi, C., Giovannelli, D., Damiani, E., Astolfi, P., et al. (2008). Sunscreens cause coral bleaching by promoting viral infections. *Environ. Health Perspect.* 116, 441–447.

Danovaro, R., and Corinaldesi, C. (2003). Sunscreen products increase virus production through prophage induction in marine bacterioplankton. *Microb. Ecol.* 45, 109–118.

Davy, S. K., Allemand, D., and Weis, V. M. (2012). Cell Biology of Cnidarian-Dinoflagellate Symbiosis. *Microbiol. Mol. Biol. Rev.* 76, 229–261.

De Nadal, E., Ammerer, G., and Posas, F. (2011). Controlling gene expression in response to stress. *Nat. Rev. Genet.* 12, 833–845.

De Villa, D., Da Silva Nagatomi, A. R., Paese, K., Guterres, S., and Cestari, T. F. (2011). Reapplication improves the amount of sunscreen, not its regularity, under real life conditions. *Photochem. Photobiol.* 87, 457–460.

DeCarlo, T. M., Cohen, A. L., Barkley, H. C., Cobban, Q., Young, C., Shamberger, K. E., et al. (2015). Coral macrobioerosion is accelerated by ocean acidification and nutrients. *Geology* 43, 7–10.

DeCarlo, T. M., Cohen, A. L., Wong, G. T. F., Davis, K. A., Lohmann, P., and Soong, K. (2017). Mass coral mortality under local amplification of 2°C ocean warming. *Sci. Rep.* 7.

Deng, X. Y., Cheng, J., Hu, X. L., Wang, L., Li, D., and Gao, K. (2017). Biological effects of TiO_2 and CeO_2 nanoparticles on the growth, photosynthetic activity, and cellular components of a marine diatom *Phaeodactylum tricornutum*. *Sci. Total Environ.* 575, 87–96.

Desalvo, M. K., Voolstra, C. R., Sunagawa, S., Schwartz, J. A., Stillman, J. H., Coffroth, M. A., et al. (2008). Differential gene expression during thermal stress and bleaching in the Caribbean coral *Montastraea faveolata*. *Mol. Ecol.* 17, 3952–3971.

Detoni, C. B., Paese, K., Beck, R. C. R., Pohlmann, A. R., and Guterres, S. S. (2011). Nanosized and Nanoencapsulated Sunscreens. *Nanocosmetics and Nanomedicine* 3, 333–362.

Díaz-Gil, C., Cotgrove, L., Smee, S. L., Simón-Otegui, D., Hinz, H., Grau, A., et al. (2017). Anthropogenic chemical cues can alter the swimming behaviour of juvenile stages of a temperate fish. *Mar. Environ. Res.* 125, 34–41.

Dietrich, G. J., Dietrich, M., Kowalski, R. K., Dobosz, S., Karol, H., Demianowicz, W., et al. (2010). Exposure of rainbow trout milt to mercury and cadmium alters sperm motility parameters and reproductive success. *Aquat. Toxicol.* 97, 277–284.

DiNardo, J. C., and Downs, C. A. (2018). Dermatological and environmental toxicological impact of the sunscreen ingredient oxybenzone/benzophenone-3. *J. Cosmet. Dermatol.* 17, 15–19.

Donner, S. D., and Potere, D. (2007). The Inequity of the Global Threat to Coral Reefs. *Bioscience* 57, 214.

Downs, C. A., Kramarsky-Winter, E., Fauth, J. E., Segal, R., Bronstein, O., Jeger, R., et al. (2014). Toxicological effects of the sunscreen UV filter, benzophenone-2, on planulae and in vitro cells of the coral, *Stylophora pistillata*. *Ecotoxicology* 23, 175–191.

Downs, C. A., Kramarsky-Winter, E., Segal, R., Fauth, J., Knutson, S., Bronstein, O., et al. (2016). Toxicopathological Effects of the Sunscreen UV Filter, Oxybenzone (Benzophenone-3), on Coral Planulae and Cultured Primary Cells and Its Environmental Contamination in Hawaii and the U.S. Virgin Islands. *Arch. Environ. Contam. Toxicol.* 70, 265–288.

Downs, C., Fauth, J., Halas, J., Dustan, P., Bemiss, J., and Woodley, C. (2002). Oxidative stress and seasonal coral bleaching. *Free Radic. Biol. Med.* 33, 533–543.

Doyle, J. J., Ward, J. E., and Mason, R. (2016). Exposure of bivalve shellfish to titania nanoparticles under an environmental-spill scenario: Encounter, ingestion and egestion. *J. Mar. Biol. Assoc. United Kingdom* 96, 137–149.

Duckworth, C. G., Picariello, C. R., Thomason, R. K., Patel, K. S., and Bielmyer-Fraser, G. K. (2017). Responses of the sea anemone, *Exaiptasia pallida*, to ocean acidification conditions and zinc or nickel exposure. *Aquat. Toxicol.* 182, 120–128.

Dunn, J. G., Sammarco, P. W., and Lafleur, G. (2011). Effects of phosphate on growth and skeletal density in the scleractinian coral *Acropora muricata*: A controlled experimental approach.

Eakin, C. M., Liu, G., Gomez, A. M., De La Cour, J. L., Heron, S. F., Skirving, W. J., et al. (2016). Global coral bleaching 2014-2017: status and an appeal for observations. *Reef Encount.* 31, 20–25.

Eakin, C. M., Sweatman, H., and Brainard, R. E. (2019). The 2014–2017 global-scale coral bleaching event: insights and impacts. *Coral Reefs* 38, 539–545.

Edmunds, P., Gates, R., and Gleason, D. (2001). The biology of larvae from the reef coral Porites astreoides, and their response to temperature disturbances. *Mar. Biol.* 139, 981–989.

Edmunds, P. J. (2018). Implications of high rates of sexual recruitment in driving rapid reef recovery in Mo'orea, French Polynesia. *Sci. Rep.* 8, 16615.

Egerton, T. A., Everall, N. J., Mattinson, J. A., Kessell, L. M., and Tooley, I. R. (2008). Interaction of TiO_2 nano-particles with organic UV absorbers. *J. Photochem. Photobiol. A Chem.* 193, 10–17.

Ellison, M. A., Ferrier, M. D., and Carney, S. L. (2017). Salinity stress results in differential Hsp70 expression in the *Exaiptasia pallida* and *Symbiodinium* symbiosis. *Mar. Environ. Res.* 132, 63–67.

Enochs, I. C., and Glynn, P. W. (2017). "Trophodynamics of Eastern Pacific Coral Reefs," in *Coral Reefs of the Eastern Tropical Pacific: Persistence and Loss in a Dynamic Environment*, eds. P. W. Glynn, D. P. Manzello, and I. C. Enochs (Dordrecht: Springer Netherlands), 291–314.

Environmental Working Group (2019). EWG's Skin Deep Cosmetics Database.

Fabricius, K. E., Cséke, S., Humphrey, C., and De'ath, G. (2013). Does Trophic Status Enhance or Reduce the Thermal Tolerance of Scleractinian Corals? A Review, Experiment and Conceptual Framework. *PLoS One* 8.

Fan, T. Y., Li, J. J., Ie, S. X., and Fang, L. S. (2002). Lunar periodicity of larval release by pocilloporid corals in Southern Taiwan. *Zool. Stud.* 41, 288–293.

Fan, T. Y., Lin, K. H., Kuo, F. W., Soong, K., Liu, L. L., and Fang, L. S. (2006). Diel patterns of larval release by five brooding scleractinian corals. *Mar. Ecol. Prog. Ser.* 321, 133–142.

Faria, M., Navas, J. M., Soares, A. M. V. M., and Barata, C. (2014). Oxidative stress effects of titanium dioxide nanoparticle aggregates in zebrafish embryos. *Sci. Total Environ.* 470–471, 379–389.

Federici, G., Shaw, B. J., and Handy, R. D. (2007). Toxicity of titanium dioxide nanoparticles to rainbow trout (*Oncorhynchus mykiss*): Gill injury, oxidative stress, and other physiological effects. *Aquat. Toxicol.* 84, 415–430.

Fel, J.-P., Lacherez, C., Bensetra, A., Mezzache, S., Béraud, E., Léonard, M., et al. (2019). Photochemical response of the scleractinian coral *Stylophora pistillata* to some sunscreen ingredients. *Coral Reefs* 38(1), 109–122.

Ferrario, F., Beck, M. W., Storlazzi, C. D., Micheli, F., Shepard, C. C., and Airoldi, L. (2014). The effectiveness of coral reefs for coastal hazard risk reduction and adaptation. *Nat. Commun.* 5.

Figueiredo, J., Baird, A. H., Harii, S., and Connolly, S. R. (2014). Increased local retention of reef coral larvae as a result of ocean warming. *Nat. Clim. Chang.* 4, 498–502.

Finney, J. C., Pettay, D. T., Sampayo, E. M., Warner, M. E., Oxenford, H. A., and LaJeunesse, T. C. (2010). The relative significance of host-habitat, depth, and geography on the ecology, endemism, and speciation of coral endosymbionts in the genus Symbiodinium. *Microb. Ecol.* 60, 250–263.

Fitt, W. K., Brown, B. E., Warner, M. E., and Dunne, R. P. (2001). Coral bleaching: Interpretation of thermal tolerance limits and thermal thresholds in tropical corals. *Coral Reefs* 20, 51–65.

Fitt, W. K., Chang, S. S., and Trench, R. K. (1981). Motility patterns of different strains of the symbiotic dinoflagellate *Symbiodinium microadriaticum* (Freudenthal) in culture. *Bullettin Mar. Sci.* 31, 436–443.

Fitt, W. K., Gates, R. D., Hoegh-Guldberg, O., Bythell, J. C., Jatkar, A., Grottoli, A. G., et al. (2009). Response of two species of Indo-Pacific corals, *Porites cylindrica* and *Stylophora pistillata*, to short-term thermal stress: The host does matter in determining the tolerance of corals to bleaching. *J. Exp. Mar. Bio. Ecol.* 373, 102–110.

Fitzpatrick, J. L., Nadella, S., Bucking, C., Balshine, S., and Wood, C. M. (2008). The relative sensitivity of sperm, eggs and embryos to copper in the blue mussel (*Mytilus trossulus*). *Comp. Biochem. Physiol. - C Toxicol. Pharmacol.* 147, 441–449.

Foltête, A.-S., Masfaraud, J.-F., Bigorgne, E., Nahmani, J., Chaurand, P., Botta, C., et al. (2011). Environmental impact of sunscreen nanomaterials: Ecotoxicity and genotoxicity of altered TiO_2 nanocomposites on *Vicia faba*. *Environ. Pollut.* 159, 2515–2522.

Fonseca, J. da S., Marangoni, L. F. de B., Marques, J. A., and Bianchini, A. (2017). Effects of increasing temperature alone and combined with copper exposure on biochemical and physiological parameters in the zooxanthellate scleractinian coral *Mussismilia harttii*. *Aquat. Toxicol.* 190, 121–132.

Fordyce, A. J., Ainsworth, T. D., Heron, S. F., and Leggat, W. (2019). Marine Heatwave Hotspots in Coral Reef Environments: Physical Drivers, Ecophysiological Outcomes, and Impact Upon Structural Complexity. *Front. Mar. Sci.* 6, 1–17.

Fouqueray, M., Dufils, B., Vollat, B., Chaurand, P., Botta, C., Abacci, K., et al. (2012). Effects of aged TiO_2 nanomaterial from sunscreen on *Daphnia magna* exposed by dietary route. *Environ. Pollut.* 163, 55–61.

Fragoso Ados Santos, H., Duarte, G. A. S., Rachid, C. T. D. C., Chaloub, R. M., Calderon, E. N., Marangoni, L. F. D. B., et al. (2015). Impact of oil spills on coral reefs can be reduced by bioremediation using probiotic microbiota. *Sci. Rep.* 5.

Franklin, D. J., Hoegh-Guldberg, O., Jones, R. J., and Berges, J. A. (2004). Cell death and degeneration in the symbiotic dinoflagellates of the coral *Stylophora pistillata* during bleaching. *Mar. Ecol. Prog. Ser.* 272, 117–130.

Frölicher, T. L., Fischer, E. M., and Gruber, N. (2018). Marine heatwaves under global warming. *Nature* 560, 360–364.

Frölicher, T. L., and Laufkötter, C. (2018). Emerging risks from marine heat waves. *Nat. Commun.* 9.

Gago-Ferrero, P., Alonso, M. B., Bertozzi, C. P., Marigo, J., Barbosa, L., Cremer, M., et al. (2013). First determination of UV filters in marine mammals. octocrylene levels in Franciscana dolphins. *Environ. Sci. Technol.* 47, 5619–5625.

Gallo, A., and Tosti, E. (2019). Effects of ecosystem stress on reproduction and development. *Mol. Reprod. Dev.*

Gao, F., Liu, C., Qu, C., Zheng, L., Yang, F., Su, M., et al. (2008). Was improvement of spinach growth by nano-TiO_2 treatment related to the changes of Rubisco activase? *BioMetals* 21, 211–217.

Gates, R. D., and Edmunds, P. (1999). The physiological mechanisms of acclimatization in tropical reef corals. *Am. Zool.* 39, 30–43.

Gattuso, J.-P., Allemand, D., and Frankignoulle, M. (1999). Photosynthesis and calcification at cellular, organismal and community levels in coral reefs: a review on interactions and control by carbonate chemistry. *Am. Zool.* 39, 160–183.

Gegner, H. M., Ziegler, M., Rädecker, N., Buitrago-López, C., Aranda, M., and Voolstra, C. R. (2017). High salinity conveys thermotolerance in the coral model *Aiptasia*. *Biol. Open* 6, 1943–1948.

George, J., and Sabapathi, S. N. (2015). Cellulose nanocrystals: Synthesis, functional properties, and applications. *Nanotechnol. Sci. Appl.* 8, 45–54.

Giokas, D. L., Salvador, A., and Chisvert, A. (2007). UV filters: From sunscreens to human body and the environment. *TrAC - Trends Anal. Chem.* 26, 360–374.

Gissi, F., Reichelt-Brushett, A. J., Chariton, A. A., Stauber, J. L., Greenfield, P., Humphrey, C., et al. (2019). The effect of dissolved nickel and copper on the adult coral *Acropora muricata* and its microbiome. *Environ. Pollut.*, 792–806.

Gissi, F., Stauber, J., Reichelt-Brushett, A., Harrison, P. L., and Jolley, D. F. (2017). Inhibition in fertilisation of coral gametes following exposure to nickel and copper. *Ecotoxicol. Environ. Saf.* 145, 32–41.

Glasl, B., Webster, N. S., and Bourne, D. G. (2017). Microbial indicators as a diagnostic tool for assessing water quality and climate stress in coral reef ecosystems. *Mar. Biol.* 164, 91.

Goldberg, W. M. (2018). "Coral Food, Feeding, Nutrition, and Secretion: A Review," in *Marine Organisms as Model Systems in Biology and Medicine*, eds. M. Kloc and J. Z. Kubiak (Cham: Springer International Publishing), 377–421.

Gondikas, A., von der Kammer, F., Kaegi, R., Borovinskaya, O., Neubauer, E., Navratilova, J., et al. (2017). Where is the nano? Analytical approaches for the detection and quantification of TiO_2 engineered nanoparticles in surface waters. *Environ. Sci. Nano* 5, 313–326.

Gondikas, A., von der Kammer, F., Reed, R. B., Wagner, S., Ranville, J. F., and Hofmann, T. (2014). Release of TiO_2 nanoparticles from sunscreens into surface waters: A one-year survey at the old danube recreational lake. *Environ. Sci. Technol.* 48, 5415–5422.

Goodson, S. G., Zhang, Z., Tsuruta, J. K., Wang, W., and O'Brien, D. A. (2011). Classification of Mouse Sperm Motility Patterns Using an Automated Multiclass Support Vector Machines Model1. *Biol. Reprod.* 84, 1207–1215.

Gössling, S., Scott, D., and Hall, C. M. (2018). Global trends in length of stay: implications for destination management and climate change. *J. Sustain. Tour.* 26, 2087–2101.

Gottschalk, F., Sonderer, T., Scholz, R. W., and Nowack, B. (2009). Modeled environmental concentrations of engineered nanomaterials ($TiO_{(2)}$, ZnO, Ag, CNT, Fullerenes) for different regions. *Environ. Sci. Technol.* 43, 9216–22.

Goulet, T. L., Cook, C. B., and Goulet, D. (2005). Effect of short-term exposure to elevated temperatures and light levels on photosynthesis of different host-symbiont combinations in the *Aiptasia pallida/Symbiodinium* symbiosis.

Graham, E. M., Baird, A. H., and Connolly, S. R. (2008). Survival dynamics of scleractinian coral larvae and implications for dispersal. *Coral Reefs* 27, 529–539.

Graham, N. A. J., and Nash, K. L. (2013). The importance of structural complexity in coral reef ecosystems. *Coral Reefs* 32, 315–326.

Grajales, A., Rodriguez, E., and Rodríguez, E. (2014). Morphological revision of the genus *Aiptasia* and the family Aiptasiidae (Cnidaria, Actiniaria, Metridioidea). *Zootaxa* 3826, 55.

Granados-Cifuentes, C., Neigel, J., Leberg, P., and Rodriguez-Lanetty, M. (2015). Genetic diversity of free-living *Symbiodinium* in the Caribbean: the importance of habitats and seasons. *Coral Reefs* 34, 927–939.

Grégoire, V., Schmacka, F., Coffroth, M. A., and Karsten, U. (2017). Photophysiological and thermal tolerance of various genotypes of the coral endosymbiont *Symbiodinium* sp. (*Dinophyceae*). *J. Appl. Phycol.* 29, 1893–1905.

Griffitt, R. J., Luo, J., Gao, J., Bonzongo, J.-C., and Barber, D. S. (2008). Effects of particle composition and species on toxicity of metallic nanomaterials in aquatic organisms. *Environ. Toxicol. Chem.* 27, 1972–1978.

Grimaldi, A. M., Belcari, P., Pagano, E., Cacialli, F., and Locatello, L. (2013). Immune responses of *Octopus vulgaris* (Mollusca: Cephalopoda) exposed to titanium dioxide nanoparticles. *J. Exp. Mar. Bio. Ecol.* 447, 123–127.

Grottoli, A. G., Rodrigues, L. J., and Palardy, J. E. (2006). Heterotrophic plasticity and resilience in bleached corals. *Nature* 440, 1186–1189.

Guillard, R. R. L. (1975). "Culture of phytoplankton for feeding marine invertebrates," in *Culture of marine invertebrate animals* (Springer), 29–60.

Gustavs, L., Schumann, R., Eggert, A., and Karsten, U. (2009). In vivo growth fluorometry: Accuracy and limits of microalgal growth rate measurements in ecophysiological investigations. *Aquat. Microb. Ecol.* 55, 95–104.

Hansen, S. F., Baun, A., Michelson, E. S., Kamper, A., Borling, P., and Stur-Lauridsen, F. (2009). Nanomaterials in consumer products. *Nanomater. Risks Benefits*, 359–367.

Harii, S., Nadaoka, K., Yamamoto, M., and Iwao, K. (2007). Temporal changes in settlement, lipid content and lipid composition of larvae of the spawning hermatypic coral Acropora tenuis. *Mar. Ecol. Prog. Ser.* 346, 89–96.

Harrington, L., Fabricius, K., De, G., and Negri, A. (2004). Recognition and Selection of Settlement Substrata Determine Post-Settlement Survival in Corals.

Harrison, P. L. (2011). "Sexual reproduction of scleractinian corals," in *Coral Reefs: An Ecosystem in Transition*, 59–85.

Harrison, P. L., and Wallace, C. C. (1990). Reproduction, dispersal and recruitment of scleractinian corals. *Coral Reefs. Ecosyst. World*, 132–207.

Hartmann, N. B., Legros, S., Von der Kammer, F., Hofmann, T., and Baun, A. (2012). The potential of TiO_2 nanoparticles as carriers for cadmium uptake in *Lumbriculus variegatus* and *Daphnia magna*. *Aquat. Toxicol.* 118–119, 1–8.

Hartmann, N. B., Von der Kammer, F., Hofmann, T., Baalousha, M., Ottofuelling, S., and Baun, A. (2010). Algal testing of titanium dioxide nanoparticles-Testing considerations, inhibitory effects and modification of cadmium bioavailability. *Toxicology* 269, 190–197.

Harvell, D., Jordán-Dahlgren, E., Merkel, S., Rosenberg, E., Raymundo, L., Smith, G., et al. (2007). Coral disease, environmental drivers, and the balance between coral and microbial associates. *Oceanography* 20, 172–195.

Hassan, T. H., Metz, H., and Mäder, K. (2014). Novel semisolid SNEDDS based on PEG-30-dipolyhydroxystearate: Development and characterization. *Int. J. Pharm.* 477, 506–518.

Hawkins, T. D., and Davy, S. K. (2012). Nitric oxide production and tolerance differ among symbiodinium types exposed to heat stress. *Plant Cell Physiol.* 53, 1889–1898.

Hawkins, T. D., and Warner, M. E. (2017). Warm preconditioning protects against acute heat-induced respiratory dysfunction and delays bleaching in a symbiotic sea anemone. *J. Exp. Biol.* 220, 969–983.

Hayashibara, T., Shimoike, K., Kimura, T., Hosaka, S., Heyward, A., Harrison, P., et al. (1993). Patterns of coral spawning at Akajima Island, Okinawa, Japan. *Mar. Ecol. Prog. Ser.* 101, 253–262.

Haynes, V. N., Ward, J. E., Russell, B. J., and Agrios, A. G. (2017). Photocatalytic effects of titanium dioxide nanoparticles on aquatic organisms—Current knowledge and suggestions for future research. *Aquat. Toxicol.* 185, 138–148.

He, T., Tsui, M. M. P., Tan, C. J., Ma, C. Y., Yiu, S. K. F., Wang, L. H., et al. (2019a). Toxicological effects of two organic ultraviolet filters and a related commercial sunscreen product in adult corals. *Environ. Pollut.* 245, 462–471.

He, T., Tsui, M. M. P., Tan, C. J., Ng, K. Y., Guo, F. W., Wang, L. H., et al. (2019b). Comparative toxicities of four benzophenone ultraviolet filters to two life stages of two coral species. *Sci. Total Environ.* 651, 2391–2399.

Hédouin, L., and Gates, R. D. (2013). Assessing fertilization success of the coral *Montipora capitata* under copper exposure: Does the night of spawning matter? *Mar. Pollut. Bull.* 66, 221–224.

Hédouin, L., Pilon, R., and Puisay, A. (2015). Hyposalinity stress compromises the fertilization of gametes more than the survival of coral larvae. *Mar. Environ. Res.* 104, 1–9.

Hennige, S. J., Suggett, D. J., Warner, M. E., McDougall, K. E., and Smith, D. J. (2009). Photobiology of *Symbiodinium* revisited: Bio-physical and bio-optical signatures. *Coral Reefs* 28, 179–195.

Henry, T. B., McPherson, J. T., Rogers, E. D., Heah, T. P., Hawkins, S. A., Layton, A. C., et al. (2009). Changes in the relative expression pattern of multiple vitellogenin genes in adult male and larval zebrafish exposed to exogenous estrogens. *Comp. Biochem. Physiol. - A Mol. Integr. Physiol.* 154, 119–126.

Heron, S. F., Maynard, J. A., van Hooidonk, R., and Eakin, C. M. (2016). Warming Trends and Bleaching Stress of the World's Coral Reefs 1985–2012. *Sci. Rep.* 6, 38402.

Heyward, A. J., and Babcock, R. C. (1986). Self- and cross-fertilization in scleractinian corals. *Mar. Biol.* 90, 191–195.

Heyward, A. J., and Negri, A. P. (2010). Plasticity of larval pre-competency in response to temperature: Observations on multiple broadcast spawning coral species. *Coral Reefs* 29, 631–636.

Hill, R., and Ralph, P. J. (2006). Photosystem II Heterogeneity of in hospite Zooxanthellae in Scleractinian Corals Exposed to Bleaching Conditions. *Photochem. Photobiol.* 82, 1577.

Hirose, M., Yamamoto, H., and Nonaka, M. (2008). Metamorphosis and acquisition of symbiotic algae in planula larvae and primary polyps of *Acropora* spp. *Coral Reefs* 27, 247–254.

Hoadley, K. D., Pettay, D. T., Grottoli, A. G., Cai, W. J., Melman, T. F., Schoepf, V., et al. (2015). Physiological response to elevated temperature and pCO_2 varies across four Pacific coral species: Understanding the unique host+symbiont response. *Sci. Rep.* 5, 18371.

Hobday, A. J., Alexander, L. V., Perkins, S. E., Smale, D. A., Straub, S. C., Oliver, E. C. J., et al. (2016). A hierarchical approach to defining marine heatwaves. *Prog. Oceanogr.* 141, 227–238.

Hoegh-Guldberg, O. (1999). Climate change, coral bleaching and the future of the world's coral reefs. *Mar. Freshw. Res.* 50, 839–66.

Hoegh-Guldberg, O., and Jones, R. J. (1999). Photoinhibition and photoprotection in symbiotic dinoflagellates from reef-building corals.

Hoegh-Guldberg, O., Kennedy, E. V., Beyer, H. L., McClennen, C., and Possingham, H. P. (2018). Securing a Long-term Future for Coral Reefs. *Trends Ecol. Evol.* 33, 936–944.

Hoegh-Guldberg, O., Poloczanska, E. S., Skirving, W., and Dove, S. (2017). Coral Reef Ecosystems under Climate Change and Ocean Acidification. *Front. Mar. Sci.* 4.

Holbrook, S. J., Adam, T. C., Edmunds, P. J., Schmitt, R. J., Carpenter, R. C., Brooks, A. J., et al. (2018). Recruitment Drives Spatial Variation in Recovery Rates of Resilient Coral Reefs. *Sci. Rep.* 8.

Holmstrup, M., Bindesbøl, A. M., Oostingh, G. J., Duschl, A., Scheil, V., Köhler, H. R., et al. (2010). Interactions between effects of environmental chemicals and natural stressors: A review. *Sci. Total Environ.* 408, 3746–3762.

Hong, F., Yang, F., Liu, C., Gao, Q., Wan, Z., Gu, F., et al. (2005). Influences of nano-TiO2 on the chloroplast aging of spinach under light. *Biol. Trace Elem. Res.* 104, 249–260.

Hooper, M. J., Ankley, G. T., Cristol, D. A., Maryoung, L. A., Noyes, P. D., and Pinkerton, K. E. (2013). Interactions between chemical and climate stressors: A role for mechanistic toxicology in assessing climate change risks. *Environ. Toxicol. Chem.* 32, 32–48.

Hou, J., Wang, L., Wang, C., Zhang, S., Liu, H., Li, S., et al. (2019). Toxicity and mechanisms of action of titanium dioxide nanoparticles in living organisms. *J. Environ. Sci. (China)* 75, 40–53. doi:10.1016/j.jes.2018.06.010.

Houlbrèque, F., and Ferrier-Pagès, C. (2009). Heterotrophy in tropical scleractinian corals. *Biol. Rev.* 84, 1–17.

Howe, P. L., Eichelt-Brushett, A. J., and Clark, M. W. (2012). *Aiptasia pulchella*: A tropical cnidarian representative for laboratory ecotoxicological research. *Environ. Toxicol. Chem.* 31, 2653–2662.

Howe, P. L., Reichelt-Brushett, A. J., Clark, M. W., and Seery, C. R. (2017). Toxicity estimates for diuron and atrazine for the tropical marine cnidarian *Exaiptasia pallida* and in-hospite Symbiodinium spp. using PAM chlorophyll-a fluorometry. *J. Photochem. Photobiol. B Biol.* 171, 125–132.

Howe, P. L., Reichelt-Brushett, A. J., Krassoi, R., and Micevska, T. (2015). Comparative sensitivity of the cnidarian *Exaiptasia pallida* and a standard toxicity test suite: testing whole effluents intended for ocean disposal. *Environ. Sci. Pollut. Res.* 22, 13225–13233.

Hughes, T. P. (2019). There's insufficient evidence your sunscreen harms coral reefs. *Conversat.*

Hughes, T. P., Anderson, K. D., Connolly, S. R., Heron, S. F., Kerry, J. T., Lough, J. M., et al. (2018a). Spatial and temporal patterns of mass bleaching of corals in the Anthropocene. *Publ. Sci.* 5, 80–83.

Hughes, T. P., Barnes, M. L., Bellwood, D. R., Cinner, J. E., Cumming, G. S., Jackson, J. B. C., et al. (2017a). Coral reefs in the Anthropocene. *Nature* 546, 82–90.

Hughes, T. P., Connolly, S. R., Eakin, C. M., Dietzel, A., McWilliam, M. J., Hoey, A. S., et al. (2018b). Global warming transforms coral reef assemblages. *Nature* 556, 492–496.

Hughes, T. P., Kerry, J. T., Álvarez-Noriega, M., Álvarez-Romero, J. G., Anderson, K. D., Baird, A. H., et al. (2017b). Global warming and recurrent mass bleaching of corals. *Nature* 543, 373–377.

Hughes, T. P., Kerry, J. T., Baird, A. H., Connolly, S. R., Chase, T. J., Dietzel, A., et al. (2019). Global warming impairs stock–recruitment dynamics of corals. *Nature* 568, 387–390.

Humanes, A., Noonan, S. H. C., Willis, B. L., Fabricius, K. E., and Negri, A. P. (2016). Cumulative effects of nutrient enrichment and elevated temperature compromise the early life history stages of the coral acropora tenuis. *PLoS One* 11.

Humphrey, C., Weber, M., Lott, C., Cooper, T., and Fabricius, K. (2008). Effects of suspended sediments, dissolved inorganic nutrients and salinity on fertilisation and embryo development in the coral *Acropora millepora* (Ehrenberg, 1834). *Coral Reefs* 27, 837–850.

Hund-Rinke, K., and Simon, M. (2006). Ecotoxic effect of photocatalytic active nanoparticles (TiO_2) on algae and daphnids. *Environ. Sci. Pollut. Res.* 13, 225–232.

Hussain, S., Iqbal, N., Brestic, M., Raza, M. A., Pang, T., Langham, D. R., et al. (2019). Changes in morphology, chlorophyll fluorescence performance and Rubisco activity of soybean in response to foliar application of ionic titanium under normal light and shade environment. *Sci. Total Environ.* 658, 626–637.

Iglesias-Prieto, R., Matta, J. L., Robins, W. A., and Trench, R. K. (1992). Photosynthetic response to elevated temperature in the symbiotic dinoflagellate *Symbiodinium microadriaticum* in culture. *Proc. Natl. Acad. Sci. U. S. A.* 89, 10302–5.

Iguchi, A., Suzuki, A., Sakai, K., and Nojiri, Y. (2015). Comparison of the effects of thermal stress and CO_2-driven acidified seawater on fertilization in coral *Acropora digitifera*. *Zygote* 23, 631–634.

IPCC (2014). *Climate Change 2014: Synthesis Report. Contribution of Working Groups I, II and III to the Fifth Assessment Report of the Intergovernmental Panel on Climate Change*.

IPCC (2018). Global Warming of 1.5°C.

Ishibashi, H., Minamide, S., and Takeuchi, I. (2018). Identification and characterization of heat shock protein 90 (HSP90) in the hard coral *Acropora tenuis* in response to Irgarol 1051. *Mar. Pollut. Bull.* 133, 773–780.

Jensen, K. A. (2014). The NANOGENOTOX dispersion protocol for NANoREG.

Johnson, A. C., Bowes, M. J., Crossley, A., Jarvie, H. P., Jurkschat, K., Jürgens, M. D., et al. (2011). An assessment of the fate, behaviour and environmental risk associated with sunscreen TiO_2 nanoparticles in UK field scenarios. *Sci. Total Environ.* 409, 2503–10.

Jokiel, P. L., and Coles, S. L. (1990). Response of Hawaiian and other Indo-Pacific reef corals to elevated temperature.

Jomini, S., Labille, J., Bauda, P., and Pagnout, C. (2012). Modifications of the bacterial reverse mutation test reveals mutagenicity of TiO_2 nanoparticles and byproducts from a sunscreen TiO_2-based nanocomposite. *Toxicol. Lett.* 215, 54–61.

Jones, R. J. (2004). Testing the "photoinhibition" model of coral bleaching using chemical inhibitors. *Mar. Ecol. Prog. Ser.* 284, 133–145.

Jones, R. J., Hoegh-Guldberg, O., Larkum, A. W. D., and Schreiber, U. (1998). Temperature-induced bleaching of corals begins with impairment of the CO_2 fixation mechanism in zooxanthellae. *Plant, Cell Environ.* 21, 1219–1230.

Jones, R. J., and Kerswell, A. P. (2003). Phytotoxicity of Photosystem II (PSII) herbicides to coral. *Mar. Ecol. Prog. Ser.* 261, 149–159.

Jones, R. J., Kildea, T., and Hoegh-Guldberg, O. (1999). PAM chlorophyll fluorometry: A new in situ technique for stress assessment in scleractinian corals, used to examine the effects of cyanide from cyanide fishing. *Mar. Pollut. Bull.* 38, 864–874.

Jones, R., Ricardo, G. F., and Negri, A. P. (2015). Effects of sediments on the reproductive cycle of corals. *Mar. Pollut. Bull.* 100, 13–33.

Jovanović, B. (2015). Review of titanium dioxide nanoparticle phototoxicity: Developing a phototoxicity ratio to correct the endpoint values of toxicity tests. *Environ. Toxicol. Chem.* 34, 1070–1077.

Jovanović, B., and Guzmán, H. M. (2014). Effects of titanium dioxide (TiO_2) nanoparticles on caribbean reef-building coral (*Montastraea faveolata*). *Environ. Toxicol. Chem.* 33, 1346–1353.

Kalman, J., Paul, K. B., Khan, F. R., Stone, V., and Fernandes, T. F. (2015). Characterisation of bioaccumulation dynamics of three differently coated silver nanoparticles and aqueous silver in a simple freshwater food chain. *Environ. Chem.* 12, 662–672.

Kalmar, B., and Greensmith, L. (2009). Induction of heat shock proteins for protection against oxidative stress. *Adv. Drug Deliv. Rev.* 61, 310–318.

Kaniewska, P., Campbell, P. R., Kline, D. I., Rodriguez-Lanetty, M., Miller, D. J., Dove, S., et al. (2012). Major cellular and physiological impacts of ocean acidification on a reef building coral. *PLoS One* 7, 34659.

Kaplan, E. L., and Meier, P. (1958). Nonparametric estimation from incomplete samples. *J. ASA* 73, 457–481.

Karim, W., Nakaema, S., and Hidaka, M. (2015). Temperature effects on the growth rates and photosynthetic activities of *Symbiodinium* cells. *J. Mar. Sci. Eng.* 3, 368–381.

Kathiravan, P., Kalatharan, J., Karthikeya, G., Rengarajan, K., and Kadirvel, G. (2011). Objective Sperm Motion Analysis to Assess Dairy Bull Fertility Using Computer-Aided System - A Review. *Reprod. Domest. Anim.* 46, 165–172.

Kegler, P., Baum, G., Indriana, L. F., Wild, C., and Kunzmann, A. (2015). Physiological response of the hard coral *Pocillopora verrucosa* from Lombok, Indonesia, to two common pollutants in combination with high temperature. *PLoS One* 10.

Keller, A. A., Wang, H., Zhou, D., Lenihan, H. S., Cherr, G., Cardinale, B. J., et al. (2010). Stability and aggregation of metal oxide nanoparticles in natural aqueous matrices. *Environ. Sci. Technol.* 44, 1962–1967.

Keshavmurthy, S., Fontana, S., Mezaki, T., González, L. D. C., Chen, C. A., Del Caño González, L., et al. (2014). Doors are closing on early development in corals facing climate change. *Sci. Rep.* 4, 5633.

Kimberly, D. A., and Salice, C. J. (2014). Complex interactions between climate change and toxicants: Evidence that temperature variability increases sensitivity to cadmium. *Ecotoxicology* 23, 809–817.

Kime, D. E., Van Look, K. J. W., McAllister, B. G., Huyskens, G., Rurangwa, E., and Ollevier, F. (2001). Computer-assisted sperm analysis (CASA) as a tool for monitoring sperm quality in fish. *Comp. Biochem. Physiol. Part C Toxicol. Pharmacol.* 130, 425–433.

Kiser, M. A., Westerhoff, P., Benn, T., Wang, Y., Pérez-Rivera, J., and Hristovski, K. (2009). Titanium nanomaterial removal and release from wastewater treatment plants. *Environ. Sci. Technol.* 43, 6757–6763.

Kitchen, S. A., and Weis, V. M. (2017). The sphingosine rheostat is involved in the cnidarian heat stress response but not necessarily in bleaching. *J. Exp. Biol.* 220, 1709–1720.

Klaus, J. S., Janse, I., Heikoop, J. M., Sanford, R. A., and Fouke, B. W. (2007). Coral microbial communities, zooxanthellae and mucus along gradients of seawater depth and coastal pollution. *Environ. Microbiol.* 9, 1291–1305.

Knowlton, N. (2001). The future of coral reefs. *Proc. Natl. Acad. Sci.* 98, 5419–5425.

Koop, K., Booth, D., Broadbent, A., Brodie, J., Bucher, D., Capone, D., et al. (2001). ENCORE: The effect of nutrient enrichment on coral reefs. Synthesis of results and conclusions. *Mar. Pollut. Bull.* 42, 91–120.

Krämer, W. E., Caamaño-Ricken, I., Richter, C., and Bischof, K. (2012). Dynamic regulation of photoprotection determines thermal tolerance of two phylotypes of symbiodinium clade a at two photon fluence rates. *Photochem. Photobiol.* 88, 398–413.

Krueger, T., Becker, S., Pontasch, S., Dove, S., Hoegh-Guldberg, O., Leggat, W., et al. (2014). Antioxidant plasticity and thermal sensitivity in four types of *Symbiodinium* sp. *J. Phycol.* 50, 1035–1047.

Krueger, T., Hawkins, T. D., Becker, S., Pontasch, S., Dove, S., Hoegh-Guldberg, O., et al. (2015). Differential coral bleaching-Contrasting the activity and response of enzymatic antioxidants in symbiotic partners under thermal stress. *Comp. Biochem. Physiol. -Part A Mol. Integr. Physiol.* 190, 15–25.

Krueger, T., Horwitz, N., Bodin, J., Giovani, M.-E. E., Escrig, S., Meibom, A., et al. (2017). Common reef-building coral in the Northern Red Sea resistant to elevated temperature and acidification. *R. Soc. Open Sci.* 4, 170038.

Kruskopf, M., and Flynn, K. J. (2006). Chlorophyll content and fluorescence responses cannot be used to gauge reliably phytoplankton biomass, nutrient status or growth rate. *New Phytol.* 169, 525–536.

Kvitt, H., Rosenfeld, H., and Tchernov, D. (2016). The regulation of thermal stress induced apoptosis in corals reveals high similarities in gene expression and function to higher animals. *Sci. Rep.* 6, 30359.

Kvitt, H., Rosenfeld, H., Zandbank, K., and Tchernov, D. (2011). Regulation of apoptotic pathways by *Stylophora pistillata* (Anthozoa, Pocilloporidae) to survive thermal stress and bleaching. *PLoS One* 6.

Kwok, C. K., and Ang, P. O. (2013). Inhibition of larval swimming activity of the coral (*Platygyra acuta*) by interactive thermal and chemical stresses. *Mar. Pollut. Bull.* 74, 264–273.

Kwok, C. K., Lam, K. Y., Leung, S. M., Chui, A. P. Y., and Ang, P. O. (2016). Copper and thermal perturbations on the early life processes of the hard coral *Platygyra acuta*. *Coral Reefs* 35, 827–838.

Labille, J., Feng, J., Botta, C., Borschneck, D., Sammut, M., Cabie, M., et al. (2010). Aging of TiO_2 nanocomposites used in sunscreen. Dispersion and fate of the degradation products in aqueous environment. *Environ. Pollut.* 158, 3482–3489.

LaJeunesse, T. C., Loh, W. K. W., van Woesik, R., Hoegh-Guldberg, O., Schmidt, G. W., and Fitt, W. K. (2003). Low symbiont diversity in southern Great Barrier Reef corals relative to those of the Caribbean. *Limnol. Oceanogr.* 48, 2046–2054.

LaJeunesse, T. C., Parkinson, J. E., Gabrielson, P. W., Jeong, H. J., Reimer, J. D., Voolstra, C. R., et al. (2018). Systematic Revision of *Symbiodiniaceae* Highlights the Antiquity and Diversity of Coral Endosymbionts. *Curr. Biol.* 28, 2570-2580.e6.

LaJeunesse, T. C., Pettay, D. T., Sampayo, E. M., Phongsuwan, N., Brown, B., Obura, D. O., et al. (2010). Long-standing environmental conditions, geographic isolation and host-symbiont specificity influence the relative ecological dominance and genetic diversification of coral endosymbionts in the genus *Symbiodinium*. *J. Biogeogr.* 37.

Lam, E. K. Y., Chui, A. P. Y., Kwok, C. K., Ip, A. H. P., Chan, S. W., Leung, H. N., et al. (2015). High levels of inorganic nutrients affect fertilization kinetics, early development and settlement of the scleractinian coral *Platygyra acuta*. *Coral Reefs* 34, 837–848.

Lapied, E., Nahmani, J. Y., Moudilou, E., Chaurand, P., Labille, J., Rose, J., et al. (2011). Ecotoxicological effects of an aged TiO_2 nanocomposite measured as apoptosis in the anecic earthworm *Lumbricus terrestris* after exposure through water, food and soil. *Environ. Int.* 37, 1105–1110.

Lapointe, B. E. (1997). Nutrient thresholds for bottom-up control of macroalgal blooms on coral reefs in Jamaica and southeast Florida. *Limnol. Oceanogr.* 42, 1119–1131.

Le Nohaïc, M., Ross, C. L., Cornwall, C. E., Comeau, S., Lowe, R., McCulloch, M. T., et al. (2017). Marine heatwave causes unprecedented regional mass bleaching of thermally resistant corals in northwestern Australia. *Sci. Rep.* 7.

Leal, M. C., Ferrier-Pagès, C., Petersen, D., and Osinga, R. (2016). Coral aquaculture: Applying scientific knowledge to ex situ production. *Rev. Aquac.* 8, 136–153.

Leggat, W. P., Camp, E. F., Suggett, D. J., Heron, S. F., Fordyce, A. J., Gardner, S., et al. (2019). Rapid Coral Decay Is Associated with Marine Heatwave Mortality Events on Reefs. *Curr. Biol.* 29, 2723-2730.e4.

Leggat, W., Seneca, F., Wasmund, K., Ukani, L., Yellowlees, D., and Ainsworth, T. D. (2011). Differential responses of the coral host and their algal symbiont to thermal stress. *PLoS One* 6.

Lehnert, E. M., Burriesci, M. S., and Pringle, J. R. (2012). Developing the anemone Aiptasia as a tractable model for cnidarian-dinoflagellate symbiosis: the transcriptome of aposymbiotic A. pallida. *BMC Genomics* 13.

Lehnert, E. M., Mouchka, M. E., Burriesci, M. S., Gallo, N. D., Schwarz, J. A., and Pringle, J. R. (2014). Extensive Differences in Gene Expression Between Symbiotic and Aposymbiotic Cnidarians. *Genes|Genomes|Genetics* 4, 277–295.

Leichter, J. (2015). MCR LTER: Coral Reef: Benthic Water Temperature, ongoing since 2005. *Moorea Coral Reef LTER; Long Term Ecol. Res. Netw.*

Leigh-Smith, J., Reichelt-Brushett, A., and Rose, A. L. (2018). The characterization of iron (III) in seawater and related toxicity to early life stages of scleractinian corals. *Environ. Toxicol. Chem.* 37, 1104–1114.

Lesser, M. P. (1996). Elevated temperatures and ultraviolet radiation cause oxidative stress and inhibit photosynthesis in symbiotic dinoflagellates. *Limnol. Oceanogr.* 41, 271–283.

Lesser, M. P. (2006). Oxidative stress in marine environments: Biochemistry and Physiological Ecology. *Annu. Rev. Physiol.* 68, 253–278.

Lesser, M. P. (2011). Coral Bleaching: Causes and Mechanisms. *Coral Reefs An Ecosyst. Transit.*, 405–419.

Lesser, M. P. (2019). Phylogenetic signature of light and thermal stress for the endosymbiotic dinoflagellates of corals (Family Symbiodiniaceae). *Limnol. Oceanogr.* 9999, 1–12.

Levy, O., Kaniewska, P., Alon, S., Eisenberg, E., Karako-Lampert, S., Bay, L. K., et al. (2011). Complex Diel Cycles of Gene Expression in Coral-Algal Symbiosis. *Science (80-.).* 331, 175–175.

Levy, O., Karako-Lampert, S., Ben-Asher, H. W., Zoccola, D., Pagès, G., and Ferrier-Pagès, C. (2016). Molecular assessment of the effect of light and heterotrophy in the scleractinian coral *Stylophora pistillata*. *Proc. R. Soc. B Biol. Sci.* 283, 20153025.

Lewicka, Z. A., Benedetto, A. F., Benoit, D. N., Yu, W. W., Fortner, J. D., and Colvin, V. L. (2011). The structure, composition, and dimensions of TiO_2 and ZnO nanomaterials in commercial sunscreens. *J. Nanoparticle Res.* 13, 3607–3617.

Lewis, C., and Ford, A. T. (2012). Infertility in male aquatic invertebrates: A review. *Aquat. Toxicol.* 120–121, 79–89.

Li, F., Liang, Z., Zheng, X., Zhao, W., Wu, M., and Wang, Z. (2015). Toxicity of nano-TiO_2 on algae and the site of reactive oxygen species production. *Aquat. Toxicol.* 158, 1–13.

Louis, Y. D., Bhagooli, R., Kenkel, C. D., Baker, A. C., and Dyall, S. D. (2017). Gene expression biomarkers of heat stress in scleractinian corals: Promises and limitations. *Comp. Biochem. Physiol. Part C Toxicol. Pharmacol.* 191, 63–77.

Loya, Y., Lubinevsky, H., Rosenfeld, M., and Kramarsky-Winter, E. (2004). Nutrient enrichment caused by in situ fish farms at Eilat, Red Sea is detrimental to coral reproduction. *Mar. Pollut. Bull.* 49, 344–353.

Loya, Y., Sakai, K., Nakano, Y., and Woesik, R. Van (2001). Coral bleaching: the winners and the losers. *Ecol. Lett.* 4, 122–131.

Lürig, M., and Kunzmann, A. (2015). Effects of episodic low aragonite saturation and elevated temperature on the physiology of *Stylophora pistillata*. *J. Sea Res.* 99, 26–33.

Manaia, E. B., Kaminski, R. C. K., Corrêa, M. A., and Chiavacci, L. A. (2013). Inorganic UV filters. *Brazilian J. Pharm. Sci.* 49, 201–209.

Manzo, S., Buono, S., Rametta, G., Miglietta, M. L., Schiavo, S., and Di Francia, G. (2015). The diverse toxic effect of SiO_2 and TiO_2 nanoparticles toward the marine microalgae *Dunaliella tertiolecta*. *Environ. Sci. Pollut. Res.* 22, 15941–15951.

Maor-Landaw, K., Karako-Lampert, S., Waldman Ben-Asher, H., Goffredo, S., Falini, G., Dubinsky, Z., et al. (2014). Gene expression profiles during short-term heat stress in the red sea coral *Stylophora pistillata*. *Glob. Chang. Biol.* 20, 3026–35.

Marchello, A. E., Barreto, D. M., and Lombardi, A. T. (2018). Effects of Titanium Dioxide Nanoparticles in Different Metabolic Pathways in the Freshwater Microalga *Chlorella sorokiniana* (Trebouxiophyceae). *Water. Air. Soil Pollut.* 229.

Marisa, I., Matozzo, V., Martucci, A., Franceschinis, E., Brianese, N., and Marin, M. G. (2018). Bioaccumulation and effects of titanium dioxide nanoparticles and bulk in the clam *Ruditapes philippinarum*. *Mar. Environ. Res.* 136, 179–189.

Marshall, D. J. (2006). Reliably estimating the effect of toxicants on fertilization success in marine broadcast spawners. *Mar. Pollut. Bull.* 52, 734–738.

McClanahan, T. R., Darling, E. S., Maina, J. M., Muthiga, N. A., D'agata, S., Jupiter, S. D., et al. (2019). Temperature patterns and mechanisms influencing coral bleaching during the 2016 El Niño. *Nat. Clim. Chang.*, 1–7.

McCloskey, L. R. (1978). Measurement and interpretation of photosynthesis and respiration in reef corals. *Coral Reefs Res. Methods.*, 379–396.

McCook, L. J., Jompa, J., and Diaz-Pulido, G. (2001). Competition between corals and algae on coral reefs: A review of evidence and mechanisms. *Coral Reefs* 19, 400–417.

McDevitt-Irwin, J. M., Baum, J. K., Garren, M., and Vega Thurber, R. L. (2017). Responses of coral-associated bacterial communities to local and global stressors. *Front. Mar. Sci.* 4, 1–16.

McGinty, E. S., Pieczonka, J., and Mydlarz, L. D. (2012). Variations in Reactive Oxygen Release and Antioxidant Activity in Multiple *Symbiodinium* Types in Response to Elevated Temperature. *Microb. Ecol.* 64, 1000–1007.

Metzler, D. M., Li, M., Erdem, A., and Huang, C. P. (2011). Responses of algae to photocatalytic nano-TiO_2 particles with an emphasis on the effect of particle size. *Chem. Eng. J.* 170, 538–546.

Middlebrook, R., Anthony, K. R. N., Hoegh-Guldberg, O., and Dove, S. (2010). Heating rate and symbiont productivity are key factors determining thermal stress in the reef-building coral *Acropora formosa*. *J. Exp. Biol.* 213, 1026–1034.

Middlebrook, R., Anthony, K. R. N., Hoegh-Guldberg, O., and Dove, S. (2012). Thermal priming affects symbiont photosynthesis but does not alter bleaching susceptibility in *Acropora millepora*. *J. Exp. Mar. Bio. Ecol.* 432–433, 64–72.

Middlebrook, R., Hoegh-Guldberg, O., and Leggat, W. (2008). The effect of thermal history on the susceptibility of reef-building corals to thermal stress. *J. Exp. Biol.* 211, 1050–1056.

Mieog, J. C., Olsen, J. L., Berkelmans, R., Bleuler-Martinez, S. A., Willis, B. L., and van Oppen, M. J. H. (2009). The roles and interactions of symbiont, host and environment in defining coral fitness. *PLoS One* 4.

Miller, K., and Mundy, C. (2003). Rapid settlement in broadcast spawning corals: Implications for larval dispersal. *Coral Reefs* 22, 99–106.

Miller, R. J., Bennett, S., Keller, A. A., Pease, S., and Lenihan, H. S. (2012). TiO_2 nanoparticles are phototoxic to marine phytoplankton. *PLoS One* 7.

Miller, R. J., Lenihan, H. S., Muller, E. B., Tseng, N., Hanna, S. K., and Keller, A. a (2010). Impacts of metal oxide nanoparticles on marine phytoplankton. *Environ. Sci. Technol.* 44, 7329–7334.

Minetto, D., Libralato, G., and Volpi Ghirardini, a. (2014). Ecotoxicity of engineered TiO2 nanoparticles to saltwater organisms: An overview. *Environ. Int.* 66, 18–27.

Mitchelmore, C. L., He, K., Gonsior, M., Hain, E., Heyes, A., Clark, C., et al. (2019). Occurrence and distribution of UV-filters and other anthropogenic contaminants in coastal surface water, sediment, and coral tissue from Hawaii. *Sci. Total Environ.* 670, 398–410.

Moberg, F. F., and Folke, C. (1999). Ecological goods and services of coral reef ecosystems. *Ecol. Econ.* 29, 215–233.

Mohammadi, R., Maali-Amiri, R., and Mantri, N. L. (2014). Effect of TiO_2 Nanoparticles on Oxidative Damage and Antioxidant Defense Systems in Chickpea Seedlings during Cold Stress. *Russ. J. Plant Physiol.* 61, 768–775.

Morelli, E., Gabellieri, E., Bonomini, A., Tognotti, D., Grassi, G., and Corsi, I. (2018). TiO_2 nanoparticles in seawater: Aggregation and interactions with the green alga Dunaliella tertiolecta. *Ecotoxicol. Environ. Saf.* 148, 184–193.

Morimoto, R. (1993). Cells in Stress: Transcriptional Activation of Heat Shock Genes. *Science (80-.).* 259, 1409–1410.

Morita, M., Suwa, R., Iguchi, A., Nakamura, M., Shimada, K., Sakai, K., et al. (2010). Ocean acidification reduces sperm flagellar motility in broadcast spawning reef invertebrates. *Zygote* 18, 103–107.

Moya, A., Ganot, P., Furla, P., and Sabourault, C. (2012). The transcriptomic response to thermal stress is immediate, transient and potentiated by ultraviolet radiation in the sea anemone *Anemonia viridis*. *Mol. Ecol.* 21, 1158–1174.

Mueller, N. C., and Nowack, B. (2008). Exposure modeling of engineered nanoparticles in the environment. *EMPA Act.* 41, 63.

Muscatine, L. (1990). The role of symbiotic algae in carbon and energy flux in coral reefs. *Ecosyst. world* 25, 75–87.

Muscatine, L., Mccloskey, L. R., and Marian, R. E. (1981). Estimating the daily contribution of carbon from zooxanthellae to coral animal respiration. *Limnol. Oceanogr.* 26, 601–611.

Musee, N. (2011). Simulated environmental risk estimation of engineered nanomaterials: A case of cosmetics in Johannesburg City. *Hum. Exp. Toxicol.* 30, 1181–1195.

Nakamura, M., and Morita, M. (2012). Sperm motility of the scleractinian coral Acropora digitifera under preindustrial, current, and predicted ocean acidification regimes. *Geochemistry, Geophys. Geosystems* 15, 299–302.

Nakamura, T., Iguchi, A., Suzuki, A., Sakai, K., and Nojiri, Y. (2017). Effects of acidified seawater on calcification, photosynthetic efficiencies and the recovery processes from strong light exposure in the coral *Stylophora pistillata*. *Mar. Ecol.* 38, 1–7.

Nakata, H., Murata, S., and Filatreau, J. (2009). Occurrence and Concentrations of Benzotriazole UV Stabilizers in Marine Organisms and Sediments from the Ariake Sea, Japan. *Environ. Sci. Technol.* 43, 6920–6926.

Negri, A. P., and Heyward, A. J. (2000). Inhibition of fertilization and larval metamorphosis of the coral *Acropora millepora* (Ehrenberg, 1834) by petroleum products. *Mar. Pollut. Bull.* 41, 420–427.

Negri, A. P., and Hoogenboom, M. O. (2011). Water contamination reduces the tolerance of coral larvae to thermal stress. *PLoS One* 6, 19703.

Negri, A. P., Marshall, P. A., and Heyward, A. J. (2007). Differing effects of thermal stress on coral fertilization and early embryogenesis in four Indo Pacific species. *Coral Reefs* 26, 759–763.

Negri, A., Vollhardt, C., Humphrey, C., Heyward, A., Jones, R., Eaglesham, G., et al. (2005). Effects of the herbicide diuron on the early life history stages of coral. in *Marine Pollution Bulletin*, 370–383.

Nickel, C., Hellack, B., Nogowski, A., Babick, F., Stintz, M., Maes, H., et al. (2013). Mobility, fate and behaviour of TiO_2 nanomaterials in different environmental media. *Fed. Environ. Agency Ger. Proj. No.(FKZ) 3710.65* 414.

Nicklisch, A., and Köhler, J. (2001). Estimation of primary production with Phyto-PAM-fluorometry. *Ann Rep. Inst Freshw Ecol Inl. Fish Berlin* 13, 47–60.

Nikinmaa, M. (2013). Climate change and ocean acidification-Interactions with aquatic toxicology. *Aquat. Toxicol.* 126, 365–372.

Nitschke, M. R., Davy, S. K., Cribb, T. H., and Ward, S. (2015). The effect of elevated temperature and substrate on free-living *Symbiodinium* cultures. *Coral Reefs* 34, 161–171.

NOAA (2019). Sunscreen Chemicals and Marine Life.

Nohynek, G. J., Antignac, E., Re, T., and Toutain, H. (2010). Safety assessment of personal care products/cosmetics and their ingredients. *Toxicol. Appl. Pharmacol.* 243, 239–259.

Noonan, S. H. C. C., and Fabricius, K. E. (2016). Ocean acidification affects productivity but not the severity of thermal bleaching in some tropical corals. *ICES J. Mar. Sci.* 73, 715–726.

Nordemar, I., Nyström, M., and Dizon, R. (2003). Effects of elevated seawater temperature and nitrate enrichment on the branching coral *Porites cylindrica* in the absence of particulate food. *Mar. Biol.* 142, 669–677.

Nowack, B., Ranville, J. F., Diamond, S., Gallego-Urrea, J. A., Metcalfe, C., Rose, J., et al. (2012). Potential scenarios for nanomaterial release and subsequent alteration in the environment. *Environ. Toxicol. Chem.* 31, 50–9.

Nozawa, Y., and Harrison, P. L. (2002). Larval settlement and the effect dispersal of temperature on settlement of larvae *Platygyra* of the reef coral , from the Great Reef. *Proc. 9th Int. Coral Reef Symp.* I, 409–416.

Nozawa, Y., and Harrison, P. L. (2007). Effects of elevated temperature on larval settlement and post-settlement survival in scleractinian corals, *Acropora solitaryensis* and *Favites chinensis*. *Mar. Biol.* 152, 1181–1185.

NPS Protect Yourself, Protect The Reef! US National Park Service, https://cdhc.noaa.gov/_d.

Núñez-Pons, L., Bertocci, I., and Baghdasarian, G. (2017). Symbiont dynamics during thermal acclimation using cnidarian-dinoflagellate model holobionts. *Mar. Environ. Res.* 130, 303–314.

Nyström, M., Nordemar, I., and Tedengren, M. (2001). Simultaneous and sequential stress from increased temperature and copper on the metabolism of the hermatypic coral *Porites cylindrica*. *Mar. Biol.* 138, 1225–1231.

Ohno, T., Tokieda, K., Higashida, S., and Matsumura, M. (2003). Synergism between rutile and anatase TiO_2 particles in photocatalytic oxidation of naphthalene. *Appl. Catal. A Gen.* 244, 383–391.

Oliver, E. C. J., Donat, M. G., Burrows, M. T., Moore, P. J., Smale, D. A., Alexander, L. V, et al. (2018). Longer and more frequent marine heatwaves over the past century. *Nat. Commun.* 9.

Oliver, J., and Babcock, R. (1992). Aspects of the fertilization ecology of broadcast spawning corals: sperm dilution effects and in situ measurements of fertilization. *Biol. Bull.* 183, 409–417.

Olsen, K., Ritson-Williams, R., Ochrietor, J. D., Paul, V. J., and Ross, C. (2013). Detecting hyperthermal stress in larvae of the hermatypic coral *Porites astreoides*: The suitability of using biomarkers of oxidative stress versus heat-shock protein transcriptional expression. *Mar. Biol.* 160, 2609–2618.

Omori, M., Fukami, H., Kobinata, H., and Hatta, M. (2001). Significant drop of fertilization of *Acropora* corals in 1999: An after-effect of heavy coral bleaching? *Limnol. Oceanogr.* 46, 704–706.

Osterwalder, U., Sohn, M., and Herzog, B. (2014). Global state of sunscreens. *Photodermatol. Photoimmunol. Photomed.* 30, 62–80.

Overmans, S., Nordborg, M., Díaz-Rúa, R., Brinkman, D. L., Negri, A. P., and Agustí, S. (2018). Phototoxic effects of PAH and UVA exposure on molecular responses and developmental success in coral larvae. *Aquat. Toxicol.* 198, 165–174.

Özgür, M. E., Balcıoğlu, S., Ulu, A., Özcan, İ., Okumuş, F., Köytepe, S., et al. (2018). The in vitro toxicity analysis of titanium dioxide (TiO_2) nanoparticles on kinematics and biochemical quality of rainbow trout sperm cells. *Environ. Toxicol. Pharmacol.* 62, 11–19.

PADI The Best Coral Reef Safe Sunscreen for Scuba Diving? https://www2.padi.com/blog/2013/06/27/coral-reef-s.

Padilla-Gamiño, J. L., Bidigare, R. R., Barshis, D. J., Alamaru, A., Hédouin, L., Hernández-Pech, X., et al. (2013). Are all eggs created equal? A case study from the Hawaiian reef-building coral Montipora capitata. *Coral Reefs* 32, 137–152.

Palmer, C. V. (2018). Warmer water affects immunity of a tolerant reef coral. *Front. Mar. Sci.* 5, 1–9.

Pandolfi, J. M., Connolly, S. R., Marshall, D. J., and Cohen, A. L. (2011). Projecting Coral Reef Futures Under Global Warming and Ocean Acidification. *Science (80-.).* 333, 418–422.

Patel, P. P., and Bielmyer-Fraser, G. K. (2015). The influence of salinity and copper exposure on copper accumulation and physiological impairment in the sea anemone, *Exaiptasia pallida*. *Comp. Biochem. Physiol. Part - C Toxicol. Pharmacol.* 168, 39–47.

Patsiou, D., Kalman, J., Fernandes, T. F., and Henry, T. B. (2019). Differences in Engineered Nanoparticle (NP) Surface Physicochemistry Revealed by Investigation of Changes in Copper Bioavailability during Sorption to NPs in the Aqueous Phase. *Environ. Toxicol. Chem.*

Perez, S. F., Cook, C. B., and Brooks, W. R. (2001). The role of symbiotic dinoflagellates in the temperature-induced bleaching response of the subtropical sea anemone *Aiptasia pallida*. *J. Exp. Mar. Bio. Ecol.* 256, 1–14.

Pernice, M., Dunn, S. R., Miard, T., Dufour, S., Dove, S., and Hoegh-Guldberg, O. (2011). Regulation of apoptotic mediators reveals dynamic responses to thermal stress in the reef building coral acropora millepora. *PLoS One* 6.

Pfaffl, M. W. (2001). A new mathematical model for relative quantification in real-time RT-PCR. *Nucleic Acids Res.* 29, e45.

Piccinno, F., Gottschalk, F., Seeger, S., and Nowack, B. (2012). Industrial production quantities and uses of ten engineered nanomaterials in Europe and the world. *J. Nanoparticle Res.* 14, 1–11.

Pochon, X., Stat, M., Takabayashi, M., Chasqui, L., Chauka, L. J., Logan, D. D. K., et al. (2010). Comparison of endosymbiotic and free-living *Symbiodinium* (dinophyceae) diversity in a hawaiian reef environment. *J. Phycol.* 46, 53–65.

Poiger, T., Buser, H. R., Balmer, M. E., Bergqvist, P. A., and Müller, M. D. (2004). Occurrence of UV filter compounds from sunscreens in surface waters: Regional mass balance in two Swiss lakes. *Chemosphere* 55, 951–963.

Poquita-Du, R. C., Huang, D., Chou, L. M., Mrinalini, and Todd, P. A. (2019). Short Term Exposure to Heat and Sediment Triggers Changes in Coral Gene Expression and Photo-Physiological Performance. *Front. Mar. Sci.* 6, 1–15.

Porra, R. J., Thompson, W. A., and Kriedemann, P. E. (1989). Determination of accurate extinction coefficients and simultaneous equations for assaying chlorophylls a and b extracted with four different solvents: verification of the concentration of chlorophyll standards by atomic absorption spectroscopy. *Biochim. Biophys. Acta* 975, 143–196.

Porter, J. W., Lewis, S. K., and Porter, K. G. (1999). The effect of multiple stressors on the Florida Keys coral reef ecosystem: A landscape hypothesis and a physiological test. *Limnol. Oceanogr.* 44, 941–949.

Portune, K. J., Voolstra, C. R., Medina, M., and Szmant, A. M. (2010). Development and heat stress-induced transcriptomic changes during embryogenesis of the scleractinian coral *Acropora palmata*. *Mar. Genomics* 3, 51–62.

Pratchett, M. S., Anderson, K. D., Hoogenboom, M. O., Widman, E., Baird, A. H., Pandolfi, J. M., et al. (2015). Spatial, temporal and taxonomic variation in coral growth-implications for the structure and function of coral reef ecosystems. *Oceanogr. Mar. Biol. An Annu. Rev.* 53, 215–295.

Puisay, A., Pilon, R., Goiran, C., and Hédouin, L. (2018). Thermal resistances and acclimation potential during coral larval ontogeny in *Acropora pulchra*. *Mar. Environ. Res.* 135, 1–10.

Puisay, A., Pilon, R., and Hédouin, L. (2015). High resistance of *Acropora* coral gametes facing copper exposure. *Chemosphere* 120, 563–567.

Putnam, H. M., Edmunds, P. J., and Fan, T.-Y. (2010). Effect of a fluctuating thermal regime on adult and larval reef corals. *Invertebr. Biol.* 129, 199–209.

Qi, M., Liu, Y., and Li, T. (2013). Nano-TiO_2 improve the photosynthesis of tomato leaves under mild heat stress. *Biol. Trace Elem. Res.* 156, 323–328.

Qiang, L., Shi, X., Pan, X., Zhu, L., Chen, M., and Han, Y. (2015). Facilitated bioaccumulation of perfluorooctanesulfonate in zebrafish by nano-TiO_2 in two crystalline phases. *Environ. Pollut.* 206, 644–651.

R Core Team (2017). R: A language and environment for statistical computing.

Råberg, S., Nyström, M., Erös, M., and Plantman, P. (2003). Impact of the herbicides 2,4-D and diuron on the metabolism of the coral *Porites cylindrica*. *Mar. Environ. Res.* 56, 503–514.

Rädecker, N., Raina, J. B., Pernice, M., Perna, G., Guagliardo, P., Kilburn, M. R., et al. (2018). Using *Aiptasia* as a model to study metabolic interactions in Cnidarian-*Symbiodinium* symbioses. *Front. Physiol.* 9.

Radonić, A., Thulke, S., Mackay, I. M., Landt, O., Siegert, W., and Nitsche, A. (2004). Guideline to reference gene selection for quantitative real-time PCR. *Biochem. Biophys. Res. Commun.* 313, 856–862.

Raffa, R. B., Jr, J. V. P., Jr, R. T., and Rph, J. M. K. (2018). Sunscreen bans : Coral reefs and skin cancer. *Clin. Pharm. Ther.*, 1–6.

Ragni, M., Airs, R. L., Hennige, S. J., Suggett, D. J., Warner, M. E., and Geider, R. J. (2010). PSII photoinhibition and photorepair in *Symbiodinium* (Pyrrhophyta) differs between thermally tolerant and sensitive phylotypes. *Mar. Ecol. Prog. Ser.* 406, 57–70.

Ralph, P. J., Smith, R. A., MacInnis-Ng, C. M. O. O., and Seery, C. R. (2007). Use of fluorescence-based ecotoxicological bioassays in monitoring toxicants and pollution in aquatic systems: Review. Taylor & Francis Group.

Randall, C. J., and Szmant, A. M. (2009). Elevated temperature affects development, survivorship, and settlement of the elkhorn coral, *Acropora palmata* (Lamarck 1816). *Biol. Bull.* 217, 269–282.

Reed, R. B., Martin, D. P., Bednar, A. J., Montaño, M. D., Westerhoff, P., Ranville, J. F., et al. (2017). Multi-day diurnal measurements of Ti-containing nanoparticle and organic sunscreen chemical release during recreational use of a natural surface water. *Environ. Sci. Nano* 4, 69–77.

Reich, A., Harupa, M., Bury, M., Chrzaszcz, J., and Starczewska, A. (2009). Application of sunscreen preparations: A need to change the regulations. *Photodermatol. Photoimmunol. Photomed.* 25, 242–244.

Reichelt-Brushett, A., and Hudspith, M. (2016). The effects of metals of emerging concern on the fertilization success of gametes of the tropical scleractinian coral *Platygyra daedalea*. *Chemosphere* 150, 398–406.

Reichelt-Brushett, A. J., and Harrison, P. L. (1999). The effect of copper, zinc and cadmium on fertilization success of gametes from scleractinian reef corals. *Mar. Pollut. Bull.* 38, 182–187.

Reichelt-Brushett, A. J., and Harrison, P. L. (2000). The effect of copper on the settlement success of larvae from the scleractinian coral *Acropora tenuis*. *Mar. Pollut. Bull.* 41, 385–391.

Ricardo, G. F., Jones, R. J., Clode, P. L., Humanes, A., and Negri, A. P. (2015). Suspended sediments limit coral sperm availability. *Sci. Rep.* 5, 18084.

Richardson, S. D., and Ternes, T. A. (2018). Water Analysis: Emerging Contaminants and Current Issues. *Anal. Chem.* 90, 398–428.

Richier, S., Sabourault, C., Courtiade, J., Zucchini, N., Allemand, D., and Furla, P. (2006). Oxidative stress and apoptotic events during thermal stress in the symbiotic sea anemone, Anemonia viridis. *FEBS J.* 273, 4186–4198.

Richmond, R. H. (1987). Energetics, competency, and long-distance dispersal of planula larvae of the coral *Pocillopora damicornis*. *Mar. Biol.* 93, 527–533.

Richmond, R. H., and Hunter, C. L. (1990). Reproduction and recruitment of corals: comparisons among the Caribbean, the Tropical Pacific, and the Red Sea. *Mar. Ecol. Prog. Ser. Oldend.* 60, 185–203.

Richmond, R. H., Tisthammer, K. H., and Spies, N. P. (2018). The Effects of Anthropogenic Stressors on Reproduction and Recruitment of Corals and Reef Organisms. *Front. Mar. Sci.* 5, 1–9.

Richter, K., Haslbeck, M., and Buchner, J. (2010). The Heat Shock Response: Life on the Verge of Death. *Mol. Cell* 40, 253–266.

Ritson-Williams, R., Arnold, S., Fogarty, N., Steneck, R. S., Vermeij, M., and Paul, V. J. (2009). New perspectives on ecological mechanisms affecting coral recruitment on reefs. *Smithson. Contrib. Mar. Sci.*, 437–457.

Ritson-Williams, R., Paul, V. J., Arnold, S. N., and Steneck, R. S. (2010). Larval settlement preferences and post-settlement survival of the threatened Caribbean corals *Acropora palmata* and *A. cervicornis*. *Coral Reefs* 29, 71–81.

Rivest, E. B., and Hofmann, G. E. (2014). Responses of the metabolism of the larvae of *Pocillopora damicornis* to ocean acidification and warming. *PLoS One* 9, 96172.

Rivest, E. B., and Hofmann, G. E. (2015). Effects of temperature and pCO 2 on lipid use and biological parameters of planulae of *Pocillopora damicornis*. *J. Exp. Mar. Bio. Ecol.* 473, 43–52.

Robinson, J. P. W., Wilson, S. K., and Graham, N. A. J. (2019). Abiotic and biotic controls on coral recovery 16 years after mass bleaching. *Coral Reefs*, 1–11.

Robison, J. D., and Warner, M. E. (2006). Differential impacts of photoacclimation and thermal stress on the photobiology of four different phylotypes of *Symbiodinium* (Pyrrhophyta). *J. Phycol.* 42, 568–579.

Rodrigues, L. J., and Grottoli, A. G. (2007). Energy reserves and metabolism as indicators of coral recovery from bleaching. *Limnol. Oceanogr.* 52, 1874–1882.

Rodriguez-Lanetty, M., Harii, S., and Hoegh-Guldberg, O. (2009). Early molecular responses of coral larvae to hyperthermal stress. *Mol. Ecol.* 18, 5101–5114.

Rodríguez-Román, A., and Iglesias-Prieto, R. (2005). Regulation of photochemical activity in cultured symbiotic dinoflagellates under nitrate limitation and deprivation. *Mar. Biol.* 146, 1063–1073.

Rodríguez-Romero, A., Ruiz-Gutiérrez, G., Viguri, J. R., and Tovar-Sánchez, A. (2019). Sunscreens as a New Source of Metals and Nutrients to Coastal Waters. *Environ. Sci. Technol.* 53, 10177–10187.

Rogers, J. E., and Davis, R. H. (2006). Application of a new micro-culturing technique to assess the effects of temperature and salinity on specific growth rates of six *Symbiodinium* isolates. *Bull. Mar. Sci.* 79, 113–126.

Rohwer, F., Seguritan, V., Azam, F., and Knowlton, N. (2002). Diversity and distribution of coral-associated bacteria. *Mar. Ecol. Prog. Ser.* 243, 1–10.

Roman, M. (2015). Toxicity of Cellulose Nanocrystals: A Review. *Ind. Biotechnol.* 11, 25–33.

Rosenberg, E., Koren, O., Reshef, L., Efrony, R., and Zilber-Rosenberg, I. (2007). The role of microorganisms in coral health, disease and evolution. *Nat. Rev. Microbiol.* 5, 355–362.

Rosic, N., Kaniewska, P., Chan, C. K. K., Ling, E. Y. S., Edwards, D., Dove, S., et al. (2014). Early transcriptional changes in the reef-building coral *Acropora aspera* in response to thermal and nutrient stress. *BMC Genomics* 15.

Rosic, N. N., Pernice, M., Dove, S., Dunn, S., and Hoegh-Guldberg, O. (2011). Gene expression profiles of cytosolic heat shock proteins Hsp70 and Hsp90 from symbiotic dinoflagellates in response to thermal stress: Possible implications for coral bleaching. *Cell Stress Chaperones* 16, 69–80.

Roth, M. S. (2014). The engine of the reef: photobiology of the coral-algal symbiosis. *Front. Microbiol.* 5, 422.

Rowan, R. (2004). Thermal adaptation in reef coral symbionts. *Nature* 430, 742.

Sánchez-Quiles, D., and Tovar-Sánchez, A. (2014). Sunscreens as a source of hydrogen peroxide production in coastal waters. *Environ. Sci. Technol.* 48, 9037–42.

Sánchez-Quiles, D., and Tovar-Sánchez, A. (2015). Are sunscreens a new environmental risk associated with coastal tourism? *Environ. Int.* 83, 158–170.

Santaella, C., Allainmat, B., Simonet, F., Labille, J., Auffan, M., Rose, J., et al. (2014). Aged TiO_2 based nanocomposite used in sunscreens produces singlet oxygen under long wave UV and sensitises escherichia coli to cadmium. *Environ. Sci. Technol.* 48, 5245–5253.

Santos, A. J. M., Miranda, M. S., and Esteves da Silva, J. C. G. (2012). The degradation products of UV filters in aqueous and chlorinated aqueous solutions. *Water Res.* 46, 3167–3176.

Santos, S. R., Gutierrez-Rodriguez, C., and Coffroth, M. A. (2003). Phylogenetic identification of symbiotic dinoflagellates via length heteroplasmy in domain V of chloroplast large subunit (cp23S)—ribosomal DNA sequences. *Mar. Biotechnol.* 5, 130–140.

Sayes, C. M., Wahi, R., Kurian, P. A., Liu, Y., West, J. L., Ausman, K. D., et al. (2006). Correlating nanoscale titania structure with toxicity: A cytotoxicity and inflammatory response study with human dermal fibroblasts and human lung epithelial cells. *Toxicol. Sci.* 92, 174–185.

Schaffelke, B., and Klumpp, D. W. (1998). Short-term nutrient pulses enhance growth and photosynthesis of the coral reef macroalga *Sargassum baccularia*. *Mar. Ecol. Prog. Ser.* 170, 95–105.

Schiavo, S., Oliviero, M., Philippe, A., and Manzo, S. (2018). Nanoparticles based sunscreens provoke adverse effects on marine microalgae *Dunaliella tertiolecta*. *Environ. Sci. Nano* 5, 3011–3022.

Schiedek, D., Sundelin, B., Readman, J. W., and Macdonald, R. W. (2007). Interactions between climate change and contaminants. *Mar. Pollut. Bull.* 54, 1845–1856.

Schilling, K., Bradford, B., Castelli, D., Dufour, E., Nash, J. F., Pape, W., et al. (2010). Human safety review of "nano" titanium dioxide and zinc oxide. *Photochem. Photobiol. Sci.* 9, 495–509.

Schuhmacher, H., and Zibrowius, H. (1985). What is hermatypic? *Coral reefs* 4, 1–9.

Schwarz, J. A., Mitchelmore, C. L., Jones, R., O'Dea, A., and Seymour, S. (2013). Exposure to copper induces oxidative and stress responses and DNA damage in the coral *Montastraea franksi*. *Comp. Biochem. Physiol. - C Toxicol. Pharmacol.* 157, 272–279.

Sendra, M., Moreno-garrido, I., Yeste, M. P., Gatica, J. M., Blasco, J., Sánchez-quiles, D., et al. (2017a). Toxicity of TiO2 in nanoparticle or bulk form to freshwater and marine microalgae under visible light and UV-A radiation. *Environ. Pollut.* 227, 39–48.

Sendra, M., Sánchez-quiles, D., Blasco, J., Moreno-garrido, I., and Lubián, L. M. (2017b). Effects of TiO2 nanoparticles and sunscreens on coastal marine microalgae: Ultraviolet radiation is key variable for toxicity assessment. *Environ. Int.* 98, 62–68.

Sendra, M., Yeste, M. P., Gatica, J. M., Moreno-Garrido, I., and Blasco, J. (2017c). Homoagglomeration and heteroagglomeration of TiO_2, in nanoparticle and bulk form, onto freshwater and marine microalgae. *Sci. Total Environ.* 592, 403–411.

Seneca, F. O., and Palumbi, S. R. (2015). The role of transcriptome resilience in resistance of corals to bleaching. *Mol. Ecol.* 24, 1467–1484.

Seo, G.-Y., Lee, J. H., Kim, J. H., Shim, J. B., Hong, H. J., Kim, E., et al. (2018). Effects of emulsifying agents on the safety of titanium dioxide and zinc oxide nanoparticles in sunscreens. *J. Dispers. Sci. Technol.* 0, 1–6.

Serpone, N., Dondi, D., and Albini, A. (2007). Inorganic and organic UV filters: Their role and efficacy in sunscreens and suncare products. *Inorganica Chim. Acta* 360, 794–802.

Seveso, D., Montano, S., Strona, G., Orlandi, I., Galli, P., and Vai, M. (2016). Hsp60 expression profiles in the reef-building coral *Seriatopora caliendrum* subjected to heat and cold shock regimes. *Mar. Environ. Res.* 119, 1–11.

Shandilya, N., and Capron, I. (2017). Safer-by-design hybrid nanostructures: an alternative to conventional titanium dioxide UV filters in skin care products. *RSC Adv.* 7, 20430–20439.

Shantz, A. A., and Burkepile, D. E. (2014). Context-dependent effects of nutrient loading on the coral–algal mutualism. *Ecology* 95, 1995–2005.

Shaver, E. C., Burkepile, D. E., and Silliman, B. R. (2018). Local management actions can increase coral resilience to thermally-induced bleaching. *Nat. Ecol. Evol.* 2, 1075–1079.

Shick, J. M. (2012). *A functional biology of sea anemones*. Springer Science & Business Media.

Siddiqui, S., and Bielmyer-Fraser, G. K. (2015). Responses of the sea anemone, *Exaiptasia pallida*, to ocean acidification conditions and copper exposure. *Aquat. Toxicol.* 167, 228–239.

Silverstein, R. N., Cunning, R., and Baker, A. C. (2015). Change in algal symbiont communities after bleaching, not prior heat exposure, increases heat tolerance of reef corals. *Glob. Chang. Biol.* 21, 236–249.

Smijs, T. G., and Pavel, S. (2011). Titanium dioxide and zinc oxide nanoparticles in sunscreens: Focus on their safety and effectiveness. *Nanotechnol. Sci. Appl.* 4, 95–112.

Smith, D. J., Suggett, D. J., and Baker, N. R. (2005). Is photoinhibition of zooxanthellae photosynthesis the primary cause of thermal bleaching in corals? *Glob. Chang. Biol.* 11, 1–11.

Sørensen, J. G., Kristensen, T. N., and Loeschcke, V. (2003). The evolutionary and ecological role of heat shock proteins. *Ecol. Lett.* 6, 1025–1037.

Spalding, M. D., Burke, L., Wood, S. A., Ashpole, J., Hutchison, J., and zu Ermgassen, P. (2017). Mapping the global value and distribution of coral reef tourism. *Mar. Policy* 82, 104–113.

Spalding, M. D., Ravilious, C., and Green, E. P. (2001). *World Atlas of Coral Reefs*.

Srinivasan, M. (2003). Depth distributions of coral reef fishes: the influence of microhabitat structure, settlement, and post-settlement processes. *Oecologia* 137, 76–84.

Stambler, N. (2011). Zooxanthellae: The Yellow Symbionts Inside Animals. *Coral Reefs An Ecosyst. Transit.*, 87–106.

Stat, M., Carter, D., and Hoegh-Guldberg, O. (2006). The evolutionary history of *Symbiodinium* and scleractinian hosts-Symbiosis, diversity, and the effect of climate change. *Perspect. Plant Ecol. Evol. Syst.* 8, 23–43.

Stat, M., Pochon, X., Franklin, E. C., Bruno, J. F., Casey, K. S., Selig, E. R., et al. (2013). The distribution of the thermally tolerant symbiont lineage (*Symbiodinium* clade D) in corals from Hawaii: Correlations with host and the history of ocean thermal stress. *Ecol. Evol.* 3, 1317–1329.

Stien, D., Clergeaud, F., Rodrigues, A. M. S., Lebaron, K., Pillot, R., Romans, P., et al. (2018). Metabolomics reveal that octocrylene accumulates in *Pocillopora damicornis* tissues as fatty acid conjugates and triggers coral cell mitochondrial dysfunction. *Anal. Chem.*, in press.

Stimson, J., and Kinzie, R. A. (1991). The temporal pattern and rate of release of zooxanthellae from the reef coral *Pocillopora damicornis* (Linnaeus) under nitrogen-enrichment and control conditions. *J. Exp. Mar. Bio. Ecol.* 153, 63–74.

Strahl, J., Stolz, I., Uthicke, S., Vogel, N., Noonan, S. H. C., and Fabricius, K. E. (2015). Physiological and ecological performance differs in four coral taxa at a volcanic carbon dioxide seep. *Comp. Biochem. Physiol. -Part A Mol. Integr. Physiol.* 184, 179–186.

Sun, T. Y., Gottschalk, F., Hungerbühler, K., and Nowack, B. (2014). Comprehensive probabilistic modelling of environmental emissions of engineered nanomaterials. *Environ. Pollut.* 185, 69–76.

Sunagawa, S., Wilson, E. C., Thaler, M., Smith, M. L., Caruso, C., Pringle, J. R., et al. (2009). Generation and analysis of transcriptomic resources for a model system on the rise: the sea anemone *Aiptasia pallida* and its dinoflagellate endosymbiont. *BMC Genomics* 10, 258.

Sureda, A., Capó, X., Busquets-Cortés, C., and Tejada, S. (2018). Acute exposure to sunscreen containing titanium induces an adaptive response and oxidative stress in *Mytillus galloprovincialis*. *Ecotoxicol. Environ. Saf.* 149, 58–63.

Suzuki, A., and Kawahata, H. (1999). Partial pressure of carbon dioxide in coral reef lagoon waters: Comparative study of atolls and barrier reefs in the Indo-Pacific oceans. *J. Oceanogr.* 55, 731–745.

Suzuki, A., and Kawahata, H. (2003). Carbon budget of coral reef systems: an overview of observations in fringing reefs, barrier reefs and atolls in the Indo-Pacific regions. *Tellus B Chem. Phys. Meteorol.* 55, 428–444.

Takabayashi, M., Adams, L. M., Pochon, X., and Gates, R. D. (2012). Genetic diversity of free-living *Symbiodinium* in surface water and sediment of Hawai'i and Florida. *Coral Reefs* 31, 157–167.

Takahashi, S., and Murata, N. (2008). How do environmental stresses accelerate photoinhibition? *Trends Plant Sci.* 13, 178–182.

Takahashi, S., Nakamura, T., Sakamizu, M., Van Woesik, R., and Yamasaki, H. (2004). Repair Machinery of Symbiotic Photosynthesis as the Primary Target of Heat Stress for Reef-Building Corals. *Plant Cell Physiol.* 45, 251–255.

Takahashi, S., Yoshioka-Nishimura, M., Nanba, D., and Badger, M. R. (2013). Thermal acclimation of the symbiotic alga *Symbiodinium* spp. alleviates photobleaching under heat stress. *Plant Physiol.* 161, 477–85.

Tang, C. H., Lin, C. Y., Lee, S. H., and Wang, W. H. (2017). Membrane lipid profiles of coral responded to zinc oxide nanoparticle-induced perturbations on the cellular membrane. *Aquat. Toxicol.* 187, 72–81.

Tang, Y., Li, S., Qiao, J., Wang, H., and Li, L. (2013). Synergistic effects of nano-sized titanium dioxide and zinc on the photosynthetic capacity and survival of *Anabaena* sp. *Int. J. Mol. Sci.* 14, 14395–407.

Tchernov, D., Gorbunov, M. Y., de Vargas, C., Narayan Yadav, S., Milligan, A. J., Häggblom, M., et al. (2004). Membrane lipids of symbiotic algae are diagnostic of sensitivity to thermal bleaching in corals. *Proc. Natl. Acad. Sci. U. S. A.* 101, 13531–5.

The Comission of the European Communities (2006). COMMISSION RECOMMENDATION of 22 September 2006 on the efficacy of sunscreen products and the claims made relating thereto (notified under document number C(2006) 4089) (Text with EEA relevance) (2006/647/EC). *Off. J. Eur. Union*, 39–43.

Thornhill, D. J., Xiang, Y., Pettay, D. T., Zhong, M., and Santos, S. R. (2013). Population genetic data of a model symbiotic cnidarian system reveal remarkable symbiotic specificity and vectored introductions across ocean basins. *Mol. Ecol.* 22, 4499–4515.

Tovar-Sánchez, A., Sánchez-Quiles, D., Basterretxea, G., Benedé, J. L., Chisvert, A., Salvador, A., et al. (2013). Sunscreen products as emerging pollutants to coastal waters. *PLoS One* 8, e65451.

Tovar-Sánchez, A., Sánchez-Quiles, D., and Rodríguez-Romero, A. (2019). Massive coastal tourism influx to the Mediterranean Sea: The environmental risk of sunscreens. *Sci. Total Environ.* 656, 316–321.

Traylor-Knowles, N., Rose, N. H., Sheets, E. A., and Palumbi, S. R. (2017). Early transcriptional responses during heat stress in the coral *Acropora hyacinthus*. *Biol. Bull.* 232, 91–100.

Tremblay, P., Grover, R., Maguer, J. F., Legendre, L., and Ferrier-Pagès, C. (2012). Autotrophic carbon budget in coral tissue: a new 13C-based model of photosynthate translocation. *J. Exp. Biol.* 215, 1384–93.

Trenfield, M. A., van Dam, J. W., Harford, A. J., Parry, D., Streten, C., Gibb, K., et al. (2017). Assessing the chronic toxicity of copper and aluminium to the tropical sea anemone *Exaiptasia pallida*. *Ecotoxicol. Environ. Saf.* 139, 408–415.

Tsui, M. M. P., Leung, H. W., Wai, T. C., Yamashita, N., Taniyasu, S., Liu, W., et al. (2014). Occurrence, distribution and ecological risk assessment of multiple classes of UV filters in surface waters from different countries. *Water Res.* 67, 55–65.

UNEP/GPA (2006). The State of the Marine Environment: Trends and processes. The Hague, 1–111.

Van Dam, J. W., Negri, A. P., Uthicke, S., and F. Mueller, J. (2011). "Chemical Pollution on Coral Reefs: Exposure and Ecological Effects," in *Ecological Impacts of Toxic Chemicals (Open Access)*, 187–211.

Van Dam, J. W. W., Uthicke, S., Beltran, V. H. H., Mueller, J. F. F., and Negri, A. P. P. (2015). Combined thermal and herbicide stress in functionally diverse coral symbionts. *Environ. Pollut.* 204, 271–279.

van der Horst, G., Maree, L., and du Plessis, S. S. (2018). Current perspectives of CASA applications in diverse mammalian spermatozoa. *Reprod. Fertil. Dev.* 30, 875.

Van Hooidonk, R., Maynard, J. A., Manzello, D., and Planes, S. (2014). Opposite latitudinal gradients in projected ocean acidification and bleaching impacts on coral reefs. *Glob. Chang. Biol.* 20, 103–112.

van Oppen, M. J. H., and Blackall, L. L. (2019). Coral microbiome dynamics, functions and design in a changing world. *Nat. Rev. Microbiol.*

van Oppen, M. J. H., and Lough, J. M. (2009). *Coral Bleaching: Patterns, Processes, Causes and Consequences*.

van Oppen, M. J. H., Lutz, A., De'ath, G., Peplow, L., and Kininmonth, S. (2008). Genetic traces of recent long-distance dispersal in a predominantly self-recruiting coral. *PLoS One* 3.

Van Veghel, M. L. J. (1993). Multiple species spawning on Curacao reefs. *Bull. Mar. Sci.* 52, 1017–1021.

Van Woesik, R., Sakai, K., Ganase, A., and Loya, Y. (2011). Revisiting the winners and the losers a decade after coral bleaching. *Mar. Ecol. Prog. Ser.* 434, 67–76.

Veal, C. J., Holmes, G., Nunez, M., Hoegh-Guldberg, O., and Osborn, J. (2010). A comparative study of methods for surface area and three-dimensional shape measurement of coral skeletons. *Limnol. Oceanogr. Methods* 8, 241–253.

Vega Thurber, R. L., Burkepile, D. E., Fuchs, C., Shantz, A. A., Mcminds, R., and Zaneveld, J. R. (2014). Chronic nutrient enrichment increases prevalence and severity of coral disease and bleaching. *Glob. Chang. Biol.* 20, 544–554.

Venkatesan, A. K., Reed, R. B., Lee, S., Bi, X., Hanigan, D., Yang, Y., et al. (2017). Detection and Sizing of Ti-Containing Particles in Recreational Waters Using Single Particle ICP-MS. *Bull. Environ. Contam. Toxicol.* 100, 1–7.

Venn, A. A., Loram, J. E., and Douglas, A. E. (2008). Photosynthetic symbioses in animals. in *Journal of Experimental Botany*, 1069–1080.

Venn, A. A., Quinn, J., Jones, R., and Bodnar, A. (2009). P-glycoprotein (multi-xenobiotic resistance) and heat shock protein gene expression in the reef coral *Montastraea franksi* in response to environmental toxicants. *Aquat. Toxicol.* 93, 188–195.

Venn, A. A., Wilson, M., Trapido-Rosenthal, H. G., Keely, B. J., and Douglas, A. E. (2006). The impact of coral bleaching on the pigment profile of the symbiotic alga, Symbiodinium. *Plant, Cell Environ.* 29, 2133–2142.

Veron, J. E. N. (2000). *Corals of the World*.

Vijayavel, K., and Richmond, R. H. (2012). The preparation of the rice coral *Montipora capitata* nubbins for application in coral-reef ecotoxicology. *Ecotoxicology* 21, 925–930.

von Moos, N., Bowen, P., and Slaveykova, V. I. (2014). Oxidative stress induced by inorganic nanoparticles in bacteria and aquatic microalgae - State of the art and knowledge gaps. *Nanotoxicology* 8, 605–630.

Voolstra, C. R. (2013). A journey into the wild of the cnidarian model system Aiptasia and its symbionts. *Mol. Ecol.* 22, 4366–4368.

Voolstra, C. R., and Berumen, M. L. (2019). *Coral Reefs of the Red Sea*.

Voolstra, C. R., Schnetzer, J., Peshkin, L., Randall, C. J., Szmant, A. M., and Medina, M. (2009). Effects of temperature on gene expression in embryos of the coral *Montastraea faveolata*. *BMC Genomics* 10.

Voss, J. D., and Richardson, L. L. (2006). Nutrient enrichment enhances black band disease progression in corals. *Coral Reefs* 25, 569–576.

Wahie, S., Lloyd, J. J., and Farr, P. M. (2007). Sunscreen ingredients and labelling: a survey of products available in the UK. *Clin. Exp. Dermatol.* 32, 359–64.

Wang, J., and Douglas, A. E. (1997). Nutrients , Signals , and Photosynthate Release by Symbiotic Algae. *Plant Physiol.* 114, 631–636.

Wang, L., Shantz, A. A., Payet, J. P., Sharpton, T. J., Foster, A., Burkepile, D. E., et al. (2018a). Corals and their microbiomes are differentially affected by exposure to elevated nutrients and a natural thermal anomaly. *Front. Mar. Sci.* 5, 1–16.

Wang, S. Q., and Lim, H. W. (2016). *Principles and practice of photoprotection*. Adis.

Wang, X., Jiang, D., and Lang, X. (2018b). Climate Change of 4°C Global Warming above Pre-industrial Levels. *Adv. Atmos. Sci.* 35, 757–770.

Wang, X., Sharma, R. K., Gupta, A., George, V., Thomas, A. J., Falcone, T., et al. (2003). Alterations in mitochondria membrane potential and oxidative stress in infertile men: A prospective observational study. *Fertil. Steril.* 80, 844–850.

Wang, Y., Hu, M., Li, Q., Li, J., Lin, D., and Lu, W. (2014). Immune toxicity of TiO_2 under hypoxia in the green-lipped mussel *Perna viridis* based on flow cytometric analysis of hemocyte parameters. *Sci. Total Environ.* 470–471, 791–799.

Wang, Y., Zhu, X., Lao, Y., Lv, X., Tao, Y., Huang, B., et al. (2016). TiO_2 nanoparticles in the marine environment: Physical effects responsible for the toxicity on algae *Phaeodactylum tricornutum*. *Sci. Total Environ.* 565, 818–826.

Warner, M. E., Fitt, W. K., and Schmidt, G. W. (1999). Damage to photosystem II in symbiotic dinoflagellates: a determinant of coral bleaching. *Proc. Natl. Acad. Sci. U. S. A.* 96, 8007–12.

Webster, N. S., Smith, L. D., Heyward, A. J., Watts, J. E. M., Webb, R. I., Blackall, L. L., et al. (2004). Metamorphosis of a scleractinian coral in response to microbial biofilms. *Appl. Environ. Microbiol.* 70, 1213–21.

Weir, A., Westerhoff, P., Fabricius, L., and von Goetz, N. (2012). Titanium Dioxide Nanoparticles in Food and Personal Care Products. *Environ. Sci. Technol.* 46, 2242–2250.

Weis, V. M. (2008). Cellular mechanisms of Cnidarian bleaching: stress causes the collapse of symbiosis. *J. Exp. Biol.* 211, 3059–66.

Weis, V. M. (2019). Cell Biology of Coral Symbiosis: Foundational Study Can Inform Solutions to the Coral Reef Crisis. *Integr. Comp. Biol.* 59, 845–855.

Weis, V. M., Davy, S. K., Hoegh-Guldberg, O., Rodriguez-Lanetty, M., and Pringle, J. R. (2008). Cell biology in model systems as the key to understanding corals. *Trends Ecol. Evol.* 23, 369–376.

Wernberg, T., Smale, D. A., Tuya, F., Thomsen, M. S., Langlois, T. J., De Bettignies, T., et al. (2013). An extreme climatic event alters marine ecosystem structure in a global biodiversity hotspot. *Nat. Clim. Chang.* 3, 78–82.

Westerhoff, P., Song, G., Hristovski, K., and Kiser, M. A. (2011). Occurrence and removal of titanium at full scale wastewater treatment plants: implications for TiO_2 nanomaterials. *J. Environ. Monit.* 13, 1195–1203.

Wiedenmann, J., D'Angelo, C., Smith, E. G., Hunt, A. N., Legiret, F. E., Postle, A. D., et al. (2013). Nutrient enrichment can increase the susceptibility of reef corals to bleaching. *Nat. Clim. Chang.* 3, 160–164.

Wietheger, A., Fisher, P. L., Gould, K. S., and Davy, S. K. (2015). Sensitivity to oxidative stress is not a definite predictor of thermal sensitivity in symbiotic dinoflagellates. *Mar. Biol.* 162, 2067–2077.

Wild, C., Hoegh-Guldberg, O., Naumann, M. S., Colombo-Pallotta, M. F., Ateweberhan, M., Fitt, W. K., et al. (2011). Climate change impedes scleractinian corals as primary reef ecosystem engineers. *Mar. Freshw. Res.* 62, 205–215.

Willis, B. L., Babcock, R., Harrison, P. L., and Wallace, C. C. (1997). Experimental hybridization and breeding incompatibilities within the mating systems of mass spawning reef corals. *Coral Reefs* 16, S53–S65.

Wood, E. (2018). Impacts of sunscreens on coral reefs. *Rep. by Int. Coral Reef Initiat.*

Woods, R. M., Baird, A. H., Mizerek, T. L., and Madin, J. S. (2016). Environmental factors limiting fertilisation and larval success in corals. *Coral Reefs* 35, 1433–1440.

Wooldridge, S. A. (2012). A hypothesis linking sub-optimal seawater pCO_2 conditions for cnidarian-*Symbiodinium* symbioses with the exceedence of the interglacial threshold (>260 ppmv). *Biogeosciences* 9, 1709–1723.

Woolsey, E. S., Keith, S. A., Byrne, M., Schmidt-Roach, S., and Baird, A. H. (2015). Latitudinal variation in thermal tolerance thresholds of early life stages of corals. *Coral Reefs* 34, 471–478.

Wurl, O., and Obbard, J. P. (2004). A review of pollutants in the sea-surface microlayer (SML): A unique habitat for marine organisms. *Mar. Pollut. Bull.* 48, 1016–1030.

Xia, B., Chen, B., Sun, X., Qu, K., Ma, F., and Du, M. (2015). Interaction of TiO_2 nanoparticles with the marine microalga *Nitzschia closterium*: Growth inhibition, oxidative stress and internalization. *Sci. Total Environ.* 508, 525–533.

Xiong, D., Fang, T., Yu, L., Sima, X., and Zhu, W. (2011). Effects of nano-scale TiO_2, ZnO and their bulk counterparts on zebrafish: Acute toxicity, oxidative stress and oxidative damage. *Sci. Total Environ.* 409, 1444–1452.

Yakovleva, I. M., Baird, A. H., Yamamoto, H. H., Bhagooli, R., Nonaka, M., and Hidaka, M. (2009). Algal symbionts increase oxidative damage and death in coral larvae at high temperatures. *Mar. Ecol. Prog. Ser.* 378, 105–112.

Yamashita, H., and Koike, K. (2013). Genetic identity of free-living *Symbiodinium* obtained over a broad latitudinal range in the Japanese coast. *Phycol. Res.* 61, 68–80.

Zafiriou, O. C. (1986). “Photochemistry and the Sea-Surface Microlayer: Natural Processes and Potential as a Technique,” in *Dynamic processes in the chemistry of the upper ocean* (Springer), 129–135.

Zaitsev, Y. (2005). *Neuston of seas and oceans*. , eds. P. S. Liss and R. A. Duce Cambridge University Press: Cambridge.

Zaneveld, J. R., Burkepile, D. E., Shantz, A. A., Pritchard, C. E., McMinds, R., Payet, J. P., et al. (2016). Overfishing and nutrient pollution interact with temperature to disrupt coral reefs down to microbial scales. *Nat. Commun.* 7.

Ze, Y., Liu, C., Wang, L., Hong, M., and Hong, F. (2011). The regulation of TiO_2 nanoparticles on the expression of light-harvesting complex II and photosynthesis of chloroplasts of *Arabidopsis thaliana*. *Biol. Trace Elem. Res.* 143, 1131–1141.

Zhang, C., Wang, J., Tan, L., and Chen, X. (2016). Toxic effects of nano-ZnO on marine microalgae *Skeletonema costatum*: Attention to the accumulation of intracellular Zn. *Aquat. Toxicol.* 178, 158–164.

Zhou, H., Wang, X., Zhou, Y., Yao, H., and Ahmad, F. (2014). Evaluation of the toxicity of ZnO nanoparticles to *Chlorella vulgaris* by use of the chiral perturbation approach. *Anal. Bioanal. Chem.* 406, 3689–3695.

Zhu, X., Zhou, J., and Cai, Z. (2011). The toxicity and oxidative stress of TiO_2 nanoparticles in marine abalone (*Haliotis diversicolor supertexta*). *Mar. Pollut. Bull.* 63, 334–338.